

ENHANCED BOILING OF WATER-METHANOL MIXTURES ON COATED SURFACES

A THESIS

*Submitted in partial fulfilment of the
requirements for the award of the degree*

of

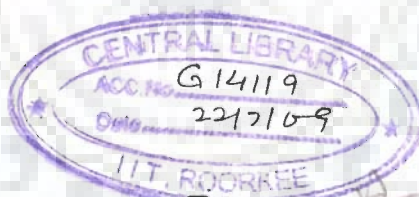
DOCTOR OF PHILOSOPHY

in

CHEMICAL ENGINEERING

By

MOHAMMAD SIRAJ ALAM



**DEPARTMENT OF CHEMICAL ENGINEERING
INDIAN INSTITUTE OF TECHNOLOGY ROORKEE
ROORKEE-247 667 (INDIA)**

JUNE, 2008



©INDIAN INSTITUTE OF TECHNOLOGY ROORKEE, ROORKEE, 2008
ALL RIGHTS RESERVED

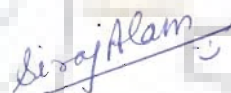


INDIAN INSTITUTE OF TECHNOLOGY ROORKEE ROORKEE

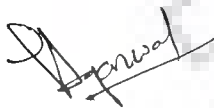
CANDIDATE'S DECLARATION

I hereby certify that the work which is being presented in this thesis entitled **ENHANCED BOILING OF WATER-METHANOL MIXTURES ON COATED SURFACES** in partial fulfilment of the requirements for the award of the Degree of Doctor of Philosophy and submitted in the Department of Chemical Engineering of the Indian Institute of Technology Roorkee, Roorkee is an authentic record of my own work carried out during the period from July 2003 to June 2008 under the supervision of Dr. S. C. Gupta, and Dr. V. K. Agarwal, Professors, Department of Chemical Engineering, Indian Institute of Technology Roorkee, Roorkee.

The matter presented in this thesis has not been submitted by me for the award of any other degree of this or any other Institute/University.


(MOHAMMAD SIRAJ ALAM)

This is to certify that the above statement made by the candidate is correct to the best of our knowledge.



(V. K. Agarwal)
Supervisor



(S. C. Gupta)
Supervisor

Date: 26-06-2008

The Ph.D. Viva-Voce examination of **Mr. Mohammad Siraj Alam**, Research Scholar, has been held on ... Oct. 24, 2008


Signature of Supervisors



Signature of External Examiner

ABSTRACT

This thesis presents an experimental investigation on nucleate pool boiling of methanol, distilled water and their binary mixtures on plain as well as copper coated stainless steel tubes at atmospheric and subatmospheric pressures. Basically, it deals with the effect of operating parameters; viz. heat flux, pressure and composition of mixture on heat transfer coefficient for the boiling of methanol, distilled water, and their mixtures on a stainless steel heating tube surface. Further, it also includes the effect of coating thickness along with the other parameters for the boiling of these liquids on stainless steel heating tubes surfaces coated with copper. In addition, thermal effectiveness of coated tubes has also been studied to obtain the range of heat flux and pressure for which enhanced boiling of liquids and their binary mixtures may occur.

The experimentation includes saturated boiling of methanol, distilled water and their binary mixtures on an electrically heated horizontal plain as well as copper coated stainless steel heating tube surfaces. The heating tube has been made of AISI 304 stainless steel cylinder having 18 mm I.D., 31.94 mm O.D. and 150 mm effective length. It is heated by placing a laboratory made electric heater inside it. Wall and liquid temperatures were measured by polytetrafluoroethylene (PTFE) coated 30 gauge copper-constantan calibrated thermocouples. The thermocouples are placed inside four holes drilled at a pitch circle diameter of 25 mm in the wall thickness of heating tube for measurement of surface temperature. Similarly, thermocouple probes are placed in liquid pool corresponding to wall thermocouple positions in heating tube for the measurement of liquid temperature. A digital multi-meter measures e.m.f. of thermocouples. The compositions of binary liquid mixtures and those of boiling liquid and vapor were measured by using HPLC system. A Novel Pack, C18 column of size 3.9 mm × 150 mm was used to measure the concentration of methanol in the binary mixture. Power input to heater is increased gradually from 240 W to 640 W in six equal steps and pressure from

44.40 kN/m² to 97.71 kN/m² in five steps. Three thicknesses of copper coating; viz. 22, 43 and 67 μm have been employed over plain heating tube by electroplating technique. The maximum uncertainty associated with the measured value of average heat transfer coefficient is of the order ±1.13%.

Experimental data for saturated boiling of distilled water on plain and copper coated tubes of various thicknesses at atmospheric and subatmospheric pressures have been processed to obtain local as well as average heat transfer coefficient. Analysis of experimental data has shown surface temperature to increase from bottom to side to top position of heating tube for a given value of heat flux at atmospheric and subatmospheric pressures. However, liquid temperature remains uniformly constant at all values of heat flux for a given pressure. Further, at a given value of heat flux, local heat transfer coefficient increases from top to side to bottom position on a heating tube surface and has been found to vary with heat flux according to power law relationship, $h_w \propto q^{0.7}$. Above observations are consistent for all the liquids of this investigation. Average value of heat transfer coefficient of a plain heating tube has also been found to be related with heat flux by the power law relationship $h \propto q^{0.7}$ for all the pressures of this investigation. This corroborates the findings of earlier investigators [4, 18, 19, 33, 34, 39, 56, 62, 83, 92, 105, 149, 150]. A dimensional equation, $h = C_1 q^{0.7} p^{0.32}$ for saturated boiling of liquids has been obtained by regression analysis within a maximum error of ±5%, where, C_1 is a constant whose value depends up on the type of boiling liquid and heating surface characteristics. To overcome the difficulty in the estimation of constant, C_1 owing to its improbable nature, above expression has been modified to the following non-dimensional form: $(h^*/h_1^*) = (p/p_1)^{0.32}$. It has been tested against experimental data of various investigators [4, 8, 16, 33, 39, 105, 106, 148, 149] for saturated boiling of several others liquids on heating surfaces with differing characteristics at various pressures, and found to correlate them excellently.

The experimental data for the pool boiling of methanol-distilled water binary mixtures at atmospheric and subatmospheric pressure showed

analogous boiling characteristic as that of pure liquids. The functional relationship of heat transfer coefficient with heat flux and pressure is same as observed for liquids and therefore, a dimensional equation, $h = C_2 q^{0.7} p^{0.32}$ for the boiling of a binary mixture, for atmospheric and subatmospheric pressures, has been developed by regression analysis. Further, above equation has also been reduced into a non-dimensional form: $(h^*/h_1^*) = (p/p_1)^{0.32}$, alike pure liquids, and found to match the experimental data of Pandey [102] within an error ranging from -12 to +20%. Furthermore, a reduction in heat transfer coefficient has been observed for the boiling of methanol-distilled water binary mixtures than the interpolated values of heat transfer coefficients of pure liquids present in the mixture. This has been due to the occurrence of mass transfer along with heat transfer in the process. Thus, an equation $h/h_{id} = [1 + |y - x|(\alpha/D)^{0.5}]^{-(0.8x+0.2)}$ has been developed for the prediction of heat transfer coefficient of a binary mixture. This equation correlates all the experimental data of this investigation within an error of $\pm 15\%$ as well as those predicted by correlations of [22, 50, 60, 76, 114, 121, 132, 134] within an average error of $\pm 25\%$.

Analysis of experimental data reveals that coating of copper on a stainless steel tube enhances heat transfer coefficient for the boiling of distilled water at atmospheric and subatmospheric pressures. In fact, enhancement is found to depend upon the thickness of coating. It has also been found that for a given value of heat flux, heat transfer coefficient increases with increase in coating thickness up to a certain value and thereafter decreases. However, increase in heat transfer coefficient is not proportional to increase in coating thickness. A functional relationship amongst heat transfer coefficient, heat flux and pressure has been established as $h = C_3 q^r p^s$, where the value of constant, C_3 and exponents, r and s depend upon heating surface characteristics and thickness of coating on heating tube surface.

Further, enhancement on a 43 μm thick coated tube surface is found to be more than any other coated surface of this investigation. Hence, a 43 μm thick coated tube surface has been selected to conduct experiments for the boiling of methanol and various compositions of methanol-distilled water binary

mixtures. Boiling of methanol and the binary mixtures on a 43 μm thick coated tube at atmospheric and subatmospheric pressures has also shown similar behavior as observed on a plain tube. However, increase in magnitude of heat transfer coefficient has differed due to difference in physico-thermal properties of methanol, distilled water and their binary mixtures. A dimensional relationship, $h = C_4 q^{0.60} p^{0.39}$, correlating heat transfer coefficient, heat flux and pressure is of the same form as obtained for liquids, where constant, C_4 depends upon the composition of methanol in the mixture and heating surface characteristics. In addition, it has been found that application of copper coating on stainless steel heating tube surface does not alter the methanol turnaround concentration. Therefore, the correlation, $h/h_{id} = [1 + |y - x|(\alpha/D)^{0.5}]^{-(0.8x+0.2)}$ developed for boiling of methanol-distilled water binary mixtures on a plain tube is also valid for the boiling of those on a 43 μm thick copper coated tube as well. This correlation has been compared against the experimental data for the boiling of methanol-distilled water mixtures on a 43 μm thick copper coated tube and found to match within an error of $\pm 20\%$.

Performance of a coated heating tube surface has been evaluated in terms of thermal effectiveness, ζ which is defined as a ratio of heat transfer coefficient on a heating surface coated with a given thickness of copper to that of a plain one for the boiling of a liquid subjected to same value of heat flux and pressure. It has been related to heat flux and pressure by the following equation, $\zeta = k q^\alpha p^\beta$, where constant, k and exponents, α and β depend upon heat flux, pressure, boiling liquid and thickness of coating. Using the condition, $\zeta > 1$, a criterion $q^{-\alpha} p^{-\beta} < k$ has been established for enhanced boiling of a liquid on a stainless steel heating tube surface coated with copper of a given thickness. This criterion can also be used to determine the range of heat flux for enhanced boiling of liquids on a copper coated stainless steel tube surface at a given pressure. Alternatively, it can also be used to obtain the range of pressure for enhanced boiling of liquids at a given value of heat flux. This criterion is also applicable to enhanced boiling of methanol-distilled water mixtures on a stainless steel heating tube surface coated with copper of a given thickness.

ACKNOWLEDGEMENTS

I wish to heartily express deep sense of gratitude to my supervisors Dr. S.C. Gupta, Retd. Professor, and Dr. V.K Agarwal, Professor, Department of Chemical Engineering, Indian Institute of Technology Roorkee for their proper guidance, inspiration and encouragement throughout course of this investigation. Their efforts and immense care in going minutely through the manuscript, thought provoking discussion and suggestions for its improvement are greatly acknowledged. In fact, I have no words to express my gratefulness towards my venerable supervisors for all the help received from time to time.

I would like to take this opportunity to put on record my respect to Prof. Shri Chand, Head of the Department, and Prof. Bikash Mohanty, former Head of the Department, for providing me the best of facilities during my research work. My sincere and grateful thanks are also due to Prof. Surendra Kumar, Professor, Prof. I. M. Mishra, Professor, Dr. B. Prasad, Associate Professor, and Dr. Ravindra Bhargava, Assistant Professor, Department of Chemical Engineering, IIT Roorkee for their kind assistance and encouragement.

I would also like to thank M/s Plating Sheen Chem. India Pvt. Ltd., New Delhi (India), for providing copper coating over heating tubes and its coating thickness measurement.

An enthusiastic association, cooperation and support provided by Dr. Mihir Kumar Das, former research scholar, during my experimentation, and M.Tech. students Amitosh Tiwari, Vimlesh Singh and Mohd. Rashid during correction and checking of manuscript is highly appreciated.

I owe my grateful thanks to my friends especially Dr. Vimal Chandra Srivastava, Mr. K. Upendar Reddy, Dr. Kaleem Khan, Dr. A.H. Bhatt, Dr. Anil Kumar Mathur, Dr. Arvind Kumar, Mr. Anil Kumar, Mr. Shamsuddin Ahmed, Mr. Shakir Ali, Dr. Rehana and many others who generously helped and encouraged me during my research work.

Thanks are also due to technical and ministerial staff of the Department, especially Mr. U.C. Sharma, Vijay Singh, Raj Kumar, S.C. Sharma, Shadab Ali,

Acknowledgements

S.P. Singh, Smt. Kamlesh, Smt. Anuradha, Satpal Singh, Tara Chand, B.K. Arora, Harbansh Singh, R. Bhatnagar, Vipin Ekka, J.S. Chowdhury, A.K. Chopra, Narender, Sudesh and Akhilesh Sharma for their kind help.

I am thankful to Prof. A. B. Samaddar, Director, MNNIT Allahabad, Prof. R. Kumar, Head of the Department; Prof. Satish Chandra, Prof. P.K. Mishra, Prof. Vinod Yadav and entire faculty of the Mechanical Engineering Department, MNNIT Allahabad for their sincere advice, cooperation and encouragement in the final phase of my research work.

I express my sincere gratitude to Mrs. Suman Gupta and Mrs. Alka Agarwal for their affection and encouragement during entire period of the work.

I sincerely thank the IIT Roorkee and Ministry of Human Resource and Development, Government of India, for providing financial support to undertake the work. The facilities and the environment at the Institute are great and are highly conducive for research work.

I deeply express my heartiest regards and ever ending heart felt affection to my reverend parents, my brother, Mr. Taj Mohammad, my father in-law, Mr. Jahangir and my entire family for their patience, love, encouragement and blessing without which it was not possible to complete my research work. Their faith in God and confidence made me to materialize their dream.

Last but not the least, I feel extremely grateful to *my wife*, Anjum, and *son*, Faiz who faced every difficult moment during this doctoral programme smilingly and always stood along with me. The care, support and encouragement provided by them are unforgettable.

I fully understand that the research experience and knowledge that I have gain during the course of my doctoral program would be highly useful in my carrier profession. This work was possible due to contribution of many. I am thankful to all of them and extremely sorry if any one is left out to acknowledge. I thank God for helping me in one way or the other and providing me and to my family members to the pain of remaining away from them for long duration.

MOHAMMAD SIRAJ ALAM

CONTENTS

	Title	Page No
	CANDIDATE'S DECLARATION	i
	ABSTRACT	ii
	ACKNOWLEDGMENTS	vi
	CONTENTS	viii
	LIST OF FIGURES	xii
	LIST OF TABLES	xx
	NOMENCLATURE	xxii
CHAPTER 1	INTRODUCTION	1
	1.1 OBJECTIVES OF THE PRESENT STUDY	4
	1.2 ORGANIZATION OF THESIS	5
CHAPTER 2	LITERATURE REVIEW	7
	2.1 NUCLEATE POOL BOILING HEAT TRANSFER FROM A PLAIN HEATING SURFACE	7
	2.2 BOILING HEAT TRANSFER CORRELATIONS FOR PURE LIQUIDS	8
	2.3 BOILING HEAT TRANSFER ON ENHANCED SURFACES	11
	2.3.1 Boiling on roughened surfaces	12
	2.3.2 Boiling on non-metallic coated surfaces	14
	2.3.3 Boiling on metal coated surfaces	18
	2.4 BOILING HEAT TRANSFER CORRELATIONS FOR MIXTURES	30
	2.5 MOTIVATION FOR PRESENT INVESTIGATION	56
CHAPTER 3	EXPERIMENTAL SET-UP	58
	3.1 DESIGN CONSIDERATIONS	58

		Page No
3.2	DETAILS OF EXPERIMENTAL SET-UP	60
3.2.1	Vessel	60
3.2.2	Heating tube	61
3.2.3	Condenser	66
3.2.4	Air-liquid separator	67
3.2.5	Liquid and vapor sampling arrangements	67
3.2.6	Vacuum pump	67
3.2.7	Instrumentation	68
CHAPTER 4	EXPERIMENTAL PROCEDURE	70
4.1	INTEGRITY TEST	70
4.2	CHECKING OF MECHANICAL AND ELECTRICAL LEAKAGE	71
4.3	THERMOCOUPLE INSTALLATION	72
4.4	PRELIMINARY OPERATIONS	73
4.5	DATA ACQUISITION	75
4.6	REPRODUCIBILITY AND CONSISTENCY	76
4.7	OPERATIONAL CONSTRAINT	76
CHAPTER 5	RESULTS AND DISCUSSION	79
5.1	LIMITATIONS OF PRESENT ANALYSIS	79
5.2	NUCLEATE BOILING OF SATURATED LIQUIDS ON AN UNCOATED HEATING TUBE	81
5.2.1	Circumferential variation of surface temperature	81
5.2.2	Variation of local heat transfer coefficient	84
5.2.3	Variation of average heat transfer coefficient	89
5.2.4	Heat transfer correlation for boiling of liquids at subatmospheric pressure	96

	Page No
5.3 NUCLEATE BOILING OF A BINARY MIXTURE ON AN UNCOATED HEATING TUBE	99
5.3.1 Circumferential variation of heat transfer coefficient	99
5.3.2 Heat transfer coefficient-heat flux relationship for a binary mixture	100
5.3.3 Variation of heat transfer coefficient of mixtures with composition	113
5.3.4 Development of a semi-empirical correlation for heat transfer coefficient of a binary mixture	121
5.4 NUCLEATE BOILING OF DISTILLED WATER ON COATED HEATING TUBES	127
5.4.1 Heat transfer coefficients on coated heating surfaces	127
5.4.2 Boiling of distilled water on copper coated tubes	130
5.4.3 Heat transfer coefficient-heat flux relationship for distilled water on coated tubes	134
5.4.4 Comparison between boiling characteristics for distilled water on a coated heating tube and those on an uncoated heating tube	135
5.5 NUCLEATE BOILING OF METHANOL ON A COATED HEATING TUBE	142
5.5.1 Boiling heat transfer characteristics for methanol on a coated tube	142
5.5.2 Heat transfer coefficient-heat flux relationship for methanol on a coated tube	143

	Page No
5.5.3 Comparison of boiling heat transfer characteristics on a coated and uncoated tube surfaces for methanol	143
5.6 NUCLEATE BOILING OF A BINARY MIXTURE ON A COATED HEATING TUBE	147
5.6.1 Boiling heat transfer characteristics for a binary mixture on a coated heating tube	147
5.6.2 Heat transfer coefficient-heat flux relationship for a binary mixture on a coated heating tube	148
5.6.3 Comparison of boiling heat transfer characteristics on a coated and uncoated tube surfaces for a binary mixture	155
5.6.4 Variation of heat transfer coefficient of mixtures with composition for boiling on a coated tube	156
5.7 THERMAL EFFECTIVENESS OF A COATED HEATING TUBE	171
CHAPTER 6 CONCLUSIONS AND RECOMMENDATIONS	184
6.1 CONCLUSIONS	184
6.2 RECOMMENDATIONS	188
ANNEXURE A PREPARATION OF COATED HEATING TUBES	190
ANNEXURE B TABULATION OF EXPERIMENTAL DATA	196
ANNEXURE C SAMPLE CALCULATION	236
ANNEXURE D UNCERTAINTY ANALYSIS	244
ANNEXURE E PHYSICO-THERMAL PROPERTIES EVALUATION	252
REFERENCES	263

LIST OF FIGURES

	Title	Page No.
Fig. 1.1	Techniques for enhanced heat transfer	3
Fig. 1.2	Organization of thesis	6
Fig. 3.1	Schematic diagram of the experimental set-up	62
Fig. 3.2	Photographic view of the experimental set-up	63
Fig. 3.3	Photographic view of the heating tubes	64
Fig. 3.4	Schematic diagram of the heating tube along with heater	65
Fig. 4.1	Calibration curve for measurement of methanol concentration using HPLC system	77
Fig. 5.1	Variation of liquid and surface temperature along circumference at bottom, two sides and top position of an uncoated heating tube with heat flux as a parameter for boiling of distilled water at atmospheric and subatmospheric pressures	83
Fig. 5.2	Variation of liquid and surface temperature along circumference at bottom, two sides and top position of an uncoated heating tube with heat flux as a parameter for boiling of methanol at atmospheric and subatmospheric pressures	86
Fig. 5.3	Variation of local heat transfer coefficient with heat flux along the circumference of an uncoated heating tube for boiling of distilled water and methanol at atmospheric pressure	87
Fig. 5.4	Comparison of experimental local heat transfer coefficients with those predicted from Eq. (5.3) for pool boiling of distilled water and methanol at atmospheric and subatmospheric pressures	90

	Title	Page No.
Fig. 5.5	Comparison of experimental data of this investigation with those of earlier investigators for boiling of distilled water at atmospheric pressure	91
Fig. 5.6	Variation of heat transfer coefficient with heat flux for boiling of distilled water and methanol over an uncoated heating tube with pressure as a parameter	94
Fig. 5.7	Comparison of experimental heat transfer coefficients with those predicted from Eq. (5.4) for boiling of saturated liquids on an uncoated heating tube surface at atmospheric and subatmospheric pressures	95
Fig. 5.8	A plot between (h^*/h^*_i) and $(p/p_1)^{0.32}$ for the boiling of various liquid on an uncoated heating surface at atmospheric and sub-atmospheric pressures	98
Fig. 5.9	Variation of liquid and surface temperature along circumference at bottom, two sides and top positions of uncoated heating tube with heat flux as a parameter for boiling of methanol-distilled water mixtures at atmospheric pressure	101
Fig. 5.10	Variation of liquid and surface temperature along circumference at bottom, two sides and top positions of uncoated heating tube with heat flux as a parameter for boiling of methanol-distilled water mixtures at 71.06 kN/m ² pressure	102
Fig. 5.11	Variation of liquid and surface temperature along circumference at bottom, two sides and top positions of uncoated heating tube with heat flux as a parameter for boiling of methanol-distilled water mixtures at 44.40 kN/m ² pressure	103

	Title	Page No.
Fig. 5.12	Comparison of experimental saturation temperature with those of calculated values for methanol-distilled water mixture at atmospheric and subatmospheric pressures	104
Fig. 5.13	Variation of heat transfer coefficient with heat flux for boiling of 5 mol% methanol-distilled water mixture on an uncoated heating tube with pressure as a parameter	105
Fig. 5.14	Variation of heat transfer coefficient with heat flux for boiling of 10 and 30 mol% methanol-distilled water mixture on an uncoated heating tube with pressure as a parameter	106
Fig. 5.15	Variation of heat transfer coefficient with heat flux for boiling of 50 and 80 mol% methanol-distilled water mixture on an uncoated heating tube with pressure as a parameter	107
Fig. 5.16	Variation of heat transfer coefficient with heat flux for boiling of 90 and 95 mol% methanol-distilled water mixture on an uncoated heating tube with pressure as a parameter	108
Fig. 5.17	Comparison of experimental heat transfer coefficients with those predicted from Eq. (5.7) for boiling of methanol-distilled water mixtures on an uncoated heating tube surface at atmospheric and subatmospheric pressures	111
Fig. 5.18	Comparison of experimental values of (h^*/h_1^*) with those predicted from Eq. (5.8) for pool boiling of binary liquid mixtures at atmospheric and subatmospheric pressures	112
Fig. 5.19	Variation of heat transfer coefficient, and $ y - x $ with mole fraction of methanol for methanol-distilled water mixtures on uncoated tube at atmospheric pressure	115
Fig. 5.20	Variation of heat transfer coefficient, and $ y - x $ with mole fraction of methanol for methanol-distilled water mixtures on uncoated tube at 84.39 kN/m ² pressure	116

	Title	Page No.
Fig. 5.21	Variation of heat transfer coefficient, and $ y - x $ with mole fraction of methanol for methanol-distilled water mixtures on uncoated tube at 44.40 kN/m ² pressure	117
Fig. 5.22	Phase equilibrium curves for methanol-distilled water binary mixtures at atmospheric and subatmospheric pressures	118
Fig. 5.23	Comparison of experimental heat transfer coefficients with those predicted from Eq. (5.13) for boiling of methanol-distilled water mixture on an uncoated heating tube surface at atmospheric and subatmospheric pressures	125
Fig. 5.24	Comparison of experimental heat transfer coefficients with those predicted from Eq. (5.13) for boiling of methanol-distilled water mixture on an uncoated heating tube surface at atmospheric	126
Fig. 5.25	Variation of heat transfer coefficient with heat flux for saturated boiling of distilled water from uncoated and coated surfaces due to present and earlier investigators at atmospheric pressure	129
Fig. 5.26	Variation of heat transfer coefficient with heat flux for boiling of distilled water on a 22 μm thick copper coated heating tube surface with pressure as a parameter	132
Fig. 5.27	Variation of heat transfer coefficient with heat flux for boiling of distilled water on 43 and 67 μm thick copper coated heating tubes with pressure as a parameter	133
Fig. 5.28	Comparison of experimental heat transfer coefficients with those predicted from Eq. (5.14) for boiling of distilled water on coated heating tube surfaces at atmospheric and subatmospheric pressures	136

	Title	Page No.
Fig. 5.29	Variation of heat transfer coefficient with heat flux for boiling of distilled water on copper coated tubes and on an uncoated tube at atmospheric pressure	137
Fig. 5.30	Variation of heat transfer coefficient with heat flux for boiling of distilled water on copper coated tubes and uncoated tube at 84.39 kN/m ² and 71.06 kN/m ² subatmospheric pressures	140
Fig. 5.31	Variation of heat transfer coefficient with heat flux for boiling of distilled water on copper coated tubes and uncoated tube at 57.73 kN/m ² and 44.40 kN/m ² subatmospheric pressures	141
Fig. 5.32	Variation of heat transfer coefficient with heat flux for boiling of methanol on a 43 μm thick copper coated heating tube surface with pressure as a parameter	144
Fig. 5.33	Comparison of experimental heat transfer coefficients with those predicted from Eq. (5.15) for boiling of methanol on a 43 μm coated heating tube surfaces at atmospheric and subatmospheric pressures	145
Fig. 5.34	Variation of heat transfer coefficient with heat flux for boiling of methanol on a 43 μm thick copper coated tube and on an uncoated tube at atmospheric pressure	146
Fig. 5.35	Variation of heat transfer coefficient with heat flux for boiling of methanol on a 43 μm thick copper coated tube and on an uncoated tube at 84.39 and 71.06 kN/m ² pressures	149
Fig. 5.36	Variation of heat transfer coefficient with heat flux for boiling of methanol on a 43 μm thick copper coated tube and on an uncoated tube at 57.73 and 44.40 kN/m ² pressures	150
Fig. 5.37	Variation of heat transfer coefficient with heat flux for boiling of 5 mol% methanol-distilled water mixture on a 43 μm thick copper coated heating tube surface with pressure as a parameter	151

	Title	Page No.
Fig. 5.38	Variation of heat transfer coefficient with heat flux for boiling of 10 and 30 mol% methanol-distilled water mixtures on a 43 μm thick copper coated heating tube surface with pressure as a parameter	152
Fig. 5.39	Variation of heat transfer coefficient with heat flux for boiling of 50 and 80 mol% methanol-distilled water mixtures on a 43 μm thick copper coated heating tube surface with pressure as a parameter	153
Fig. 5.40	Variation of heat transfer coefficient with heat flux for boiling of 90 and 95 mol% methanol-distilled water mixtures on a 43 μm thick copper coated heating tube surface with pressure as a parameter	154
Fig. 5.41	Comparison of experimental heat transfer coefficients with those predicted from Eq. (5.16) for boiling of methanol-distilled water mixtures on a 43 μm coated heating tube surfaces at atmospheric and subatmospheric pressures	157
Fig. 5.42	Variation of heat transfer coefficient with heat flux for boiling of various methanol-distilled water mixtures on a 43 μm thick copper coated tube and on an uncoated tube at atmospheric pressure	158
Fig. 5.43	Variation of heat transfer coefficient with heat flux for boiling of various methanol-distilled water mixtures on a 43 μm thick copper coated tube and on an uncoated tube at 84.39 kN/m^2 pressure	159
Fig. 5.44	Variation of heat transfer coefficient with heat flux for boiling of various methanol-distilled water mixtures on a 43 μm thick copper coated tube and on an uncoated tube at 57.73 kN/m^2 pressure	160

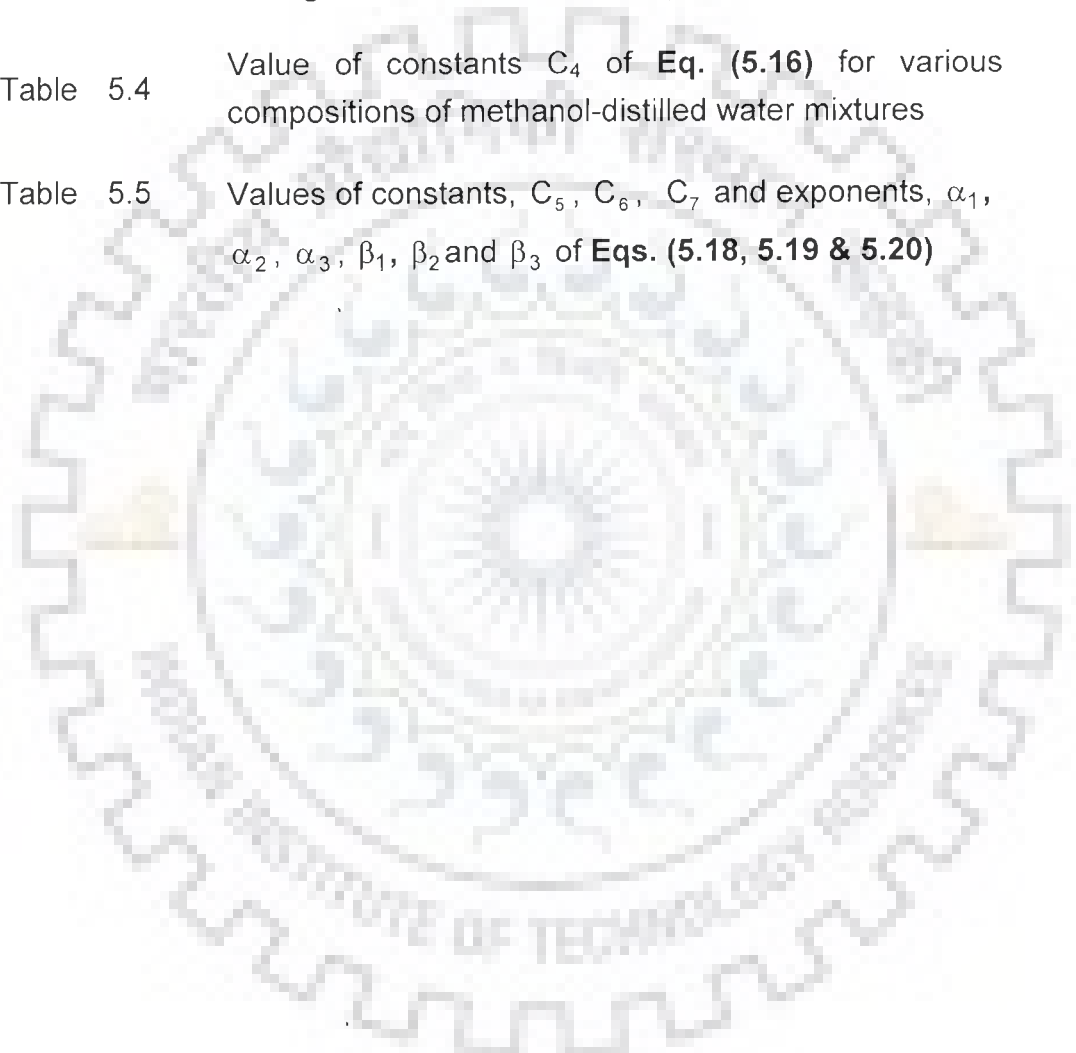
	Title	Page No.
Fig. 5.45	Variation of heat transfer coefficient with heat flux for boiling of various methanol-distilled water mixtures on a 43 μm thick copper coated tube and on an uncoated tube at 44.40 kN/m^2 pressure	161
Fig. 5.46	Variation of heat transfer coefficient, and $ y - x $ with mole fraction of methanol for methanol-water mixtures on 43 μm thickness copper coated tube at atmospheric pressure	162
Fig. 5.47	Variation of heat transfer coefficient, $ y - x $ with mole fraction of methanol for methanol-water mixtures on 43 μm thickness copper coated tube at 84.39 kN/m^2 pressure	165
Fig. 5.48	Variation of heat transfer coefficient, $ y - x $ with mole fraction of methanol for methanol-water mixtures on 43 μm thickness copper coated tube at 57.73 kN/m^2 pressure	166
Fig. 5.49	Variation of heat transfer coefficient, $ y - x $ with mole fraction of methanol for methanol-water mixtures on 43 μm thickness copper coated tube at 44.40 kN/m^2 pressure	167
Fig. 5.50	Comparison of experimental heat transfer coefficients with those predicted from Eq. (5.13) for boiling of methanol-distilled water mixtures on a 43 μm copper coated heating tube surface at atmospheric pressure	168
Fig. 5.51	Comparison of experimental heat transfer coefficients with those predicted from Eq. (5.13) for boiling of methanol-distilled water mixture on a 43 μm copper coated heating tube surface at subatmospheric pressures	169
Fig. 5.52	Variation of thermal effectiveness with heat flux and pressure for the boiling of distilled water over a 22 μm thick copper coated heating tube surface	174

	Title	Page No.
Fig. 5.53	Variation of thermal effectiveness with heat flux and pressure for the boiling of distilled water over a 43 μm thick copper coated heating tube surface	175
Fig. 5.54	Variation of thermal effectiveness with heat flux and pressure for the boiling of distilled water over a 67 μm thick copper coated heating tube surface	176
Fig. 5.55	Variation of thermal effectiveness with heat flux and pressure for the boiling of Methanol over a 43 μm thick copper coated heating tube surface	179
Fig. 5.56	Variation of thermal effectiveness with heat flux and pressure for the boiling of 5 mol% Methanol over a 43 μm thick copper coated heating tube surface	180
Fig. 5.57	Variation of thermal effectiveness with heat flux and pressure for the boiling of 50 mol% Methanol over a 43 μm thick copper coated heating tube surface	181
Fig. 5.58	Variation of thermal effectiveness with heat flux and pressure for the boiling of 90 mol% Methanol over a 43 μm thick copper coated heating tube surface	182

LIST OF TABLES

	Title	Page No.
Table 2.1	Dimensional correlations of nucleate pool boiling of liquids various investigators	9
Table 2.2	Values of constant a and b in Cryder & Finalborgo [39] correlation	10
Table 2.3	Values of constant C and exponent n in Sciance et al. [116] correlation	10
Table 2.4	Non-dimensional correlations of nucleate pool boiling of liquids various investigators	10
Table 2.5	Values of Rohsenow constant, C_{sf} obtained by Vachon et al. [144] & Piro [104] for various surface-liquid combinations	11
Table 2.6	Values of constant E of Rice & Calus [111] correlation	11
Table 2.7	Values of constant, C_{sf} and exponents, r and s of Rohsenow [112] correlation due to Vachon et al. [143]	16
Table 2.8	Summary of important investigations related to boiling of liquids on non-wetting surfaces	30
Table 2.9	Values of constant E of Calus & Rice [22] correlation	38
Table 2.10	Values for Constant C and index b of Eq. (2.54)	56
Table 3.1	Dimensions of Heating Tube	66
Table 4.1	Operating parameters of present investigation	78
Table 5.1	Values of constant C_{ψ} of Eq. (5.3) for various saturated liquids at various circumferential positions	88

	Title	Page No.
Table 5.2	Values of constant, C_2 of Eq. (5.7) for various compositions of methanol-distilled water mixtures	109
Table 5.3	Values of constant, C_3 and exponents, r and s for boiling of distilled water of Eq. (5.14)	134
Table 5.4	Value of constants C_4 of Eq. (5.16) for various compositions of methanol-distilled water mixtures	155
Table 5.5	Values of constants, C_5 , C_6 , C_7 and exponents, α_1 , α_2 , α_3 , β_1 , β_2 and β_3 of Eqs. (5.18, 5.19 & 5.20)	173



NOMENCLATURE

A	heat transfer surface area, m^2
C_d	Drag coefficient
C_p	specific heat, J/kg-K
D	mass diffusivity, m^2/s
d	diameter of heating tube, m
d_o	diameter of pore, m
d_p	particle diameter, m
f	bubble emission frequency, s^{-1}
G	mass flux
g	gravitational acceleration, m/s^2
h	heat transfer coefficient, $W/m^2 \text{ } ^\circ C$
h_b	heat transfer coefficient of binary mixture, $W/m^2 \text{ } ^\circ C$
k	thermal conductivity, $W/m \text{ } ^\circ C$
l	effective length of heating tube, m
M	molecular weight, kg/kmol
Na	nucleation site density, m^{-2}
P	pressure, kN/m^2
P_c	critical pressure, kN/m^2
P_r	reduced pressure (= p/p_c)
ΔP	pressure drop, kN/m^2
Q	total heat transfer, W
q	heat flux, W/m^2
R	bubble radius, m
R_a	surface roughness, m
R_p	radius of particle, m
r_c	critical radius of active site, m
t	time, s

Nomenclature

T	temperature, °C or K
ΔT_w	wall superheat, °C or K
ΔT_{bp}	boiling range defined as the dew point minus bubble point temperatures at constant mole fraction, °C or K
ΔT_{id}	ideal wall superheat, °C or K
V	velocity, m/s
V_b	bubble volume, m ³
x	mole fraction of high volatile component of binary mixture in liquid-phase
y	mole fraction of high volatile component of binary mixture in vapor-phase

Greek letters

α	thermal diffusivity, m ² /s
β	contact angle, degree
β_L	mass transfer coefficient in the liquid, m/s
δ	coating thickness, m
ε	porosity
λ	latent heat of vaporization, J/kg
μ	dynamic viscosity, N-s/m ²
ρ	density, kg/m ³
σ	surface tension, N/m
ν	kinematic viscosity, m ² /s
ζ	effectiveness factor

Subscripts

1	high volatile component
2	low volatile component
A	arithmetic average
b	bubble
c	cavity

cr	critical
exp.	experimental
h	pitch circle
H	horizontal orientation
i	inner
id	Ideal or weighted mean
inf	influence
l	liquid
LH	latent heat
m	measured
mix.	mixture
o	outer
p	particle
pred.	predicted
s	saturation
sf	surface liquid combination factor
T	total
v	vapor
W	wall
ψ	circumferential position

Dimensionless Group

Ar	Archimedes number	$\frac{g}{V^2} \left[\frac{\sigma}{(\rho_l - \rho_v)} \right]^{3/2} \left[\frac{\rho_l - \rho_v}{\rho_v} \right]$
Bu	Buoyancy number	$\frac{\rho_l - \rho_v}{\rho_l}$
Ga	Gallelian number	$\frac{g}{v^2} \left[\frac{\sigma}{g(\rho_l - \rho_v)} \right]^{3/2}$
Ja	Jakob number	$\frac{\rho_l C_{pl} \Delta T_w}{\rho_v \lambda}$

Nomenclature

K_P	Criterion for pressure term in boiling	$\frac{P}{\sqrt{g\sigma(\rho_l - \rho_v)}}$
K_{sub}	Criterion for sub cooling term	$\left[1 + \sqrt{\frac{\rho_l}{\rho_v} \left(\frac{T_s - T_l}{T_s} \right)} \right]$
K_t	Criterion for bubble break of frequency	$\frac{[\rho_v \lambda]^2}{C_{pl} T_s \rho_l \sqrt{g\sigma(\rho_l - \rho_v)}} = \frac{1}{K_u}$
Nu	Nusselt number	$\frac{h d}{k}$
Nu_B^*	Modified Nusselt number	$\frac{h}{k_l} \sqrt{\frac{\sigma}{g(\rho_l - \rho_v)}}$
Pr	Prandtl number	$\frac{C_p \mu}{k}$
Re	Reynolds number	$\frac{\rho v d}{\mu}$
St	Stanton number	$\frac{Nu}{Pr Re}$

Chapter-1

Introduction

This chapter deals with the introduction, need and objectives of this study

INTRODUCTION

Nucleate pool boiling, an intensive area of heat transfer, finds wide applications in chemical, petrochemical, food processing, space, refrigeration, nuclear, and other allied industries due to its ability to transfer enormous amount of heat at a low temperature gradient. It is also becoming increasingly important in the modern era, where many intriguing problems imposed by scarcity of space, energy, materials etc., leads to the development of energy efficient and compact heat transfer equipment. Heat transfer coefficient is one of the important factors contributing to the design of these equipment as it directly affects the material of construction, energy economy and thereby cost of the equipment. Therefore, the precise estimation of heat transfer coefficient is of vital significance.

Since its inception, boiling heat transfer has been a most challenging and dynamic field of contemporary heat transfer research. Although numerous experimental and theoretical investigations have been carried out over various surfaces for boiling of liquids and mixtures, yet they do not seem to be conclusive in nature. In fact, research has been carried out on various aspects of boiling such as mechanism, design correlations, parametric effects on heat transfer rate etc., but hardly there is single approach to deal with various problems involving boiling of liquids. Literature has a plethora of correlations both for pure liquids and mixtures, unfortunately, they shows a large discrepancy when they are applied to the surfaces other than used by the authors of these correlations. This is quite natural as almost all of them are empirical and semi-empirical in nature and include surface-liquid combination factor in them. In fact, each one of them holds true for a particular set of heating surface, liquid and operating conditions therein. In addition, most of the correlations have been developed using flat surfaces and hence their applicability for the design of tubular boiling equipment is questionable. This is quite obvious as boiling heat transfer coefficient on a flat surface remains

uniformly constant whereas on a tubular surface it is not likely to be so. Further, most of the investigations have been confined to boiling of liquids and mixtures at atmospheric pressure only. However, situations do exist in industries where boiling of liquids and mixtures is required to take place at subatmospheric pressures either due to process condition or to safeguard them against any possible deterioration. Further, very few studies are available mentioning the effect of heat flux, pressure, coating thickness and composition of liquid mixture on boiling characteristics. Therefore, it is necessary to generate experimental data for boiling of industrially important liquids at subatmospheric pressures on tubular surfaces and to study the effect of heat flux, pressure, thickness of coating, and composition of liquid mixture on heat transfer coefficient and thereby to develop a correlation free from surface-liquid combination factor.

Enhanced boiling is a solution to the challenges imposed by the advancement in technology due to rapid stride in various industries, exploitation of low heat flux non-conventional energy resources and necessity to conserve material and energy resources. Its importance lies in the facts that it has been employed to augment performance of flooded evaporators in refrigeration system, in reboilers on distillation towers for non fouling services and in evaporators of cascade refrigeration systems in refineries and chemical processing plants, for cooling high power density components by improved cooling rates and thereby lower start up and operational temperature of dissipating components to enhance their service life and reliability in the electronic industry, to augment boiling heat transfer and to obtain compact design, in air separation and gas processing industries and, to reduce size and cost of new unit as well as energy related operating cost in heat exchangers. Accordingly, several techniques for enhancement of boiling heat transfer have been developed during last few decades. These techniques have been reviewed by various investigators [12, 14, 135, 152], and classified as active passive and compound technique. A brief description of these techniques is provided in **Fig. 1.1**. An active technique includes the use of an external agency to enhance heat transfer. Thus, these techniques are difficult to implement at large scale due to economical reasons. Passive techniques offer

a significant enhancement in boiling heat transfer rate, and fabrication of such surfaces is easy and economical as it does not require power from any external source for this purpose.

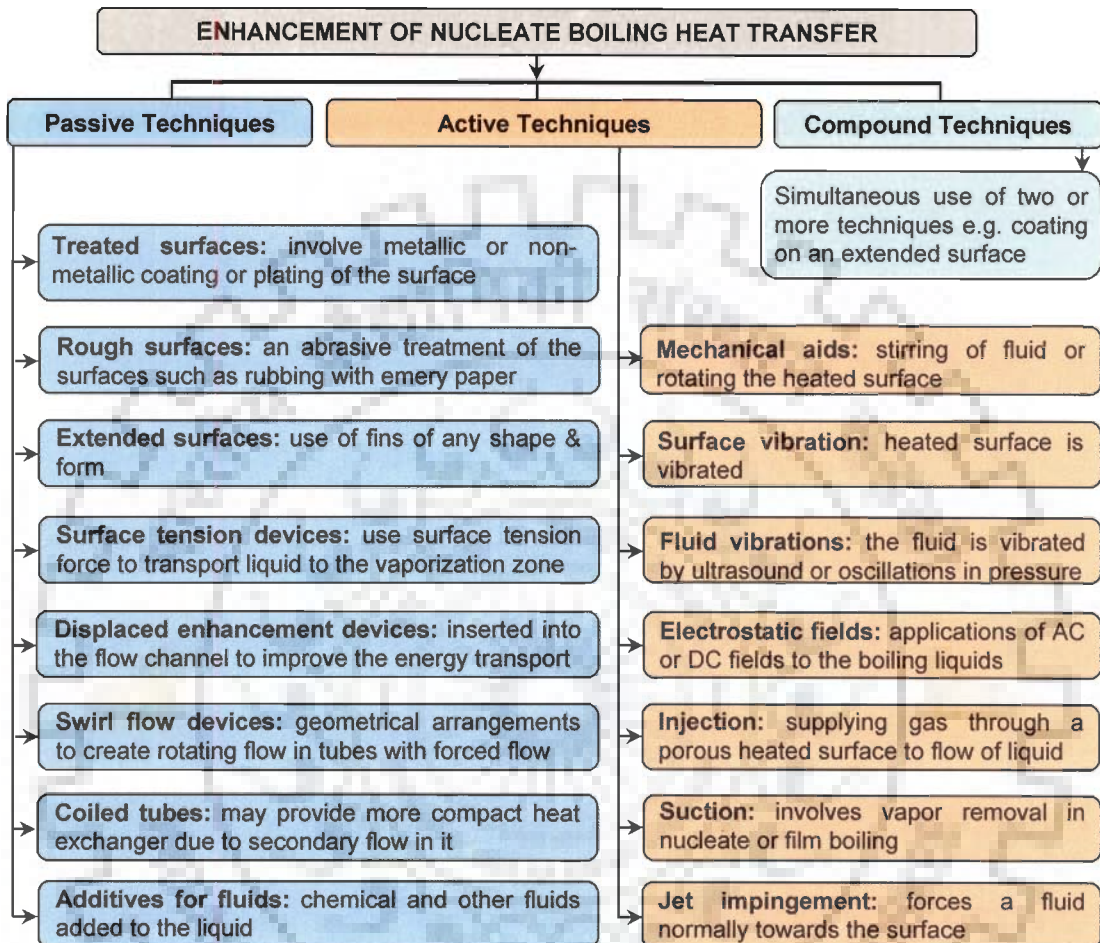


Fig. 1.1 Techniques for enhanced heat transfer

One of the important passive techniques involves modification of heating surfaces by altering their characteristics. These include either roughening or coating of metallic and non-metallic materials over heating surfaces. Many investigators [13, 16, 52, 54, 61, 90, 113, 143, 148] have used various non-metallic coating such as polytetrafluoroethylene (PTFE), tetrafluoroethylene (TFE), methane, paraffin carbon tetrachloride solution, etc, on heating surfaces and have reported substantial enhancement in boiling heat transfer rate. However, the surfaces coated with non-metallic materials have been found of limited durability because of their deterioration and surface's wetting

characteristics. Therefore, such surfaces apparently do not seem to be suitable for commercial applications. On the other hand, the surfaces coated with metallic materials such as copper, silver, nickel, cadmium, bronze, zinc, tin, chromium, aluminium etc., as reported by various investigators [1, 17, 24, 34, 62, 64, 95, 117, 119, 131, 147] have been found to last long and to enhance heat transfer coefficient many folds as compared to non-metallic coated surfaces. Besides, it is also important to point out that the properties of coating material and technique of coating influence heat transfer performance of the heating surface markedly. In fact, the heating surfaces coated with high thermal conductivity and high permeability materials provide better heat transfer performance than that of other coated materials. Another aspect is that, most of the investigations are confined to boiling of liquids – refrigerants, water, cryogenics and their mixtures at atmospheric pressure only. Therefore, it calls for an investigation to generate experimental data for boiling of industrially important liquids and mixtures at subatmospheric pressures on a metallic coated heating surface and thereby to study the effect of various parameters on boiling heat transfer coefficient.

1.1 OBJECTIVES OF THE PRESENT STUDY

Keeping the above in view, an experimental investigation on nucleate pool boiling of saturated liquids and their binary mixtures on an electrically heated ($q = \text{constant}$) horizontal stainless steel heating tube coated with various thicknesses of copper at atmospheric and subatmospheric pressures has been undertaken with the following objectives :

1. To conduct experiments for nucleate pool boiling of saturated distilled water, methanol and their binary mixtures on a horizontal plain stainless steel heating tube surface at atmospheric and subatmospheric pressures to determine the effects of operating parameters on local as well as average boiling heat transfer coefficients.

Further, to formulate a correlation of average heat transfer coefficient as a function of heat flux and pressure and thereby to recommend an equation, free from surface-liquid combination factor, for boiling heat transfer coefficient.

2. To conduct experiments for saturated boiling of distilled water on a stainless steel heating tube coated with various thicknesses of copper at atmospheric and subatmospheric pressures and to obtain the effect of operating parameters – heat flux, pressure, and coating thickness on heat transfer coefficient and thereby to develop correlations relating above parameters with heat transfer coefficient for the identification most suitable coated tube.
3. To conduct experiments for saturated boiling of methanol and various composition of methanol-distilled water binary mixture on a copper coated stainless steel heating tube at atmospheric and subatmospheric pressures and thereby to obtain the effect of operating parameters – heat flux, pressure, and composition on heat transfer coefficient and to formulate correlations.
4. To carry out a semi-theoretical analysis of nucleate pool boiling of liquids and their binary mixtures on both plain and copper coated surfaces for the prediction of heat transfer coefficient of binary liquid mixtures from that of pure liquids.
5. To compare heat transfer coefficient of a coated heating tube surface with that of plain one to determine the enhancement of heat transfer coefficient as a function of heat flux, pressure and thickness of coating.
6. To evaluate thermal effectiveness of coated heating tube surfaces for boiling of liquids and mixtures and to establish criteria for enhanced boiling on coated tube surfaces.

1.2 ORGANIZATION OF THESIS

Present investigation is broadly divided into two parts: First part deals with saturated boiling of distilled water, methanol, and various compositions of their binary mixtures on a plain stainless steel heating tube surface and second part deals with saturated boiling of these liquids and mixtures on coated stainless heating tube surfaces. Each part involves the study of boiling characteristics and effect of parameters along with formulation of correlations for determination of boiling heat transfer coefficient on respective surfaces. The details of overall organization of thesis are presented in **Fig. 1.2**.

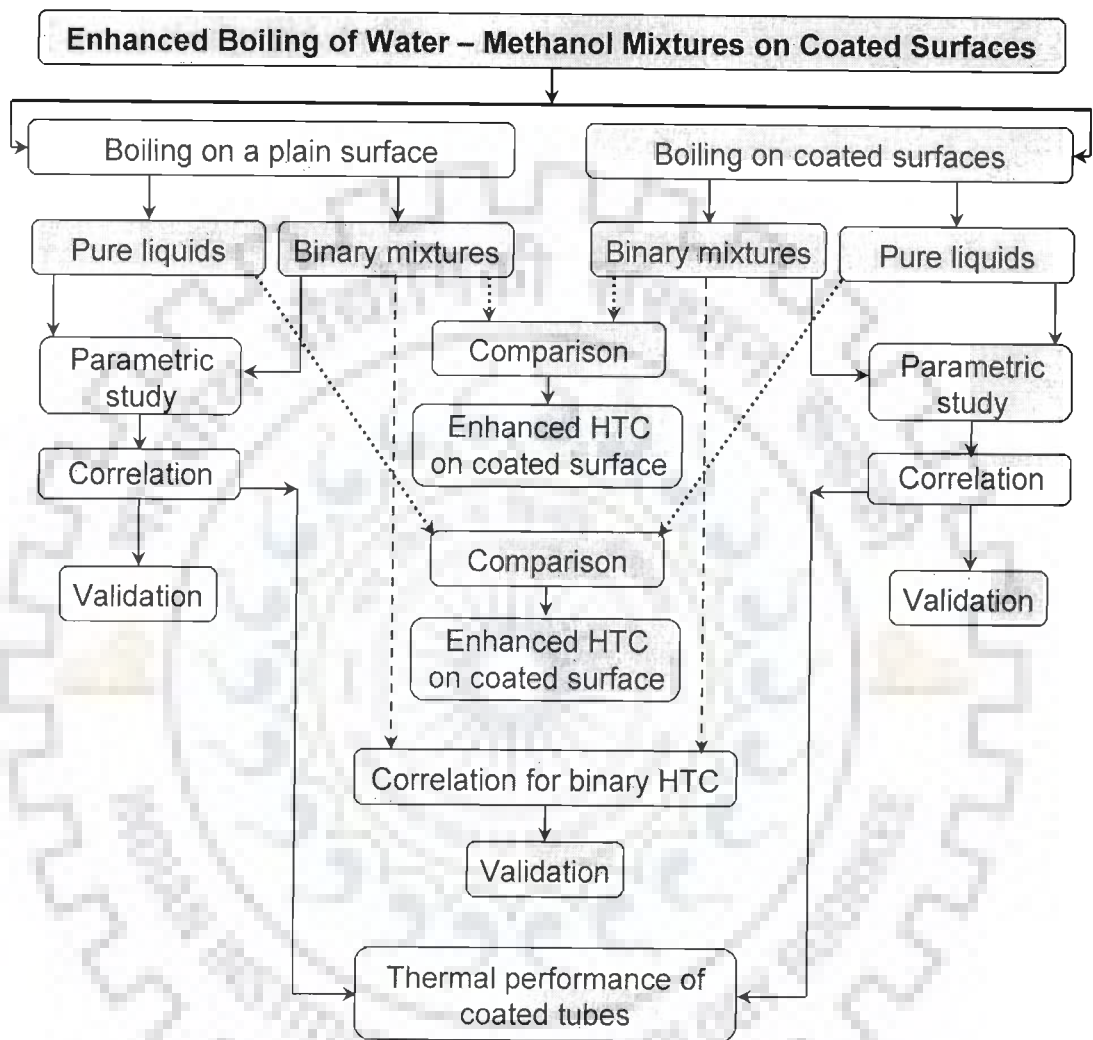


Fig. 1.2 Organization of thesis

Chapter-2

Literature Review

This chapter deals with the literature related to this study

LITERATURE REVIEW

This chapter discusses literature pertaining to various aspects of nucleate pool boiling heat transfer and its enhancement. It includes the published literature related to mechanism and dimensional and non-dimensional correlations developed by various investigators for saturated boiling of liquids and their mixtures on various surfaces. It also briefly reviews on enhancement of boiling heat transfer by the use of different passive techniques. Following sections are devoted to above aspects:

2.1 NUCLEATE POOL BOILING HEAT TRANSFER FROM A PLAIN HEATING SURFACE

Nucleate pool boiling heat transfer of liquids and mixtures is an important area of research due to its ultimate application in improving the design of heat transfer equipment largely employed in many industries. It has been a subject of active research for many years to understand the mechanism during boiling heat transfer, the effect of parameters and to develop generalized design correlations for boiling equipment. Perhaps, Nukiyama [100] pioneer work was the first systematic research in this area, in which he boiled distilled water on an electrically heated platinum wire submerged in it at atmospheric pressure. He presented his data in the form of a curve between heat flux and excess temperature i.e. difference between temperature of platinum wire and temperature of liquid. He could not obtain complete boiling curve due to burning out of the wire beyond a certain value of heat flux. He also could not ascribe any reason for this behaviour. Later, Drew and Mueller [44], on the basis of their experimental work, supported the findings of Nukiyama. They conducted experiments by using a temperature controlled heating surface and obtained a complete boiling curve. Thereafter, Insinger and Bliss [70], Westwater & Strangelò [153], Borishanskii et al. [19], and Kutateladze [84], studied it and confirmed its general shape. These investigators have also

identified various regimes in it and governing mechanism to explain high rate of heat transfer associated with the boiling of liquids. As a result, a voluminous literature covering its different facets has been carried out for boiling of liquids to understand its mechanism, to obtain correlations for the design of boiling heat transfer equipment and also to determine the effect of operating parameters such as heat flux, pressure, boiling liquid, heating surface characteristics, etc. on heat transfer coefficient.

The mechanism of heat transfer during nucleate pool boiling has been postulated by various investigators [46, 47, 58, 59, 108, 159]. These models, apart from their diversified nature, provide an insight of heat transfer phenomena occurring during boiling of liquids. In general, nucleate boiling is characterized by the formation of vapor-bubbles at preferred sites which are in the form of cavities, scratches, depressions, projections, etc. distributed randomly on the heating surface. The vapor-bubble grows in size till it attains a maximum size which is controlled by number of forces acting on it and afterward departs from the surface. It travel upwards in liquid pool and ultimately collapses at free surface of liquid. The vapor-bubble leaves a void space, while departing from the surface, which is immediately filled by the nearby cold liquid for the formation of next vapor bubble. This completes the ebullition cycle. In this process, nucleation site density, bubble departure diameter and bubble emission frequency are important parameters.

2.2 BOILING HEAT TRANSFER CORRELATIONS FOR PURE LIQUIDS

A large number of heat transfer correlations are available in literature to predict heat transfer coefficient for nucleate pool boiling of liquids. These correlations are empirical and semi-empirical in nature and are presented in both dimensional and non-dimensional form. In dimensional form, heat transfer coefficient is generally expresses as a function of heat flux and system pressure:

$$h = C q^m p^n \quad (2.1)$$

Where, the values of constant, C and exponent's m and n depend upon heating surface characteristics and boiling liquid.

The general form of non-dimensional equation for boiling heat transfer coefficient is as follows:

$$h = B \text{Re}^{n_1} \text{Pr}^{n_2} \text{Ga}^{n_3} k_p^{n_4} k_t^{n_5} \quad (2.2)$$

where, the value of constant B and exponents of various non-dimensional groups depends upon the system conditions.

An exhaustive literature review for dimensional and non-dimensional correlations for nucleate boiling of pure liquids has been reported recently by Das [42]. Therefore, only some of the important dimensional and non-dimensional correlations are enlisted in **Table 2.1 & 2.4** for quick reference.

Table 2.1 Dimensional correlations of nucleate pool boiling of liquids by various investigators

Investigator	Correlation
Jakob and Linke [72]	$(hd_{b,1}/k_i) = \beta \left[\left(\frac{q}{\rho_v \lambda} \right) \left(\frac{1}{fd_{b,1}} \right) \right]$ For spherical Bubbles where, $d_{b,1}$ bubble departure diameter at 1atm pressure
Jakob [73]	$\frac{h}{k_i} \sqrt{\frac{\sigma}{(\rho_l - \rho_v)g}} = 31.6 \frac{v_{l,a}}{v_l} \left[\frac{\rho_{l,a} \sigma}{\rho_l \sigma_a \rho_{v,a} \lambda_a d_{b,a} f} \frac{q}{\rho_l \sigma_a \rho_{v,a} \lambda_a d_{b,a} f} \right]^{0.8}$
Cryder & Finalborgo [39]	$\log h = a + 2.5 \log \Delta t + bt$ and $\log(h/h_n) = b(t - t_n)$ where, values of constant a and b are listed in Table 2.2
Bonilla & Perry [18]	$\frac{h}{k_i} \sqrt{\frac{\sigma}{\rho_l}} = 16.6 \left(\frac{v_a}{v} \right) \left[\left(\frac{\sigma}{\sigma_a} \right) \left(\frac{\rho_{l,a}}{\rho_l} \right) \left(\frac{q}{\rho_{v,a} \lambda W} \right) \right]^{0.73} \left[\left(\frac{C_p \mu}{k_i} \right) \right]^{0.5}$ where, Jakob constant, $W = 918 \text{ ft/hr}$
Hughmark [65]	$q = 2.67 \times 10^{-7} \left[\frac{(\Delta P)^{1.867} (\rho_l - \rho_v) (C_{pl}) T_s^{1.618}}{(\rho_v)^{1.385} (\mu_l)_w^{1.630} (\lambda)_w^{1.150} (P/P_c)^{0.202}} \right]$
Tien [136]	$q_{ex} = 61.3 \text{ k} (\text{Na})^{0.5} \text{Pr}^{0.33} \Delta T_w$
Mostinskii [93]	$h = A^* q^{0.7} F(P)$; $A^* = 3.596 \times 10^{-5} P_c^{0.69}$; & $F(P) = 1.8P_r^{0.17} + 4P_r^{1.2} + 10P_r^{10}$
Science et al. [116]	$\left[q \sqrt{\sigma / (\rho_l - \rho_v)} \right] / \lambda \mu_l = C \left[\left\{ (C_{pl} \Delta T_w) / \lambda \right\} (T_r / \text{Pr})^{1.18} \right]^n$ where, constant, C and exponent n are given in Table 2.3
Gupta and Varshney [56, 57]	For distilled water $\frac{h}{h_o} = \left(\frac{p}{p_o} \right)^{-0.355} \left(\frac{\lambda}{\lambda_o} \right)^{4.5} \left(\frac{T_{so}}{T_s} \right)^{2.833} \left(\frac{k_{lo}}{k_o} \right)^{0.7} \left(\frac{\rho_l}{\rho_o} \right)^{0.25} \left(\frac{\rho_v}{\rho_{v,o}} \right) \left(\frac{\sigma_o}{\sigma} \right)^{1.25} \left(\frac{C_{plo}}{C_{pl}} \right)^{2.133} \left(\frac{q}{q_o} \right)$ For organic liquids $\frac{h}{h_o} = \left(\frac{p}{p_o} \right)^{-0.194} \left(\frac{\lambda}{\lambda_o} \right)^{4.5} \left(\frac{T_{so}}{T_s} \right)^{2.833} \left(\frac{k_{lo}}{k_i} \right)^{0.7} \left(\frac{\rho_l}{\rho_o} \right)^{0.25} \left(\frac{\rho_v}{\rho_{v,o}} \right) \left(\frac{\sigma_o}{\sigma} \right)^{1.25} \left(\frac{C_{plo}}{C_{pl}} \right)^{2.133} \left(\frac{q}{q_o} \right)$ where, subscript o refers 1 atmosphere condition.
Cooper [36]	$F'(P) = 43000^{(n-0.75)} \left[1.2P_r^{0.27} + (2.5 + \{1/(1-P_r)\})P_r \right]$ where, constant, C is equal to 55, for Cu-plate or stainless steel cylinders and 93.5 for copper cylinders

Table 2.2 Values of constant a and b in Cryder and Finalborgo [39] correlation

Liquids	a	B
Water	-2.05	0.014
Methanol	-2.23	0.015
n-butanol	-4.06	0.014
Carbon tetrachloride	-2.57	0.012
Kerosene	-5.15	0.012
26.3% glycerine solution	-2.65	0.015
10.1% sodium sulphate solution	-2.62	0.016
24.2% sodium chloride solution	-3.61	0.017

Table 2.3 Values of constant C and exponent n in Science et al. [116] correlation

Liquid	C x 10 ⁻⁵	N
Methane	3.25	2.89
Propane	5.77	2.60
n-Butane	2.83	2.80

Table 2.4 Non-dimensional correlations of nucleate pool boiling of liquids various investigators

Investigator	Correlation
Cryder & Gilliland [40]	$Nu^*_B = 0.38(Pr)^{0.425} (\Delta T S^2 d^2 k_t / \mu_l^3)^{2.34} (\mu^2 / (Sd\sigma))^{1.65}$
Insinger and Bliss [70]	$\frac{h\sqrt{\sigma}}{\sqrt{k_L \rho_l^{0.82}}} = 4J^{0.41} g^{-0.09} (10)^{-3.2} \left(\frac{q^{0.68} c_L^{0.5}}{\rho_v^{0.5} \lambda^{0.27}} \right)$
Rohsenow [112]	$(1/St) = C_{sf} Re^{0.33} Pr^s$ s = 1.0 for water, and 1.3 to 1.8 for other liquids where, values of C _{sf} are given in Table 2.5
McNelly [91]	$Nu^*_B = 0.255(qd/\mu\lambda)^{0.69} (Pd/\sigma)^{0.31} (Bu)^{0.33} Pr^{0.69}$
Kruzhilin & Averin [82]	$Nu^*_B = 0.082(Pe_b)^{0.7} (Pr)^{-0.5} (K_t)^{0.377}$
Gilmour [53]	$(h/CG) = 0.001 (Re_b)^{-0.30} (Pr)^{-0.6} (P^2/\rho_l\sigma)^{0.425}$
Labuntsov [85]	$Nu^*_B = 0.125(Pe_b)^{0.65} (Pr)^{-0.32} (k_t)^{0.35}$
Kutateladze [84]	$Nu^*_B = 7.0 \times 10^{-4} (Pe_B)^{0.7} (Pr)^{-0.35} (K_p)^{0.7}$
Minchenko & Firsova [92]	$Nu^*_B = 0.55(K_p Re_b)^{0.7}$
Rice & Calus [111]	$(Nu/K_p^{0.7}) [T_s/T_{sw}]^4 = E Pe_B^{0.7}$; where, values of E are given in Table 2.6
Alam and Varshney [5]	$Nu^*_B = 0.084(Pe_B)^{0.6} (K_{sub})^{-0.5} (K_t)^{0.37}$
Tolubinskii and Kostanchuk [137]	$Nu^*_B = 75 K^{0.7} Pr^{-0.2}$
Gupta and Varshney [57]	$Nu^*_B = 1.391(Pe_b)^{0.7} (\rho_v/\rho_l) (Pr)^{-0.32}$
Cornwell & Houston [37]	$Nu^*_B = A F(P) Re_b^{0.67} Pr^{0.4}$; A = 9.7 P _c ^{0.5} ; where, F(P) = 1.8 P _r ^{0.17} + 4 P _r ^{1.2} + 10 P _r ¹⁰
Borishanskii and Minchenko [cf 84]	$Nu^*_B = 8.7 \times 10^{-4} (Pe_B)^{0.7} (K_p)^{0.7}$

Table 2.5 Values of Rohsenow constant, C_{sf} obtained by Vachon et al. [144] & Piore [104] for various surface-liquid combinations

Liquid -surface combination	C_{sf}
Water on polished copper	0.0128
Water on ground and polished stainless steel	0.0080
Water on mechanically polished stainless steel	0.0132
Water on nickel	0.0060
Water on platinum	0.0130
Water on brass	0.0060
n-Pentane on polished copper	0.0154
n-Pentane on polished nickel	0.0127
n-Pentane on chromium	0.0150
Carbon tetrachloride on polished copper	0.0070
Benzene on chromium	0.0100
Ethyl alcohol on chromium	0.0027
Isopropyl alcohol on copper	0.0025
n-Butyl alcohol on polished copper	0.0030
35% K_2CO_3 on copper	0.0054

Table 2.6 Values of constant E of Rice & Calus [111] correlation

Investigators	Heating surface	$E \times 10^4$
Rice & Calus [111]	Ni-Al wire	6.30
Cichelli & Bonilla [33]	Cu electroplated with Cr	3.92
Borishanskii et al. [19]	Stainless steel	8.90

2.3 BOILING HEAT TRANSFER ON ENHANCED SURFACES

In recent years, development of enhanced heat transfer surfaces used in various thermal processes based on the improved understanding of boiling phenomena on plain surfaces which led to the ideas about modification of certain aspects of the process to increase boiling heat transfer coefficient. It has been well established that nucleate pool boiling heat transfer is depend on characteristics of the boiling surface. This fact encouraged researchers for the development of various methods to enhance boiling heat transfer rate. Accordingly, numerous techniques have been developed to augment boiling heat transfer either by means of external aids, active techniques, or by altering the surface characteristics, passive techniques, as discussed in Chapter-1. A lot of information is now available in literature on different facets of boiling of

liquids from various modified surfaces. A critical review of the literature concerning boiling on such surfaces has been provided in this section.

2.3.1 Boiling on roughened surfaces

Apparently Jacob and Fritz [cf 135] were the first to study the effect of surface finish on nucleate pool boiling heat transfer. They used a sand blasted surface and a machined surface for the boiling of water at atmospheric pressure. They reported that the sand blasted surface increased the boiling heat transfer coefficient up to 4 folds and the machined groove surface about 3 folds higher than that of a smooth chrome plate surface at a fixed heat flux. However their final observation indicated that boiling performance of these surfaces weaken rapidly with time, tending towards the smooth chrome plate's boiling curve.

Berenson [11] obtained significant variation in heat transfer coefficient for boiling of n-pentane on a copper plate, whose surface was roughened using different grades of emery paper. He reported a large enhancement in boiling heat transfer with increased roughness. However, he did not measure the degree of roughness of the surface. Similar results were also observed by Corty and Foust [38], who found that though roughness enhances heat transfer coefficient, but higher roughness has little effect on boiling process. Further, they observed different nucleation site densities for copper and nickel surface for the boiling of similar liquid. In addition, Kurihara and Myers [83] studied the relationship between the boiling site density and the boiling heat transfer coefficient for water and several organic liquids boiling on a surface roughened with emery paper. Their results for five test liquids showed that $h \propto (Na)^{0.43}$. Finally, they also concluded that boiling heat transfer coefficient increases with increase in surface roughness and boiling site density also increased concurrently.

In their experimental investigation, Chaudri and McDougall [26] boiled several organic liquids on copper and steel tubes to measure the long term performance up to 500 hr of standard abrasive treated tubes. The abrasive treatment formed parallel scratches of 0.25 mm or less in width over the

surfaces. They found only temporary benefits of the surface treatment. After several hundred hours the treated tubes showed essentially the same performance as the untreated tubes.

Chowdhury and Winterton [30] carried out experiments using a simple quenching technique with aluminum copper cylinder of 18 mm diameter and 40 mm long immersed in saturated water or methanol. They had given particular emphasis on the role of surface roughness, measured by centre line average (CLA), and surface energy, measured by contact angle, on nucleate boiling heat transfer. Their result showed that copper cylinder quenched in methanol, nucleate boiling heat transfer improved steadily with increased roughness. But for aluminum cylinder that were first roughened and then anodized, when quenched in water, become virtually independent of measured roughness in spite of the fact that anodizing process did not affect the roughness. They explained to this behavior that it is not surface roughness in itself that influences nucleate boiling but the number of active nucleation site. They also reported that low contact angle increases with heat flux at a given superheat.

Luke [88] carried out experiments with propane boiling on copper and mild steel tube to study the effect of surface roughness on heat transfer coefficient. The copper tube of 8 mm diameter was ground with 400 grade emery cloth whereas the mild steel tube of 7.6 mm diameter was sand blasted to get fine or sand blasted surface. The experiments were carried out for a wide range of heat fluxes and saturation pressures (10% to 80% of the critical pressure). The activation of nucleation sites, the bubble departure diameter, d_b , nucleation site density, N_a , and bubble frequency, f were also examined by high speed video technique. He reported that the effect of surface roughness on heat transfer decreases with increasing pressure and with increasing heat flux. He also found that production of densities of active nucleation site using the theoretical model could be improved for high heat fluxes at low pressures by incorporating the additional heat transfer $Q_{\delta V}$ by evaporation into the bubbles sliding along the tube surfaces.

Chun & Kang [31] in an effort to improve the thermal design of passive residual heat removal (PRHR) system of advanced light water reactor (ALWR)

carried out experiment to determine the combined effects of tube diameter, surface roughness and tube orientation on nucleate pool boiling heat transfer. They performed the experiments for boiling of water at atmospheric pressure over four different diameter tubes (9.7, 14.0, 19.06 and 25.4 mm) having roughness 15.1, 26.2 and 60.9 nm and with two different orientation (horizontal and vertical). They reported that increased surface roughness increases heat transfer coefficient for both horizontal and vertical tubes. However, the effect of surface roughness on nucleate boiling heat transfer for vertical tube is more than for horizontal tubes. Also, for a given surface roughness of the tube, the effect of the tube diameter on the nucleate pool boiling heat transfer for vertical tube is more than that for horizontal tubes.

In an experimental investigation, Kang [78] studied the effect of surface roughness and heating tube orientation on heat transfer coefficient for the saturated boiling of water at atmospheric pressure. He took three different diameters (9.7, 19.05 and 25.4 mm) tubes of three different lengths (100, 300 and 530 mm) and two different surface roughness (15.1 and 60.9 nm) to obtain the heat flux (q'') versus wall superheat (ΔT) data for various combinations of test parameters. He also studied the effect of tube orientation. His experimental results reveal that increased surface roughness gives no reasonable change in pool boiling heat transfer for horizontal tubes in high heat flux region. However, its effect magnified as the orientation of tube changed from the horizontal to the vertical. He further concluded that the increase in the ratio of a tube length to its diameter magnified the effect of surface roughness on pool boiling heat transfer for vertically installed tubes.

The author suggested that the net effect of surface roughness on pool boiling heat transfer can be obtained if active nucleation site density, the intensity of liquid agitation, bubble agglomeration on the surface and the formation of a rapid flow around the tube surface is considered.

2.3.2 Boiling on non-metallic coated surfaces

Griffith & Wallis [54] were perhaps the first to report a work on non-metallic coated surface. They recognize that a thin coating of non-metallic

material may improve the nucleation characteristics of the heating surface for the boiling of water. They found that a non-wetting coating on interior walls of cavity enhances its ability as nucleation site. Thus, a lower temperature level will be needed to deactivate the cavity. They observed that this type of coating does not affect the temperature at which a cavity nucleates. They also found that it is easy to maintain boiling and get reproducible results from paraffin cavity than from a clean metal surface and thus concluded those un-wetted cavities are more stable than wetted surface.

Gaertner [52] carried out an extensive work with artificial nucleation sites covering the inside surface of the cavities with a non-wetting material. He boiled water on various surfaces having closely spaced nucleation sites formed by needle sharp punches and parallel scratches. The low surface energy material was coated over the surface containing the artificial sites and then removed from the flat surface by abrasion, leaving a thin film of the material deposited in each cavity. Further, he found that coated surface promotes boiling at lower superheat and remained active for much longer time. In contrast, heat transfer coefficient was considerably reduced when the coating was left on the entire surface.

Young & Hummel [155] boiled water on a spray Teflon coated stainless steel surface having 30-60 spots/m² with each spot of 0.25 mm diameter or less. They found an enhancement in boiling heat transfer with a nucleation occurring at $\Delta T < 0.5$ K. Their results showed that the performance of the pitted surface has been marginally better than the smooth surface when both surfaces have Teflon spots. They argued that it is undesirable to have Teflon coat over the entire surface as vapor formed tend to blanket a large area of the surface and thereby reducing heat transfer coefficient.

In fact, Teflon spotting method, should be effective only for surface-liquid combinations that have high interfacial surface energy, e.g., when the liquid normally wets the surface. Bergles et al. [13] confirmed this in their tests with refrigerants, which have low surface tension and large contact angles, e.g. 40°. Their result showed that the Teflon spotting method did not favorably affect the boiling performance of the refrigerants.

Marto et al. [90] boiled liquid nitrogen on a flat copper heating surface coated with grease and Teflon. The grease coating is found to significantly decrease heat transfer coefficient while Teflon coating show very little effect on heat transfer coefficient.

Vachon et al. [143] carried out experiments for nucleate pool boiling on a stainless steel surface coated with Teflon of 7.6, 30.4 and 35.6 μm using green enamel for boiling of water at atmospheric pressure. Spraying method was adopted for coating. Results indicate a substantial enhancement in heat transfer coefficient for 7.6 μm thick coating. However, heat transfer coefficient decreases for thicker coatings because of their insulating effect. Further, they have also compared their data with Rohsenow [112] correlation. **Table 2.7** lists the values of constant, C_{sf} and exponents, r and s of the correlation as obtained by them for various thicknesses of teflon coated as well as uncoated surface.

Table 2.7 Values of constant, C_{sf} and exponents, r and s of Rohsenow [112] correlation due to Vachon et al. [143]

Liquid-surface combination	C_{sf}	r	S
Water-stainless steel	0.0141	0.25	1.0
Water-7.6 μm teflon coat	0.0071	0.26	1.0
Water-30.4 μm teflon coat	0.0269	0.71	1.0
Water-35.6 μm teflon coat	0.0523	0.87	1.0

Warner et al. [151] investigated the effect of plasma deposited tetrafluoroethylene (TFE) coating over copper surface for the boiling of liquid nitrogen. Their result reveals that heat transfer coefficient of coated surface is five times more than that over an uncoated surface for the same temperature difference. Thicker coating provides higher heat transfer rate as it has many nucleation sites for activating bubbles. It is also found that transition from nucleate to film boiling is much slower for TFE coated surface than that for uncoated one.

Schade & Park [113] carried out similar experiments to obtain the effect of plasma deposited polymer coating on heating surface during nucleate boiling

of Freon-113. They used two copper heating surfaces which were coated by polymethylmethacrylate monomer. They concluded that heat transfer enhancement is not dependent on coating material alone, but surface topography and coating thickness also play important roles.

Hinrichs et al. [61] used plasma deposited polymers on copper heating surface for the boiling of water under atmospheric pressure. Tetrafluoroethylene (TFE) and methane were coated over copper surface by them. Their results showed that an 18 nm thick coating of TFE enhances heat transfer rate while 150 nm thick coating reduces heat transfer rate. The enhancement was explained by surface energy effect. They explained that high interfacial surface energy increases the chemical potential of the liquid in the cavity which reduces wall superheat required for incipience of nucleation. On the basis of above argument and contact angle data for water over TFE and methane coated surface, they showed that 18 nm thick coated heating surface enhances nucleation as observed by the experimental results. However, 15 nm methane coated surface reduces nucleation due to attainment of lower interfacial surface energy and unable to alter the chemical potential of the liquid in cavity enough to enhance the boiling. Further, they also stated that thick coating decreases nucleation due to deactivation of some of boiling sites and concluded that enhanced boiling is a strong function of surface energy.

Vittala et al. [148, 149] conducted experiments for nucleate pool boiling of distilled water on PTFE coated brass heating tubes at atmospheric and subatmospheric pressures. The tube was coated with 21, 39 and 51 μm thickness of PTFE. They found significant enhancement in heat transfer coefficient due to PTFE coating on tube surface. However, enhancement is found to be a function of heat flux, pressure and coating thickness. They also obtained similar results during the boiling of alcohols (ethanol, methanol and isopropanol) on PTFE coated tubes.

Bhaumik [16] carried out experimentation for nucleate pool boiling of distilled water, benzene and toluene at atmospheric and subatmospheric

pressures on plain and PTFE coated stainless steel heating tubes. He used five coating thicknesses, viz. 14, 27, 30, 45 and 50 μm . He observed an enhancement in boiling heat transfer coefficient for 14 μm thick tube at all pressures. However, plain tube outperforms all PTFE coated tube for boiling of benzene and toluene at atmospheric as well as subatmospheric pressures.

2.3.3 Boiling on metal coated surfaces

In an extensive work, Bliss et al. [17] boiled water under atmospheric condition on stainless steel tube coated with copper, zinc, tin, nickel, cadmium & chromium to obtain the effect of plating material on boiling heat transfer coefficient. Thickness of plated material for all specimens in the experiment was about 0.005 inch. They observed that boiling phenomena occurring during boiling on various coated materials is solely because of their thermal properties, and thermal properties of base material has no influence on it. They also found that heat transfer coefficient enhanced by 2 to 3 folds for boiling on copper and chromium plated surfaces whereas reduced for boiling on zinc, nickel, cadmium and tin plated surfaces.

Magrini & Nannei [89] carried out experiments for saturated boiling of water over epoxy-resin rods electroplated with copper, silver, zinc, nickel, and tin at atmospheric pressure. The heating surface was of 10 mm in diameter and 190 mm in length and coating thickness of 5 to 250 μm was varied over it. The average surface roughness was of the order of 0.7 to 1.0 μm . They found that heat transfer coefficient increases with decrease in thickness of coating in case of lower thermal conductivity coating material such as zinc, tin & nickel surfaces. The enhancement was found to be 5 to 7 folds for nickel or tin and one fold for zinc. They further observed that when coating thickness exceeds to a certain limiting value, the influence of coating thickness on the heat transfer coefficient become insignificant. This limiting value was 70 μm for zinc and 15 μm for both nickel & tin. No appreciable effect of coating thickness was observed for higher thermal conductivity material such as copper & silver.

Nishikawa et al. [99] conducted experiments to investigate the effect of particle size and thickness of coating of porous surfaces for boiling of R-11 and

R-113 on an 18 mm diameter horizontal tube. Heating tubes have been coated with sintered spherical shaped copper and bronze particles. The particle size of bronze varied from 0.1 to 1 mm and the porosity from 38 to 71%. They found that particles of 250 μm diameter have shown better performance in comparison to particles of other diameters, viz. 100, 500, 750 and 1000 μm . Further, they observed that for four times of particle diameter that thickness of copper coating, highest heat transfer coefficient has been obtained in the region of $10 < q < 100 \text{ kW/m}^2$. Besides, coating of spherical bronze particles on heating tube shows little effect on boiling heat transfer coefficient. However, coating thickness equal to four times of particle diameter yielded in highest boiling heat transfer coefficient when $q > 50 \text{ kW/m}^2$.

Nishikawa & Ito [98] carried out experiments for boiling of R-11, R-113 and benzene at atmospheric pressure on porous surfaces made of copper and bronze particles. They developed following empirical correlation using their experimental data by regression analysis within a maximum error of $\pm 30\%$:

$$\frac{q\delta}{k_m(T_w - T_s)} = 0.001 \left(\frac{\sigma^2 \lambda}{q^2 \delta^2} \right)^{0.0284} \left(\frac{\delta}{d_p} \right)^{0.88} \left(\frac{q d_p}{\varepsilon \lambda \mu_v} \right)^{0.593} \left(\frac{k_l}{k_m} \right)^{0.708} \left(\frac{\rho_l}{\rho_v} \right)^{0.67} \quad (2.3)$$

where, $k_m = k_l - (1 - \varepsilon)k_p$ and above correlation holds true for:

$$0.1 < d_p < 1 \text{ mm}, 1.6 < (\delta/d_p) < 20, 0.38 < \varepsilon < 0.71 \text{ and } 61 < k_p < 372 \text{ W/mK}.$$

Nakayama et al. [96, 97] investigated heat transfer performance of various structured enhanced surfaces composed of interconnected internal cavities in the form of tunnels and small pores connecting the pool of liquid and the tunnel. They carried out experiments for boiling of water, R-11 and liquid nitrogen at atmospheric pressure on these structured surfaces and found that surface structure having pore diameter of around 0.1 mm is highly efficient in reducing 80-90% reduction of wall superheat required to transfer same heat flux as that on plain surface. They observed that latent heat flux is a significant contributor for enhancement of heat transfer coefficient. They also developed an analytical model on the basis that interconnecting cavities remain in contact with the liquid outside the porous matrix and found it to be in well agreement with experimental data.

Nakayama et al. [95] have investigated the effect of pore diameter of porous structured surfaces and pressure on the saturated boiling of R-11. Pore diameters of 50, 100 and 150 μm and pressures of 0.04, 0.1 and 0.23 MPa were employed. They used various combinations of pore diameter and pressure and observed that if pores of different sizes are present on the surface, the most populous pore govern the rate of heat transfer for heat flux greater than 3-4 W/cm^2 . However, at low values of heat flux, pore of largest size play important role in heat transfer. They postulated that intense bubble formation does not necessarily yield a high rate of heat transfer.

Kajikawa et al. [77] studied heat transfer performances of metal fiber sintered stainless steel tubes for boiling of R-11. Stainless steel fiber was characterized with respect to metal fiber diameter, amount of metal fiber web/area and porosity. Twenty six types of surface configurations were studied with diameter of fiber ranging from 4 to 50 μm , amount of metal fiber web/area ranging from 0.08 to 2.0 kg/m^2 and porosity ranging from 50 to 80%. Their results indicates a ten folds increment in heat transfer coefficient for sintered surfaces in comparison to that on a smooth surface. It was also observed that heat transfer coefficient varies with thickness of porous coating and an optimum value of thickness exists. Besides, they also reported that along with thickness, diameter of fiber used for sintering and porosity also affect heat transfer coefficient significantly.

Danilova and Tikhonov [41] suggested a method for experimental modeling of porous layers with regular screen or fiber metal structures. They modeled these surfaces using several thin layers of wire wound on a tube. Experiments were carried out for boiling of R-113 at atmospheric pressure and for heat fluxes from 7 kW/m^2 to 100 kW/m^2 . They reported that their modeling enabled to find accurate geometrical parameters for porous layers and to estimate their effect on heat transfer performance. It also enabled to measure the temperature field across the height of a layer. They also observed that boiling of R-113 on modeled surface resulted in enhancement of heat transfer for small value of heat flux and thin layers and degradation performance at high value of heat flux and thick layers.

Afgan et al. [1] carried out experiments to obtain heat transfer coefficient for boiling of water, ethanol and R-113 from porous surfaces at atmospheric pressure. Five numbers of heating surfaces were made using sintering of Cr-Ni stainless steel on Cr-Ni, and one Cr-Ni stainless steel surface was sintered with titanium porous layer. Dendrite shaped and spherical 63-100 μm particles were sintered. The porosity and porous layer thickness varied from 30 to 70% and 0.45 to 2.2 mm, respectively. They obtained boiling curves of different shapes depending on the mode of operation namely, bubble mode, transient mode and film formation mode. However, authors did not suggest any criterion for any mode of boiling. In bubble mode, boiling occurs at small temperature difference. At high heat flux, a vapor film appears at the base of the porous layer. Thus, a qualitative change of mechanism of bubble boiling occurs. They found that in relatively thick porous layers, the transition to this new mode of boiling occurs at critical heat flux values 2 to 3 times greater than for smooth surface.

Jung et. al. [75] studied the pool boiling heat transfer of a flat copper surface and two specially prepared metal coated surface (UNB#1, UNB#2) in R-11 with surface orientations varying from horizontally facing upward (0°), to vertical (90°), to horizontally facing downward (180°). A flat 7.8 cm diameter test surface was used. The plain copper surface was prepared by polishing with a coarse emery paper where as the enhanced surfaces were prepared by depositing metal particles on plain mild steel plates. They found that enhanced surfaces (UNB#1 & UNB#2) show 2-3 times higher heat transfer coefficient at constant heat flux as compared to the plain copper surface in the fully developed nucleate boiling regime. For all surfaces investigated, the super heat decreases by 15-25 % as the inclination angle changes from 0° to 165° in the relatively low heat flux range i.e. 10-40 kW/m^2 . Beyond this heat flux range, the super heat remains constant regardless of the surface orientation.

Lu & Chang [87] analyzed the problem of boiling heat transfer from a porous layer sintered on a horizontal heating surface for laminar to turbulent region. They determined the effect of porous layer particle diameter, porosity, pore size distribution and properties of liquid on boiling heat transfer rate. Their analysis was based on Ergun equation for pressure drop in granular beds and

solved for different cases of dry out of the bed. On the basis of this, they found that for thick porous bed, thickness does not affect heat transfer coefficient whereas for thin bed, it plays an important role. Further, they also carried out experiments by boiling methanol over copper heating surface coated with porous matrix and validated their model with their experimental data.

Hongji & Li [62] conducted experiments for pool boiling of water and ethyl alcohol on porous surfaces prepared by sintering spherical bronze powder particles of 16 different sizes over the copper surface at atmospheric pressure. Their result reveals that heat transfer coefficient of prepared surfaces increases by 3 -10 times than that on a plain surface. They have proposed a model based on annular countercurrent two-phase flow in porous surface enabling explanation to enhanced boiling on porous surfaces. Their model can be expressed by the following equations:

For $3 < (\delta/d_p) < 10$

$$Nu = 34.34(Re/We)^{0.5089} (S_r)^{-0.4757} (Pr)^{0.4335} (\delta/d_p)^{-0.6913} (\rho_l/\rho_v)^{0.3427} \quad (2.4a)$$

and for $10 < (\delta/d_p) < 40$

$$Nu = 0.3318 (Re/We)^{0.2253} (S_r)^{0.1309} (Pr)^{1.041} (\delta/d_p)^{-0.7993} (\rho_l/\rho_v)^{0.7583} \quad (2.4b)$$

where, S_r is the superheat ratio criteria which is equal to $(C_{pl} \Delta T)/\lambda$ and (Re/We) is equal to $q\mu_l/(g \lambda \sigma \varepsilon)$.

Shi & Liu [119] carried out experiment for boiling of distilled water and ethanol at atmospheric pressure on an electrically heated stainless steel tube electroplated with various metallic material, viz. copper, zinc, nickel and chromium. The thickness of coating has been varied from 6 to 120 μm . They found that heat transfer coefficient increases with thickness of coating up to critical value and attain a constant value for coating thicknesses beyond critical value. In addition, they also found that boiling characteristics on coated surface remain same as that on the surface made of coating material itself.

Tehvir [130] investigated the effect of aluminum particles coated over aluminum rod of 22 mm diameter by plasma spraying method for the boiling of R-113 and liquid nitrogen at atmospheric pressure. He used eight samples and varied heat flux from low value to burn out condition. Pore diameter, porosity

and porous layer thickness were varied from 6 to 14.2 μm , 26 to 37% and 0.15 to 1.5 mm, respectively. He observed that period of macro layer evaporation extended due to liquid absorbed by porous coating during the contact period with bulk liquid, which in turn delays the boiling crisis.

Tehvir et al. [131] carried out experiments for pool boiling of R-113 at atmospheric pressure on a wide range of porous surfaces to determine relationship between the effectiveness of heat transfer and structural parameters of a plasma sprayed coating. They used 113 different porous surfaces with base material of copper and aluminum plate. The heating surfaces were coated by various combinations of materials such as aluminum-bronze, copper-bronze, copper-copper, aluminum-copper, aluminum-corundum and aluminum-aluminum using plasma spraying technique. The parameters of surface include porous layer thickness from 0.01 to 0.60 mm, porosity from 5 to 61%, and mean pore diameter from 2 to 31.4 μm . They generated data up to burn out heat flux point. They found that porous surface parameters such as porosity, mean pore radius and porous layer thickness of porous coating have profound effect on heat transfer performance and determined optimal values of these three parameters analytically. Further, they remarked that porous coating material of higher thermal conductivity provides higher rate of heat transfer.

Zhang & Zhang [156] investigated boiling heat transfer phenomena of distilled water, ethyl alcohol and R-113 from thin powder porous surfaces with low and moderate heat flux at atmospheric pressure. The heating surface has been prepared by sintering bronze powder over a cylindrical copper block. Particle size of bronze varied from 0.105 mm to 0.392 mm and matrix thickness from 0.94 to 4.6 mm. They developed an analytical model using their own boiling experimental data based on two phase flow and heat transfer in thin porous layers. They proposed following correlation based on their model and found the model to fit experimental data within an error of $\pm 23.5\%$:

$$\text{Nu} = 1.6746 \times 10^{-5} \left(\frac{\text{Fr}}{\text{We}} \right)^{0.4254} \left(\frac{\text{Re}_l \rho_l}{\rho_v} \right)^{-0.6032} \text{We}_1^{1.1605} \text{We}_2^{-0.811} \left(\frac{\delta^2 \epsilon^3}{4d_p^2} \right)^{0.2626} \left(\frac{v_l}{v_v} \right)^{0.2999} \quad (2.5)$$

$$\text{where, } \text{We}_1 = \frac{\sigma}{d_p (\rho_l - \rho_v) g} \quad \text{and} \quad \text{We}_2 = \frac{\sigma}{d_p \rho_l g d_p}$$

Scurlock [117] conducted experiments for saturated boiling of liquid nitrogen, argon and R-12 on enhanced porous surfaces at atmospheric pressure. Heating surfaces were coated with pure aluminum or a mixture of aluminium/10% silicon powder and polyester on to a 5 mm thick aluminum back plates using plasma spraying technique. Coating thickness was varied from 0.13 to 1.32 mm. They observed that heat transfer coefficient enhances up to 10 folds than those for smooth surfaces. However, they pointed out that there is an optimum thickness of plasma sprayed coating for each liquid and selected heat flux in order to achieve maximum heat transfer coefficient. They also studied the effect of fouling by impurities and found that smooth surfaces may show greater degradation in heat transfer performance than porous surfaces.

Chang & You [25] conducted experiments for nucleate pool boiling of FC-72 at atmospheric pressure to examine the effect of various uncoated and coated heating surface orientation on critical heat flux. They used plain, copper particles (1-50 μm) coated, and aluminum particles (1-20 μm) coated surfaces. They found that for microporous surface, incipient boiling superheat gets reduced by 80% and heat transfer coefficient increases by 330% and critical heat flux enhances by 100% as compared to those on plain one. They also observed that the rotation of plain surface from horizontal to vertical orientation improves heat transfer in nucleate boiling regime. However, boiling superheats of micro-porous layer are found to be independent of tube orientation.

Chang & You [23] performed experiments to obtain the effect of coating on boiling heat transfer performance of diamond coated particle surfaces immersed in saturated FC-72. Diamond particles of five different sizes (2, 10, 20, 45 & 70 μm) were used for coating. The thickness of coating was varied from 30 to 250 μm and porosity from 40 to 48%. They used transient thermal boundary layer concept to determine the activation of cavities during nucleation and classified coatings into two groups – microporous, i.e. coating thickness less than 100 μm , and porous, i.e. coating thickness greater than 100 μm . They

observed that heating surface with microporous coating showed dissimilar boiling characteristics as compared to that with porous coating.

In another experimental work, Chang & You [24] determined boiling characteristics of various enhanced surfaces immersed in FC-87 and R-123 at atmospheric pressure. A total of six different types of tube geometries i.e. plain, micro-porous enhanced, integral fin with 709 fins/m, microporous enhanced low fin, Turbo-B and High flux have been studied. They found that microporous (ABM coated) plain tube shows enhancement of heat transfer coefficient of 200-380% for FC-87 and 140-280% for R-123 over the plain one. The increased number of active nucleation sites due to creation of micro-porous structure is basically responsible for the enhancement of heat transfer coefficient. ABM coated low finned tube shows enhancement of heat transfer coefficient of 220-270% for FC-87 whereas High flux surface produced an enhancement of 260-810% for FC-87 and 460-1500% for R-123 as compared to uncoated one. Turbo-B surface has also shown a significant enhancement in boiling heat transfer coefficient.

Hsieh & Weng [64] carried out experiment for saturated boiling of R-34a & R-407c on copper surface, coated with porous aluminum, copper, and molybdenum. Three types of coating technique have been employed, viz. plasma spraying, flame spraying and pitted coatings. Copper & molybdenum were coated by plasma spraying with a coating thickness of 35 μm & 100 μm respectively. Aluminum & zinc were coated by flame spraying with a coating thickness of 50-300 μm of aluminum and 150 μm of zinc. Four different numbers of meshes of the pitted particles were treated with pitted coating using a sand blasting technique. The coating thicknesses obtained by pitted coatings are 18, 30, 31 & 32 μm , respectively for the four different numbers of meshes of the pitted particles. They observed that at $q > 10 \text{ kW/m}^2$, the R-34a has better heat transfer performance than that of the corresponding coated surface in R-407c. They also reported that pitted coating surfaces give the best performance over a range of heat flux in R-134a, while the plasma spraying

surface performs well in R-407c. The authors also correlated their experimental data for plasma and flame spray coating surfaces by the following equation:

$$Ja = 0.137(Re)^{0.292} (d_o/\delta)^{-0.190} [N_{cf}]^{0.065} \quad (2.6)$$

where, $N_{cf} \left(= \frac{\mu_l^2}{d_o \rho_l \sigma} \right)$ is constant heat flux number, and the above equation

hold true for:

$$6.909 \times 10^{-3} \leq Re \leq 1.899 \times 10^{-1}; \quad 6.667 \times 10^{-3} \leq (d_o/\delta) \leq 1.667 \times 10^{-1}$$

$$\text{and} \quad 7.773 \times 10^{-3} \leq N_{cf} \leq 4.787 \times 10^{-2}$$

Zhou & Bier [158] carried out experiment to study the pool boiling heat transfer from a horizontal copper tube coated with 0.2 mm of Aluminum-oxide-titanium oxides ceramics with four refrigerants i.e. R-12, R-113, R-114 and R-134a and three hydrocarbons i.e. propane, n-butane & n-pentane. The heat transfer coefficient shows a similar dependence on heat flux and normalized saturation pressure as with a metallic heating tube. For hydrocarbons, the absolute value of the heat transfer coefficient are just as high as for a sand blast copper tube of similar surface roughness at normalized saturation pressure $p/p_c \geq 0.1$ and at lower saturation pressures even higher. The negative influence of the low thermal conductivity of the ceramics is completely compensated or even over compensated by the positive influence of the microstructure, which results in a higher nucleation site density. This is especially effective in pool boiling of mixture

Chien & Webb [29] investigated boiling characteristics of R-123 over five different structured enhanced surfaces at atmospheric pressure. They observed that bubble growth mechanism on enhanced surfaces is different from that on plain surface. According to them, a significant fraction of vaporization occurs at menisci in the corner of the tunnels which control bubble frequency and nucleation site density. Further, evaporation and bubble growth occurs after the bubble emerges from the surface pores. Smaller bubbles are generated on the enhanced surfaces at a greater frequency as compared to

those on plain surface for the same heat flux condition. The enhanced surface has greater nucleation site density than that on plain surface.

Rainey and You [107] conducted experiments to obtain the effect of heater orientation and size on the pool boiling performance of plain and microporous coated surfaces immersed in saturated FC-72. They used flush mounted 2 cm x 2 cm and 5 cm x 5 cm copper surfaces and compare their performance with the previous result of Chang and You [25] who studied a 1 cm x 1 cm surface. They observed that the boiling performance of plain surface increased slightly from 0° to 45° and decreased from 90° to 180° . In addition, larger surfaces exhibited diminished enhancement from 0° to 45° in the lower heat flux region and increased enhancement from 0° to 45° in the higher heat flux region. Unlike plain surfaces, the boiling performance of microporous enhanced surfaces was insensitive to both inclination angle and heater size due to the higher number of active nucleation sites. Further, the plain and microporous coated surfaces exhibited similar CHF behavior with respect to heater size.

In an experimental work, Kim et al. [79] studied nucleate pool boiling heat transfer mechanism of microporous surface immersed in saturated FC-72 at atmospheric pressure. They used consecutive photo method for measurement of bubble size, frequency and vapor flow rate from a plain and microporous coated 390 μm diameter platinum wire to determine the effect of the coating on the convective and latent heat transfer mechanisms. They concluded that microporous coating augments nucleate boiling performance through increased latent heat transfer in the low heat flux region and through increased convection heat transfer in the high heat flux region. In addition, the higher active nucleation site density of microporous coating reduces bubble diameters and increases bubble frequency. Further, the CHF for the microporous coated surface is significantly enhanced over the plain surface due to decreased latent heat transfer and/or increased hydrodynamic stability from increased vapor inertia.

Cieslinski [34] carried out experiments for saturated boiling of distilled water on electrically heated stainless steel tubes of various diameters and flat horizontal plates at atmospheric pressure. Various materials, viz. aluminum, copper, molybdenum, zinc, brass and stainless steel particles were used to form coatings. A variety of deposition techniques such as dispersive electrolytic treatment, plasma spraying, gas flame spraying and modified gas flame spraying were used to coat flat horizontal surfaces and on stainless steel tubes. The parameters such as surface roughness were varied from 0.3 to 4 μm , coating thickness from 0.08 to 2 mm, porosity from 10 to 65% and mean pore radius from 1.11 to 10.5 μm . They found that boiling commences at lower wall superheat for all coated surfaces as compared to that on a smooth surface but the rate of enhancement decreases with the increase in heat flux. Further, aluminum deposited heating surface has shown superiority over other material coated surfaces in promoting nucleate boiling. However, the porosity and coating thickness of porous surface influences the boiling phenomenon irrespective of deposition technique used in the investigation. Burnout heat flux has been found essentially to be independent of surface finish.

Vasiliev et al. [146] performed experiments for saturated boiling of propane on single horizontal stainless steel pipes with smooth and porous surfaces. They also studied the loop heat pipe evaporator wick structure made from aluminum oxide ceramic with heat generation inside the wick. The coating on stainless steel pipes were applied by the method of gas thermal spraying. They varied heat flux densities from 0.1 to 100 kW/m^2 , saturation pressure from 3.45 to 13.8 bar, thickness of coating from 0.1 to 0.3 mm and thereby porosity from 4 to 17%. They found that porous surface enhances heat transfer coefficient up to 3 to 5 folds in the region of low heat flux and up to 2.3 to 3 folds in the region of high heat flux. They also observed that increase in porosity enhances heat transfer coefficient. Further, at the same porosity, heat transfer coefficient of porous surface having coating thickness 0.2 mm is lower than that for with coating thickness of 0.1 and 0.3 mm.

In their experimental work Vemuri & Kim [147] studied pool boiling heat transfer from nano-porous surface immersed in saturated FC-72 at atmospheric pressure. They used a plain reference heating surface made of aluminum of thickness about 105 μm and a plain surface attached with nano-porous coating of aluminum oxide of thickness about 70 μm . The nano-porous coating has been attached to the plain surface using Omega bond 200 high thermal conductivity epoxy (thermal conductivity $\approx 1.4 \text{ W/m-K}$). They have taken SEM photographs of the nano-porous coating and found that diameter of pores were lies in the range of 50 to 250 nm. They reported that the incipient superheat for the nano-porous coated surface has been reduced by 30% as compared to that of a plain surface.

Das [42] conducted experiments for the pool boiling of saturated liquids viz. distilled water, methanol and isopropanol on copper heating tubes coated with various thicknesses of copper by wire flame spraying technique. He used four coating thicknesses namely, 29, 63, 85 & 118 μm . He observed that application of copper coating on an uncoated surface result an enhancement in the value of heat transfer coefficient.

Recently, Prasad et al. [105] carried out experiments for the boiling of saturated methanol on uncoated as well as five copper coated mild steel heating tubes at atmospheric and subatmospheric pressures. Heat flux was progressively increased from 1.6 to 4.3 kW/m^2 in six steps and pressure from 23.02 to 98.68 kN/m^2 in five steps. They studied the boiling characteristics on coated surfaces and compared with those on uncoated ones. Later, Alam et al. [4] conducted experiments for the boiling of saturated water on the same surfaces with identical operating condition to obtain generalized conclusions. Both the studies finally concluded that heat transfer coefficient enhances with application of copper coating. In fact, it increases with increase in coating thickness. Further, at a given pressure, it was found that heat transfer coefficient is maximum for 26 μm copper coated tube both for methanol and distilled water.

Table 2.8 Summary of important investigations related to boiling of liquids on non-wetting surfaces

Investigator(s)	Substrate material	Coating materials	Coating thickness	Test fluid	Pressure (atm)
Bliss et al.[17]	Stainless Steel	Copper, Tin, Zinc, Nickel, Cadmium and Chromium	127 μ m	Water	1
Magrini & Nannei [89]	Epoxy resin	Copper, Tin, Zinc& Nickel	5 to 250 μ m	Water	1
Afgan et al. [1]	Chromium; Nickel Stainless Steel	Titanium & Cr-Ni	63 to 100 μ m	Water, Ethyl alcohol & R-113	1
Scurlock [117]	Aluminum	Pure Al & Al/Silica (10%)	0.13 to 1.32 mm	Liq. Nitrogen, Argon, Oxygen, & R-12	1
Zhang & Zhang [156]	Copper	Bronze powder	0.94 to 4.60mm	Distilled water, Ethyl alcohol & R-113	1
Chang & You [23]	Copper	Diamond particles	30 to 250 μ m	FC-72	1
Cieslinski [34]	Stainless steel	Cu, Al, Mo, Zn, Brass	0.08 to 2.0mm	Distilled water	1
Rainy & You [107]	Copper	DOM	50 μ m	FC-72	1
Kim et al. [79]	Platinum wire	DOM	35 μ m	FC-72	1
Vemuri & Kim [147]	Aluminum	Aluminum oxide	70 μ m	FC-72	1

2.4 BOILING HEAT TRANSFER CORRELATIONS FOR MIXTURES

Perhaps, Cryder & Finalborgo [39] were the first who started investigation in the area of nucleate pool boiling of binary liquid mixture. In their effort to generate experimental data, they carried out experimentation for boiling of pure as well as binary mixtures at atmospheric and subatmospheric pressures. The binary mixtures were 26 wt% glycerol, 10 wt% sodium sulfate

and 24 wt% sodium chloride in water. The saturation temperature of water-glycerol ranged from 68.88 °C to 113.3 °C and heat flux from 8141 W/m² to 41,868 W/m².

Bonilla & Perry [18] boiled six binary mixtures of water-ethanol, water-acetone, water-butanol, ethanol-butanol, ethanol-acetone, and butanol-acetone with a wide range of compositions. A horizontal chromium plate surface was used as a heating surface. In some of their mixtures, they found that maximum heat flux in nucleate boiling exceeded slightly to that of either of pure components. However, no systematic study about the effects of concentration was made and the increase of maximum heat flux mentioned by them was very moderate. Further, they found that the plating of copper/gold on copper surface results in higher heat transfer coefficient than that on aged surface.

Cichelli & Bonilla [33] investigated the effect of chromium coating on copper surface for boiling of water, ethanol, benzene, propane, n-heptane, n-pentane and their mixtures. A thickness of 0.002 inch of chromium was obtained by electroplating technique. They varied pressure from 4 to 32 bars and heat flux from 2.9075 to 5.8150 kW/m². They proposed a correlation as function of heat flux and pressure for calculation of heat transfer coefficient. The noteworthy point about the correlation was that it does not contain any concentration terms. The correlation is as follows:

$$h = 0.232 \times q^{0.7} P^{0.53} \quad (2.7)$$

Chernobylskii & Lukach [28] determined the heat transfer coefficient for boiling of two binary mixtures, benzene-toluene and ethanol-water for various compositions. In their experimentation, they varied heat flux from 18.61 to 151.20 kW/m² at atmospheric pressure. They expressed their results in the conventional power law form i.e. $h = Cq^n$. The values of C and n vary with concentration of the more volatile component in the mixture.

In an experimental work, Sternling & Tichacek [125], determine the heat transfer coefficient for boiling of various non-azeotropic and azeotropic binary mixtures at atmospheric pressure. They used a thin stainless steel tube of diameter 4.51 mm for the experiments. They found that heat transfer coefficient for all the binary mixtures, at a given heat flux, decreased noticeably with the

addition of more volatile component up to a specific composition and thereafter started increasing. This behavior has been attributed to the change in bubble dynamics with the addition of more volatile component in a pure liquid.

Perhaps, Palen & Small [101] were the first to propose a correlation for estimation of heat transfer coefficient for binary mixtures. The proposed correlation is as follows:

$$(h/h_{id}) = \exp[-0.027(T_{bo} - T_{bi})] \quad (2.8)$$

They determined the ideal heat transfer coefficient using the McNelly [91] correlation for pure liquids using average physico-thermal properties:

$$h_{id} = 0.225 \left(\frac{k_l}{d_b} \right) \left(\frac{d_b q}{\lambda \mu_l} \right)^{0.69} \left(\frac{Pd_b}{\sigma} \right)^{0.31} \left(\frac{\rho_l}{\rho_v} - 1 \right)^{0.33} \left(\frac{C_{pl} \mu_l}{k_l} \right)^{0.69} \quad (2.9)$$

The term $(T_{bo} - T_{bi})$ is the temperature difference between the vapor leaving and liquid feed to a kettle reboiler and is equal to the boiling range i.e. the temperature difference between the dew point and the bubble point at the liquid feed composition if all the feed is evaporated.

Tolubinskii & Ostrovskii [138] carried out an investigation to measure the vapor bubble growth rate in pool boiling of ethanol-water and ethanol-butanol mixtures at atmospheric pressure. They reported that the vapor bubble growth decreased with increase in the difference of concentrations of more volatile component in vapor and liquid phases. The correlation proposed by them for the experimental values of Nusselt number for the ethanol-water mixture is as follows:

$$Nu_B = 75Kq^{0.7} Pr^{-0.2} [1 - (y - x)]^{1.85} \quad (2.10)$$

where the values of K depends on the individual components of the mixture

Afgan [2] conducted experiments for the boiling ethanol, benzene and various compositions of their mixtures on a cylindrical tube of diameter 5.12 mm heated by direct-current. The pressure varied from 6 atm to 15 atm. He proposed following correlation for pure liquids:

$$Nu = 9.44 \times 10^{-4} Re^{0.7} Kp^{0.7} Pr^{0.35} \quad (2.11)$$

where, Kp is the criterion for the pressure term, and the bubble departure diameter in the above equation is that of Fritz [48].

Further, he found that plots between heat transfer coefficient and concentration, at a constant heat flux, showed maxima and minima which corresponded to minima and maxima of the absolute values of the differences of equilibrium concentration, $(y - x)$. On the basis of this observation, he included a multiplier which depends on $(y - x)$ in above equation to correlated mixture data. The multiplier suggested by him for boiling of a mixture was $[1 - K(y - x)]$, where the value of K depends on the individual components of the mixture.

Ivanov [71] studied the boiling heat transfer of refrigerant mixtures of F-12 and F-22 for heat fluxes varying from 2 to 25 kW/m² and temperature from 240 K to 293 K. The experimental data showed a minimum value of heat transfer coefficient between 15 to 55 percent concentration of less volatile component, F-22. He employed the method of corresponding state which was suggested by Borishanskii [20] for boiling of liquids in their pure state. He recommended following equation for computation of heat transfer coefficient:

$$\left[\frac{(h/q)^{0.75}}{(h^*/q^*)^{0.75}} \right] = f(P/P^*) \quad (2.12)$$

Where $P^* = 0.03 P_c^{Ps}$ and P_c^{Ps} is the pseudo critical pressure of the mixture.

Tolubinskii & Ostrovskii [140] conducted experiments to study the mechanism of heat transfer in nucleate pool boiling of binary mixtures. They generated data for heat transfer coefficients, bubble departure diameters and bubble frequency for boiling of methanol-water, ethanol-water, ethanol-n-butanol and ethanol-benzene on a stainless steel tube of diameter 4.5 mm heated by direct-current. They found that nucleation site density for the boiling of mixtures is different as compared to that for boiling of pure liquids. In addition, it was also found that at a given heat flux, h , d_b and the product fd_b attain minima when $(y - x)$ is at its maxima.

Further, they recommended following equation for experimental data of ethanol-water over the entire range of concentration by dimensional analysis:

$$(fd_b)_m = [(fd_b)_{\text{water}} (1 - x) + (fd_b)_{\text{ethanol}} x] \left[1 - \frac{(y^* - x)^2}{y^* - (1 - x)} \right]^{1.15} \quad (2.13)$$

$$Nu = \left\{ \frac{q}{\lambda P_v [(fd_b)_{\text{water}} (1-x) + (fd_b)_{\text{ethanol}} x]} \right\}^{0.7} \left\{ \frac{C_l \mu_l}{k_l} \right\}^{-0.2} \left[1 - \frac{(y^* - x)^2}{y^* - (1-x)} \right]^{-1.6} \quad (2.14)$$

Above equations requires prior determination of fd_b factor even for ethanol-water mixtures, so are not of general use for all mixtures

Filatkin [45] studied the pool boiling heat transfer of water-ammonia solution on a horizontal tube 28 mm diameter and 450 mm length. He observed that the solution with an ammonia concentration of approximately 0.4 has the minimum heat transfer coefficient. One of the reasons attributed to this reduction in heat transfer coefficient is that as the concentration difference between the vapor and liquid phase i.e. $(y-x)$ increases the number of nucleation sites decrease and so the heat transfer coefficient. Further, he proposed the following correlation:

$$\frac{h}{k} \sqrt{\frac{\sigma}{(\rho_l - \rho_v)}} = D \left(\frac{\alpha}{v} \right)^{0.45} \left[\frac{C_l \sigma^{0.5} T_s \rho_l (\rho_l - \rho_v)^{0.5}}{J(\lambda \rho_v)^2} \right]^{0.33} \left[\frac{J \rho_v \lambda q}{T_s k (\rho_l - \rho_v)} \right]^n \quad (2.15)$$

The equation is applicable for the following conditions:

- (i) $Pr = 1.3$ to 4.8 (ii) $\frac{J \rho_v \lambda q}{T_s k (\rho_l - \rho_v)} = 0.3$ to 40.4
- (iii) $\frac{C_l \sigma^{0.5} T_s \rho_l (\rho_l - \rho_v)^{0.5}}{J(\lambda \rho_v)^2} = 1.0 \times 10^{-4}$ to 206.0×10^{-4}

The values of n and D are calculated by the following equations:

$$n = 0.70 - 0.24 (y - x) \quad (2.16)$$

$$D = 0.083 + 0.33 (y - x) \quad (2.17)$$

Finally he concluded that the effect of Prandtl number on heat transfer coefficient is less noticeable and pressure appears to increase the system heat transfer coefficient at low rate.

In an extensive work, Stephan & Körner [121] proposed another empirical correlation for calculating heat transfer coefficients. They carried out experimentation for various binary mixtures for pressures ranging from 1 to 10 bar. On analysis of their data they observed that calculated value of the ideal heat transfer coefficient, interpolated values of pure component heat

transfer coefficients, is less than that of actual value by an amount proportional to $(y - x)$. The proposed correlation is given below:

$$\frac{\Delta T_{\text{sat},W}}{\Delta T_{\text{sat},W,\text{ideal}}} = 1 + \theta \quad (2.18)$$

$$\text{Where, } \Delta T_{\text{sat},W,\text{ideal}} = X_{\infty} \Delta T_{\text{sat},W,A} + (1 - X_{\infty}) \Delta T_{\text{sat},W,B} \quad (2.19)$$

$$\Delta T_{\text{sat},W,\text{ideal}} = X_{\infty} + (L - X_{\infty})$$

$\Delta T_{\text{sat},W,A}$ and $\Delta T_{\text{sat},W,B}$ are wall superheats for boiling of pure components on the same surface and at the same heat flux as the mixture in consideration. $\Delta T_{\text{sat},W,A}$ is actual wall superheat for the mixture and θ represents the deviation from the ideal situation due to mass transfer resistance and is defined as:

$$\theta = A(y^* - x) \quad (2.20)$$

where A is a function of pressure and is different for every binary mixture.

$$A = A_0(0.88 + 0.12P) \quad (2.21)$$

Pressure, P in above equation is in bar and A_0 is a constant which depends only on the nature of the two components and is independent of concentration. Further, they provided the calculated values of A_0 for various binary mixtures in the same investigation. The generalized value of A_0 , as reported by them is equal to 1.53.

Tolubinskii & Ostrovskii [141] undertook an investigation to understand the heat transfer mechanism to saturated boiling water-glycerin mixtures at atmospheric pressure. The glycerin concentration was taken up to 96 wt. percent. They observed that with increasing glycerin concentration up to 70 wt. percent the bubble departure diameter increased slightly and bubble emission frequency reduced, but for that of greater than 70 wt. percent, both the bubble departure diameter and frequency reduced rapidly.

Contrary to low-boiling liquids, they also observed in this case that the value of heat transfer coefficient reduces continuously with increase in glycerin concentration and no intermediate minima has been observed even up to 96 wt. percent of glycerin.

Takeda et al. [129] carried out experiments for boiling of pure water, methanol, ethanol, MEK, acetone and their mixtures on a copper surface and a

thin platinum wire. They proposed a general correlation both for pure liquids and mixtures by dimensional analysis, which is given below:

$$\left(\frac{\rho_v \lambda}{C_l \rho_l \Delta T_{\text{sat}}} \right) \left(\frac{C_l \mu_l}{k_l} \right)^{0.67} = 1.0 \times 10^{-2} \left(\frac{d_b q \rho_l}{\mu_l \lambda \rho_v} \right)^{-0.35} \left(\frac{P^2}{g \sigma \rho_l} \right)^{0.25}$$

$$\text{or } \text{St.Pr}^{0.67} = 1.0 \times 10^{-2} \text{Re}^{-0.35} \Pi^{0.25} \quad (2.22)$$

Wright et al. [154] studied nucleate and film boiling behavior of pure ethane, ethylene and their mixtures containing 0.25, 0.50 and 0.75 mole fraction of ethylene. They carried out experiments on a gold-plated tube of diameter 20.6 mm and length 89 mm, which was heated by direct current power source at atmospheric and subatmospheric pressures. The data were compared with the correlations of Borishanskii et al. [19], Kutateladze [84] and McNelly [91] and found large deviation. Therefore, they developed following correlation, which fitted their data by modifying the Rohsenow correlation:

$$\frac{q d_b}{\lambda \mu_l} = 683.3 \left[\frac{C_l \Delta T}{\lambda} \left(\frac{T_r}{P_r} \right)^{1.18} \right]^{1.243} \quad (2.23)$$

Clements & Colver [35] extended work of Wright et al. [154] for saturated boiling of propane, n-butane and n-pentane and their mixtures on the same test section with extended range of pressure up to $3 \times 10^6 \text{ N/m}^2$. In their plot of experimental data between wall superheat and concentration for each heat flux, they observed that the position of the maxima is nearly coinciding with maximum of $(y-x)$, which implies that the value of heat transfer coefficient is minimum at maximum $(y-x)$. They also compared their data with the correlations of Borishanskii et al. [19], Kutateladze [84] and McNelly [91]. These correlations have been found to suitable for pure liquids data but showed large discrepancy with binary mixtures data. Therefore, to correlate the data for binary mixtures, they modified above correlations by introducing a factor, $\alpha_\infty^{-0.5}$ in terms of relative volatility, α_∞ into each of the basic correlation. This factor takes into account the mass transfer resistance effects. The modified correlations are as follows:

Modified Borishanskii et al. correlation:

$$\frac{qd_b}{k\Delta T_w} = 8.7 \times 10^{-4} \alpha_\infty^{-0.5} \left[\frac{qd_b}{\alpha \rho_v \lambda} \right]^{0.7} \left[\frac{Pd_b}{\sigma} \right]^{0.7} \quad (2.24)$$

Modified Kutateladze correlation:

$$\frac{qd_b}{k\Delta T_w} = 7.0 \times 10^{-4} \alpha_\infty^{-0.5} \left[\frac{qd_b}{\alpha \rho_v \lambda} \right]^{0.7} \left[\frac{Pd_b}{\sigma} \right]^{0.7} \left[\frac{C_l \mu_l}{k_l} \right]^{-0.35} \quad (2.25)$$

Modified McNelly correlation:

$$\frac{qd_b}{k\Delta T_w} = 0.255 \alpha_\infty^{-0.5} \left[\frac{qd_b}{\lambda \mu_l} \right]^{0.69} \left[\frac{Pd_b}{\sigma} \right]^{0.31} \left[\frac{\rho_l}{\rho_v} - 1 \right]^{0.33} \left[\frac{C_l \mu_l}{k_l} \right]^{0.69} \quad (2.26)$$

where d is a characteristic dimension of heating surface.

They finally concluded that the modified forms of the Kutateladze [84] & McNelly [91] correlations predict the data for mixtures as accurate as the original equations predict for pure liquids.

Calus & Rice [22] carried out a comprehensive investigation for pool boiling of water, isopropanol, acetone and their binary mixtures on nickel-aluminum-alloy wires of 0.315 mm diameter and 89 mm length (72.6 mm length for acetone-water mixtures), heated by direct current. They proposed a correlation for binary liquid mixtures that included the heat and mass transfer term $1 + (y^* - x)(\alpha/D)^{0.5}$ in the Borishanskii et al. [19] correlation modified earlier by Rice & Calus [111] for pure liquids. The proposed correlation is given below:

$$\left[\frac{Nu}{(K_p)^{0.7}} \right] \left[\frac{T_s}{T_{sw}} \right]^4 = E \left[\frac{Pe}{1 + (y^* - x)(\alpha/D)^{0.5}} \right]^{0.7} \quad (2.27)$$

The constant, E in above equation depends upon surface and liquid under consideration. They determined the values of E for their experimental data for pure as well binary mixtures and those for Sternling & Tichacek [125] data for aqueous solutions of glycol and glycerol. The values of E are given in

Table 2.9:

Table 2.9 Values of constant E of Calus and Rice [22] correlation

System	Heat transfer Surface	E
Isopropanol-Water	Nickel-aluminum alloy, Wire 200 [22]	5.8×10^{-4}
Acetone-Water	Nickel-aluminum alloy, Wire 24 [22]	4.7×10^{-4}
Water-Glycerol	Stainless steel hypodermic tubing [125]	12.2×10^{-4}
Water-Glycol	Stainless steel hypodermic tubing [125]	11.4×10^{-4}
Seven pure liquids	Nickel-aluminum alloy [111]	6.3×10^{-4}

Tolubinskii et al. [137] studied the effect of pressure on the boiling heat transfer rate in water-ethanol mixtures, at pressures up to 15 bars and over the entire range of concentrations. The mixture under study was boiled in a vertical test element consisting of a stainless steel tube heated by direct current. The heat flux density, q at the heated section was varied from 0.5×10^4 to 0.8×10^6 W/m². They observed that boiling of water-ethanol mixtures at elevated pressures involves the same mechanism as boiling at atmospheric pressure i.e. reduction in the heat transfer rate in the range of maximum excess concentration $(y^* - x)$ of the more volatile component as a result of simultaneous reduction in the rate of growth of vapor bubbles and in the number of effective nucleation sites as compared with pure components. Consequently, the boiling of binary mixtures at elevated pressures involves the same regularities as at atmospheric pressure. This made it possible to use an empirical expression for the boiling heat transfer coefficient for mixtures at atmospheric pressure by supplementing it by a term which provides allowance for the pressure:

$$h_{\text{mix}} = \{[A_{h,b}(1-x') + A_{l,b}x'] - (A_{h,b}/A_{l,b})\} \Delta x^{0.7} P^n q^{0.7} \quad (2.28)$$

where for the water-ethanol mixtures under consideration, $A_{h,b} = 3.05 \times P^{0.2}$, $A_{l,b} = 1.5 \times P^{0.4}$, $n = 0.4$. The above correlation fitted their experimental data within ± 20 percent.

Calus & Leonidopoulos [21], in an attempt to modify the correlations of Calus & Rice [22] and Stephan & Körner [121], carried out an extensive study for pool boiling of n-propanol, water and their eleven mixtures at atmospheric pressure. The main purpose of this work was to modify the constant A of

Stephan & Körner [121] correlation. Stephan and Körner have stated that the value of A can be regarded as constant for the entire range of concentrations in the case of mixtures having a vapor-liquid equilibrium relationship approaching ideal behavior. But it is observed and also indicated by Stephan & Körner themselves that to treat A as a constant is a major approximation for the binary-mixtures behaving as highly non-ideal. Thus, Calus & Leonidopoulos [21], attempted to replace the constant A in terms of the vapor-liquid equilibrium relationship, the transport properties and the thermodynamic properties of the binary mixture. The correlation proposed by them for ideal and non-ideal mixtures finally emerges in the following form:

$$\Delta T = (\Delta T_1 x_1 + \Delta T_2 x_2) \left[1 + (y^* - x) \left(\frac{\alpha}{D} \right)^{0.5} \left(\frac{C_1}{\lambda} \right) \left(\frac{dT}{dx} \right) \right] \quad (2.29)$$

where ΔT , ΔT_1 and ΔT_2 are the differences between wall superheat and saturation temperature i.e. $(T_{\text{wall}} - T_{\text{sat}})$ for the mixture of concentration x , and for the pure components 1 and 2, respectively, required for obtaining the same heat flux. All the quantities in above equation are based on the weight fraction concentrations.

Happel & Stephan [60] conducted experiments to study the boiling phenomena occurring during boiling of binary mixtures in both the nucleate and film boiling regimes. Here only the work related to nucleate boiling is discussed. He obtained boiling heat transfer coefficient for mixtures of benzene-toluene, ethanol-benzene and water-isobutanol in a pressure range of 0.5-2 bar as well as with refrigerants in a pressure range of 0.5-30 bar. The test surface was a nickel tube of 14 mm outside diameter with 0.43 μm integrated roughness. Provision was made to heat the tube both by the electricity and passing a hot stabilized fluid through the tube.

During the discussion of the mechanism of nucleate pool boiling in binary liquid mixtures, he also reaffirmed the occurrence of mass transfer along with heat transfer. Thus, heat transfer coefficient for the mixture is reduced due to additional diffusion resistance. He concluded that larger the concentration difference $(y - x)$, stronger is the reduction in heat transfer coefficient. They

developed following correlation, to account the reduction of heat transfer as compared with that for pure substances

$$(h_{\text{eff}}/h_{\text{id}}) = 1 - K_{\text{st}}(y - x)^n \quad (2.30)$$

where, h_{eff} is the effective heat transfer coefficient and h_{id} is defined as:

$$h_{\text{id}} = h_1(1 - x) + h_2x \quad (2.31)$$

Thus, h_{id} is obtainable from the knowledge of heat transfer coefficient of the pure components h_1 and h_2 . The constant, K_{st} depends upon system pressure and boiling mixture. At a given pressure, the values of K_{st} and index n can be determined by experiments at only two different mixture compositions. They reported that the value K_{st} and n is equal to 1.5 and 1.4, respectively, for benzene-toluene system at atmospheric pressure.

Thome & Bold [133] have studied the nucleate pool boiling for cryogenic binary mixtures. They obtained the pool boiling curves for liquid nitrogen, argon and their mixtures at 1 atm and 1.3 atm pressures. They observed a minimum heat flux in the mixtures and compared their results with the existing correlations of Happpel & Stephan [60] and Calus & Leonidopoulos [21] but none of these is found to correlate their experimental data satisfactory.

In their experimental work, Stephan & Preusser [122] studied heat transfer in nucleate boiling for various compositions of binary and ternary mixtures of acetone, methanol and water. They used a horizontal Nickel tube of 14 mm O.D., 550 mm length and a mean roughness of about 0.25 μm . They observed a reduction in heat transfer for the boiling of mixtures as compared to that for pure substances. Further, in order to explain this effect they argued that the more readily evaporation of the volatile fraction in binary mixtures which creates a concentration difference between the liquid and the vapor bubble, and building up a diffusion resistance in addition to the thermal resistance. In binary mixtures, the reduction in heat transfer coefficients depends on the difference in the mole fractions between both phases. It increases with the difference in mole fractions and vanishes at azeotropic points.

Stephan & Preusser [123, 124], in these two investigation attempted to calculate the boiling heat transfer coefficient of ternary mixtures from the data

of pure components and binary mixtures. They conducted experiments with two ternary mixtures of organic components and of binary mixtures at atmospheric pressure boiling on a horizontal nickel tube. They have recommended that for rough estimation, the heat transfer coefficient in the boiling of ternary mixtures can be calculated from the data of corresponding binary mixtures with the expanded formulation of the correlation of Stephan & Körner [121] for binary mixtures. Further, an equation is derived for heat transfer coefficient in the boiling of mixtures, in which the nonlinear variation of the material properties has been taken into account.

Stephan & Abdelsalam [120] attempted to present guidelines for predicting heat transfer coefficients in natural convection boiling. In order to establish correlations with wide application, the methods of regression analysis were applied to nearly 5000 existing experimental data points for natural convection boiling heat transfer. As demonstrated by the analysis, these data can be represented by subdividing the substances into four groups depending upon their physico-thermal properties. The four groups were water, hydrocarbons, cryogenic fluids and refrigerants. Each set of group employed a different set of dimensionless numbers to correlate the data for the calculation of approximate value of heat transfer coefficient.

Jungnickel et al. [76] experimentally determined heat transfer during nucleate pool boiling for the mixtures R-12/R-113, R-22/R-12, R-13/R-12, R-13/R-22 and R-23/R-13 and also that of for the respective five pure refrigerants. Dependent upon the mixture, the measurements were made at boiling pressures of 0.1 to 2 MPa within the temperature region of 198 to 333 K and at heat fluxes of 4 to 100 kW/m². A horizontal, electronically heated copper plate of 3 cm² was used. The following quantities were measured: pressure; temperature difference between the heating surface and the boiling liquid; composition and temperature in the liquid and vapor phases; and heat flow rate. They observed deterioration in the heat transfer coefficient for an evaporating mixture as compared to the pure components and also obtained parameters, pressure, difference between vapor and liquid composition and heat flux influencing the reduction.

$$\frac{h}{h_{id}} = \frac{1}{1 + K_{ST} |y_1 - x_1| (\rho_v / \rho_l) q^{0.48 + 0.1x_1}} \quad (2.32)$$

In the above correlations, the ideal heat transfer coefficient, h_{id} is defined as:

$$h_{id} = \frac{1}{x_1/h_1 + (1-x_1)/h_2} \quad (2.33)$$

K_{ST} in Eq. (2.32) is an empirical constant. They determined the value of K_{ST} to all the mixtures and gave a smooth curve of K_{ST} , as a function of the temperature difference between the normal boiling points of the two pure components.

Pandey [102], in an exhaustive work, carried out experiments for nucleate boiling of various pure liquids, viz. distilled water, methanol, ethanol, and isopropanol, and for a wide range of compositions of binary liquid mixtures, viz. distilled water-methanol, distilled water-ethanol, distilled water-isopropanol at atmospheric and subatmospheric pressures. She used a horizontal stainless steel cylinder with electrical heating facility for her experimentation. The heat flux ranges from 9.618 to 31.354 kW/m² and the system pressure from 25.33 to 98.63 kN/m². She observed reduction in heat transfer coefficient for binary mixture as compared to that of its pure constituents. Further, she found that the concentration at the heat transfer coefficient is minimum corresponds to a maximum values of heat (y-x). It is 31.10 wt. percent for ethanol, 30.80 percent for methanol and 22.5 wt. percent for isopropanol for distilled water-ethanol, distilled water-methanol, distilled water-isopropanol mixtures, respectively. She also proposed following correlation for calculation of heat transfer coefficient for binary mixtures, which correlates their data excellently:

$$\overline{Nu}^* (P_1/P)^{0.32} = 3.70 \times 10^{-2} (x')^{-0.60} \quad \text{for } 0 < x' \leq 22.0 \quad (2.34)$$

$$\overline{Nu}^* (P_1/P)^{0.32} = 2.51 \times 10^{-4} (x')^{0.90} \quad \text{for } 30 < x' \leq 78.0 \quad (2.35)$$

where, \overline{Nu}^* , represents the average value of the modified Nusselt number and x' the wt. percent of the more volatile liquid in the mixture.

Thome [132] developed a particularly simple correlation based on the assumption that all the liquid arriving to the wall is evaporated, hence the local

boiling temperature rises to the condensation temperature (dew point). This situation is mainly representative for high heat fluxes close to burnout, and conservative at lower heat fluxes. The correlation is as follows:

$$\frac{h}{h_{id}} = \frac{1}{1 + (\Delta T_{bp} / \Delta T_{id})} \quad (2.36)$$

$$\text{where, } h_{id} = \frac{1}{(x_1/h_1) + (x_2/h_2)}$$

Schlünder [114] proposed a semi-empirical correlation developed on the basis of mass transfer film theory for nucleate boiling:

$$\frac{h}{h_{id}} = 1 + \frac{1}{1 + \frac{(T_{s2} - T_{s1})y_1 - x_1}{\Delta T_{id}} \left[1 - \exp\left(\frac{-B_0 q}{\beta_L \rho_L \lambda}\right) \right]} \quad (2.37)$$

The ideal heat transfer coefficient was obtained using linear mixing laws. He assumed that the dominant mass transfer resistance is in the liquid phase near the growing bubble and the vapor side mass transfer resistance can be neglected. In above equation, parameter B_0 represents the fraction of the total heat flux used as latent heat of evaporation, and it is assumed to be 1.0. The binary mass transfer coefficients for fluid combinations, β_L were set to a constant value of 0.0002 m/s in correlating other investigators data. Further, he assumed that all the heat transfer from the heated surface in nucleate boiling passes into the bubble in the form of latent heat.

Hui & Thome [66] measured boiling site densities and heat-transfer coefficients for ethanol-water and ethanol-benzene mixtures at 1.01 bar for a heated vertical brass disk. They observed a strong effect of composition on the boiling site density, which was attributed to the nature of the activation of the boiling surface and mass diffusion effects. They also found that boiling heat transfer coefficient decreases with increasing subcooling, but for the mixtures at a given level of subcooling the decrease was less than that for the single components and azeotropic mixtures. They further observed that heat transfer coefficient at a given heat flux is quite insensitive to the very large increase in boiling site density in comparing the pure water and the ethanol-water azeotrope results, leading one to question pool boiling models that predict heat transfer rates on the basis of boiling site density.

Ünal [142] established a correlation to predict nucleate pool boiling heat transfer coefficients for binary mixtures. The 388 data taken with 13 binary mixtures (including highly non-ideal mixtures) were considered; the ranges of operating conditions for the data were: $P/P_c = 0.015-0.95$; $q = 5.8-400 \text{ kW/m}^2$; $x = 0.001-0.95$. The correlation predicts the heat transfer coefficient from these data accurate to 30% for 97% of the time. The r.m.s. error for the 388 data analyzed was 14.8%. The correlation developed is as follows:

$$\frac{h}{h_{id}} = \frac{1}{[1 + (b_2 + b_3)(1 + b_4)][1 + b_5]} \quad (2.38)$$

where, $b_2 = (1-x) \ln \frac{1.01-x}{1.01-y} + x \ln \frac{x}{y} + |1-x|^{1.5}$

$$b_3 = 0 \quad \text{for } x \geq 0.01; \quad b_3 = (y/x)^{0.1} - 1 \quad \text{for } x \leq 0.01$$

$$b_4 = 152(P/P_c)^{3.9}; \quad b_5 = 0.92|y-x|^{0.001}(P/P_c)^{0.66}$$

$$\text{and } x/y = 1 \quad \text{for } x = y = 0$$

Thome & Shakir [134] in their investigation analyzed the expression for the slope of the curve used by Schlünder [114] and concluded that the actual slope is predicted by the expression due to Schlünder [114] only at one composition. Thus they used the boiling range, which is the difference between the dew point and the bubble point at constant mole fraction to approximate the slope of the bubble point curve and obtained the following correlation:

$$\frac{h}{h_{id}} = \left\{ 1 + \frac{\Delta T_{bp}}{\Delta T_{id}} \left[1 - \exp\left(\frac{-B_0 q}{\beta_L \rho_L h_{fg}}\right) \right] \right\}^{-1} \quad (2.39)$$

Further, they used the Stephan & Abdelsalam [120] correlation for pure components with mixture properties to calculate the ideal heat transfer coefficient, which is as follows:

$$h_{id} = 0.0546 \left(\frac{k_f}{d_b} \right) \left[\left(\frac{\rho_v}{\rho_l} \right)^{0.5} \left(\frac{q d_b}{k_f T_s} \right) \right]^{0.67} \left(\frac{\rho_l - \rho_v}{\rho_l} \right)^{-4.33} \left(\frac{\lambda d_b^2}{\alpha_l^2} \right)^{0.248}$$

Alpay & Balkan [6] measured nucleate pool boiling heat transfer coefficients for acetone-ethanol and methylene chloride-ethanol binary mixtures at pressures ranging from 2.0 to 5.0 bar and varied heat fluxes from 10 to

40 kW/m². They tested their experimental results with the others correlations, and found that the correlations are in good agreement with the experimental results.

Fujita & Tsutsui [50] in their investigation carried out experiments to measure heat transfer coefficients for nucleate pool boiling of binary mixtures on a circular copper plate facing upwards. They were tested various mixtures viz. methanol-water, ethanol-water, methanol-ethanol, ethanol-n-butanol, and methanol-benzene, each in the saturated state at atmospheric pressure. Special stress was laid on elucidating the dependence of heat transfer reduction on mixture composition, physical properties, phase equilibrium diagram, and heat flux. They compared their experimental data with available correlations in literature developed for binary mixtures. They found that among the compared correlations, Stephan & Körner's [121] and Thome's [132] correlations give reasonably good results while their accuracy varies considerably with mixtures and heat flux levels. A modification of Thome's [132] correlation so as to include the effect of heat flux succeeded in correlating the present data within $\pm 20\%$ accuracy. The modified correlation is given below:

$$\frac{h}{h_{id}} = \frac{1}{1 + [1 - 0.8 \exp(-q/10^5)] (\Delta T_{bp} / \Delta T_{id})} \quad (2.40)$$

Inoue & Monde [67] in an experimental investigation studied heat transfer during nucleate pool boiling on a horizontal platinum wire in non-azeotropic binary mixtures of R12-R113, R134a-R113, R22-R113 and R22-R11 at a pressure from 2 to 8 bar and at heat flux up to 100 kW/m². The substances employed were chosen such that the components of a given mixture have a large difference in saturation temperatures. They also modified Thome's [132] correlation, which is given below, by adding a constant, k in that.

$$\frac{h}{h_{id}} = \frac{1}{1 + k(\Delta T_{bp} / \Delta T_{id})} \quad (2.41)$$

$$\text{and } k = 0.45 \times 10^{-5} q + 0.25, \quad 10^4 \leq q \leq 10^5$$

The obtained correlation predicted the heat transfer coefficients for the mixtures within an accuracy of ± 25 percent. It is also shown that the correlation can be applicable for mixtures with a small difference in saturation

temperatures within accuracy of ± 20 percent. They found that the heat transfer coefficients for the mixtures are smaller than that for the single components over the entire concentration range. The heat transfer coefficients for the mixtures depend on the system pressures and heat fluxes at a lesser extent than that for the single components.

Ahmed & Carey [3] conducted experiments with 0.015, 0.025 and 0.1 molar concentration of water/2-propanol mixtures under reduced gravity, normal gravity and high gravity in order to investigate Marangoni effects and their interaction with the gravitational effect in the pool boiling of binary mixtures. The system pressure was subatmospheric (8 kPa at 1 g) and the bulk liquid temperature varied from low sub cooling to near saturation. The reduced and high gravity experiments were carried out at DC-9 aircraft at NASA Lewis Research Center. They obtained boiling curves both for high gravity (2 g) and reduced gravity (0.01 g). For each concentration of 2-propanol, they determined critical heat flux for normal and reduced gravity conditions. The experimental data were compared with the available predictive correlations available in open literature for binary mixture boiling heat transfer and critical heat flux conditions. On the basis of comparison of boiling curves obtained from the experiment under 2 g, 1 g, and reduced gravity conditions they found that the boiling mechanism in these mixtures is nearly independent of gravity. The critical heat flux values determined under reduced gravity conditions for each concentration did not change significantly from those measured under 1 g, conditions. They finally concluded that the Marangoni effect, an active mechanism in the boiling of binary mixtures, arises from the surface tension gradients due to concentration gradients is strong enough in these mixtures to sustain stable nucleate boiling under reduced gravity conditions.

Köster et al. [80] investigated heat transfer for nucleate pool boiling of the binary and ternary refrigerant mixtures R404A, R407C and R507 on a horizontal tube with emery ground surface for wide range of pressures and heat fluxes. The results of this investigation were used to comparative study of the influence of heat flux on the heat transfer coefficient as predicted by various correlations for nucleate boiling of mixtures. At comparatively high saturation

pressures with experimental heat transfer values markedly smaller than the molar average of the pure components. They found that the predicted values of heat flux and heat transfer coefficient by various relationships significantly differ from the experimental values, particularly for wide boiling mixtures. On the basis of the comparison they suggested that various assumptions in the development of the correlations should be improved in order to achieve a better prediction of the heat transfer coefficients at high saturation pressures.

Bajorek & Lloyd [7] proposed a model considering the diffusion of the more volatile components to the interface of a growing bubble. According to them, the diffusion of multicomponent mixtures is different from binary mixtures and considered cross-diffusion terms in that. Thus, they incorporated cross-diffusion coefficients in their model. Considering Schlünder's [114] approach, they arrived at the following expression for a ternary mixture.

$$\frac{h}{h_{id}} = \left\{ 1 + \frac{h_{id}}{q} \left[\left(\frac{dT}{dx} \right) (y_1 - x_1) \left[1 - \phi_1 \frac{\exp(-\psi_1)}{\zeta_1 - \zeta_2} + \phi_2 \frac{\exp(-\psi_2)}{\zeta_1 - \zeta_2} \right] \right] \right\}^{-1} \quad (2.42)$$

$$\text{where, } \phi_1 = D_{22} - D_{21} \left(\frac{y_2 - x_2}{y_1 - x_1} \right) - \zeta_2; \quad \phi_2 = D_{22} - D_{21} \left(\frac{y_2 - x_2}{y_1 - x_1} \right) - \zeta_1$$

$$\psi_1 = \frac{k_1 q \zeta_1}{\rho \lambda \det[D] h_{id} \sqrt{Le}}; \quad \psi_2 = \frac{k_1 q \zeta_2}{\rho \lambda \det[D] h_{id} \sqrt{Le}}$$

Where ζ_1 and ζ_2 are the eigen values of the matrix of diffusion coefficients [D]. They suggested the slope (dT/dx) of the bubble point curve can be replaced with the boiling range. They used the Stephan & Abdelsalam [120] correlation for pure components, with mixture properties to calculate the ideal heat transfer coefficient.

Inoue et al. [68] carried out experiments on a horizontal platinum wire during nucleate pool boiling in non-azeotropic binary mixtures of R12-R113, R134a-R113, R22-R113 and R22-R11, at pressures of 0.25 to 0.7 MPa and at heat fluxes up to critical heat flux. They photographically studied the features of boiling phenomenon occurring during boiling of the mixtures and the pure substances. The relationship between the boiling features and the reduction in heat transfer coefficient in binary mixtures is discussed in order to propose a

correlation useful for predicting the experimental data measured over a wide range of low and high heat fluxes. They modified Thome's [132] correlation by adding a constant k to account the effect of heat flux on the reduction in heat transfer coefficient. Further, they argued that the correlation developed by them is also applicable to alcoholic mixtures, since its predictions closely matched with the experimental data for alcohols due to Fujita & Tsutsui [50]. The correlation proposed by them is as follows:

$$\frac{h}{h_{id}} = \frac{1}{1 + k(\Delta T_{bp}/\Delta T_{id})} \quad (2.43)$$

$$\text{and } k = 0.75 \exp(-0.75 \times 10^{-5} q)$$

Krupiczka et al. [81] studied the effect of mass transport on the boiling heat transfer coefficient. On the basis of that they described a mathematical model of the process based on multi-component mass transfer. The results of the model were compared with their experimental pool boiling data for the ternary system methanol–isopropanol–water along with others data. The model presented by them is as follows:

$$\frac{h}{h_{id}} = [1 + (h_{id}/q)(T_i - T_N)]^{-1} \quad (2.44)$$

Where T_i is the interfacial temperature and T_N is boiling point of the liquid. As evident from above equation it is necessary to know the interfacial temperature in order to obtain the actual heat transfer coefficients during the boiling of multi-component mixtures.

Shen et al. [118] investigated systematically nucleate pool boiling heat transfer for refrigerant mixture R32-R125 in a wide range of pressure and heat flux under saturation conditions using a horizontal platinum wire ($d = 0.1$ mm). The platinum wire served as both heating element and resistance thermometer. They developed a correlation for heat transfer coefficient by modifying Jungnickel et al. [76], which is given below:

$$\frac{h}{h_{id}} = \frac{1}{1 + k_0 |y_1 - x_1| q^{(0.48+0.1x)} (\rho_V/\rho_L)} \quad (2.45)$$

Where k_0 is an empirical parameter. Jungnickel et al. [76] determined the value of k_0 for five refrigerant mixtures. In a diagram they give a smooth

curve of k_o as a function of the temperature difference between the normal boiling points of the two pure components. According to the curve the value k_o for R32-R125 mixtures should be between 0.5 and 0.6. But they found that the experimental values of k_o range from about 1 to 0.1, depending on the normalized pressure. Therefore, they introduced an equation for k_o as a function of the normalized pressure P^* :

$$k_o = -1.14 \log(P^*) - 0.06$$

The results indicated that the pressure and the heat flux dependence of the heat transfer coefficient for the R32-R125 mixtures do not differ from those of pure components. In order to describe the composition dependence of the heat transfer the empirical parameter k_o in the correlation by Jungnickel et al. [76] was modified considering on the basis of their experimental data. The comparison between all calculated data and experimental data showed good agreement with a mean average deviation of $\pm 8.25\%$.

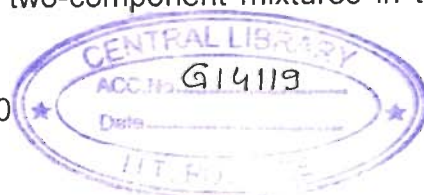
Fujita & Tsutsui [49] in their investigation measured heat transfer coefficients in nucleate boiling on a smooth flat surface for pure fluids, their binary and ternary mixtures under the saturated conditions at 0.6 MPa for a wide range of heat flux and mixture concentration. Refrigerants, R-134a, R-142b and R-123 were used to make up binary and ternary mixtures. They observed that both binary and ternary mixtures showed lower heat transfer coefficients as compared to the ideal heat transfer coefficients calculated from a mole fraction average of the wall superheats of pure components. This reduction was more pronounced as heat flux was increased. The data of binary mixtures were well reproduced by Thome & Shakir [134] and Fujita & Tsutsui [50] correlations. For ternary mixtures, dimensionless heat transfer coefficients plotted on the concentration triangle were very similar to the contour map of boiling range. This similarity suggested the boiling range is an essential parameter to account for heat transfer reduction of ternary mixtures. Fujita & Tsutsui [50] correlation was found applicable to ternary mixtures with a reasonable success.

Inoue et al. [69] in their experimental study measured nucleate boiling heat transfer coefficients for pool boiling of ammonia-water mixtures on a

horizontal heated wire. The experiment was carried out at pressures of 0.4 and 0.7 MPa, at heat fluxes below 2000 kW/m^2 and over all ranges of fraction. They also observed markedly less heat transfer coefficients in the mixtures than those in single component substances. Further, they compared their experimental data with calculated values due to existing correlations and concluded that it is difficult for any existing correlation to predict the coefficients for over all ranges of fraction. In addition, they found that in the mixtures of ammonia-water, heat of dilution and of dissolution are generated near a vapor-liquid interface, while vapor with a richer concentration of ammonia is condensed and then diffused into a bulk liquid; while in most other mixtures, little heat is generated during any dilution and dissolution.

Jung et al. [74] conducted experiments to determine nucleate boiling heat transfer coefficients of binary and ternary mixtures composed of HFC32, HFC125, and HFC134a on a horizontal smooth tube of 19.0 mm outside diameter. A cartridge heater was used to generate uniform heat flux on the tube. Data were taken in the order of decreasing heat flux from 80 kW/m^2 to 10 kW/m^2 with an interval of 10 kW/m^2 in the pool temperature at 7°C . Heat transfer coefficients of non-azeotropic mixtures of HFC32-HFC134a, HFC125-HFC134a, and HFC32-HFC125-HFC134a showed a reduction of heat transfer coefficients as much as 40% from the ideal values while the near azeotropic mixture of HFC32-HFC125 did not showed the reduction. They compared their data with four of the well known correlations for binary mixtures. Stephen & Körner's [121] and Schlünder [114] correlations yielded a good agreement with a deviation of less than 10% but they can not be easily extended to multi-component mixtures of more than three components. Thus, they developed a new correlation by utilizing only the phase equilibrium data and physical properties. On the basis of regression analysis to account for the reduction of heat transfer coefficient, they obtain the final correlation, which can be easily extended to multi-component mixtures of more than three components, yielded a deviation of 7% for all binary and ternary mixtures.

Fujita & Tsutsui [51] experimentally measured heat transfer coefficients in nucleate boiling for three-as well as two-component mixtures in the whole



range of composition with refrigerants R-134a, R-142b and R-123, as comprising pure components on the upward facing copper surface of 40 mm diameter. It was found that heat transfer coefficients of mixtures are reduced in a comparison with the ideal coefficients interpolated between pure components, with more reduction at higher heat flux. They observed that the boiling range is a key parameter to account for heat transfer reduction in boiling of mixture. Two correlations originally developed for two-components mixtures by Thome & Shakir [134] and by Fujita & Tsutsui [50], which include the boiling range as parameter, reproduced well the measured heat transfer coefficients of three- as well as two-component mixtures. Thus they finally concluded that the boiling range included in the correlations accounts for heat transfer reduction in mixture boiling.

Lee et al. [86] conducted pool boiling experiments for binary mixtures of refrigerants R11 and R113 at constant wall temperature condition. Results for binary mixtures were also compared with pure fluids. They used a micro-scale heater array and Wheatstone bridge circuits to maintain the constant temperature of the heating surface and to obtain heat flow rate measurements with high temporal and spatial resolutions. Time-triggered high-speed CCD images were captured at sampling rates of 1000 and 4000 Hz and synchronized with heat flow rate measurements to analyze the bubble motion.

They obtained geometry of the bubble from the captured bubble images and found that the equivalent radius of a sphere of the same volume showed a small shape assumption error. In the asymptotic growth region, the bubble growth rate was proportional to a value between $t^{1/6}$ and $t^{1/4}$. The bubble growth behavior was analyzed to permit comparisons with binary mixtures and pure fluids at the same scale using dimensionless parameters. There was no discernible difference in the bubble growth behavior between binary mixtures and pure fluids for a given onset of nucleate boiling temperature.

The minimum heat transfer coefficient of binary mixtures occurred near the maximum $|y - x|$ value, and the average required heat flux during bubble growth did not depend on the mass fraction of R11 as more volatile component in binary mixtures. Finally, they concluded that for binary mixtures, a higher

onset of the nucleate boiling temperature had the greatest effect on reducing the heat transfer coefficient.

Rao & Balakrishnan [109] in an exhaustive study carried out experimentation to obtain steady state pool boiling heat transfer coefficients for acetone–isopropanol–water and acetone–methyl ethyl ketone–water ternary systems. Alike other investigators, they also observed lower heat transfer coefficients for mixtures than the values obtained for pure components. The comparison of measured heat transfer coefficients with those of predicted values from others correlations showed overestimation or underestimation of the data was observed, in almost all the cases. They argued that this happen because literature correlations incorporate an 'ideal' heat transfer coefficient and a correction term for the presence of other liquids. Therefore, in this study, they tried two different correlations for the ideal heat transfer coefficient and found that the performance of the literature correlations improved considerably. To overcome these they proposed a correlation to estimate the ideal heat transfer coefficient taking into account surface–liquid interaction parameter and surface roughness group in terms of an ideal heat transfer coefficient and a correction term, which is as follows:

$$h_{id} = \frac{0.74}{\gamma^{0.1} Pr^{0.5}} \cdot \frac{k_1}{d_b} \left(\frac{qd_b}{k_1 T_s} \right)^{0.674} \left(\frac{\rho_v}{\rho_l} \right)^{0.297} \left(\frac{\lambda d_b^2}{\alpha_l^2} \right)^{0.371} \left(\frac{\alpha_l^2 \rho_l}{\sigma d_b} \right)^{0.350} \left(\frac{\rho_v - \rho_l}{\rho_l} \right)^{-1.73} \left(\frac{R_a P}{\sigma} \right)^{0.133} \quad (2.46)$$

In an earlier study, Benjamin & Balakrishnan [10] developed a model for heat flux for binary mixtures. They related the effective and superficial temperature driving forces as:

$$\frac{h}{h_{id}} = \left[1 - \left(|y - x| \sqrt{\frac{D_{AB}}{\alpha_{min}}} \right)^{0.5} \right] \quad (2.47)$$

Here D_{AB} is the binary mass diffusivity. The correction term in binary mixtures is obtained by incorporating the binary mass diffusivity of the mixture. On the basis of above equation, Rao & Balakrishnan [109] further obtained following correlation for multicomponent mixture by incorporating multicomponent diffusion coefficients:

$$\frac{h}{h_{id}} = \left[1 - \sum_{i=1}^{n-1} \left((y_i - x_i) \sqrt{\frac{(\bar{D})^{1/n-1}}{\alpha_{min}}} \right)^{0.5} \right] \quad (2.48)$$

Sun et al. [126] carried out series of experimentation to measure heat transfer coefficients in nucleate boiling on a smooth flat surface for pure fluids of R-134a, propane, isobutane and their binary mixtures at different pressure from 0.1 to 0.6 MPa. They considered different heat flux and mixture concentrations and studied the influences of pressure and heat flux on the heat transfer coefficient for pure fluids. Isobutane and propane were used to make up binary mixtures. They also observed that as compare to the pure components, binary mixtures showed lower heat transfer coefficients and this reduction was more pronounced at higher heat fluxes. They obtained several heat transfer correlations for different pure refrigerants and their binary mixtures.

According to their experimental data, the following heat transfer correlation form was adopted by them:

$$h = Cq_b^n f(p)$$

This equation includes two important influencing factors: heat flux and pressure. They obtained separate correlations for R-134a, propane and isobutane. Finally, following correlation have been proposed by them for binary mixture of propane and isobutane:

$$\frac{h}{h_{id}} = \frac{1}{1+K} \quad (2.49)$$

$$K = \left(\Delta T_{bp} / \Delta T_{id} \right) \left[1 - 0.85 \exp\left(-q / (3 \times 10^5)\right) \right]$$

$$\Delta T_{id} = \frac{q}{h_{id}} = \frac{1}{\sum (x_i / h_i)} \quad (2.50)$$

Chen et al. [27] carried out pool boiling heat transfer experiments on a conventional smooth tube and four enhanced tubes with reentrant surfaces using propane, isobutane and their mixtures as working fluids for six saturation temperatures. They observed very different heat transfer performance for different surface-fluid combinations. According to them the mixture boiling heat transfer degradation was more significant for the enhanced tubes as compared

to that of smooth tube. Further, they found boiling hysteresis for all the surfaces and mixtures showed much stronger hysteresis than the pure components.

Sun et al. [127] carried out extensive experiments for pure and mixed refrigerants at various heat fluxes from 10 kW/m² to 300 kW/m² and pressures from 0.2 to 0.6 MPa. They measured heat transfer coefficient on a smooth flat surface for pure fluids HFC134a, HC290, HC600a and their binary and ternary mixtures. On the basis of experimental results, they too found different heat transfer features of binary mixtures and ternary mixtures according to their vapor–liquid phase equilibrium behaviors as compared to smooth surface. In addition, they obtained new heat transfer correlations by regression analysis from the experimental data with average deviations within ±15% for pure refrigerants and within ±20% for mixtures. The correlations developed by them are given below.

$$\frac{h}{h_{id}} = \frac{1}{1+K}$$

For binary mixtures:

$$K = (1/\Delta T_{id})(y-x)^{-0.1} \Delta T_{bp}^{0.9} (P/10^5)^{-0.04} \times [1 - 0.85 \exp(-q/(3 \times 10^5))] \quad (2.51)$$

For ternary mixtures:

$$K = (\Delta T_{bp}/\Delta T_{id}) [1 - 0.85 \exp(-q/(3 \times 10^5))] \quad (2.52)$$

Recently, Táboas et al. [128] carried out a bibliographic revision of the information available in the open literature about nucleate pool boiling of the ammonia-water mixture and its pure components. The experimental data were compared with existing prediction correlations for the pure components and also for their mixtures. They observed that for water, all the pure component pool boiling correlations gave similar predictions, and were in good agreement with experimental data. For ammonia the prediction of the correlation and the experimental data showed more differences. Thus, they proposed a new correlation for ammonia-water mixture by combining Schlünder [114] and Thome & Shakir [134] correlations.

$$\frac{h}{h_{id}} = \frac{1}{1+K}$$

$$K = A \frac{h_{id}}{q} \left\{ x(y_1 - x_1)(T_{sat1} - T_{sat2}) + (1-x)\Delta T_{bp} \right\} \left[1 - \exp\left(\frac{B_0 q}{\rho_L h_{LV} \beta_L} \right) \right] \quad (2.53)$$

The constant, A was determined by using the least mean square method, which minimizes the error between the predicted values and the experimental data. For the value of A equal to 0.5, the above expression best fits the experimental data.

Recently, Nahra & Næss [94], in an experimental work, obtained heat transfer coefficients in nucleate pool boiling of binary and ternary non-azeotropic hydrocarbon mixtures using a vertical electrically heated cylindrical carbon steel surface at atmospheric pressure with several surface roughnesses. The fluids used were Methanol/1-Pentanol and Methanol/1-Pentanol/1,2-Propandiol at constant 1,2-Propandiol mole percent of 30%. Heat fluxes were varied in the range 25 to 235 kW/m². Comparison of his experimental data with that predicted from others correlations showed that the correlations available in literature based on the boiling range are in better qualitative agreement than correlations based on the phase envelope. He also found that increasing surface roughness resulted in an increase in the heat transfer coefficient, and the effect was observed to be dependent on the heat flux and fluid composition. The influence of the surface roughness in binary mixtures contributed to higher heat transfer coefficients at the same fluxes and mixture composition.

The heat transfer coefficients for the pure components were obtained for the different surface roughnesses in order to determine the mixture ideal heat transfer coefficients. The experimental results were fitted using simple power law equation of the following form:

$$h = Cq^b \quad (2.54)$$

The constant C and b in this depends upon surface roughness and fluid composition, and their values are reproduced in **Table 2.10** for ready reference.

Table 2.10 Values for Constant C and index b of Eq. (2.54)

Fluid	Ra = 0.2		Ra = 2.98		Ra = 4.36	
	C	b	C	b	C	b
Methanol	2.08	0.68	2.01	0.72	0.85	0.80
1-Pentanol	2.05	0.67	1.61	0.73	2.95	0.70
1,2-Propanediol	0.63	0.78	0.42	0.83		

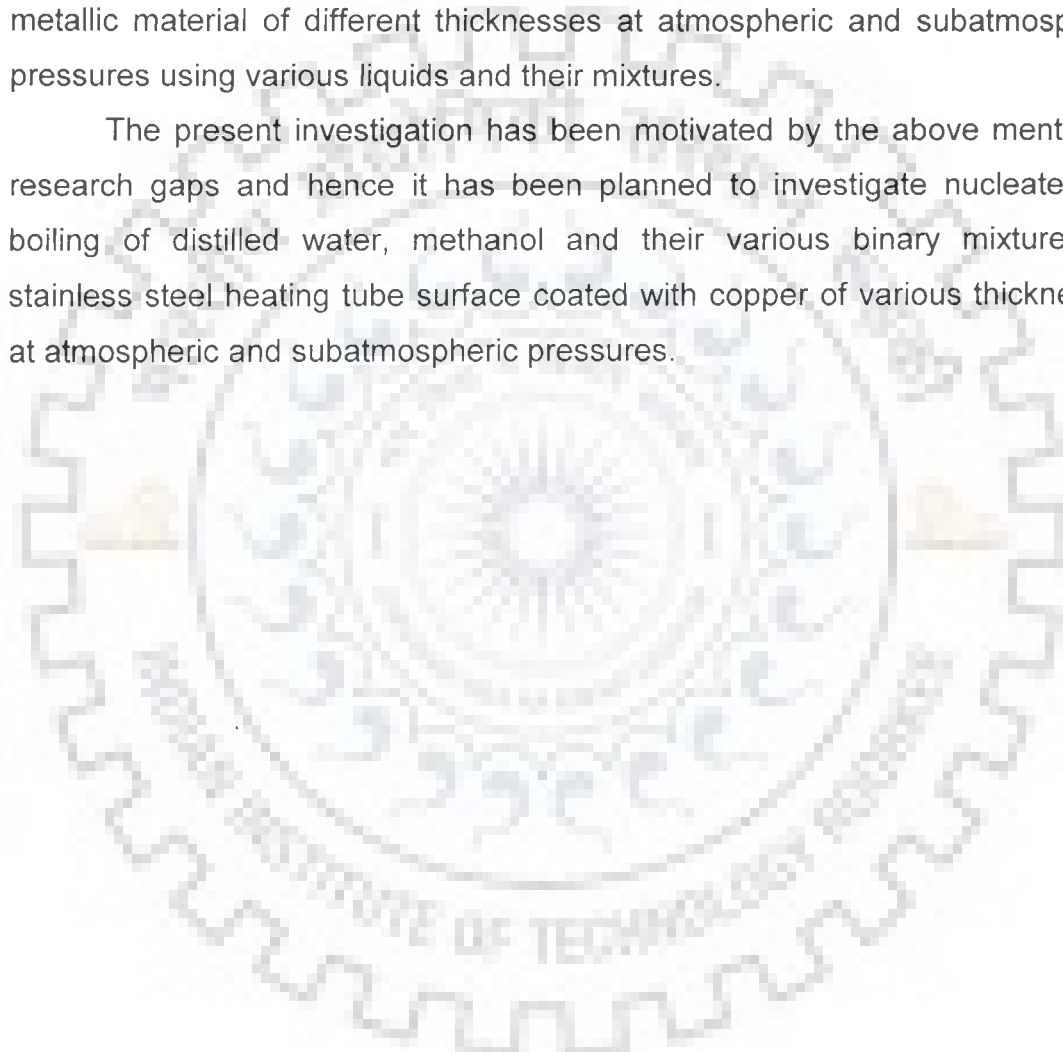
Zhao et al. [157] measured heat transfer coefficients in nucleate pool boiling for refrigerants under saturated conditions at 0.9 MPa on a horizontal copper surface. Those refrigerants were the pure components of HFC-134a, HFC-32, HFC-125 and two kinds of binary mixtures: non-azeotropic mixture HFC-32/134a, azeotropic mixture HFC-32/125 compared to pure components, and both binary mixtures showed lower heat transfer coefficients. This deterioration was more pronounced as heat flux was increased. They compared the available empirical and semi-empirical correlations developed for mixtures with the measured data. They found that none of the available correlations predicted the heat transfer coefficients well. Thus, they suggested that a new model should be developed based on exploring the heat and mass transfer mechanisms of mixture boiling.

2.5 MOTIVATION FOR PRESENT INVESTIGATION

Above literature review reveals that modified surfaces comprise one of the potential passive techniques, which can be obtained by either roughening or coating of metallic and non-metallic materials over heating surfaces, to enhance heat transfer coefficient. The surfaces coated with non-metallic materials suffer from the disadvantages of limited durability because of their continuous deterioration and surface's wetting characteristics. However, the surfaces coated with metallic materials have been found to last long and to enhance heat transfer coefficient many folds as compared to non-metallic coated surfaces. Further, coating of high thermal conductivity and high permeability material has been found to offer additional enhancement in heat transfer coefficient. Unfortunately, as summarized in **Table 2.8**, it has been

found that most of the investigations have been confined to boiling of liquids at atmospheric pressure only. However, situation do exist in various process industries where boiling of liquids and mixtures on enhanced tube is required to take place at subatmospheric pressures. Besides, very few studies are available mentioning the effect of heat flux, pressure, coating thickness and composition of liquid mixture on boiling characteristics. Thus, it is essential to investigate boiling heat transfer characteristics of a plain tube coated with metallic material of different thicknesses at atmospheric and subatmospheric pressures using various liquids and their mixtures.

The present investigation has been motivated by the above mentioned research gaps and hence it has been planned to investigate nucleate pool boiling of distilled water, methanol and their various binary mixtures on stainless steel heating tube surface coated with copper of various thicknesses at atmospheric and subatmospheric pressures.



Chapter-3

Experimental Set-up

This chapter deals with the experimental set-up and its accessories

EXPERIMENTAL SET-UP

The key objective of this investigation is to obtain experimental data of heat transfer from a horizontally placed cylindrical surface submerged in the pool of boiling liquids and their binary mixtures at atmospheric and subatmospheric pressures. This requires designing and fabrication of an experimental set-up. Following important factors were considered in the design, fabrication and commissioning of the experimental setup in order to obtain precise, consistent and reproducible experimental data:

3.1 DESIGN CONSIDERATIONS

- Since experiments are to be conducted under vacuum, a vessel of cylindrical shape was chosen so that it may withstand operating pressure without the development of excessive hoop stresses. Besides, height of the vessel was taken around twice of its diameter to provide adequate free space above liquid pool for the disengagement of vapors therein.
- Visual observation of boiling phenomenon over heating tube surface is important. Hence, a provision of two view ports on diametrically opposite sides of vessel body was considered.
- Further, an arrangement was made to hold heating tube in perfect horizontal position.
- As the process under consideration has been of closed cycle nature, a provision was made for complete condensation of vapor formed during boiling and the return of condensate, so formed, to liquid pool. Consequently, mounting of a horizontal condenser over test vessel was considered.
- To obtain heat transfer data for boiling of liquid mixtures, it is essential to determine the composition of the liquid and vapor

through out experimentation. Therefore, an arrangement was included in the experimental set-up for drawing out samples of boiling liquid and the resultant vapor for their analysis.

- In this investigation heat is to be transferred from heater to liquid pool radially. So, possibility of any heat flow in longitudinal direction was curbed by leaving an un-drilled portion of adequate thickness at one end of heating tube, and also a covering of a thick sheet of low insulating material polytetrafluoroethylene (PTFE) at un-drilled end of heating tube.
- Since heating tube was placed horizontally in the pool of liquid, a significant variation in surface temperature of heating tube may exist around its circumference. Therefore, provision was made to measure surface temperature at various circumferential positions on heating tube. For this purpose, four numbers of axial holes were made in wall thickness of heating tube at locations namely, top, bottom and two sides. These were considered adequate to represent surface temperature variation around the tube due to small diameter of heating tube. Further, insertion of thermocouple in heating tube thickness was considered as the placement of thermocouple probes on heating tube surface may affect vapor bubble dynamics. Besides, thermocouples were mounted away from the close end of heating tube to eliminate any error owing to end effects.

Liquid temperature was also measured at four locations namely top, side, bottom and side corresponding to the respective surface thermocouple positions to variation in liquid pool temperature, if any. This enabled the determination of local heat transfer coefficients. The thermocouple probes were located at a sufficient distance away from heating tube surface so that they may be outside superheated boundary layer surrounding heating tube. This was essential to measure the bulk temperature of liquid pool.

3.2 DETAILS OF EXPERIMENTAL SET-UP

On the basis of above design considerations, an experimental set-up along with all the accessories has been designed, fabricated and assembled. A schematic diagram of experimental set-up along with its various components is shown in **Fig. 3.1** and photographically in **Fig. 3.2**. The details of experimental set-up are described below:

3.2.1 Vessel

The vessel (1) used in present investigation was of cylindrical shape. It was made from AISI 304 stainless steel sheet of 3.2 mm thickness. The vessel was of an internal diameter of 250 mm and a height of 450 mm. It was closed at both ends with dished caps of same material. The dished cap attached to bottom end of the vessel had a fitting of a pipe with a valve (V_1) to drain out liquid from the vessel as and when required. Similarly, top cover of the vessel contained fittings to mount vacuum/pressure gauge (6), condenser (11), a pipe line attached with a valve (V_2) for the expulsion of air dissolved in liquid in to a bubbler (9) and a thermocouple probe (T_L) to measure the liquid pool temperature. A socket (5) was welded to vessel body at a distance of 135 mm from the bottom of vessel to hold heating tube in horizontal orientation. Two view ports (7) of 75 mm diameter were welded at diametrically opposite side positions of the vessel body for visual observation of bubble dynamics on and near the heating tube surface. A liquid level indicator (4) along with a graduated scale was fitted on one side of vessel to determine the height of liquid inside the vessel. Four liquid thermocouple probes (T_L) were inserted through the body of the vessel at suitable positions to measure liquid pool temperature corresponding to the top, two sides and bottom positions of the wall thermocouples in heating tube. An arrangement was fitted at the vessel body to draw out the liquid sample directly from the pool by the use of an air tight syringe.

The outer surface of vessel was insulated by winding asbestos rope around it, followed by the application of a thick paste of a mixture of plaster of paris, asbestos powder and magnesia powder to prevent heat loss to surrounding.

3.2.2 Heating tube

Two types of heating tubes – plain and copper coated have been used in this investigation. A photographic view of the heating tubes used in this investigation is shown in **Fig 3.3** and the details of the heating tube along with heater are shown schematically in **Fig. 3.4**.

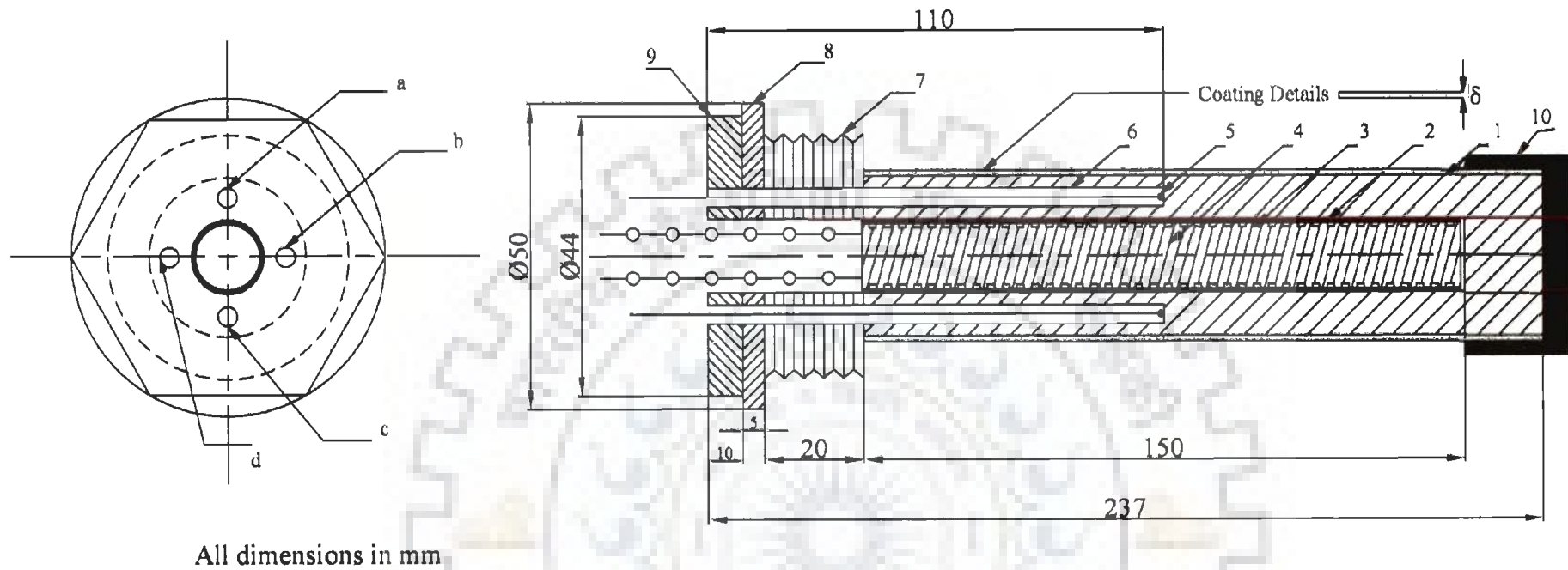
The heating tube was basically a stainless steel cylinder of 31.94 mm outside diameter, 18 mm inside diameter and 237 mm length. It was made by drilling a central hole of 18 mm diameter in a stainless steel rod up to a distance of 185 mm from its one end. A portion of 50 mm was left un-drilled at the other end of the tube. The un-drilled end of tube was covered with a thick sheet of polytetrafluoroethylene (PTFE), an inert material of very low thermal conductivity. This was carried out to abate possibility of any heat flow in longitudinal direction. Further, a length of 35 mm was left at the open end of heating tube to make provision for a hexagonal nut, a collar and a threaded portion. Thus, effective length of heating tube was 150 mm. The hexagonal nut of 10 mm length was made at the open end of heating tube surface. It was followed by a collar of 50 mm diameter and 5 mm length. The collar was used to tighten heating tube in the socket welded to the vessel body. Next to the collar was a threaded portion of 20 mm length. The threads were of 19 TPI, and were made so that heating tube can be fitted tightly in horizontal position with the socket. In order to measure wall temperature of the heating tube at top, bottom and the two side positions, four holes, equi-spaced at 90° , were made circumferentially in the wall thickness of heating tube. The holes were of 2 mm diameter and of 110 mm length measured from the open end of the heating tube. They were drilled on a pitch circle diameter of 25 mm. Their positions are clearly shown in **Fig. 3.4** by symbols a, b, c and d. The outer surface of the heating tube was made smooth by turning and rubbing against emery paper of 800 grit size followed by a very fine emery paper of 1200 grit size. Finally, the surface was polished by 4/0 grade emery paper. This procedure is carried out to obtain same roughness of all heating tubes used in this investigation. Four numbers of heating tubes prepared by above procedure were used in this investigation. Three of them are coated with various thicknesses of copper.



Fig. 3.2 Photographic view of the experimental set-up



Fig. 3.3 Photographic view of the heating tubes



- | | | |
|-----------------------------|----------------------|--------------------------------------|
| 1 Heating Tube | 5 Wall Thermocouples | 9 Hexagonal Nut |
| 2 Mica Sheet and Glass Tape | 6 Thermocouple Holes | 10 PTFE Insulation |
| 3 Porcelain Tube | 7 Threaded Portion | δ Coating Thickness |
| 4 Nichrome Wire | 8 Collar | a, b, c, & d Thermocouples Positions |

Fig. 3.4 Schematic diagram of heating tube along with heater

The coating on heating tubes is carried out by electroplating technique at M/s Plating Sheen Chem. India Pvt. Ltd., New Delhi (India). Prior to coating, preliminary treatment of heating tube was carried out to remove oil, grease, dirt and other volatile material from the substrate surface. The preliminary treatment process consists of pretreatment, alkaline cleaning, and acid dipping, followed by strike plating of copper. Thereafter, Rochelle cyanide copper plating process was used for coating of copper on stainless steel heating tubes. The desired coating thicknesses over the heating tubes were obtained using the above said processes. Details of procedure involved in producing the desired thickness of coating over the heating tube is given in Annexure-A. The dimensions of all heating tubes used in present investigation are given in **Table 3.1**.

Table 3.1 Dimensions of Heating Tube

Heating Tube Nomenclature	O.D. of Tube before Coating d , (m)	O.D. of Tube after Coating d_o , (m)	I.D. of Tube d_i , (m)	Pitch Circle Diameter d_h , (m)	Effective Length L , (m)	Coating thickness δ , (μm)
ST-00	0.031940	0.031940	0.01804	0.0250	0.1500	0
ST-22	0.031930	0.031974	0.01799	0.0250	0.1500	22
ST-43	0.031940	0.032026	0.01801	0.0250	0.1500	43
ST-67	0.031920	0.032054	0.01800	0.0250	0.1510	67

An electric heater (8), used to heat the tube, was placed inside the heating tube as shown in **Fig. 3.4**. It was prepared by winding 24 gauge nichrome wire having a current carrying capacity of 5 A over a porcelain tube of 16 mm diameter. The length of the porcelain tube was equal to the effective length of heating tube. Both the terminals of nichrome wire were taken out through porcelain beads and connected to an autotransformer (12) via a connector. The heater was insulated by wrapping several layers of mica sheet and glass tape to prevent electric short circuiting.

3.2.3 Condenser

A knockout condenser (11), made from AISI 304 stainless steel sheet, was used for the condensation of vapor formed during boiling of liquid inside

the vessel. Basically, the condenser was a double pipe heat exchanger having an inner pipe of 25 mm O.D. and outer pipe of 76 mm O.D. The length of condenser was 660 mm. The vapor passed to the inner pipe whereas coolant (water) flowed through the annular space formed between the pipes. The condenser was mounted horizontally with a slight inclination towards the end to ensure the flow of the condensate by gravity to separator.

3.2.4 Air-Liquid Separator

The purpose of installing an air-liquid separator (12) in the set-up was to provide an additional facility to remove non-condensable gases. The separator was placed between condenser and vacuum unit as depicted in **Fig. 3.2**. The air-liquid mixture entered into the separator tangentially and the separated non-condensable gasses passed to the vacuum pump through the pipe at the top of the separator, while the liquid (condensate) returned to the liquid pool through a pipe line provided at the bottom of the separator.

3.2.5 Liquid and vapor sampling arrangements

Two sampling arrangements were included in the experimental set-up for drawing out the samples of boiling liquid and the vapor for their analysis. This was necessary to ascertain the condition of equilibrium existing between the two. These arrangements were combination of two nut & cap type arrangements made of stainless steel. An axial hole of 2 mm diameter was made in nut & cap and a septum was placed between nut & cap to avoid any leakage. One of it was fitted directly to the vessel to take sample of boiling liquid while another was fitted at the outlet of separator to take vapor condensate sample.

3.2.6 Vacuum pump

The vacuum pump (14) used in this investigation was a two-stage oil sealed rotary pump driven by a 0.5 hp motor having a speed of 1440 rpm. It was supplied by M/s GE Motors India Ltd., Faridabad (India). It had a suction capacity of 8.0 l/min and an ultimate vacuum capacity of 0.002 mm Hg. The

vacuum pump was connected to the vessel through a surge tank (13) and a needle valve (V_6). The surge was used to dampen tank fluctuations in pressure and also to prevent liquid condensate to enter in to vacuum pump.

3.2.7 Instrumentation

Measurement of power input to heating tube, temperatures of liquid and heating tube wall and vacuum/pressure inside the vessel are important for the determination of boiling heat transfer. Consequently, the experimental set-up was suitably instrumented. The details of instrumentation for above parameters are described below:

The heater (8) was connected to AC mains through a constant voltage stabilizer (17), manufactured by M/s Bhurji Electronics Pvt. Ltd., Gurgaon (India) and a servo voltage stabilizer (18) manufactured by M/s Gargy Research Instruments, Delhi (India). The power input to heating tube was controlled by an autotransformer (16), manufactured by M/s Agro Transformer Company Ltd., Mumbai (India). The power input to heating tube was measured by a calibrated digital wattmeter supplied by M/s Electronics and Scientific Devices, New Delhi (INDIA) having an accuracy of $\pm 1\%$ on the full scale of (0 – 1800 W).

Vacuum in the vessel was measured by a vacuum gauge (6) mounted over the test vessel. The vacuum gauge was calibrated against a standard McLeod gauge.

Wall- and liquid- temperatures were measured by PTFE covered 30 gauge copper constantan thermocouples made by the wires supplied by M/s OMEGA Engineering Limited, United Kingdom. Thermocouples were made in the laboratory and were suitably calibrated by a temperature calibrator T-25N (temperature range $-25\text{ }^{\circ}\text{C}$ to $+125\text{ }^{\circ}\text{C}$ and accuracy $0.01\text{ }^{\circ}\text{C}$) supplied by M/s Presys Instruments Inc., USA. Four thermocouples were placed inside the holes drilled circumferentially in wall thickness of heating tube. Thermocouple probes were inserted at various positions in the vessel body with suitable

fittings to measure liquid pool temperature around the heating tube. The leads of all the thermocouples and probes were connected to a digital multimeter through a 12-point selector switch. The e.m.f. generated in thermocouple circuit was measured with the help of a digital multimeter of Keithley 177 Microvolt DMM having a least count of $0.1 \mu\text{V}$ in 20 mV range. A bath of ice and water mixture, maintained at 0°C ; was used as a reference junction.

The composition of binary liquid mixtures and those of boiling liquid and vapor were measured by using Waters Breeze HPLC system, supplied by M/s Waters (India) Pvt. Ltd., Bangalore. A Novel Pack, C18 column of size $3.9 \text{ mm} \times 150 \text{ mm}$ was used for measurement of the methanol concentration. Degassed organic free water was used as a solvent, while maintaining a flow rate of 1 ml/min, as per the specification given in the user manual of the instrument. Prior to measurement of actual composition, the instrument was calibrated for standard distilled water-methanol binary mixtures at wavelength of 210 micron.

Chapter-4

Experimental Procedure

This chapter deals with the experimental procedure and operating parameters

EXPERIMENTAL PROCEDURE

This chapter illustrates a procedure adopted in present investigation to obtain reliable experimental data. It comprises the details of integrity tests of each component and of entire experimental set-up and also the particulars of tests conducted to examine the reliability and reproducibility of the experimental data obtained.

4.1 INTEGRITY TESTS

All the components of the experimental facility were designed and fabricated according to design considerations of the system. After the fabrication of individual components of the experimental set-up certain tests, as explained below, were carried out in order to examine the reliability of individual components for smooth and trouble-free operation. Each component was tested separately and assembled with set-up and then the complete set-up was tested to ensure its proper functioning. A brief description of the tests conducted is as follows:

All the valves i.e. V_1 to V_7 were tested for leakage in a valve-testing bay against compressed air of about 200 kN/m^2 pressure. The valves detected with leakage were made leak proof prior to their fitting with the set-up.

The knock-out horizontal condenser was tested for leakage against compressed air by the following procedure. The nozzles provided in outer pipe of the condenser were connected to water inlet and outlet pipelines with proper fittings and valves. One end of the inner pipe was fitted with a pressure gauge whereas the other end was connected to a compressor through a valve. Compressed air at a pressure of 200 kN/m^2 was admitted into the condenser. After this, all the end-valves were closed and soap solution was applied to welded joints and other portions on outer surface of the condenser. The leaky points, indicated by the appearance of air bubble on the surface, were suitably attended. This process was repeated until no air bubble appeared. Further, no

drop in pressure was also noted in pressure gauge reading and then the condenser was considered to be leak-proofed. The air-liquid separator used in the experimental facility was also tested against the pressure in a similar manner as stated above for condenser to ensure the leak proof operation.

For the testing of vessel, pressure gauge was mounted and all the openings of vessel except that for liquid inlet valve V_2 were closed. The socket (5) for holding heating tube was closed by a dummy nut and valves were connected to the openings of the vessel. Then, compressed air was admitted into the vessel till a pressure of 200 kN/m^2 was indicated by the pressure gauge. After this valve V_2 was closed. The compressed air filled vessel was then submerged in the pool of water to identify leaky points. Identified leaky points, if any, were suitably attended and the vessel was tested again to ensure trouble free operation.

After testing of individual components, they were assembled to an experimental set-up, as shown in **Fig. 3.1**.

4.2 CHECKING OF MECHANICAL AND ELECTRICAL LEAKAGE

The mechanical leakage of the experimental set-up was checked by the following procedure: All valves except valve V_4 for compressed air entry were closed. Then, the set-up was pressurized up to a pressure of about 200 kN/m^2 (gauge) by admitting compressed air through inlet valve V_4 . Thereafter valve V_4 was also closed and the set up was examined for a period of 24 hours to identify leakage, if any. Any fall of pressure indicated by pressure gauge reading represents the existence of leakage in the set-up. To identify the leakage, soap-water solution was applied at all the joints of the vessel and pipelines, and each joint was examined carefully. Any leakage detected by formation of air bubbles was suitably attended. This process was repeated till no formation of air bubble was detected over the joints. Thereafter, the set-up was again filled with compressed air of a pressure of 200 kN/m^2 (gauge) and kept for a period of 48 hours. No alteration in the reading of pressure gauge was noted.

After the set-up was tested successfully against pressure, it was then tested against vacuum by creating a vacuum. For this purpose, a vacuum gauge was mounted at the vessel. A vacuum of 600 kN/m^2 (gauge) was developed inside the vessel by the use of vacuum pump. No alteration in the reading of vacuum gauge over a period of 48 hours was observed. This confirmed that the set-up was completely leak proof.

For operational safety, experimental set-up was well insulated against any electrical leakage. For this purpose, the set-up was examined for electrical leakage by passing electrical current through the heater. The leaky points were immediately repaired. However, for safe experimentation the set-up was properly earthed to eliminate any possibility of electrical short-circuiting.

4.3 THERMOCOUPLE INSTALLATION

The PTFE coated thermocouples made in the laboratory were wrapped with Teflon tape and again inserted in another PTFE sleeve to make them a little bit stiff, so that they can be inserted in the holes easily without any buckling. Each thermocouple was then inserted in hole made in wall thickness of heating tube. The insertion of thermocouples was carried out with great care so that their beads remain in perfect contact with the wall surface. It is significant to point out here that the wrapped and sleeved thermocouples occupied almost entire space in the holes. This provided very little stagnant air between thermocouple and wall surface. Thus, there was absolutely no possibility of any heat loss by convection through air present in the holes. So, the thermocouples indicated the true temperature at their respective locations.

Thermocouple probes were used for the measurement of liquid temperature. They are placed in through fittings welded in the body at top, bottom and side positions of heating tube corresponding to wall thermocouples positions. All probes were positioned at a sufficient distance away from heating tube so that they were outside the superheated boundary layer surrounding the tube. For this purpose, liquid was boiled and probes were moved away from tube gradually till they display no change in their e.m.f. values. This methodology ensured the measurement of bulk temperature of the liquid.

4.4 PRELIMINARY OPERATIONS

A set of preliminary operations was carried out before conducting series of experiments, in order to obtain precise, reliable and reproducible data. This included cleaning and rinsing of vessel, charging of liquid, stabilization of heating tube and deaeration of liquid pool. The details of these are as follows:

➤ ***Cleaning and Rinsing:***

For cleaning, all the components of experimental set-up were flushed with compressed air to remove foreign solid particles adhering to their surfaces. This was carried out by admitting compressed air on the system through valve V_4 while keeping valve V_1 and V_3 opened and valve V_5 closed. Thereafter, all valves except V_5 and V_6 were closed and vacuum was created inside vessel by vacuum pump. Now a soap-water solution was sucked through flexible tube and valve V_2 into the vessel. After this, vacuum was released and compressed air at a pressure of 200 kN/m^2 was admitted to vessel via valve V_4 . The compressed air gave a whirling motion to soap-water solution in the vessel and this helped to loosen the adherence of dust and other foreign particles on inner surface of vessel. Then, water-soap solution was drained out from the vessel through valve V_1 . Afterward, distilled water was admitted into the vessel via flexible tube and after adopting above procedure liquid was drained out. This process was repeated several times till drained-off liquid was found to be completely free from dust and other foreign particles. Subsequently heating tube surface was also cleaned with distilled water and acetone and finally with the test liquid before fitting the same in vessel.

Further, rinsing of vessel was carried out by filling liquid under investigation into the vessel, shaking it with compressed air and then draining it out from the vessel. This procedure is repeated several times to ensure rinsing of each component and surface of vessel and heating tube.

➤ ***Charging of Liquid:***

After vessel was cleaned and rinsed properly, the test liquid was charged into it by creating a vacuum inside it by adopting same procedure as

discussed above. The liquid was filled up to a height of 100 mm from top surface of heating tube.

➤ **Stabilization of Heating Tube:**

Before conducting series of experiments it was necessary to carry out aging and stabilization of the heat transfer surface. The procedure adopted for it was as follows: water (coolant) was passed into the condenser and heater was energized by supplying a power input of 600 W. The liquid temperature increased continuously till it reached to the saturation temperature corresponding to the pressure prevailing in the vessel. Usually, atmospheric pressure was maintained throughout the system during stabilization process. At this condition, liquid was boiled for several hours. The prolonged submergence of heating tube followed by vigorous boiling of about 72 hours makes the surface to be aged and thermally stabilized. This operation ensured accurate and reproducible experimental data. Further, this was confirmed by taking data at different intervals of time. The heat input was varied from 240 W to 640 W in six equal steps and set of data was taken at different intervals of time. The reproducibility of e.m.f. values of wall thermocouples, obtained during regular intervals of time, confirmed the reproducibility of experimental data.

To ensure homogeneity of heating tube surface, it was rotated by 90° and e.m.f values of wall thermocouples were noted down under the similar operating conditions by following procedure mentioned above. It was observed that the wall thermocouple readings taken before and after the rotation of the heating tube showed no change at all. This confirms homogeneity of heating tube surface.

➤ **De-aeration of Test Liquid Pool:**

Presence of dissolved air in the liquid pool and in the vessel above the liquid pool affects boiling heat transfer rate. So, it was necessary to remove dissolved air before experimentation. It was done by boiling of liquid for several hours and passing the dissolved air into a bubbler which was connected to the

vessel through valve V_2 by a PVC pipe. During this process all valves except V_2 and V_3 were closed. Continuous bubbling of air in the bubbler indicated de-aeration of liquid. This was carried out till bubbling in bubbler ceased, indicating no presence of dissolved air in liquid pool. At the end of de-aeration process valve V_2 was closed. This de-aeration procedure was exercised every time before starting a set of experimental runs.

4.5 DATA ACQUISITION

After completing all preliminary operations the set-up was ready for experimentation. Following steps were taken to conduct experiments for the boiling of liquid and their binary mixtures:

At first the vessel was subjected to atmospheric pressure by opening the valve V_4 . Then, heating tube was energized with the lowest heat input of 240 W. As a result, temperature of liquid increased gradually until it reached to the saturation temperature corresponding to atmospheric pressure. At that condition, the e.m.f readings of all thermocouples as indicated by DMM were kept under continuous observation. At steady state, no change in e.m.f. readings of all wall and liquid thermocouples were noted down. The heat input rate was then adjusted to the next prefixed higher value and procedure as mentioned above was repeated. Heat input rate was increased from 240 W to 640 W in six equal steps. After completing experiments at atmospheric pressure, the system was maintained at sub-atmospheric pressure by creating vacuum in it and above mentioned procedure was repeated to obtain boiling heat transfer data. Pressure in the test vessel was varied from 44.40 kN/m² to 97.71 kN/m². The liquids investigated in present investigation were distilled water, methanol and their seven binary mixtures.

Four number of heating tubes-one plain and three copper coated stainless steel tubes having coating thicknesses of 22, 43, and 67 μm were used in this investigation. Experimental data for distilled water were obtained at all the four tubes, and after analysis of data, so obtained, optimum coating thickness tube (ST-43) was identified. Then experiments were conducted for methanol and methanol-distilled water binary mixtures using both – plain and

43 μm copper coated stainless steel tube in the same manner as discussed above.

While conducting experiments with binary liquid mixtures the sample of liquid and vapor were taken at all heat fluxes using liquid and vapor sampling arrangements, respectively as shown in **Fig. 3.2**, with the help of an air-tight syringe. The samples collected were immediately kept in a refrigerator to avoid flashing of methanol. The samples were then analyzed with the help of HPLC in Instrumentation Laboratory of IIT Roorkee where the room temperature was maintained at 15 $^{\circ}\text{C}$. To obtain the calibration curve, samples of known composition of methanol-water mixture were prepared and their peak areas for methanol were measured. These values were plotted against composition for methanol-water mixtures as shown in **Fig. 4.1**. This plot served as a reference curve for evaluating compositions of liquid and vapor samples drawn during experimentation.

The operating parameters used in this investigation are listed in **Table 4.1**.

4.6 REPRODUCIBILITY AND CONSISTENCY

Reproducibility and consistency of experimental data was most important for their accurate and reliable analysis. Reproducibility was examined by conducting experiments at different times under the same operating condition. As no discernable variation in the readings of wall thermocouples was noted, data were considered to be reproducible.

Also, the confirmation of homogeneity of heating tube surface during preliminary operations validates the consistency of experimental data. Besides, analysis of data for circumferential variation of wall temperature around heating tube shows that surface temperature increases continuously from bottom to side to top position. This behaviour is in accordance to the literature available on variation of surface temperature of heating tube during nucleate pool boiling, as discussed in detail in Chapter-5. Thus, above tests prove that data obtained in the present investigation are consistent.

4.7 OPERATIONAL CONSTRAINT

The operating variables in present investigation were heat flux, pressure,

coating thickness and liquids. The ranges of these variables were selected on the basis of following criteria:

The maximum power input to electric heater was decided on the basis of current carrying capacity of wire used in the construction of electric heater. However, minimum heat input was decided by the value at which sustained nucleate boiling of liquid occurs. In present investigation 24-gauge Nichrome wire having a maximum current carrying capacity of 5 A was used to make the heater. Accordingly, the maximum power input to the heater was limited to 640 W, which corresponds to a heat flux of $42,524.92 \text{ W/m}^2$. The minimum power input at which sustained boiling of liquid can occur was 240 W, which is equivalent to a heat flux of $15,946.84 \text{ W/m}^2$.

The lowest pressure in vessel was established by the vacuum, which it could sustain without any mechanical vibration. It was found to be 81.00 kN/m^2 vacuum. However, the lowest pressure used in the present investigation was 44.40 kN/m^2 .

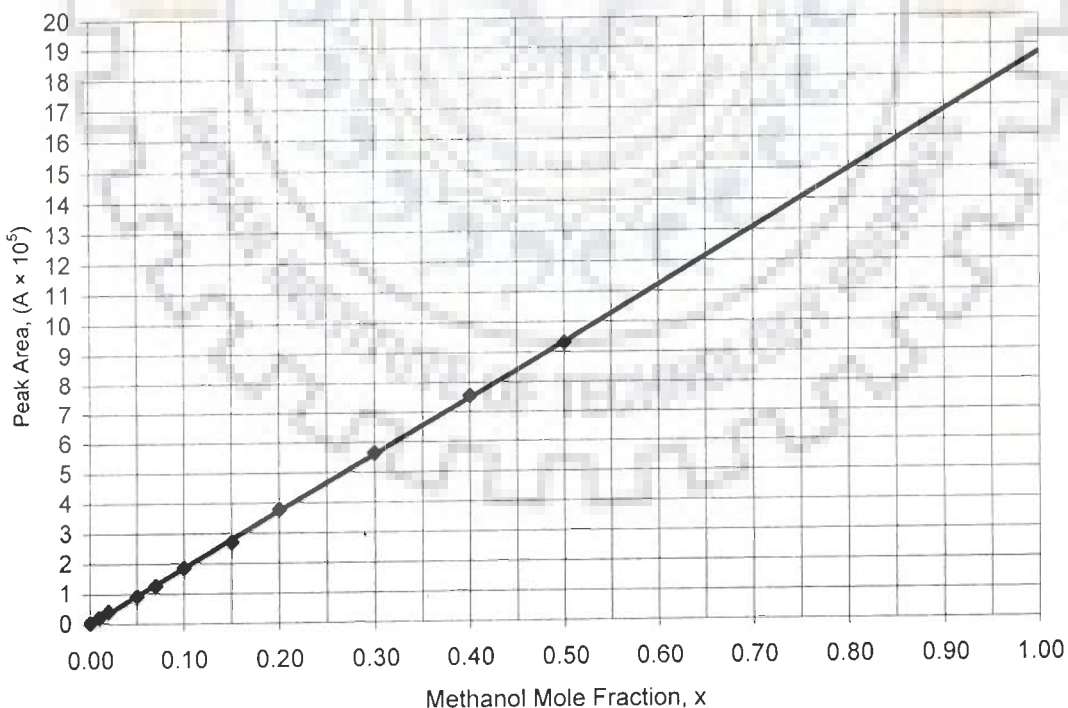


Fig. 4.1 Calibration curve for measurement of methanol concentration using HPLC system

Table 4.1 Operating parameters of present investigation

S. No.	Heating tube	Pressure (kN/m ²)			Heat flux (W/m ²)		
I. Distilled Water							
1	ST-00	97.71, 57.73,	84.39, 44.40	71.06,	15946.84, 31893.69,	21262.46, 37209.30,	26578.07, 42524.92
2	ST-22	97.77, 57.81,	84.43, 44.52	71.17,	15950.39, 31900.77,	21267.18, 37217.57,	26583.98, 42534.36,
3	ST-43	97.71, 57.68,	84.37, 44.44	71.11,	15946.84, 31893.69,	21262.46, 37209.30,	26578.07, 42524.92
4	ST-67	97.76, 58.01,	84.83, 44.72	71.67,	15855.38, 31699.44,	21273.84, 36982.68,	26416.20, 42265.91
II. Methanol							
5	ST-0	97.71, 57.73,	84.69, 45.05	71.26,	15946.84, 31893.69,	21262.46, 37209.30,	26578.07, 42524.92
6	ST-43	97.76, 58.15,	85.13, 44.82	70.97,	15946.84, 31893.69,	21262.46, 37209.30,	26578.07, 42524.92
III. 5% methanol-water mixture							
7	ST-00	97.70, 57.32,	85.05, 45.41	71.28,	15946.84, 31893.69,	21262.46, 37209.30,	26578.07, 42524.92
8	ST-43	97.71, 57.96,	84.43, 44.71	71.09,	15946.84, 31893.69,	21262.46, 37209.30,	26578.07, 42524.92
IV. 10% methanol-water mixture							
9	ST-00	97.71, 57.73,	84.49, 44.40	71.11,	15946.84, 31893.69,	21262.46, 37209.30,	26578.07, 42524.92
10	ST-43	97.77, 57.81,	84.43, 44.32	71.47,	15946.84, 31893.69,	21262.46, 37209.30,	26578.07, 42524.92
V. 30% methanol-water mixture							
11	ST-00	97.82, 57.68,	84.37, 44.84	71.00,	15946.84, 31893.69,	21262.46, 37209.30,	26578.07, 42524.92
12	ST-43	97.76, 58.08,	84.83, 45.02	71.32,	15946.84, 31893.69,	21262.46, 37209.30,	26578.07, 42524.92
VI. 50% methanol-water mixture							
13	ST-00	97.74, 58.05,	84.56, 44.61	71.00,	15946.84, 31893.69,	21262.46, 37209.30,	26578.07, 42524.92
14	ST-43	97.59, 57.56,	84.74, 44.57	70.87,	15946.84, 31893.69,	21262.46, 37209.30,	26578.07, 42524.92
VII. 80% methanol-water mixture							
15	ST-00	97.66, 57.71,	85.07, 44.32	70.95,	15946.84, 31893.69,	21262.46, 37209.30,	26578.07, 42524.92
16	ST-43	98.02, 57.83,	84.45, 44.64	71.23,	15946.84, 31893.69,	21262.46, 37209.30,	26578.07, 42524.92
VIII. 90% methanol-water mixture							
17	ST-00	97.68, 57.02,	84.55, 43.60	70.77,	15946.84, 31893.69,	21262.46, 37209.30,	26578.07, 42524.92
18	ST-43	97.71, 57.73,	84.69, 45.05	71.26,	15946.84, 31893.69,	21262.46, 37209.30,	26578.07, 42524.92
IX. 95% methanol-water mixture							
19	ST-00	97.70, 57.61,	85.07, 44.34	70.99,	15946.84, 31893.69,	21262.46, 37209.30,	26578.07, 42524.92
20	ST-43	97.86, 57.90,	84.46, 44.50	71.29,	15946.84, 31893.69,	21262.46, 37209.30,	26578.07, 42524.92

Chapter-5

Results and Discussion

This chapter deals with results and discussion of the experimental investigation for enhanced boiling conditions

RESULTS AND DISCUSSION

In this Chapter, results of experiments conducted for saturated boiling of distilled water, methanol and their binary mixtures on a horizontal copper coated stainless steel heating tube (hereafter referred as coated tube) surface and their interpretation have been discussed. It also includes a comparison between thermal effectiveness of a coated and a plain (hereafter referred as uncoated) tube to bring out the usefulness and applicability of copper coating on an uncoated tube for enhanced boiling of liquids and mixtures.

Experimental data of present investigation for boiling of saturated liquids and their mixtures on an uncoated as well as on coated heating tubes are listed in Tables B.1 to B.20 of Annexure-B. These include heat flux, liquid and surface temperatures at bottom, two sides and top positions of heating tube and heat transfer coefficient. Heat flux varied from 15946.84 W/m² to 42524.92 W/m² in 6 steps and pressure from 44.40 kN/m² to 97.71 kN/m² in 5 steps. Saturated liquids – distilled water, methanol and their binary mixtures are used in this investigation. Three thicknesses of copper coating namely; 22, 43, and 67 μm have been employed over uncoated stainless steel heating tubes.

5.1 LIMITATIONS OF PRESENT ANALYSIS

The present investigation pertains to measurement of liquid and surface temperatures of heating tube. For this purpose, copper-constantan thermocouples have been employed. They have been mounted at top, two sides and bottom positions of heating tube to measure the variation in surface temperature around tube circumference, if any. Further, thermocouples have been placed at a pitch circle diameter [$d_h = (d_i + d_o)/2$] in the wall thickness of heating tube. Thus, they have not measured the temperature of outer surface of the tube directly. So a temperature drop, δT_w across the thickness between thermocouple location and outer tube surface has been calculated by the use of following equation for heat conduction in a thin cylinder:

$$\delta T_w = \frac{qd_o}{2k_w} \ln\left(\frac{d_o}{d_h}\right) \quad (5.1)$$

The temperature drop, δT_w , so obtained, has been subtracted from the recorded temperature of heating tube measured by wall thermocouple to obtain outer surface temperature. Further, it is assumed that heat is transmitted radially to liquid pool from heating tube surface. This has also been substantiated by the fact that no significant variation in thermocouples readings was noticed when wall thermocouples were moved longitudinally. Besides, a thick plug covered with a thick sheet of PTFE provided at the closed end of the heating cylinder that diminished the possibility of any heat flow in longitudinal direction. This has already been explained in detail in Chapter-3. Arithmetic averaging has been employed to obtain the average temperature of heating surface. Thermocouple probes have also been mounted in the liquid pool at various circumferential positions corresponding to surface thermocouples i.e. at the top, the two sides and the bottom. All the probes have been placed in liquid pool at a sufficient distance away from tube surface so as to monitor bulk temperature of liquid. An arithmetic averaging has also been used to obtain the mean temperature of the liquid. Sample calculation, as given in Annexure-C clearly describes the method of calculation for heat transfer coefficient. An uncertainty analysis of each experimental run has been carried out as per procedure outlined in Annexure-D. The maximum uncertainty associated with heat transfer coefficient has been found to be of the order of $\pm 1.13\%$.

It is important to mention here that the measured values of liquid temperature have been slightly different than saturation temperature corresponding to pressure prevailing in the unit. This might be due to impurities present in the chemical used in this investigation. Besides, an insignificant difference in the values of surface temperature measured at the two side positions of the tube has also been noticed. Although difference is quite small yet it has been taken into account while computing the values of local and average heat transfer coefficient. Physico-thermal properties of liquids have been taken at arithmetic mean of liquid temperatures around the tube circumference. The physico thermal properties of binary liquid mixtures have been calculated at their saturation temperatures corresponding to the prevailing

pressure. The calculated values of the properties for pure liquids and their mixtures are given in Annexure-E.

Electroplating technique has been employed for coating copper over an uncoated stainless steel heating tube using the procedure given in Annexure-A. However, it has not been possible to get thickness of coating below 22 μm due to various constraints involved in coating operation. It is worthwhile to mention here that temperature drop across the thickness of copper coated layer has not been included in the determination of heat transfer coefficient. In other words, calculation of heat transfer coefficient for coated tube is based on substrate surface temperature only. This has enabled a comparison of heat transfer characteristics on a coated tube with that on an uncoated tube.

5.2 NUCLEATE BOILING OF SATURATED LIQUIDS ON AN UNCOATED HEATING TUBE

Experimental data for nucleate pool boiling of distilled water and methanol are given in Tables B.1 and B.5 of Annexure-B. Using these data, temperature profiles, variation of heat transfer coefficient along the circumference of an uncoated heating tube and average heat transfer coefficient for saturated boiling of liquids have been determined. It also includes the effect of heat flux, pressure and liquid on local and average heat transfer coefficient and thereby a functional relationship between heat transfer coefficient and these variables. These are discussed in the following subsections:

5.2.1 Circumferential variation of surface temperature

Figures 5.1a to 5.1e demonstrate plots representing variation of surface temperature along the circumference of an uncoated heating tube for saturated boiling of distilled water at atmospheric and subatmospheric pressures with heat flux as a parameter. Each plot is for a distinct pressure specified therein. They also include a curve to show the variation of liquid temperature around tube circumference. From an inspection of a plot, following salient features have emerged out:

- i. At a given heat flux, surface temperature increases from bottom to side to top position of heating tube.
- ii. For a given circumferential position, a rise in heat flux increases surface temperature.
- iii. The liquid temperature remains constant irrespective of circumferential position and heat flux imposed on heating tube.

These features are consistent and can be explained by the following reasoning:

In nucleate pool boiling of liquids at given pressure vapor-bubbles form at active nucleation sites randomly distributed over the heating surface. They grow in size and depart from the surface after attaining maximum size, to travel in the pool of liquid. However, when boiling occurs on a tube surface, growth of vapor-bubbles is not uniform throughout the circumference due to its cylindrical geometry. As a matter of fact, bubbles generated at top position have free access to travel upward whereas those formed at bottom and side positions do not have so. In fact, bubbles formed at bottom position slide upward along wall surface as their movement get continuously accelerated due to increase in buoyancy force. In doing so, they push the bubbles formed at adjoining circumferential positions on their way and carry them along the wall surface to reach to top position. Therefore, frequency of bubble formation increases continuously as one moves from bottom to side to top position. Coalescence of vapor-bubbles leading to form agglomerates and thereby vapor clouding occurs in this thick layer of vapor-bubbles engulfing the tube circumference. The thickness of this layer increases along the circumference from bottom to side to top position. Since this layer obstructs the passage of heat from tube surface to liquid, heat removal rate decreases from bottom to side to top position. In other words, bottom position provides the highest heat removal rate followed by side and top positions in decreasing order. As a consequence, wall temperature is found to increase continuously from bottom to side to top position. Above phenomena has also been observed by Kang [78] and Gupta et al. [55].

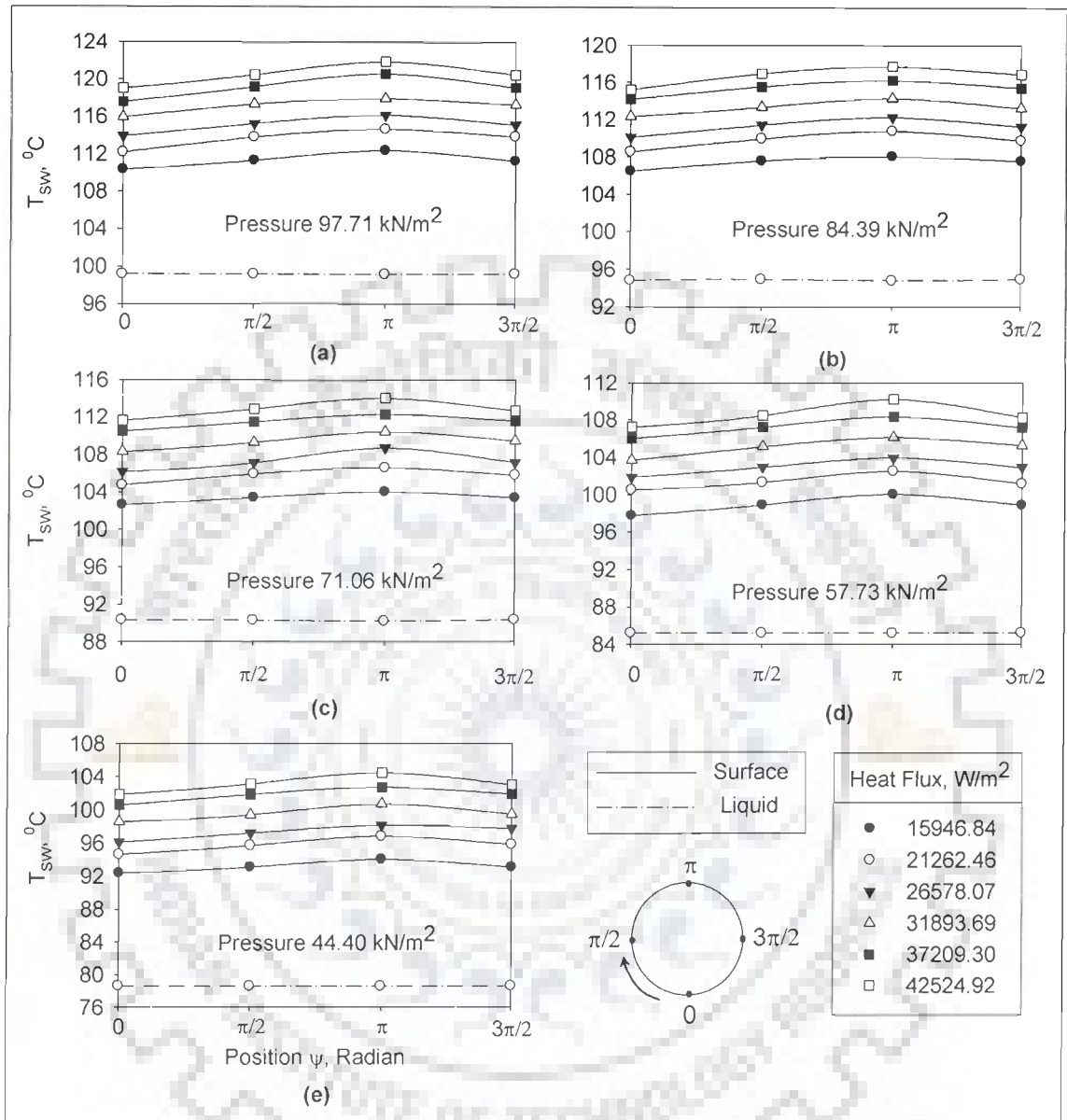


Fig. 5.1 Variation of liquid and surface temperature along circumference at bottom, two sides and top position of an uncoated heating tube with heat flux as a parameter for boiling of distilled water at atmospheric and subatmospheric pressures

At a given circumferential position, increase in surface temperature with increase in heat flux is owing to the fact that an increase in heat flux leads to higher heat transfer rate which is accompanied with higher wall superheat and thereby the surface temperature.

As a constant pressure has been maintained in the unit throughout experimentation, so the temperature of liquid pool remains constant.

Figures 5.2a to 5.2e represent plots for the variation of surface and liquid temperatures along the circumference of an uncoated heating tube for the boiling of methanol at atmospheric and subatmospheric pressures. These plots have essentially the same features, as discussed above for distilled water.

On the basis of above, it is concluded that a significant variation in surface temperature exists along the circumference of a heating tube during boiling of liquids at atmospheric and subatmospheric pressures. In other words, boiling on a heating tube is a non-uniform phenomena and therefore calls for an investigation to determine the extent of variation in heat transfer coefficient around heating tube.

5.2.2 Variation of local heat transfer coefficient

The plot shown in **Fig. 5.3a** depicts the variation of local heat transfer coefficient with heat flux for boiling of distilled water on an uncoated heating tube at atmospheric pressure. Circumferential position is a parameter in this plot. A close examination of this plot reveals the following points:

- i. At a given heat flux, value of local heat transfer coefficient increases from top to side to bottom position on heating tube.
- ii. At a given circumferential position, value of local heat transfer coefficient increases with increase in heat flux and the variation between the two can be represented by a power law, $h_{\psi} \propto q^{0.7}$.

Above features have also been found for the boiling of methanol, as shown in **Fig. 5.3b**. These features are obvious and can be explained as follows:

As mentioned in subsection 5.2.1, at a given heat flux surface temperature increases continuously from bottom to side to top position of

heating tube. So wall superheat, $\Delta T_w (= T_w - T_s)$ increases in the same order and therefore value of local heat transfer coefficient is found to decrease from bottom to side to top position on the heating tube. A rise in heat flux increases the surface temperature at a given circumferential position. This, in turn, increases the value of local wall superheat and thereby, according to following equation, value of minimum radius of nucleation site at which vapor-bubble can originate, to decrease:

$$r_c = \frac{2\sigma}{\left(\frac{dp}{dT}\right)_s \Delta T_w} \quad (5.2)$$

As the population of small sized nucleation sites on a heating surface is more than that of larger sized ones, large numbers of vapor-bubbles form, grow and detach from the surface to travel in the pool of liquid at high heat flux condition. All these activities lead to increase the intensity of turbulence and enhance heat removal rate. Consequently, local heat transfer coefficient is found to be higher at high value of heat flux.

Above features have also been observed during the boiling of liquids by earlier investigators [4, 16, 42, 105, 106]. At this stage it may be pointed out that although functional relationship between h_{ψ} and q remains unaltered irrespective of the liquid boiling on an uncoated heating tube surface, the magnitude of local heat transfer coefficient, at a given circumferential position on an uncoated heating tube, is found to differ from liquid to liquid. This is due to difference in physico-thermal properties of liquids under consideration. Further, similar behavior has also been observed during boiling of distilled water and methanol at subatmospheric pressures. Above also bring out, an important feature i.e. the variation of local heat transfer coefficient with pressure at a given circumferential position of a tube. In fact, it increases with raising pressure. This observation can be explained as follows: Raising pressure alters physico-thermal properties of the liquid. However, the most significant alteration appears in the value of surface tension. In fact, value of surface tension reduces with increase in pressure. This causes minimum radius of nucleation site at which vapor-bubble can originate to decrease, as can be

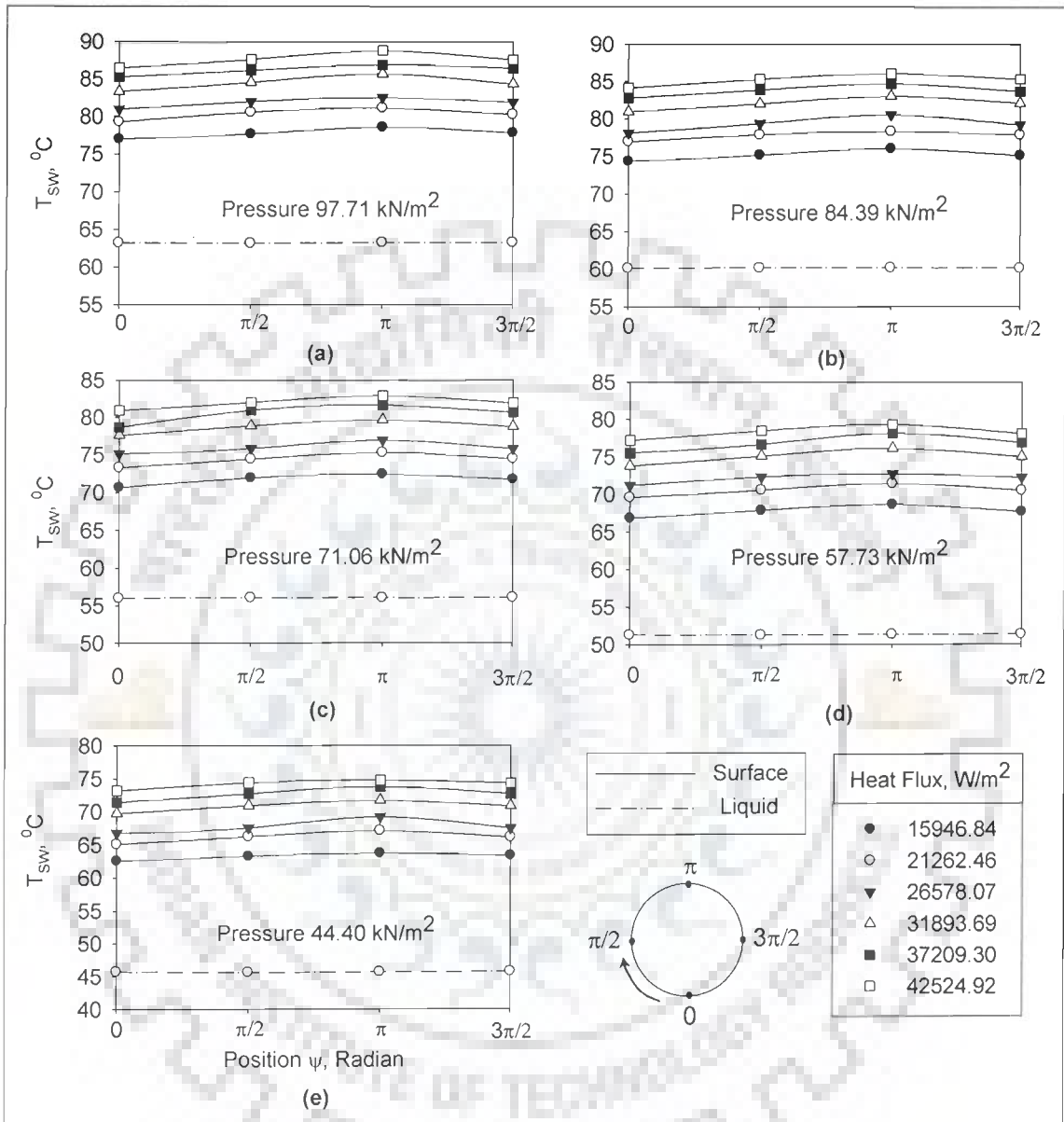


Fig. 5.2 Variation of liquid and surface temperature along circumference at bottom, two sides and top position of an uncoated heating tube with heat flux as a parameter for boiling of methanol at atmospheric and subatmospheric pressures

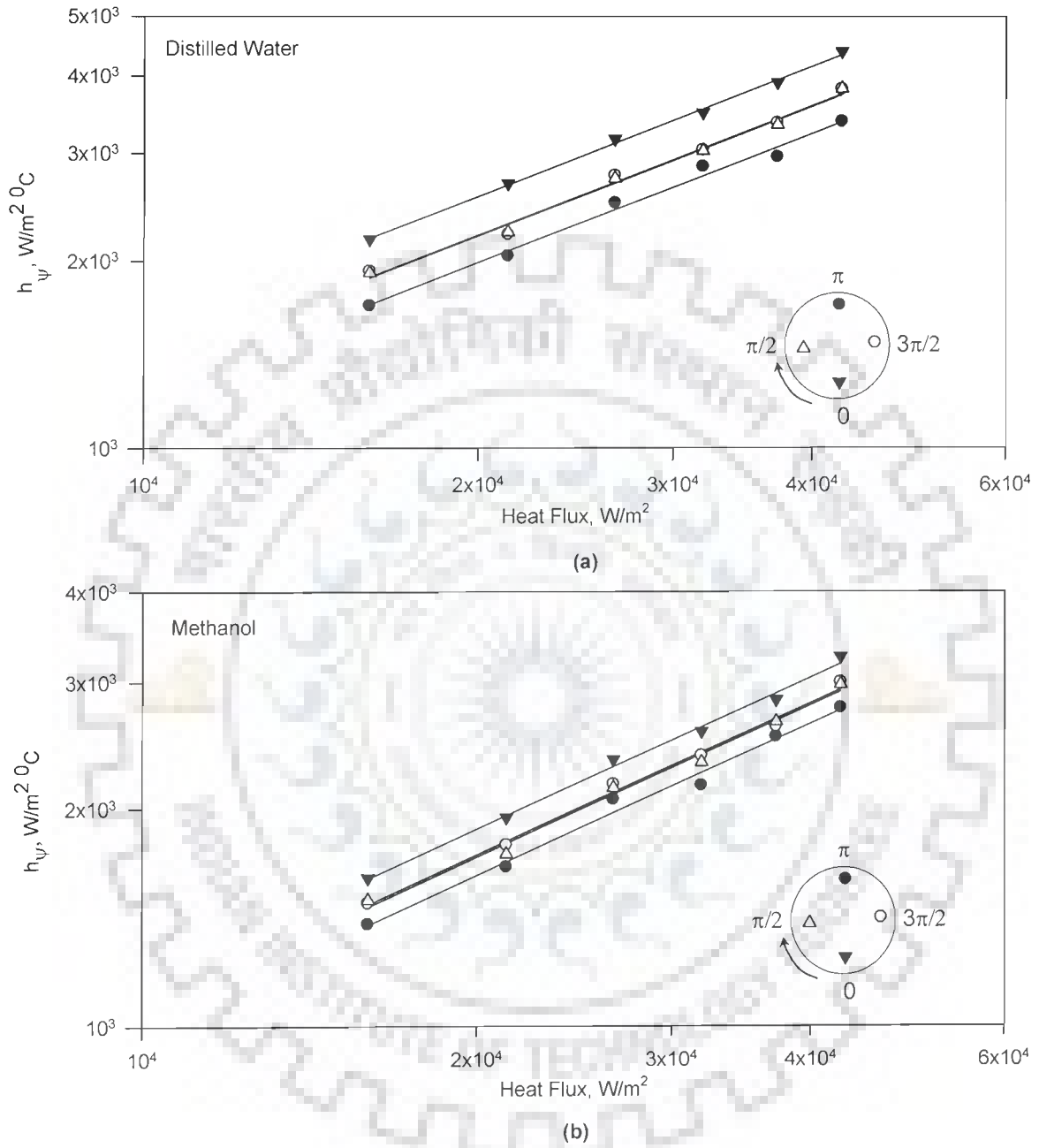


Fig. 5.3 Variation of local heat transfer coefficient with heat flux along the circumference of an uncoated heating tube for boiling of distilled water and methanol at atmospheric pressure

seen from **Eq. (5.2)**. Consequently, large numbers of small sized vapor-bubbles form, grow and detach from the surface to travel in the pool of liquid and thereby intensity of turbulence increases. This, in turn, causes higher heat removal rate and therefore heat transfer coefficient to increase.

From the above it is clear that local heat transfer coefficient for boiling of liquids on an uncoated heating tube is a function of heat flux, pressure and circumferential position. Hence, it was thought proper to develop an equation relating local heat transfer coefficient with these variables. Using method of least squares, following correlation of local heat transfer coefficient as a function of heat flux, pressure and circumferential position has been developed.

$$h_{\psi} = C_{\psi} q^{0.7} p^{0.32} \quad (5.3)$$

where, C_{ψ} is a constant whose value depends upon boiling liquid and circumferential position on a heating tube. These values are given in **Table 5.1**.

Table 5.1 Values of constant C_{ψ} of **Eq. (5.3)** for various saturated liquids at various circumferential positions

Liquids	Circumferential Position			
	Top	Side	Bottom	Side
Distilled water	0.444	0.49	0.566	0.491
Methanol	0.362	0.382	0.417	0.372

Figure 5.4 shows a plot between experimentally obtained values of local heat transfer coefficient and those computed from **Eq. (5.3)** for boiling of distilled water and methanol at atmospheric and sub-atmospheric pressures. This plot clearly shows an excellent agreement between the values predicted by **Eq. (5.3)** and experimental values within a maximum error of $\pm 7\%$. Thus, **Eq. (5.3)** can correlate experimental data of local heat transfer coefficient of various boiling liquids. In other words, above equation can be used to calculate the value of local heat transfer coefficient at any circumferential position on heating tube from the knowledge of heat flux and pressure provided the value of constant C_{ψ} is known. The value of constant C_{ψ} depends upon heating surface characteristics, circumferential position and boiling liquid.

The analytical determination of constant, C_{ψ} is highly improbable owing to variation in size, shape and number of irregularities present on a tube

surface. Hence, **Eq. (5.3)** can not be employed for the determination of local heat transfer coefficient of those heating surface-liquid combinations whose value of constant C_ψ is not experimentally known. In other words, **Eq. (5.3)** is of limited applicability.

5.2.3 Variation of average heat transfer coefficient

As discussed in preceding subsection, a significant variation in surface temperature exists along the circumference of a heating tube. Hence, values of surface temperatures measured at top, two sides and bottom positions have been averaged arithmetically to obtain true representative surface temperature of the entire tube circumference. Similarly, average temperature of liquid pool has also been calculated. Using them, average heat transfer coefficient (hereafter referred as heat transfer coefficient) has been calculated corresponding to each heat flux subjected to an uncoated heating tube for saturated boiling of distilled water and methanol at atmospheric and subatmospheric pressures. The procedure used for computation of heat transfer coefficient is given in Annexure-C, Sample Calculation. The computed values of heat transfer coefficient for each experimental run are also given in the last column of Tables B.1 and B.5 of Annexure-B.

Figure 5.5 depicts a plot between heat transfer coefficient and heat flux for saturated boiling of distilled water at an atmospheric pressure. It also contains experimental data of earlier investigators namely Alam et al. [4], Benjamin & Balakrishnan [9], Bhaumik et al. [15], Borishanskii et al. [19], Cryder & Finalborgo [39], Dhir & Liaw [43], Hinrichs et al. [61], Hsieh & Hsu [63], Kurihara & Myers [83], Wang & Dhir [150], and Young & Hummel [155], for the purpose of comparison. A close examination of this plot reveals the following features:

- i. Data of present investigation do not match with those of any of earlier investigators.
- ii. Data of earlier investigators do not match amongst themselves. However, data points of an investigator forms a distinct group and obey power law relationship, $h \propto q^{0.7}$.

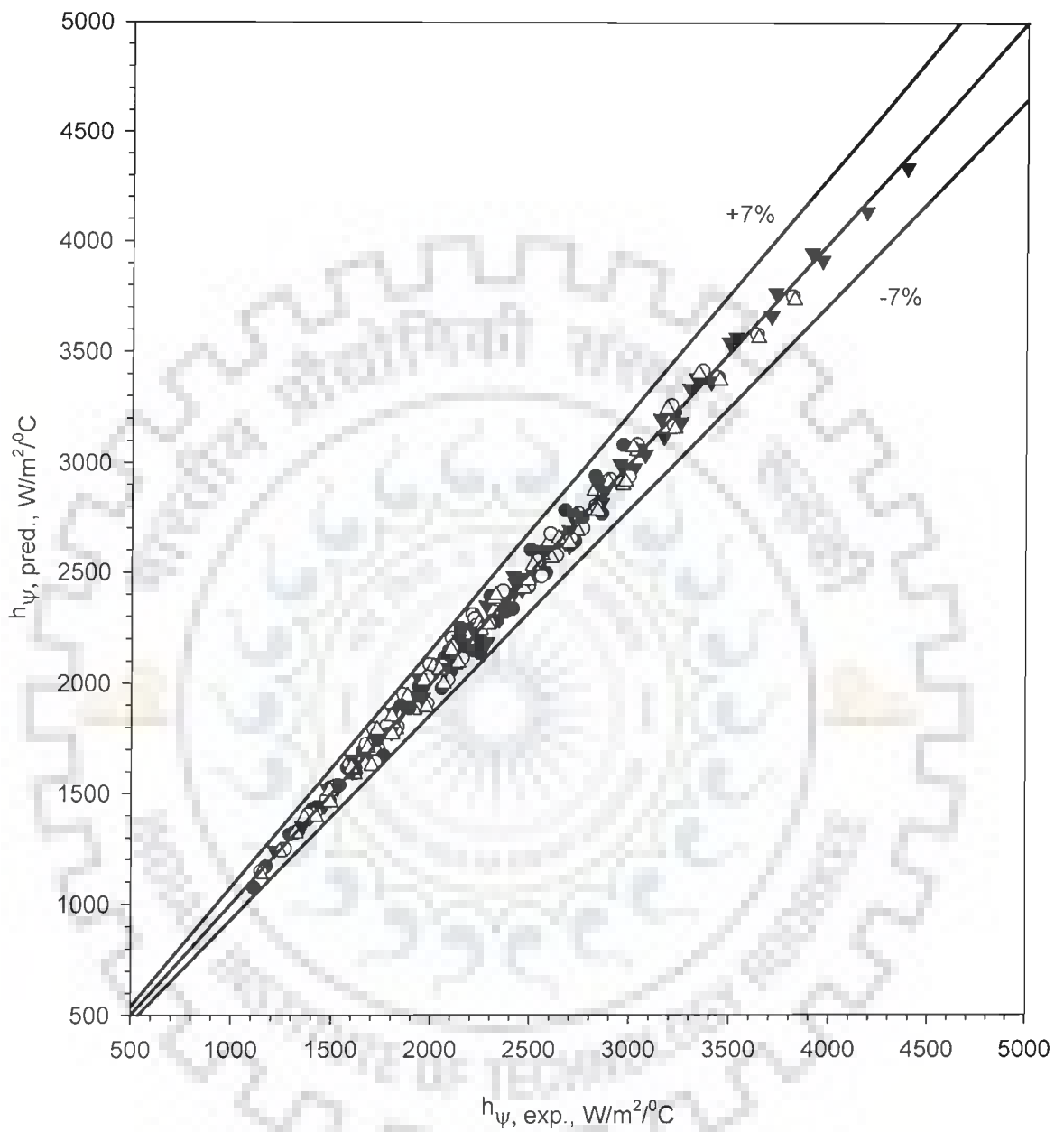


Fig. 5.4 Comparison of experimental local heat transfer coefficients with those predicted from **Eq. (5.3)** for pool boiling of distilled water and methanol at atmospheric and subatmospheric pressures

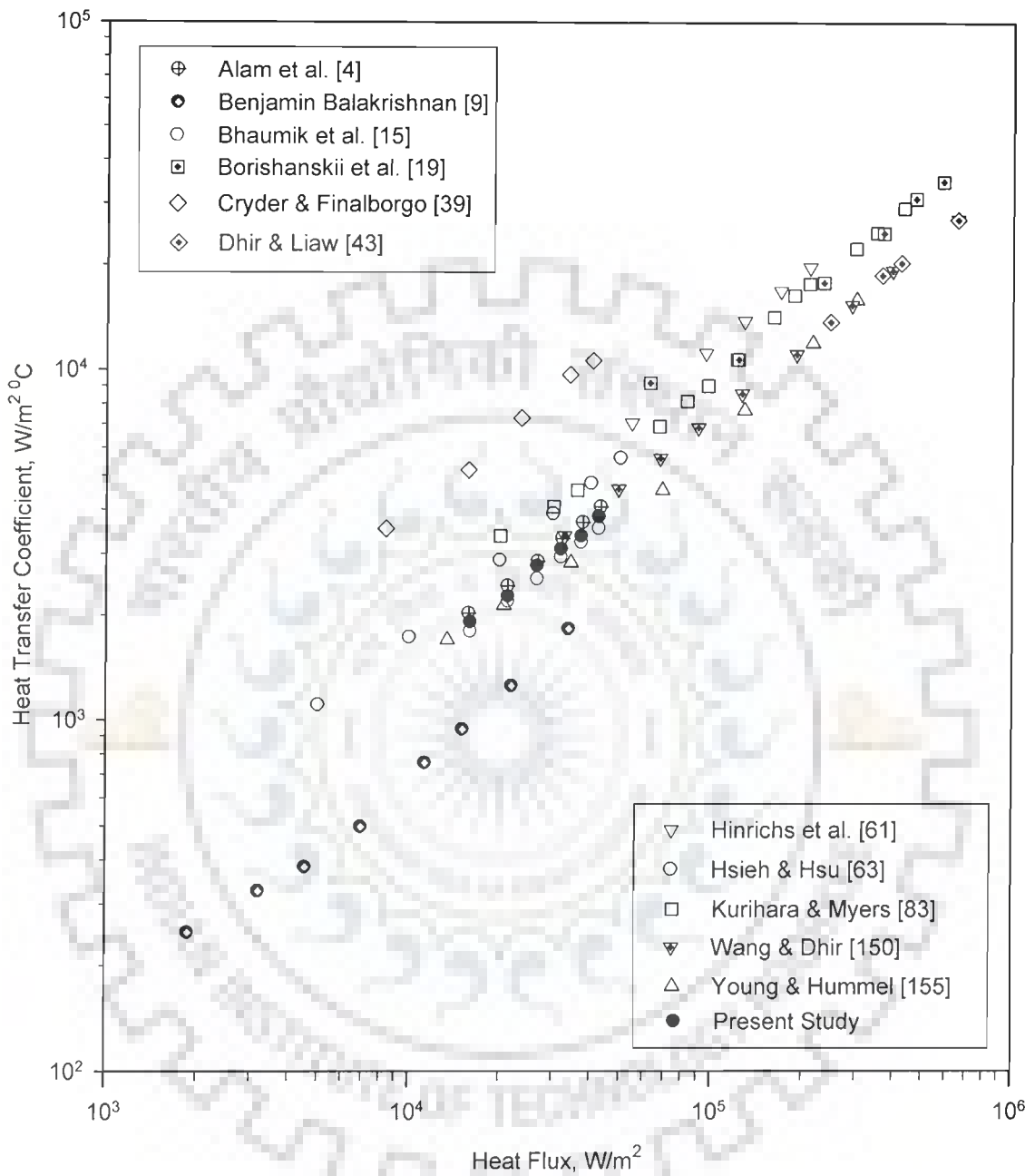


Fig. 5.5 Comparison of experimental data of this investigation with those of earlier investigators for boiling of distilled water at atmospheric pressure

These features are quite obvious as heating surfaces employed in these investigations have differed in their surface characteristics owing to differing roughness, material of construction, etc. Since boiling is a surface phenomena, above disagreement amongst data of various investigators is bound to occur. On the basis of above, it can be said that it is difficult to compare boiling heat transfer data of an investigator conducted on a heating surface with the data of other investigators.

Figure 5.6a represents a plot to show the variation of heat transfer coefficient with heat flux for saturated boiling of distilled water. Pressure is a parameter in this plot. Following key features have been drawn from this plot:

- i. For a given pressure, heat transfer coefficient increases with an increase in heat flux and the variation between the two can be described by a power law, $h \propto q^{0.7}$.
- ii. At a given heat flux, an increase in pressure enhances the value of heat transfer coefficient.

Both the above features are consistent and in accordance with the physics of boiling phenomena. Possible explanation for these features is as follows:

As explained earlier, an increase in heat flux raises local wall superheat which, in turn, leads to increase average wall superheat of heating tube. This according to equation, **Eq. (5.2)** causes the value of minimum radius of nucleation site at which vapor-bubble can originate, r_c to decrease. Consequently, nucleation sites of smaller sizes present on heating surface get activated and generate vapor-bubbles. As population of such sites is large, more number of small sized vapor-bubbles forms at enhanced value of heat flux. This increases the intensity of turbulence which in turn leads to higher rate of heat removal and thereby higher heat transfer coefficient.

An increase in pressure, as discussed in subsection 5.2.2, enhances intensity of turbulence caused by vapor-bubble dynamics due to the occurrence of large population of small sized vapor-bubbles. As a result high value of heat removal rate occurs and so heat transfer coefficient is found to be higher at an elevated pressure.

Boiling of methanol provided the same features as observed above for the boiling of distilled water. This can be easily seen from **Fig. 5.6b** which is a plot between heat transfer coefficient and heat flux for saturated boiling of methanol at atmospheric and subatmospheric pressures. It may be mentioned here that above features have also been observed by Cryder & Finalborgo [39] for boiling of water, methanol, carbon tetrachloride, and n-butanol on a brass surface, Bonilla & Perry [18] for boiling of water, ethanol, n-butanol and acetone on copper surfaces and Kurihara & Myers [83] for boiling of water, carbon tetrachloride, acetone and n-hexane on a copper surface. Thus, this investigation has corroborated the findings of earlier investigators for saturated boiling of liquids on an uncoated heating surface at atmospheric and subatmospheric pressures.

On the basis of above, it can be said that heat transfer coefficient for boiling of a liquid on an uncoated heating tube depends upon heat flux and pressure. Therefore, a functional relationship amongst them has also been developed by the method of least squares using experimental data of this investigation for the boiling of distilled water and methanol. The functional relationship is as follows:

$$h = C_1 q^{0.7} p^{0.32} \quad (5.4)$$

Where, C_1 is a constant whose value depends up on the type of boiling liquid and heating surface characteristics. The values of constant C_1 are 0.494 and 0.389 for distilled water and methanol, respectively in this investigation.

Figure 5.7 depicts a plot between experimentally determined values of heat transfer coefficient and those predicted from **Eq. (5.4)** for the boiling of distilled water and methanol at atmospheric and subatmospheric pressures on an uncoated heating tube. From this plot, it is noticed that predictions match excellently with experimental values within a maximum error of $\pm 5\%$. Therefore **Eq. (5.4)**, which is a simple and convenient one, can be used for the computation of heat transfer coefficient of a liquid boiling on an uncoated heating tube from the knowledge of heat flux and pressure provided the value of constant C_1 is known.

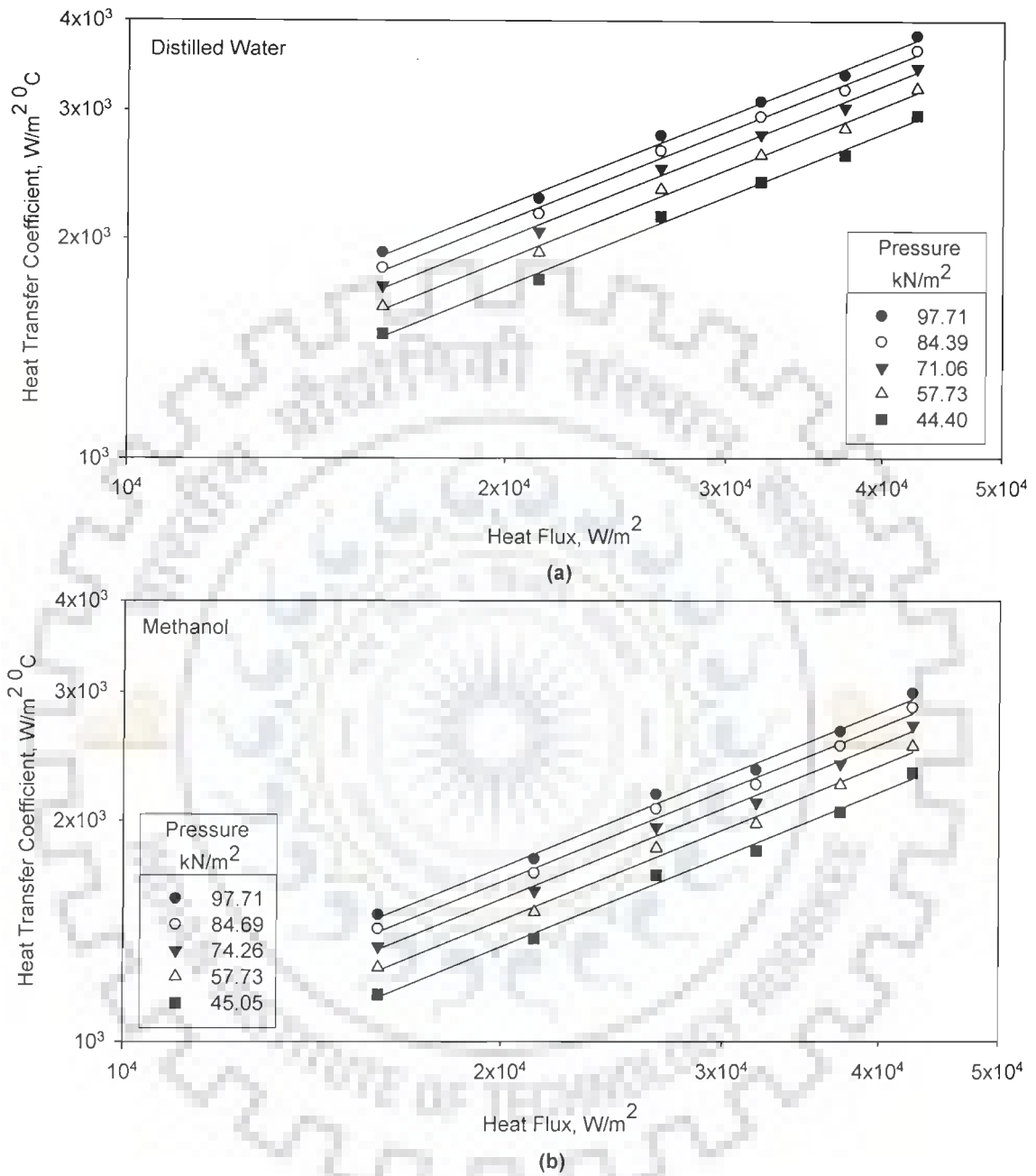


Fig. 5.6 Variation of heat transfer coefficient with heat flux for boiling of distilled water and methanol over an uncoated heating tube with pressure as a parameter

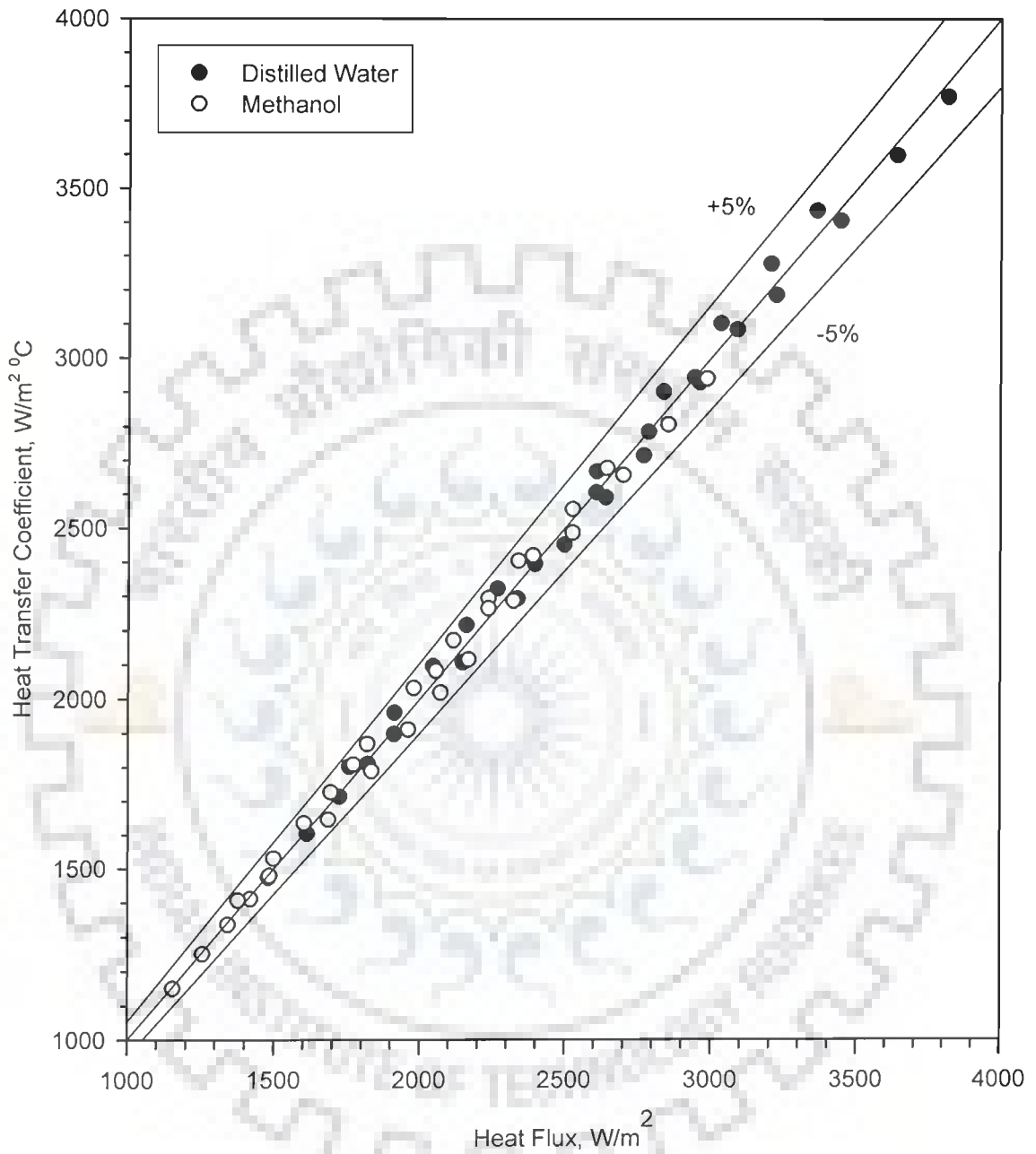


Fig. 5.7 Comparison of experimental heat transfer coefficients with those predicted from Eq. (5.4) for boiling of saturated liquids on an uncoated heating tube surface at atmospheric and subatmospheric pressures

5.2.4 Heat transfer correlation for boiling of liquids at subatmospheric pressure

Above discussion has established a simple equation, **Eq. (5.4)**, relating heat transfer coefficient with heat flux and pressure for the boiling of liquids at atmospheric and subatmospheric pressures. This equation also contains a constant, C_1 whose determination is necessary for its applicability. As pointed out above, the value of constant C_1 depend upon nature of liquid and characteristics of heating surface involved in the process. This, in turn, depends upon number and shape of irregularities present on the surface. An analytical determination of them is highly improbable. So it is quite difficult to represent C_1 in terms of measurable parameters. In other words, it calls for the development of a method which may make **Eq. (5.4)** free from the constant, C_1 . Following paragraphs attempt it:

As it has been established by this investigation as well as by earlier investigators, heat transfer coefficient of a boiling liquid is related to heat flux by power law, $h \propto q^{0.7}$ for atmospheric and subatmospheric pressures, so a term $h^* (= h/q^{0.7})$ is defined. The term, h^* incorporates the built in relationship between h and q . With this **Eq. (5.4)** reduces to:

$$h^* = C_1 p^{0.32} \quad (5.5)$$

Equation (5.5) can also be rewritten in following form if one assume that value of constant, C_1 does not depend upon pressure:

$$\frac{h^*}{h_1^*} = \left(\frac{p}{p_1} \right)^{0.32} \quad (5.6)$$

where, subscript 1 refers to one atmosphere pressure.

Equation (5.6) is tested against experimental data for the boiling of distilled water and methanol on an uncoated heating surface of this investigation; of water, methanol, carbon-tetrachloride and n-butanol on a brass tube surface by Cryder & Finalborgo [39]; of n-heptane on a copper plate surface by Cichelli & Bonilla [33]; of distilled water, methanol, ethanol and

isopropanol on a brass tube surface by Vittala et al. [148,149]; of distilled water on a stainless steel tube surface by Bansal [8]; of distilled water, benzene and toluene on a stainless steel surface by Bhaumik [16]; of distilled water on a mild steel heating tube surface by Alam et al. [4]; of methanol on a mild steel heating tube surface by Prasad et al. [105]; and of isopropanol on a mild steel heating tube surface by Prasad [106]. The comparison between predictions due **Eq. (5.6)** and the experimental values is shown in **Fig. 5.8**. As can be seen, the predictions are in excellent agreement with experimental values within an error of -12 to +9%. Thus, **Eq. (5.6)** is capable of correlating experimental data for the boiling of various liquids irrespective of heating surface involved in the process. This also proves the correctness of the hypothesis that constant, C_1 does not depend upon pressure. This corroborates the finding of Bhaumik et al. [15], Das [42], Pandey [102], Prasad [106], and Vittala et al. [148,149], they also obtained similar results.

An implication of **Eq. (5.6)** is that it enables one to generate heat transfer data for the boiling of liquids at subatmospheric pressures without resorting to experimentation from the knowledge of experimentally determined value of heat transfer coefficient at atmospheric pressure only. Another important point is that **Eq. (5.6)** can also be used to examine the consistency of heat transfer data taken for the boiling of various liquid on heating surfaces of differing surface characteristics of atmospheric and subatmospheric pressures.

Finally, it is concluded that this investigation has reaffirmed the relationship amongst heat transfer coefficient, heat flux and pressure for the boiling of liquids at atmospheric and subatmospheric pressures. It has also established a dimensionless correlation which is free from surface liquid combination factor. So the correlation is applicable to the boiling of liquids on a surface irrespective of its characteristics for subatmospheric pressures only.

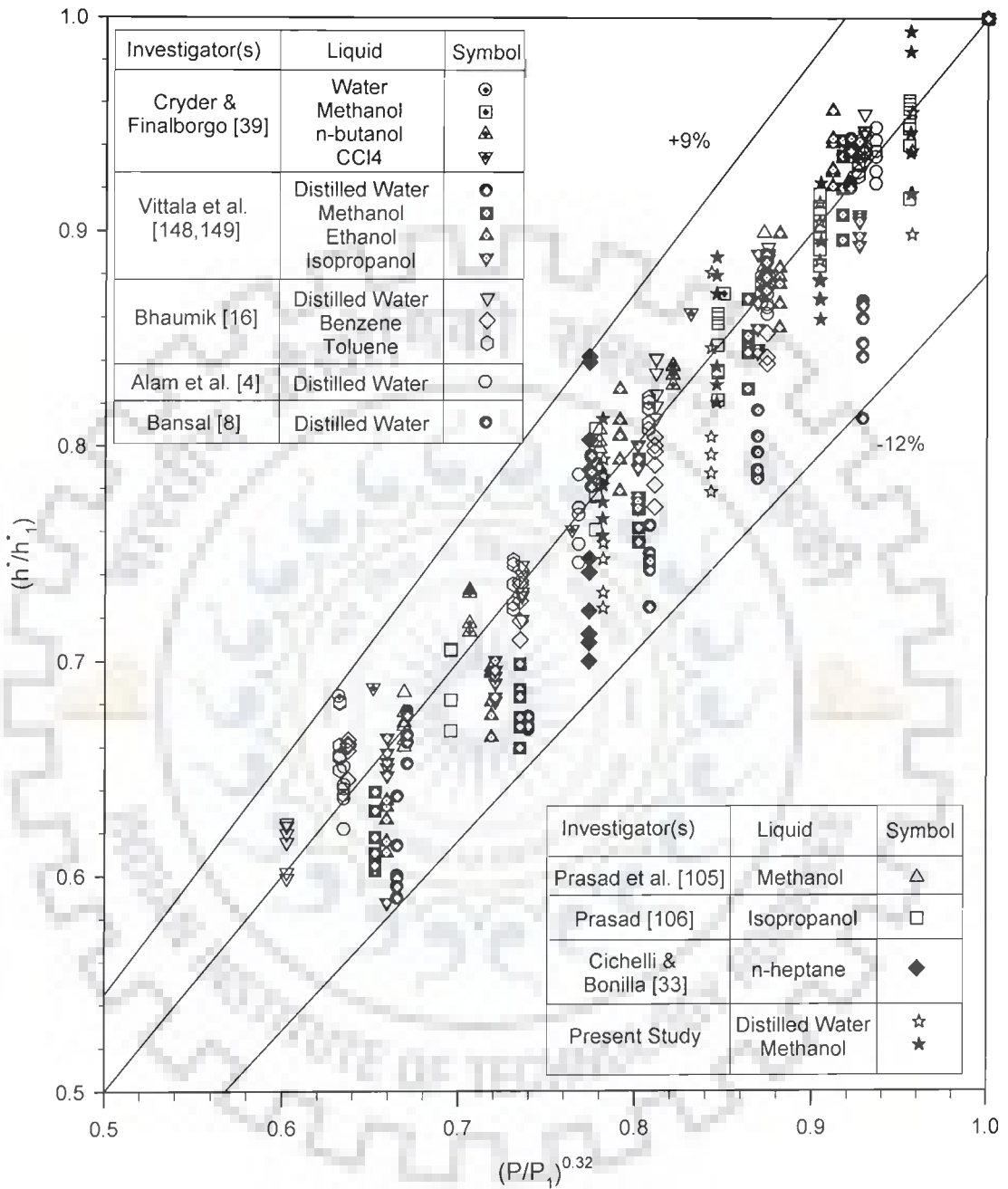


Fig. 5.8 A plot between (h^*/h^*_1) and $(p/p_1)^{0.32}$ for the boiling of various liquid on an uncoated heating surface at atmospheric and sub-atmospheric pressures

5.3 NUCLEATE BOILING OF A BINARY MIXTURE ON AN UNCOATED HEATING TUBE

The experimental data for the boiling of various compositions of methanol and distilled water are listed in Tables B.7 to B.13 of Annexure-B. It includes the measured values of temperature of heating surface and liquid pool at top, two sides and bottom positions of the tube, and heat flux as well as the calculated value of heat transfer coefficient for each composition at atmospheric and subatmospheric pressures. Based upon these data, variation of surface temperature and heat transfer coefficient around the circumferences of heating tube and thereby the effect of heat flux, pressure and composition on heat transfer coefficient for the boiling of methanol-distilled water mixture have been determined. Following subsections deal with them.

5.3.1 *Circumferential variation of heat transfer coefficient*

Figures 5.9a to 5.9e are plots to demonstrate the surface temperature profiles for the boiling of various compositions of methanol-distilled water mixtures on an uncoated tube surface at atmospheric pressure. Heat flux is parameter in each of these plots. Each plot also contains a curve to represent boiling temperature profile of the mixture. An examination of one of these plots clearly points out the following:

- i. At a given heat flux, surface temperature is found to increase continuously on moving from bottom, to side, to top position of the tube.
- ii. At a given circumferential position, an increase in heat flux increases the value of surface temperature.
- iii. Saturation temperature remains unaltered irrespective of heat flux and circumferential position.

Above features have also been found to hold true for boiling of various methanol-distilled water mixtures at various subatmospheric pressures, as clearly shown in plots of **Figs 5.10 and 5.11**.

All the above features are same as observed in case of boiling of liquids. It may be mentioned here that experimentally obtained saturation temperature

of the mixture was compared with the theoretical value calculated by Peng Robinson equation of state method [103]. The comparison indicates an indiscernible difference between the two, as evident from **Fig. 5.12**. This is a plot between the experimentally obtained values of saturation temperature with that of calculated values for methanol-water mixtures. Pressure is parameter in this plot.

Thus, it can be concluded that boiling characteristic of a given composition of methanol-distilled water mixture are same as of an individual liquid. Hence, local heat transfer coefficient of a binary mixture is likely to vary in the same way as that of a liquid. Keeping this in view it has not been included here, but a detail analysis of heat transfer coefficient with respect to heat flux, pressure and composition has been carried out.

5.3.2 Heat transfer coefficient-heat flux relationship for a binary mixture

The average value of surface temperature of the heating tube has been determined by taking arithmetic mean of the local surface temperature. Similar procedure has also been followed for the determination of average saturation temperature of the mixture. Using these values heat transfer coefficient for the boiling of various compositions of the mixtures has been determined. The method of calculation of heat transfer coefficient for binary mixture is given in section C.5 of Annexure-C, Sample Calculation.

Figure 5.13 is a plot between heat transfer coefficient and heat flux for the boiling of 5 mol percent methanol-distilled water mixture. Pressure is parameter in this plot. The features of this plot are as follows:

- i. At a given pressure, heat transfer coefficient of a mixture increases with heat flux and the variation between the two can be described by a power law, $h \propto q^{0.7}$.
- ii. A rise in pressure enhances the value of heat transfer coefficient of a mixture subjected to a given heat flux.

These features have also been observed for the boiling of other compositions of methanol-distilled water mixtures at atmospheric and various subatmospheric pressures, as can be seen from the plots in **Figs. 5.14 to 5.16**.

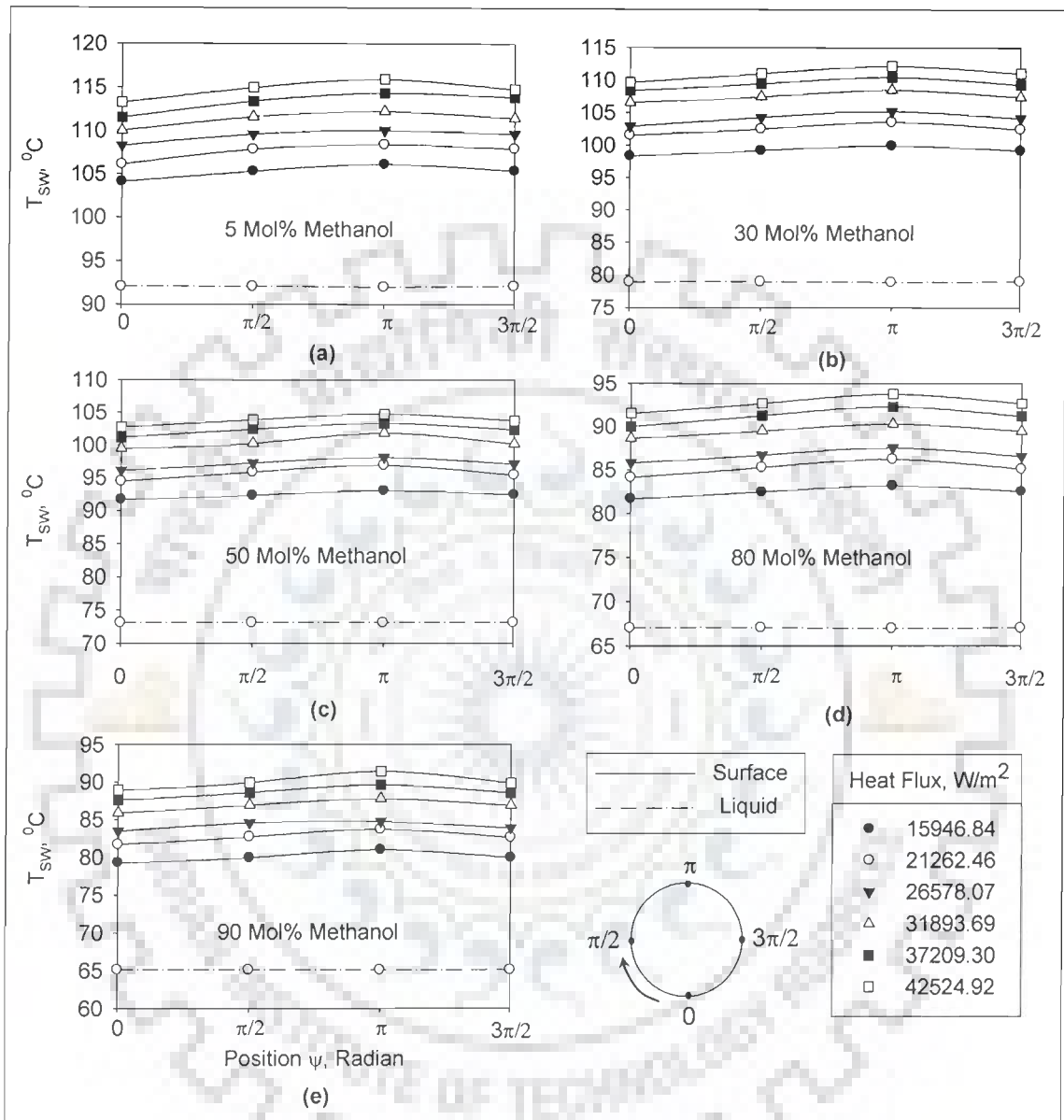


Fig. 5.9 Variation of liquid and surface temperature along circumference at bottom, two sides and top positions of uncoated heating tube with heat flux as a parameter for boiling of methanol-distilled water mixtures at atmospheric pressure

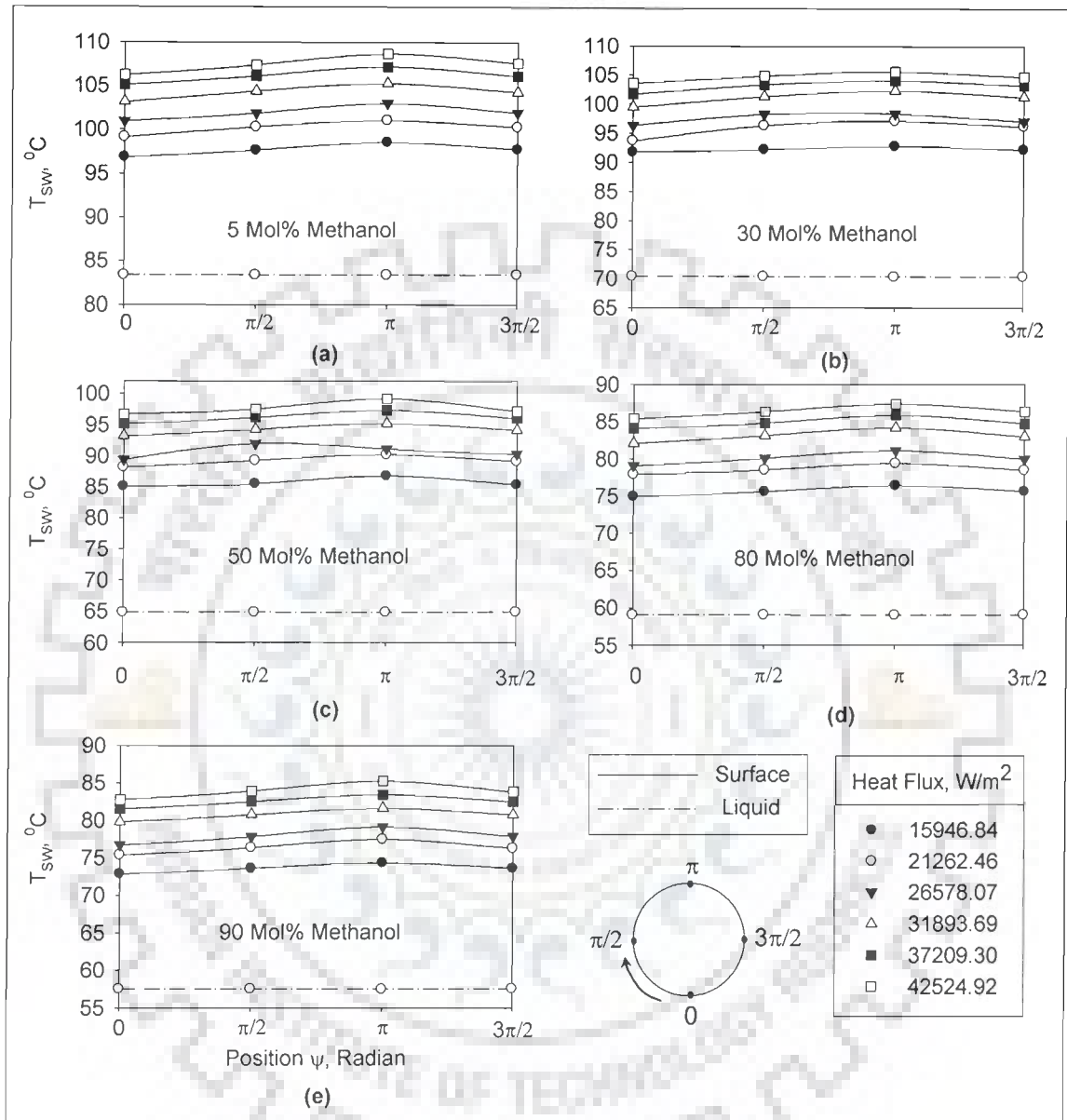


Fig. 5.10 Variation of liquid and surface temperature along circumference at bottom, two sides and top positions of uncoated heating tube with heat flux as a parameter for boiling of methanol-distilled water mixtures at 71.06 kN/m^2 pressure

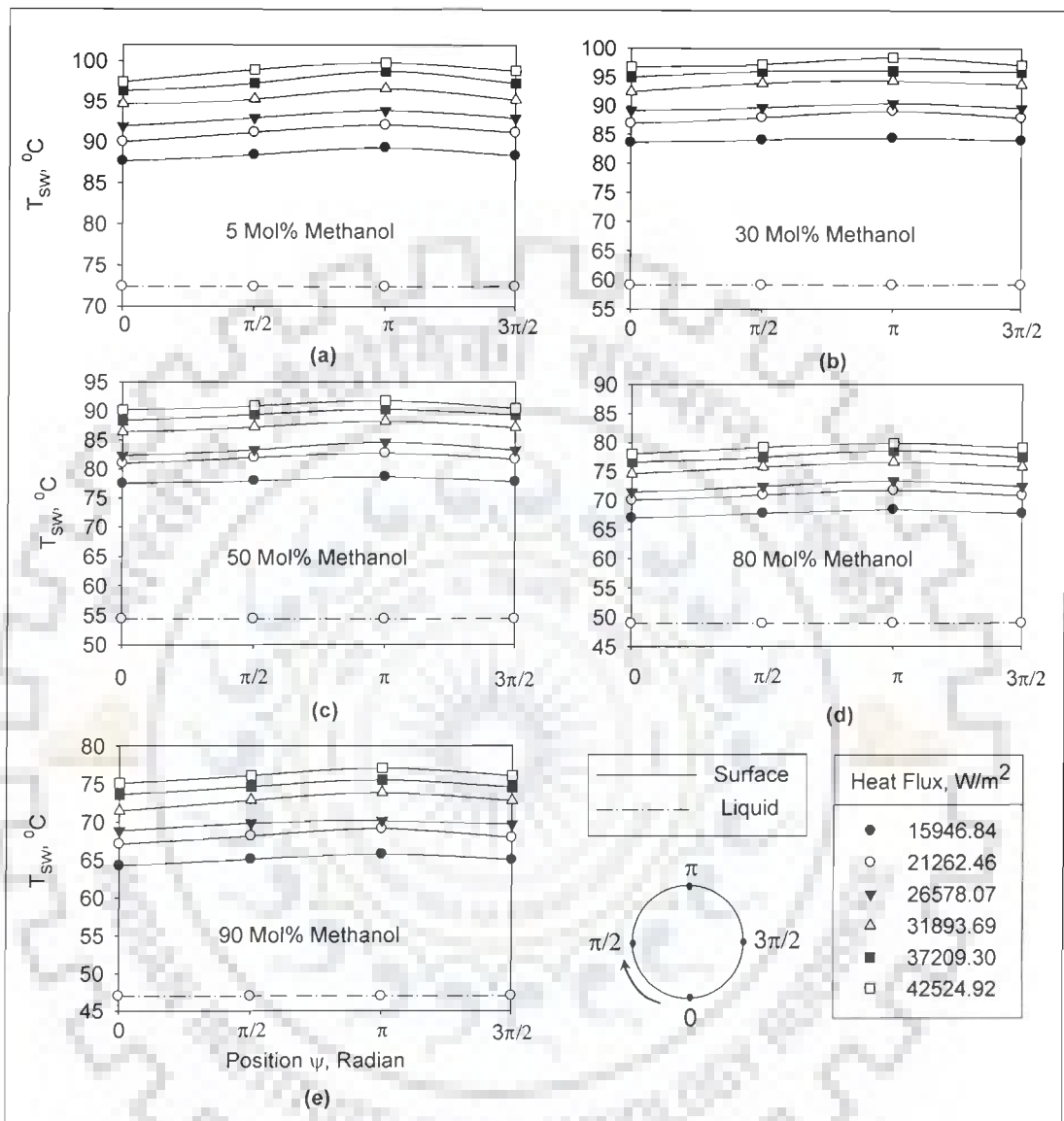


Fig. 5.11 Variation of liquid and surface temperature along circumference at bottom, two sides and top positions of uncoated heating tube with heat flux as a parameter for boiling of methanol-distilled water mixtures at 44.40 kN/m^2 pressure

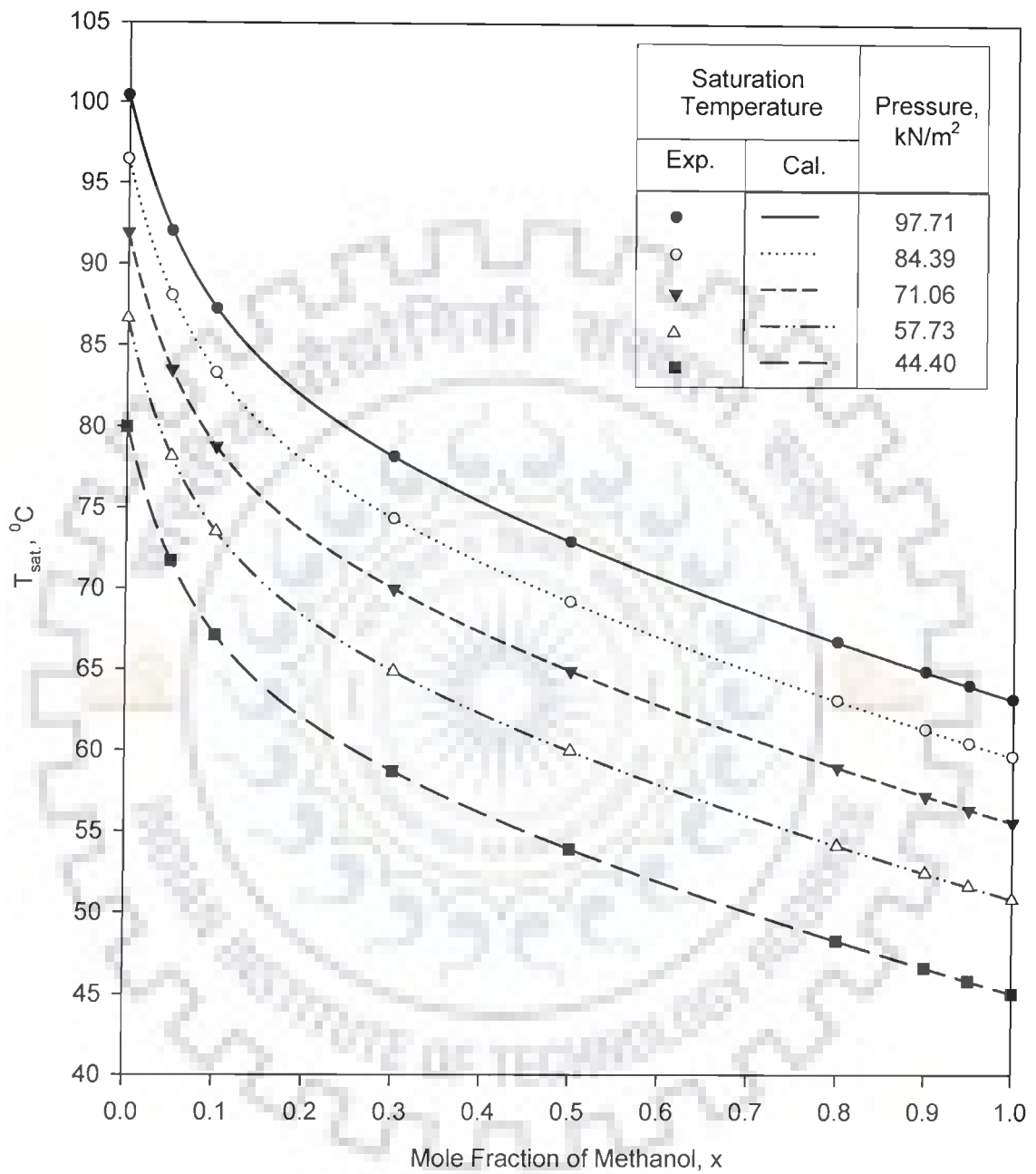


Fig. 5.12 Comparison of experimental saturation temperature with those of calculated values for methanol-distilled water mixture at atmospheric and subatmospheric pressures

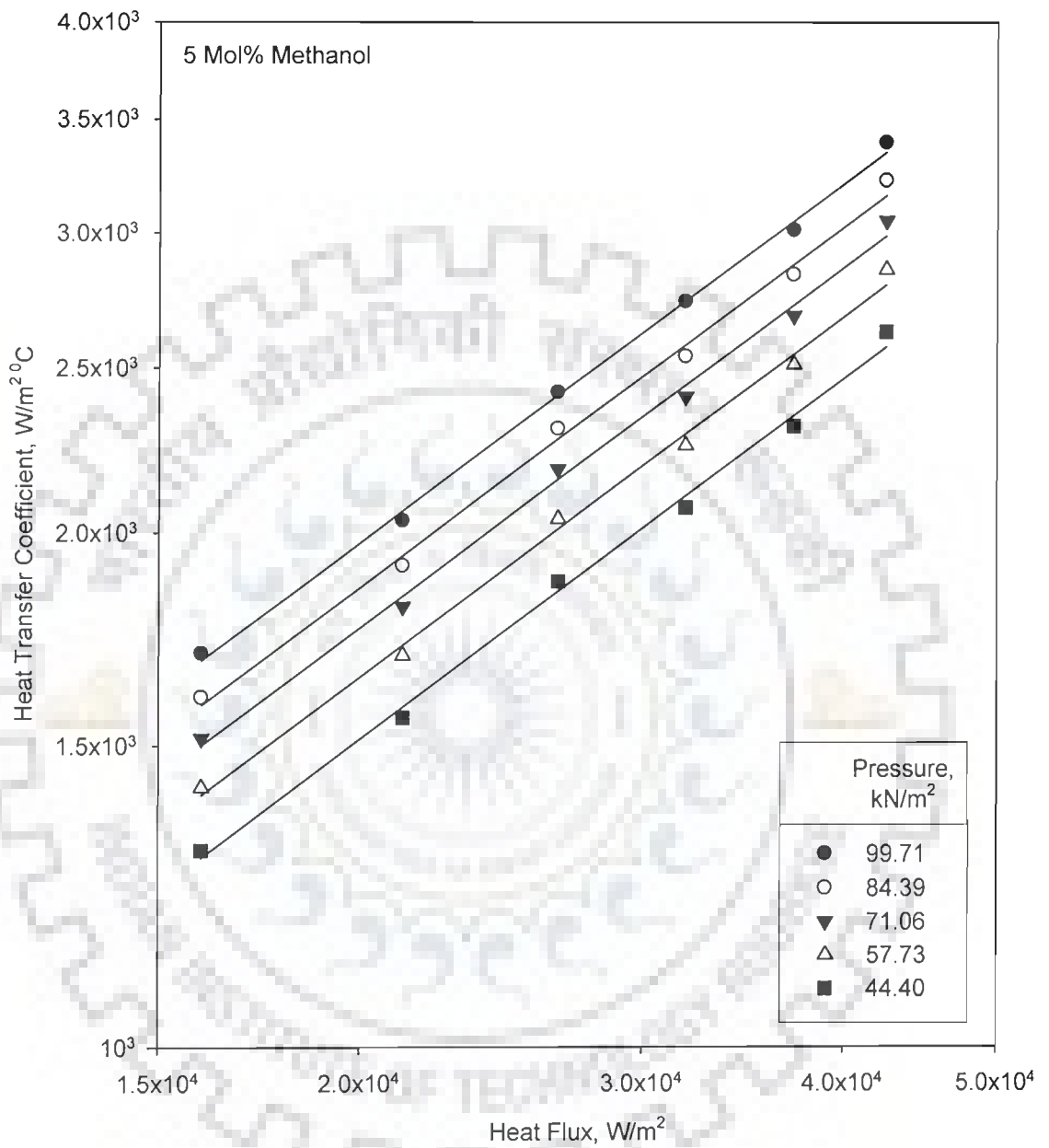


Fig. 5.13 Variation of heat transfer coefficient with heat flux for boiling of 5 mol% methanol-distilled water mixture on an uncoated heating tube with pressure as a parameter

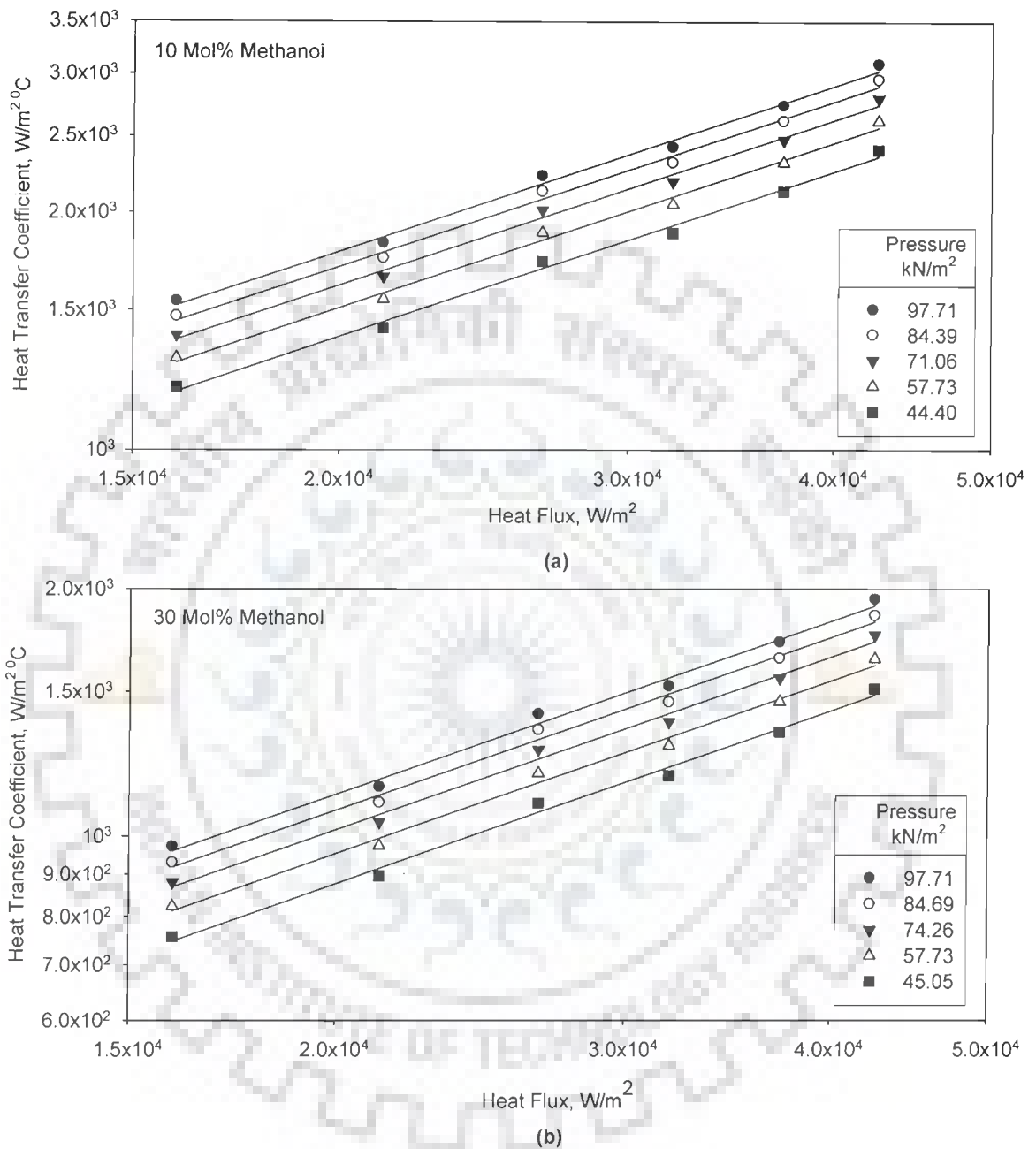


Fig. 5.14 Variation of heat transfer coefficient with heat flux for boiling of 10 and 30 mol% methanol-distilled water mixture on an uncoated heating tube with pressure as a parameter

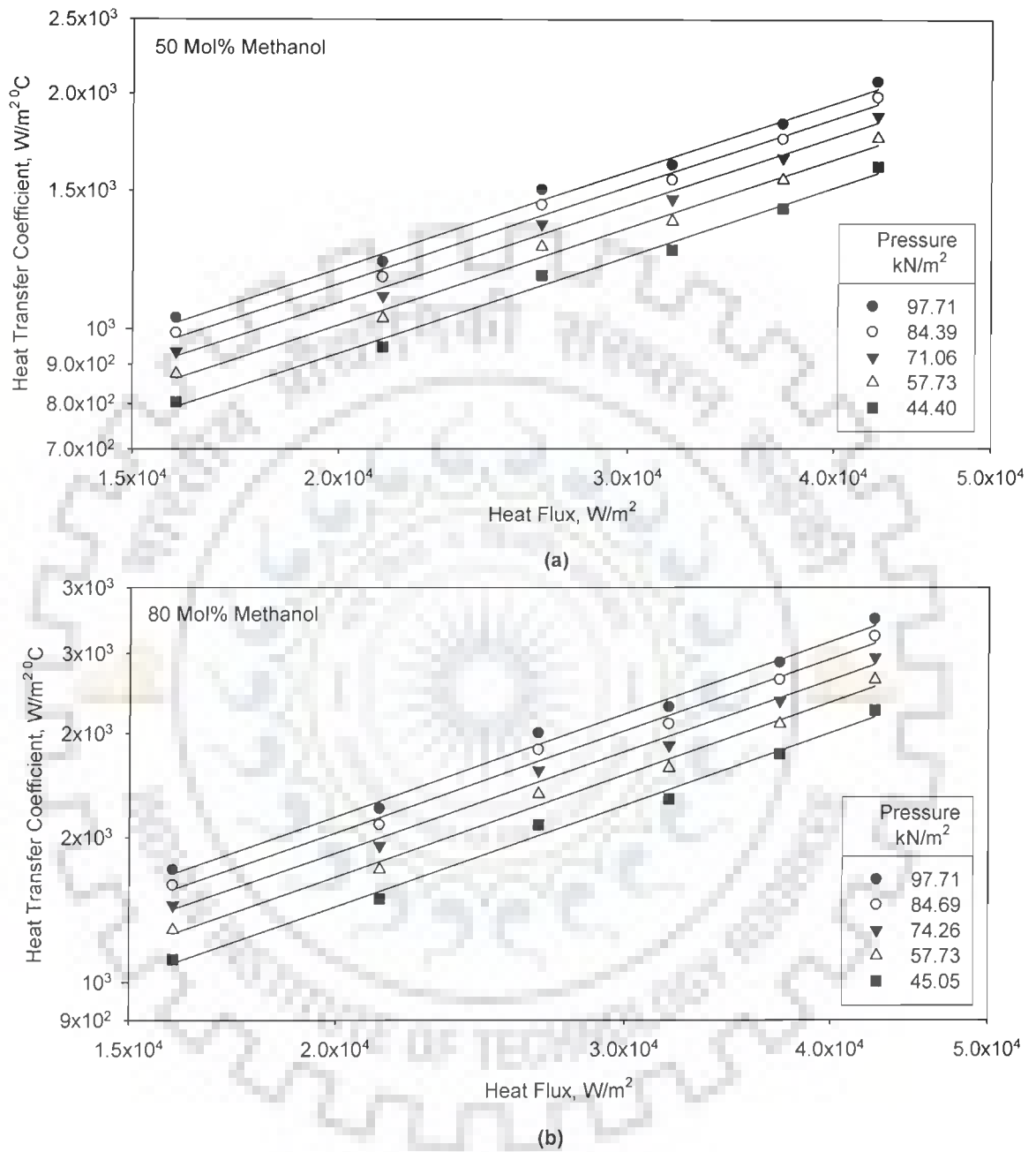


Fig. 5.15 Variation of heat transfer coefficient with heat flux for boiling of 50 and 80 mol% methanol-distilled water mixture on an uncoated heating tube with pressure as a parameter

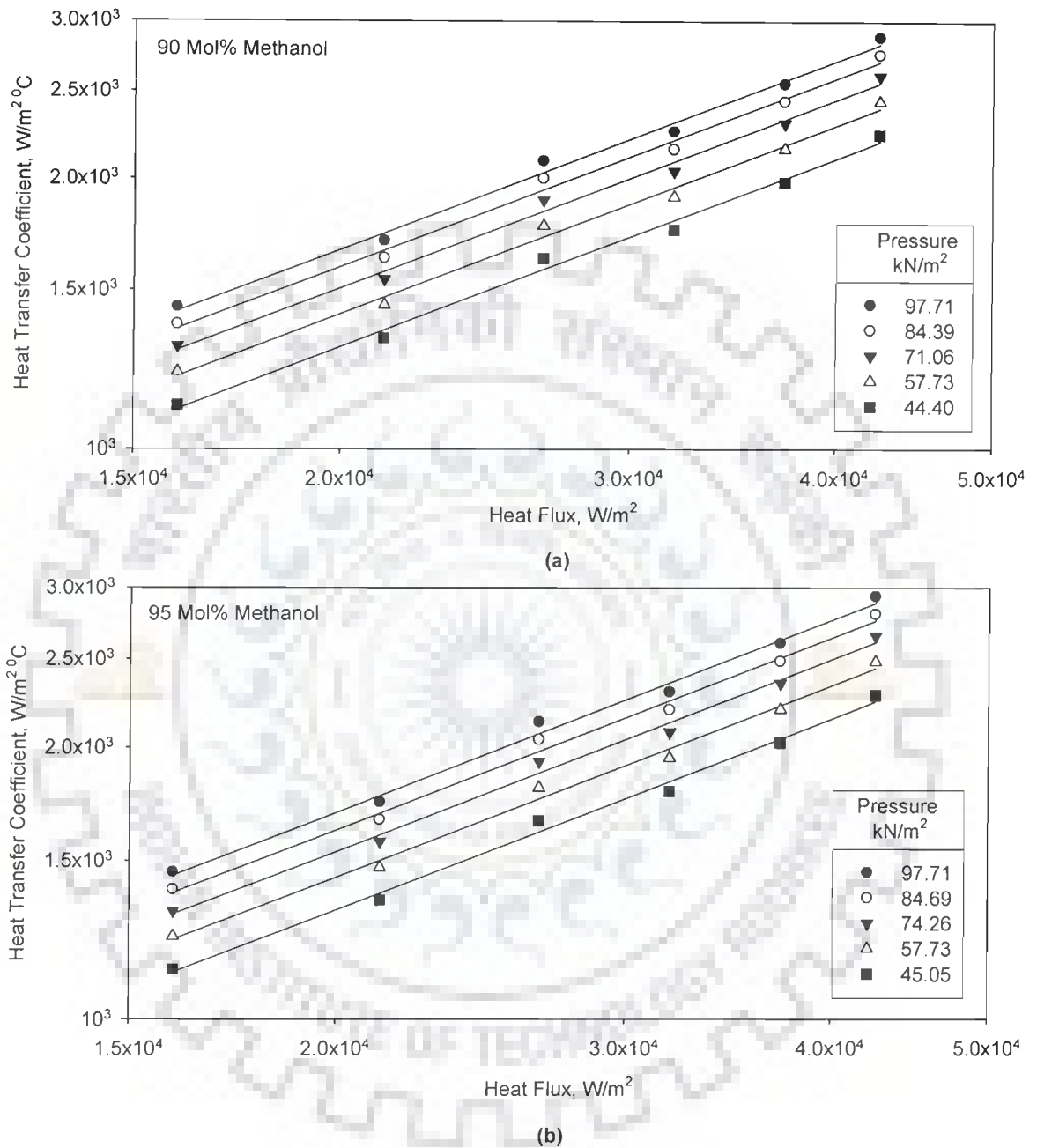


Fig. 5.16 Variation of heat transfer coefficient with heat flux for boiling of 90 and 95 mol% methanol-distilled water mixture on an uncoated heating tube with pressure as a parameter

Above motioned features are same as obtained for the boiling of liquids. Hence, same explanation as given in Section 5.2.3 hold true in this case also. It may be pointed out that this also corroborates the findings of Pandey [102] for boiling of ethanol-water, methanol-water and isopropanol-water mixtures at atmospheric and subatmospheric pressures, Alam & Varshney [5] for boiling of glycerin-water, ethylene glycol-water, acetic acid-water, and acetone-water mixtures at atmospheric and subatmospheric pressures, and Fujita et al. [50] for boiling of methanol-water, ethanol-water, methanol-ethanol, ethanol-butanol and methanol-benzene at atmospheric pressure.

Hence, boiling characteristic representing the variation of heat transfer coefficient of a binary mixture with respect to heat flux and pressure remains the same as of individual liquids. It can be described by the following equation which has been obtained by regression analysis within an error of $\pm 7.5\%$.

$$h = C_2 q^{0.7} p^{0.32} \quad (5.7)$$

where, C_2 is a constant whose value depends upon the percentage composition of the mixture, and surface characteristic. The values of constant, C_2 as determined for various compositions of distilled water-methanol mixtures are given in **Table 5.2**.

Table 5.2 Values of constant C_2 of **Eq. (5.7)** for various compositions of methanol-distilled water mixtures

S. No.	Mixture Composition	C_2
1.	5% Methanol	0.431
2.	10% Methanol	0.397
3.	30% Methanol	0.257
4.	50% Methanol	0.275
5.	80% Methanol	0.364
6.	90% Methanol	0.375
7.	95% Methanol	0.389

An important implication of **Eq. (5.7)** is that heat transfer coefficient of a given composition of methanol-distilled water mixture can be calculated from the knowledge of heat flux, q and pressure, p provided the value of constant,

C_2 appearing in **Eq. (5.7)** is experimentally known. **Figure 5.17** represents a plot between experimentally determined values of heat transfer coefficient and those predicted from **Eq. (5.7)** for the boiling of various methanol-distilled water mixtures at atmospheric and subatmospheric pressures on an uncoated heating tube. From this plot, it is observed that predicted values of heat transfer coefficient match excellently with experimental values within a maximum error of $\pm 7.5\%$.

Equation (5.7) is quite analogous to **Eq. (5.4)** which holds true for the boiling of liquids. This equation also requires the experimentally determined values of constant, C_2 for its applicability to determine heat transfer coefficient of a given composition of a binary mixture from the known values of heat flux, q and pressure, p .

The constant, C_2 is quite similar to constant, C_1 of **Eq. (5.4)**. Therefore, the strategy which has been followed to get rid of the constant in case of liquid is also used herewith. Hence, $h^* (= h/q^{0.7})$ is defined and following dimensionless correlation is obtained:

$$\frac{h^*}{h_1^*} = \left(\frac{p}{p_1} \right)^{0.32} \quad (5.8)$$

Where, subscript, 1 refers to atmospheric pressure condition.

Figure 5.18 is a plot between (h^*/h_1^*) and $(p/p_1)^{0.32}$ for the boiling of various composition of methanol-distilled water mixture on an uncoated heating surface at atmospheric and subatmospheric pressures. It also contains experimental data for the boiling of methanol-water mixtures, ethanol-water mixtures, and isopropanol-water mixtures due to Pandey [102] on a plain stainless steel surface at atmospheric and subatmospheric pressures. As can be noticed from this plot, all the data points of this investigation as well as those of Pandey [102] lie around a 45° diagonal line with the maximum deviation ranging from -12 to $+20\%$. This indicates the validity of **Eq. (5.8)**. In this way **Eq. (5.8)** has been found to hold good for the boiling of a given composition of a binary liquid mixture.

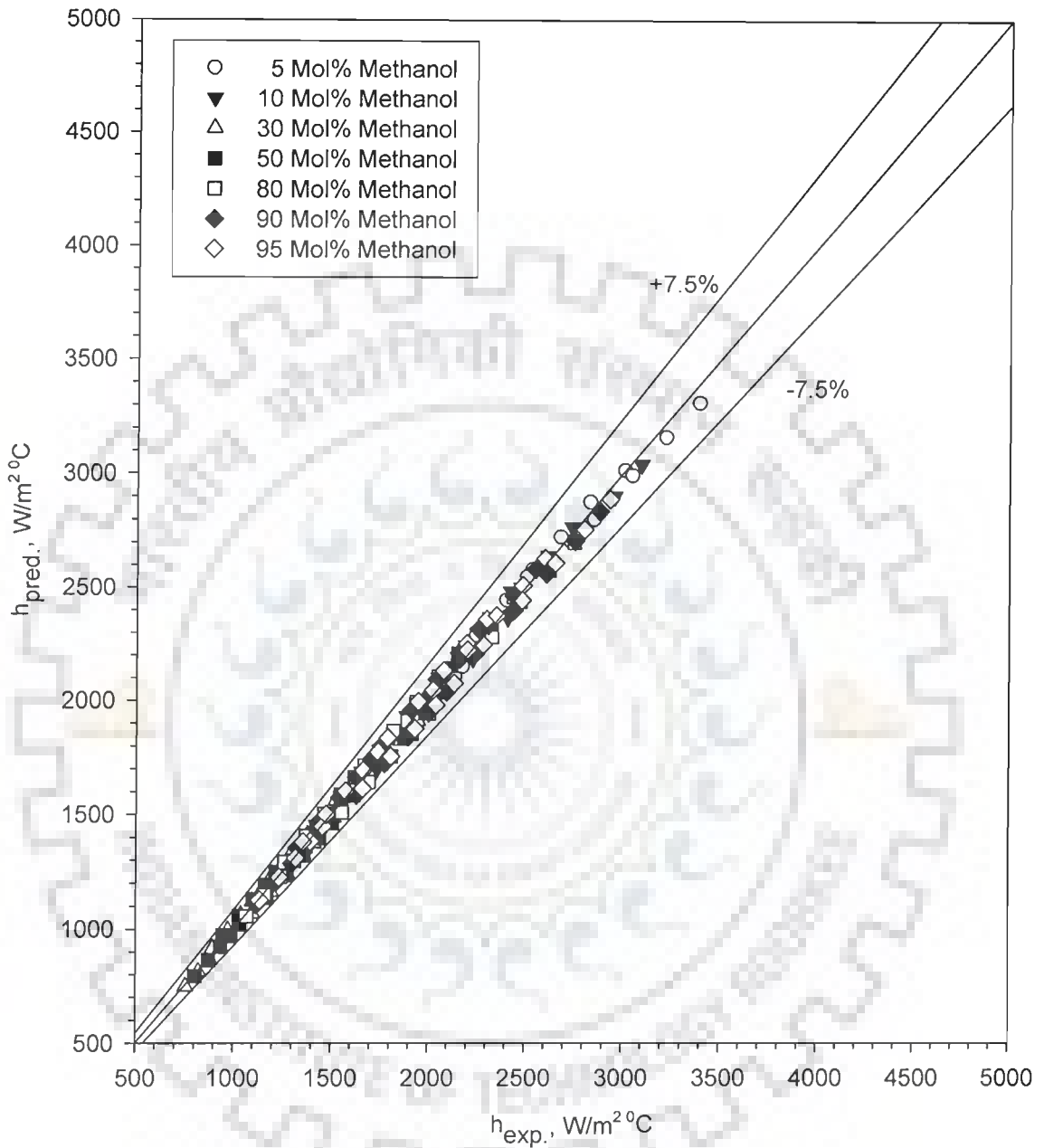


Fig. 5.17 Comparison of experimental heat transfer coefficients with those predicted from Eq. (5.7) for boiling of methanol-distilled water mixtures on an uncoated heating tube surface at atmospheric and subatmospheric pressures

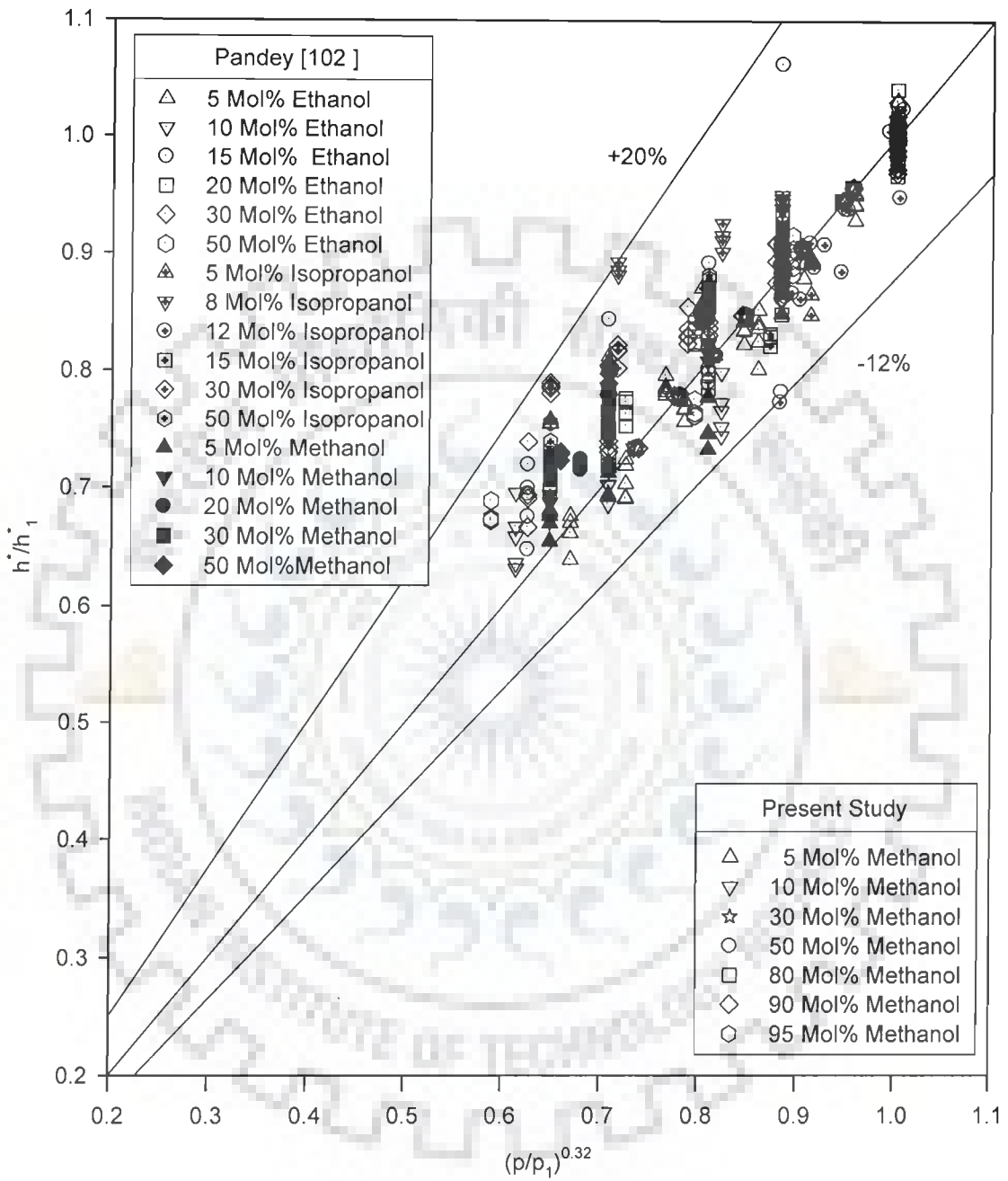


Fig. 5.18 Comparison of experimental values of (h^*/h_i) with those predicted from Eq. (5.8) for pool boiling of binary liquid mixtures at atmospheric and subatmospheric pressures

A close scrutiny of **Eq. (5.8)** reveals that it is free from surface-liquid mixture combination factor, C_2 . Therefore, it is applicable to any liquid mixture boiling on a surface. Further, it can be used to generate boiling heat transfer data of a liquid mixture at subatmospheric pressures from the knowledge of experimental data of one atmosphere pressure only. In other words, it calls for experimentation only at atmospheric pressure. Another implication of above equation is that it can be used to test the consistency of experimental data of boiling heat transfer of binary liquid mixture conducted on heating surfaces of varying characteristic at subatmospheric pressures.

5.3.3 Variation of heat transfer coefficient of mixtures with composition

The forgoing discussion has been restricted to the boiling of a given composition of a binary liquid mixture at atmospheric and subatmospheric pressures. However, it has also been found that the salient features during boiling of liquid mixtures remain the same as those of a single component liquid. So it is quite logical to determine boiling heat transfer coefficient of a given mixture from the knowledge of individual components boiling heat transfer coefficients. Keeping this in view, heat transfer coefficient of a boiling binary mixture has been computed by the following equation which represents the weighted mean of individual components heat transfer coefficient.

$$\frac{1}{h_{id}} = \frac{x}{h_1} + \frac{(1-x)}{h_2} \quad (5.9)$$

where, subscripts 1 and 2 denote high and low volatile components, respectively in the mixture.

Computations of heat transfer coefficient have been made for various compositions of methanol-distilled water mixture at atmospheric and subatmospheric pressures using **Eq. (5.9)**. The computed values, so obtained, are compared with the experimentally determined one, as shown in **Fig. 5.19b**. As it is clear from this plot, the computed values, represented by dotted curves, do not match with the experimental values, represented by solid curves. This disagreement is quite obvious due to distinct differences between the inherent nature of the boiling mixture and a single component liquid. **Fig. 5.19b** is a plot between experimental and predicted heat transfer coefficients with mole

fraction of high volatile component (methanol) in methanol-distilled water mixture at an atmospheric pressure. Heat flux is a parameter in this plot. Following points emerged out from this plot:

- i. At a given heat flux, heat transfer coefficient of a given composition of the boiling mixture is lower than those of its components. In other words, heat transfer coefficient of a binary mixture can not be predicted by interpolation of heat transfer coefficients of its components.
- ii. Left hand ordinate indicates boiling heat transfer coefficient of distilled water. At given heat flux, an addition of high volatile component (methanol) to distilled water reduces the value of boiling heat transfer coefficient. This trend continues till the mole fraction of methanol mixture reaches to 0.30. Thereafter, any further addition of methanol results in turnaround and thereby heat transfer coefficient rises to reach ultimately to the value of methanol.
- iii. An increase in heat flux makes the appearance of the region depicting lowest heat transfer coefficient in the curve to be more pronounced. Further, it also enhances the value of heat transfer coefficient of a given mol fraction of methanol in the mixture.

Figures 5.20 and 5.21 show similar plots of heat transfer coefficient verses methanol mole fraction at 84.39 kN/m^2 and 44.40 kN/m^2 pressures, respectively. These plots have essentially the same features as described above. Thus, it is clear that pressure does not alter the nature of h verses x curve.

Above observations are consistent and in agreement with the findings of many earlier investigators [2, 10, 22, 35, 50, 51, 74, 76, 109, 125, 132, 138]. Following explanation is put forward to region out the above features:

A binary mixture is composed of two component having different volatilities. They as single component liquids boil at different temperatures. So, a binary mixture boils over a range of temperature spanning from the boiling temperature of the high volatility components to that of low volatility one. It can be understood easily by vapor-liquid phase equilibrium diagrams for methanol-distilled water mixture at atmospheric pressure and various subatmospheric pressures, as shown in **Fig 5.22**. The upper curve in these plots represents the

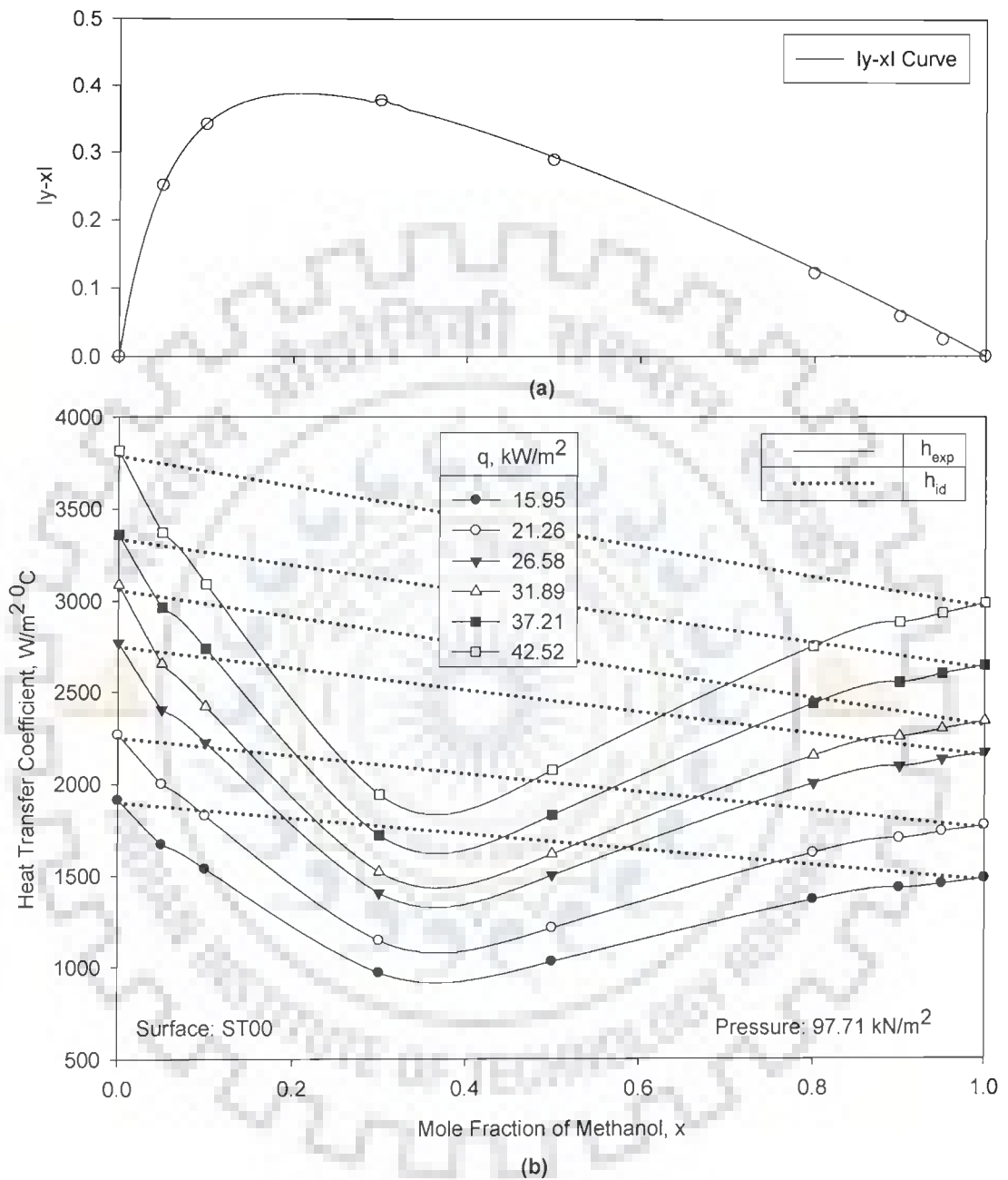


Fig. 5.19 Variation of heat transfer coefficient, and $|y - x|$ with mole fraction of methanol for methanol-distilled water mixtures on uncoated tube at atmospheric pressure

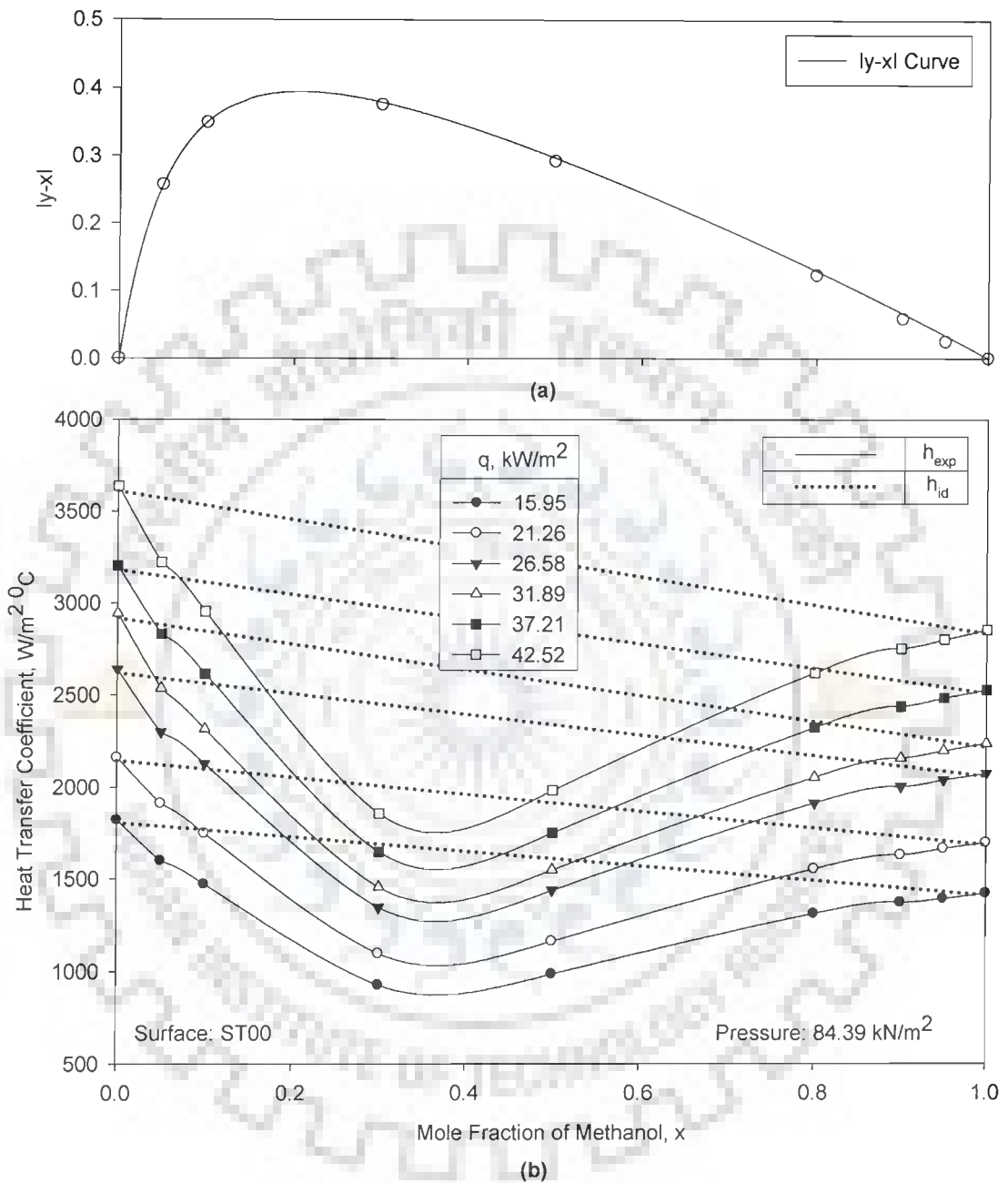


Fig. 5.20 Variation of heat transfer coefficient, and $|y-x|$ with mole fraction of methanol for methanol-distilled water mixtures on uncoated tube at 84.39 kN/m^2 pressure

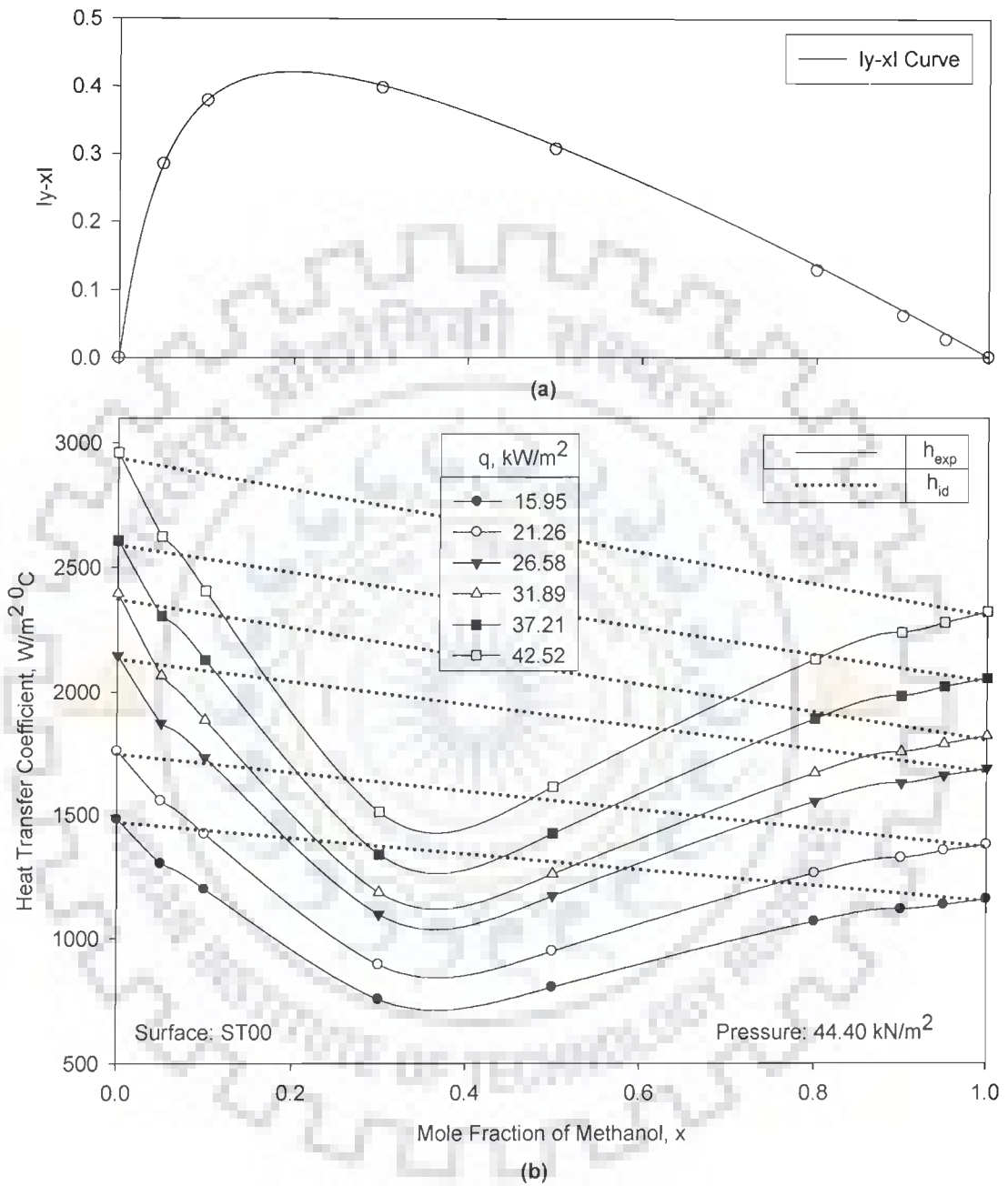


Fig. 5.21 Variation of heat transfer coefficient, and $|y - x|$ with mole fraction of methanol for methanol-distilled water mixtures on uncoated tube at 44.40 kN/m² pressure

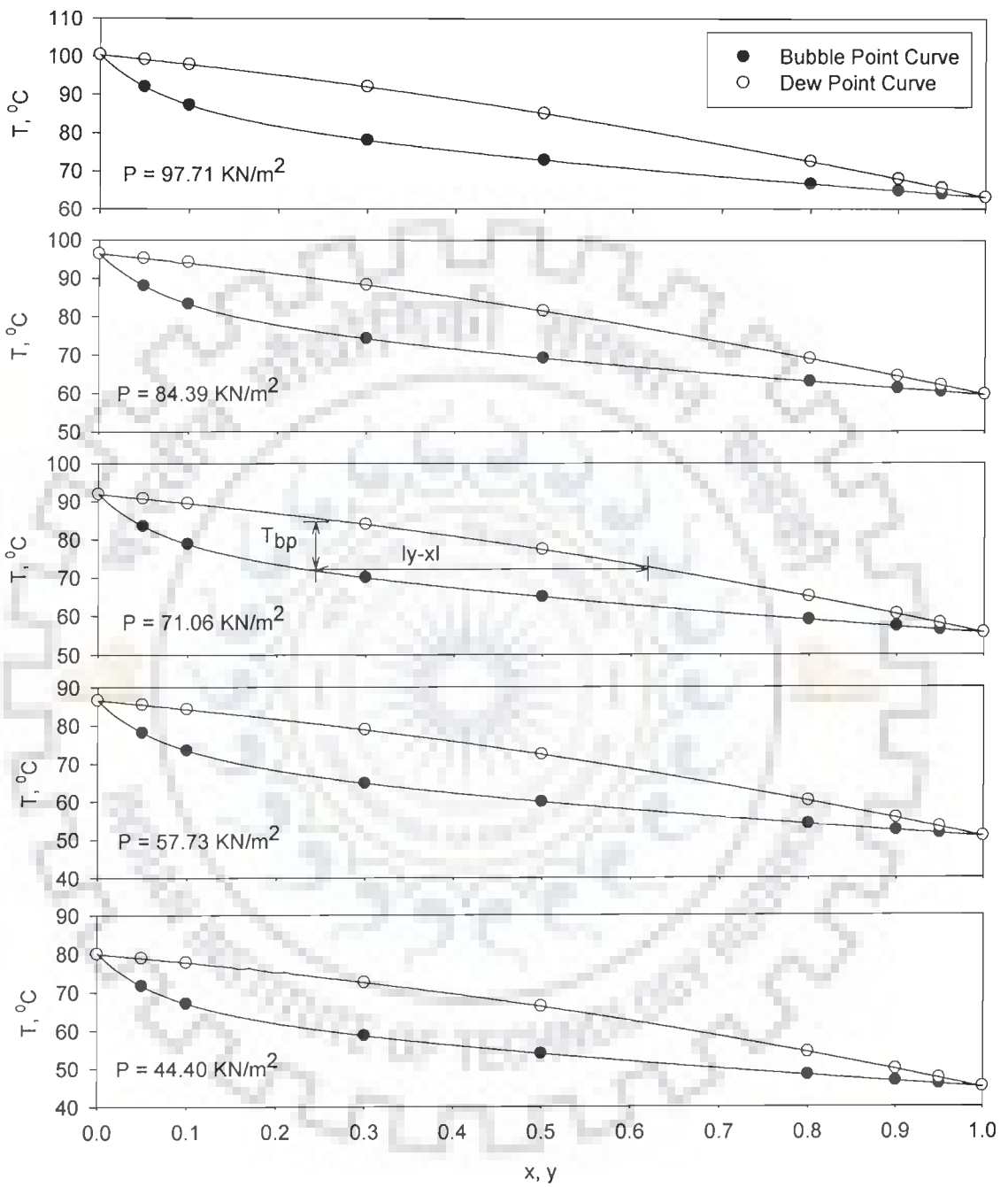


Fig. 5.22 Phase equilibrium curves for methanol-distilled water binary mixtures at atmospheric and subatmospheric pressures

vapor temperature whereas the lower one indicates liquid boiling temperature as a function of methanol mole fraction in the mixture. As can be seen from these plots, equilibrium vapor mole fraction, y^* is higher than that of the surrounding liquid mole fraction, x for the mixture vaporizing at a given temperature. Van Wijk et al. [145] have also noted this phenomenon in bubbles growing on heated surfaces. So, in order to maintain equilibrium between phases more amount of high volatile component present in liquid mixture to vaporize to provide additional vapor as bubbles grows. As a result, the local concentration of high volatile component in the liquid decreases and thereby the local boiling temperature of liquid rises. This, in turn, causes wall temperature to increase so that heat transfer may occur at a constant rate. Hence, lower values of heat transfer coefficient which is based on bulk liquid temperature are found in case of liquid mixture than that observed for single component liquids.

Boiling of a binary mixture involves simultaneous heat and mass transfer. In it, evaporation of liquid components occurs by the transfer of heat from heated surface to bubble via micro-layer existing beneath the bubble base. It is also accompanied by the diffusion of high volatility component from liquid bulk to bubble through bubble-bulk interface. The diffusion of mass makes the boiling process in mixture to be different than that in single component liquid. Mass diffusion is a slow process as compared to that of heat diffusion. Hence, it is controlling the process of boiling of a liquid mixture. In other words, mass diffusion is an impedance to heat transfer and so heat transfer rate in the boiling of liquid mixtures is lower than that in single component liquids. The rate of mass diffusion depends upon the driving force which is the difference existing between equilibrium vapor and liquid mole fraction of high volatile component. It is represented by the term, $(y^* - x)$. Higher the value of $(y^* - x)$, more is the rate of diffusion of high volatile component into the bubble and lower is the heat transfer rate and thereby heat transfer coefficient.

The variation of $(y^* - x)$ with high volatile component mole fraction, x is shown in **Fig 5.19a**. The feature of this plot is as follows:

For the boiling of a binary mixture the value of $(y^* - x)$ increases continuously with an increase in liquid mole fraction, x , and this trend continues till the value of x reaches to 0.30. Thereafter, an increase in the value of x causes $(y^* - x)$, to decrease and ultimately to vanish at unity value of mole fraction.

Both the above observations are self explanatory in nature and therefore called for no detailed analysis.

Hence, in the light of above discussion, it can be said that the variation of heat transfer coefficient of boiling binary mixture with mole fraction of high volatile component is due to alteration in the value of mass diffusion driving force, $(y^* - x)$ in it. An addition of a component to a liquid increases the value of driving forces $(y^* - x)$ which lower down heat transfer coefficient. This behavior has been observed till liquid mole fraction becomes 0.30. At this value driving force $(y^* - x)$ becomes maximum and heat transfer coefficient minimum. Thereafter, reverse trend exists due to decrease in the value of $(y^* - x)$.

A note-worthy point is that heat transfer coefficient of a boiling binary mixture is minimum for the value of x at which driving force $(y^* - x)$ is maximum. This corroborates the findings of [2, 10, 22, 35, 50, 51, 74, 76, 86, 102, 109, 128, 132, 137, 138] who have also noted similar behavior. However, some investigators [71, 127, 157] obtain a range of x for which heat transfer coefficient of a boiling binary mixture reaches to its minimum value.

Above discussion has pointed out clearly that boiling of a binary liquid mixture is different than that of single component liquids owing to the association of mass transfer with heat transfer. Consequently, heat transfer coefficient of a boiling binary mixture at atmospheric and sub atmospheric pressures is lower than that of its single component liquids. Hence its value can not be predicted by interpolation method. In fact, heat transfer coefficient varies with concentration and attains a distinct minimum value when boiling of a binary mixture is carried out at a given heat flux at atmospheric and sub atmospheric pressures. An increase in heat flux does not alter the nature of

curve h versus x but merely shifts the curve upward implying higher value of heat transfer coefficient for the boiling of a liquid mixture of a given composition at atmospheric and subatmospheric pressures.

5.3.4 Development of a semi-empirical correlation for heat transfer coefficient of a binary mixture

Previous section has demonstrated that heat transfer coefficient for the boiling of a binary liquid mixture at atmospheric and subatmospheric pressures can not be determined by the use of weighted mean of heat transfer coefficient of individual components, Eq. (5.9). This is due to the fact that mass transfer also occurs simultaneously with heat transfer in the process of boiling of binary liquid mixtures. This calls for the development of method which may be used to determine heat transfer coefficient of a boiling binary mixture from the knowledge of measurable parameters such as heat flux, pressure, concentration and physico-thermal properties of the mixture. This section has been devoted to it:

Boiling of a binary mixture is a simultaneous heat and mass transfer process. During the boiling of a liquid mixture, the vapor has a composition different than that of liquid phase owing to vapor-liquid phase equilibrium characteristic discussed above. Hence, as a liquid mixture evaporates on the heating surface, the vapor contains more mole fraction of the high volatile component than that of low volatile one. This naturally affects the composition of microlayer and it is depleted of the high volatile component and is enriched in another i.e. low volatile component. Consequently, mass diffusion of high volatile component from bulk to microlayer occurs. Since the rate of mass diffusion is much slower than heat diffusion, mass transfer of high volatile component to bulk interface becomes the limiting process and a portion of the driving force is utilized in overcoming the mass transfer resistance. As a result, an additional temperature driving force is required to obtain a given heat flux, q . Thus, wall superheat, ΔT is composed of effective temperature driving force, ΔT_{id} and an additional temperature driving force, ΔT_a . So

$$\Delta T = \Delta T_{id} + \Delta T_a \quad (5.10)$$

where, $q = h \cdot \Delta T$

If there is no mass transfer, the mixture will behave as a hypo-theoretical pure liquid and the wall superheat will be lower than that required for the actual mixture for the same heat flux. Hence,

$$q = h_{id} \cdot \Delta T_{id} \quad (5.11)$$

From **Eqs. (5.10) and (5.11)**

$$\frac{h}{h_{id}} = \frac{\Delta T_{id}}{\Delta T} \quad (5.12)$$

Thus, one can determine, the value of heat transfer coefficient for a binary liquid mixture from the knowledge of the ratio, $(\Delta T_{id}/\Delta T)$ and heat transfer coefficient of a hypo-theoretical pure liquid, h_{id} . As mentioned above, this pure liquid has same properties as the mixture but no mass transfer involved in it. Therefore, h_{id} represents heat transfer coefficient of an ideal mixture. It can be obtained from **Eq. (5.9)** which represents weighted mean temperature difference in a binary mixture. So its value can be determined from the known values of heat transfer coefficients and mole fractions of individual components present in the primary mixture.

$(\Delta T_{id}/\Delta T)$ represents the ratio of temperature driving force for the case of no mass transfer to that in presence of mass transfer occurring along with heat transfer in the boiling of a binary liquid mixture. The driving force for mass transfer of high volatile component is the concentration difference, $(y - x)$. Its value is positive for high volatile component whereas negative for low volatile component. Hence, $|y - x|$ must find a place in defining the ratio $(\Delta T_{id}/\Delta T)$. Further, as mass diffusion is rate controlling process so the term, $(\alpha/D)^{0.5}$ which represents a measure of the resistance to heat transfer, should also be included in it. Incorporation of above terms leads to the quantity, $[|y - x|(\alpha/D)^{0.5}]$ which represents effective driving force in the boiling of a binary liquid mixture.

With this following correlation has been developed to correlate the experimental data of this investigation for the boiling of various compositions of methanol-distilled water mixture at atmospheric and subatmospheric pressures.

$$\frac{h}{h_{id}} = \frac{\Delta T_{id}}{\Delta T} = \left[1 + |y - x| \left(\frac{\alpha}{D} \right)^{0.5} \right]^{-(0.8x+0.20)} \quad (5.13)$$

This equation correlates all the data of this investigation within an error of $\pm 15\%$ as can be seen from **Fig. 5.23**.

Above equation has also been tested against the predicted data due to correlations of following investigators: Calus & Rice [22], Fujita et al. [50], Happel & Stephan [60], Jungnickel et al. [76], Schlünder [114], Stephan & Körner [121], Thome [132], and Thome & Shakir [134]. The comparison between experimentally obtained values of heat transfer coefficient and those predicted by above correlations and **Eq. (5.13)** of this investigation is shown in **Fig 5.24**. As is clear from this figure, predictions have matched the experimental values within an average error of $\pm 25\%$. Thus, it can be said that correlation, **Eq. (5.13)** for boiling of binary liquid mixture is capable of correlating experimental data for the boiling of liquid mixtures taken on different heating surface.

It may be pointed out that above correlation, **Eq. (5.13)** is free from a surface-liquid combination factor, so this equation is applicable to the boiling of any liquid mixture irrespective of the characteristic of heating surface involved in it. Further, the value of heat transfer coefficient for the boiling of a binary liquid mixture can be calculated from the known values of heat transfer coefficients, diffusivity and relative volatility of the binary liquid mixture. It hold true for the boiling of non-azeotropic liquid mixtures as it has not been tested against boiling heat transfer data for azeotropic liquid mixtures. Further, its validity for superatmospheric pressure data also seems to be under doubt as no data for pressures higher than one atmosphere could be obtained and tested. Hence, **Eq. (5.13)** should be used carefully by keeping the above limitations in mind.

Equation (5.13) provides a method for the computation of heat transfer

coefficient of a boiling binary mixture from the known values of mass diffusivity, thermal diffusivity, vapor-liquid composition, heat transfer coefficients and mole fraction of individual components present in binary mixture. The values of heat transfer coefficients of pure components may be obtained experimentally or alternatively calculated by the use of a semi empirical correlation available in literature. The important correlations available in literature for the calculation of heat transfer coefficient of a liquid have been enlisted in **Table 2.1** of Chapter-2, Literature Review.

SUMMARY

On the basis of above, it can be concluded that boiling heat transfer characteristics of a binary mixture are same as that of a liquid. The functional relationship of heat transfer coefficient with heat flux and pressure is same as observed for liquids and therefore dimensional equation, $h = C_2 q^{0.7} p^{0.32}$ for the boiling of a binary mixture has been developed for atmospheric and subatmospheric pressures. This equation has also given a dimensionless correlation which can be used to estimate heat transfer coefficient for the boiling of a liquid mixture on any surface irrespective of characteristics. However, heat transfer coefficient of a boiling binary liquid mixture can not be predicted by the method of interpolation of heat transfer coefficients of individual components present in the mixture. In fact, heat transfer coefficient does not vary linearly with composition, but pass through a minimum value corresponding to a composition at which difference between vapor and liquid composition is maximum. Such a composition of the mixture can be determined from vapor-liquid phase equilibrium diagram of the binary mixture. This has been due to the occurrence of mass transfer along with heat transfer in the process. Analysis has resulted an equation for the prediction of heat transfer coefficient of a binary liquid mixture from the known values of physico-thermal properties, vapor-liquid phase equilibrium diagram, heat transfer coefficients and mole fraction of individual component present in binary mixture. The resultant equation has been found to correlate experimental data of this investigation well as those of earlier investigators very well.

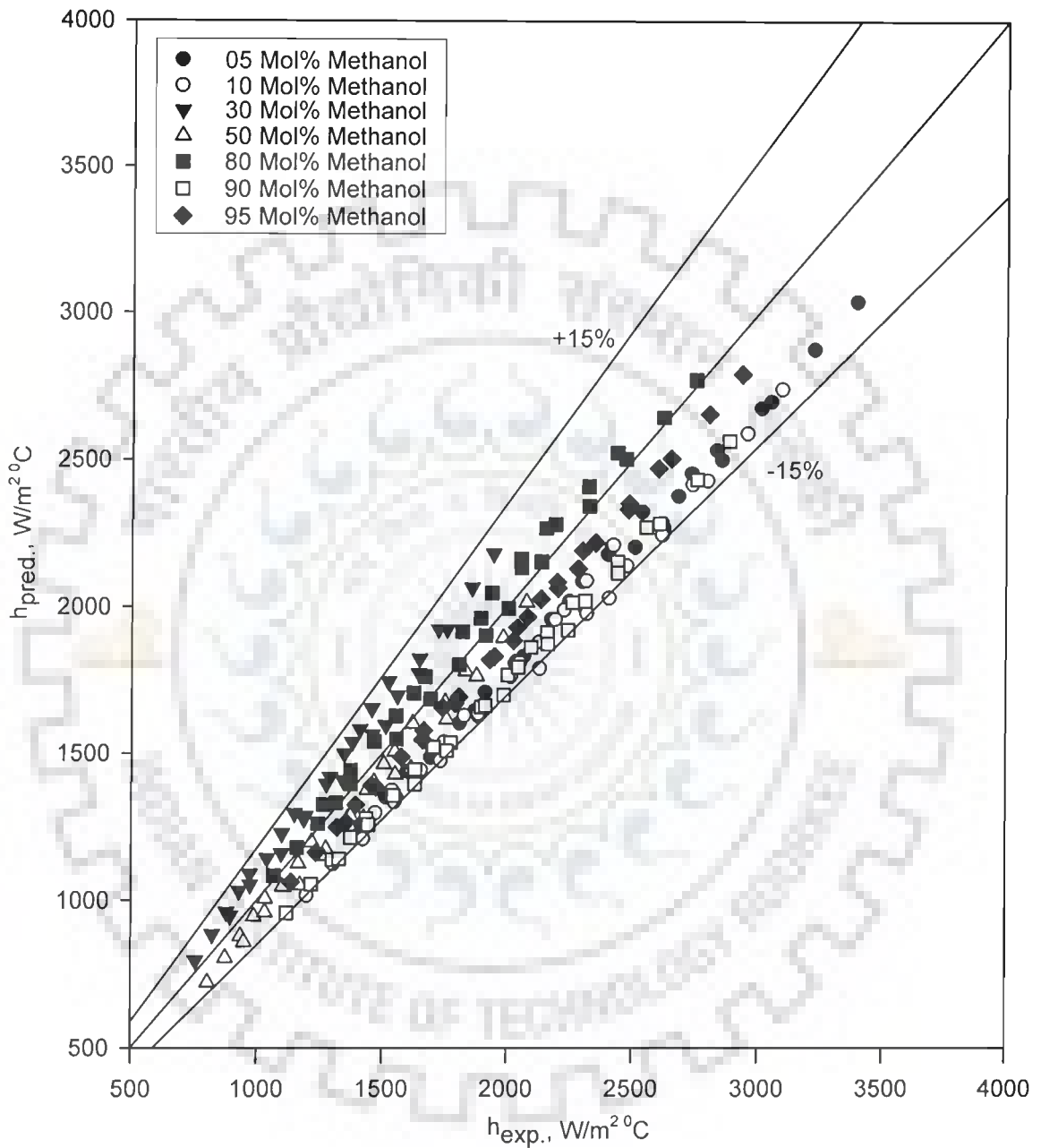


Fig. 5.23 Comparison of experimental heat transfer coefficients with those predicted from Eq. (5.13) for boiling of methanol-distilled water mixture on an uncoated heating tube surface at atmospheric and subatmospheric pressures

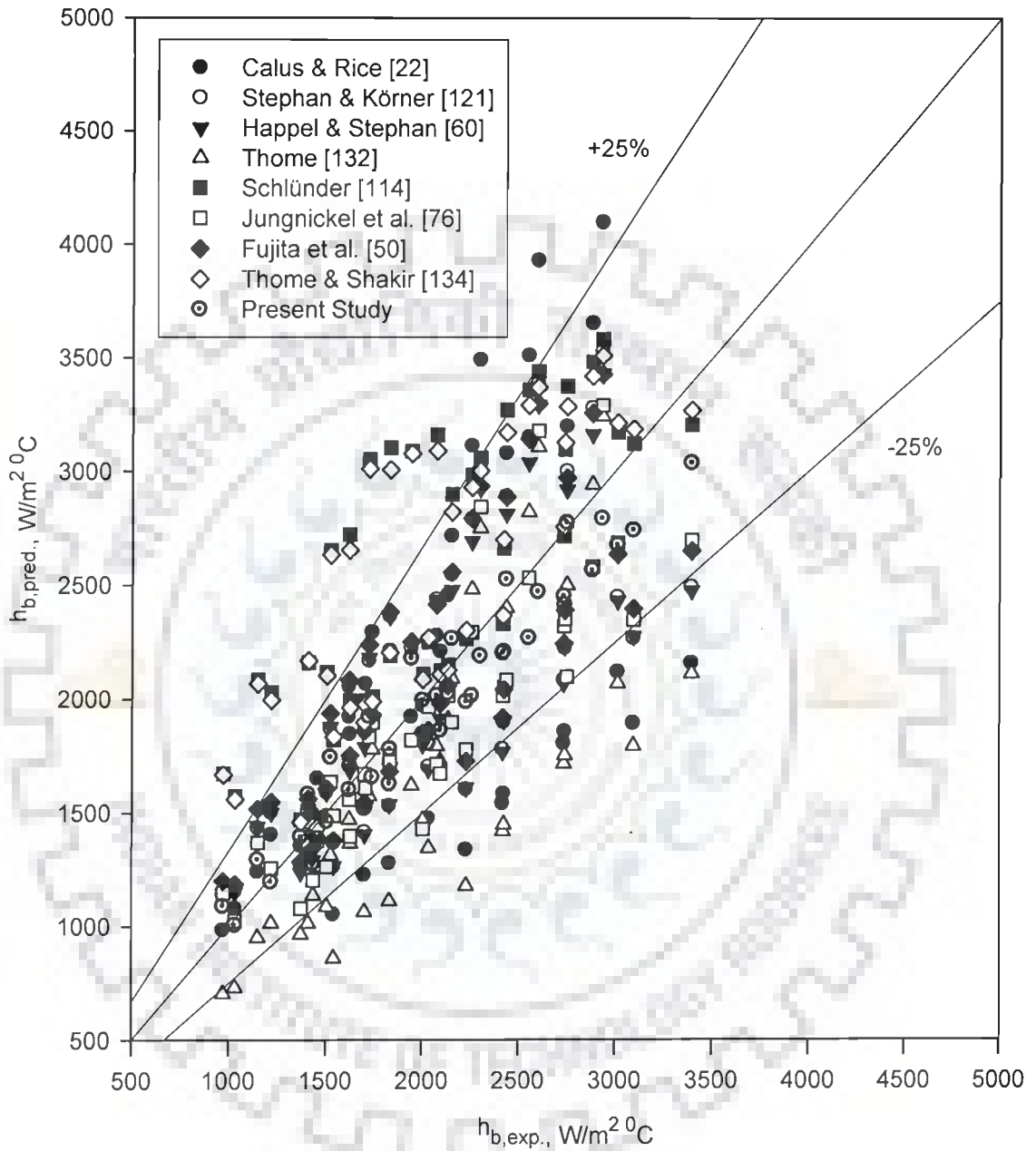


Fig. 5.24 Comparison of experimental heat transfer coefficients with those predicted from Eq. (5.13) for boiling of methanol-distilled water mixture on an uncoated heating tube surface at atmospheric

5.4 NUCLEATE BOILING OF DISTILLED WATER ON COATED HEATING TUBES

Experimental data for boiling of distilled water on horizontal stainless steel tubes coated with copper of various thicknesses are given in Tables B.2 to B.4 of Annexure-B. In this investigation, three thicknesses of copper coating namely 22, 43, and 67 μm have been used. It is important to mention here that procedure used for calculation of heat transfer coefficient in this case has been the same as used for uncoated heating tube surface. The thickness of copper coating has not been considered in the calculation of heat transfer coefficient from coated tube surfaces. Thus, heat transfer coefficient on a coated tube surface is based on substrate temperature only. This has been carried out for the sake of comparison of thermal behavior between coated and uncoated heating tube surfaces. The key objective of conducting experiment on three coated tubes for distilled water was to identify the coated tube with maximum heat transfer coefficient for boiling of distilled water. Following subsections discuss the effect of heat flux, pressure, and coating thickness on heat transfer coefficient during nucleate pool boiling of saturated water on coated heating surfaces at atmospheric and subatmospheric pressures.

5.4.1 Heat transfer coefficients on coated heating surfaces

Figure 5.25 depicts a plot between heat transfer coefficient and heat flux for saturated boiling of distilled water on a stainless steel heating surface coated with 22 μm thickness of copper by electroplating technique at atmospheric pressure. It also contains experimental data of various other investigators namely, Cieslinski [34] on stainless steel surface coated with 0.19 mm thickness of aluminum by modified gas flame spraying technique, Shi & Liu [119] on stainless steel surface coated with 90 μm thickness of copper by electroplating technique, Afgan et. al. [1] on a stainless steel surface coated with 0.45 mm thickness of Cr-Ni by sintering, Alam et al. [4] on a mild steel tube coated with 26 μm thickness of copper by plasma deposition technique, and Bliss et al. [17] on stainless steel surface coated with 127 μm thickness of copper by electroplating technique. The experimental data of

uncoated tube surfaces due to present investigation as well as of above mentioned investigators have also been included in it for the purpose of comparison between coated and uncoated tube surfaces. An examination of this plot reveals the following salient features:

- i. A substantial disagreement exists between data points of present investigation and those of others. Further, data of earlier investigators also do not match amongst themselves.
- ii. At a given heat flux, coated surface offers higher value of heat transfer coefficient than that of corresponding uncoated heating tube.
- iii. Variation of heat transfer coefficient with heat flux on a coated surface of an investigation can be represented by the relationship, $h \propto q^r$ where value of exponent r differs from investigation to investigation. However, the value of exponent r is always found to be less than 0.7 which is usually observed in the case of boiling on an uncoated heating surface.

Above features are consistent and can be explained as follows:

As reported above, heating surfaces employed in each of the above investigations have differed in material of substrate, quality of coating material, thickness of coating and the method of application of coat. Therefore, characteristics of heating surfaces are likely to differ from investigation to investigation, and hence, above noticed disagreement amongst data points of various investigations is bound to occur.

Application of copper coating on an uncoated heating tube leads to the formation of an interwoven matrix consisting of various micro-porous layers. Depending upon the method of application of coating some pores of inner layers are partially or fully exposed to distilled water. As a matter of fact, they entrap residual gas and act as nucleation sites for initiation and development of vapor-bubbles. In this way population of nucleation sites on a coated surface becomes more than that on an uncoated one. In addition, coating has also been found to affect contact angle significantly. In fact, it decreases with increase in thickness of coating, [4, 15, 16, 105, 106]. As contact angle affects surface tension directly, so coating on an uncoated tube surface decreases

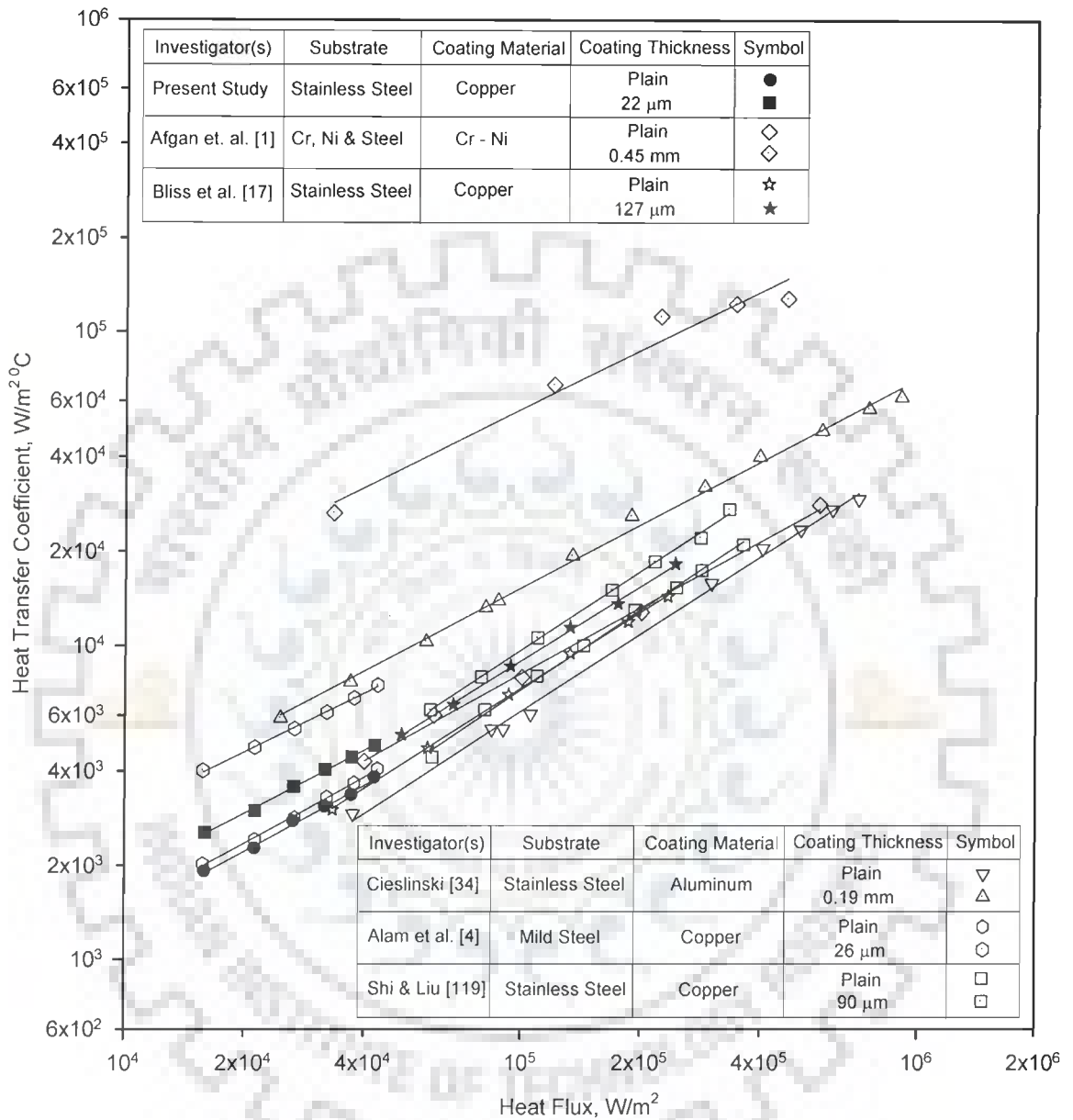


Fig. 5.25 Variation of heat transfer coefficient with heat flux for saturated boiling of distilled water from uncoated and coated surfaces due to present and earlier investigators at atmospheric pressure

surface tension. Thus, coating on an uncoated tube surface produces two significant effects i.e. multiplies nucleation site and decreases surface tension. Both these factors contribute to activate nucleation sites of smaller size to form vapor-bubbles, as can be seen from **Eq. (5.2)**. Consequently, vapor-bubble population on a coated heating surface increases. In fact, at some stage population of vapor-bubbles on coated surface become so large that many of them combine together to form agglomerates which, in turn, lead to vapor blanketing and thereby, obstruct the process of nucleation and development of vapor-bubbles on heating surface. At high values of heat flux, population of vapor agglomerates and thereby the magnitude of vapor blanketing becomes so large that heat removal occurs at a lower rate than that at low values of heat flux. Hence, heat transfer coefficient on a coated surface varies with heat flux at a lower rate than that on an uncoated surface. In other words, the value of exponent r in the relationship between h and q for boiling of distilled water on a coated heating tube surface is less than 0.7 which holds true for an uncoated heating tube surface. It may be mentioned here that almost all the investigators [1, 4, 16, 17, 34, 42, 105, 106, 119, 149] have reported the value of exponent r to be less than 0.7. Thus, experimental observations of this investigation substantiate the finding of earlier investigators too.

As mentioned above, coating on an uncoated tube surface multiplies nucleation sites and reduces surface tension. Hence, large number of small sized vapor-bubbles emit from heating surface with high emission frequency. In addition, coating also increases the magnitude of capillary action due to the formation of matrix structure over an uncoated surface. As a result, water from bulk rushes to inner layer with greater intensity and therefore, heat removal from coated surface takes place at a higher rate than that on an uncoated surface. Thus, for a given value of heat flux, heat transfer coefficient of coated surface is found to be more than that on an uncoated one.

5.4.2 Boiling of distilled water on copper coated tubes

The plot shown in **Fig. 5.26** represents a variation of heat transfer coefficient with heat flux for the boiling of distilled water on a 22 μm thick

copper coated heating tube surface. Pressure is a parameter in this plot. Following salient features emerged out from this plot:

- i. At a given pressure, heat transfer coefficient increases with heat flux and the variation between the two can be described by the relationship, $h \propto q^{0.66}$.
- ii. At a given value of heat flux, heat transfer coefficient increases with rise in pressure.

Above features have also been found for the boiling of distilled water on 43 and 67 μm thick coated tubes as can be seen from **Figs. 5.27a and 5.27b**, respectively. However, the value of exponent of q in the functional relationship between h and q has been found to be different. It is 0.60 and 0.54 for 43 and 67 μm thick coated heating tubes surfaces, respectively.

Above features are same as discussed earlier. Hence, same explanation holds true in this case also. Thus, the value of exponent of q decreases with increase in thickness of coating on heating tube surface. This might be due to the following reason:

An increase in thickness of coating of copper on a heating tube increases the number of micro-porous layers in the matrix structure. This, in turn, multiplies the number of small sized nucleation sites on heating tube surface. As a consequence of increase in the population of nucleation sites, larger number of vapor-bubbles originates in interior portion of matrix of a higher coating thickness tube surface than that on a small coating thickness tube surface. However, many of them combine together to form agglomerates. As the number of small vapor-bubbles on higher coating thickness coated tube is more than that on small coating thickness coated tube, larger number of agglomerates form on the former than that on later one. Hence, area of heating tube surface covered by vapor-agglomerates increases with increase in thickness of coating. Besides this, it is also affected by the magnitude of heat flux. At high value of heat flux, it is more pronounced than that at low heat flux value. At high heat flux value, the population of small sized vapor-bubbles is more. Therefore, the formation of vapor-agglomerates is more. As a result, heat transfer coefficient is affected by two parameters – thickness of coating and

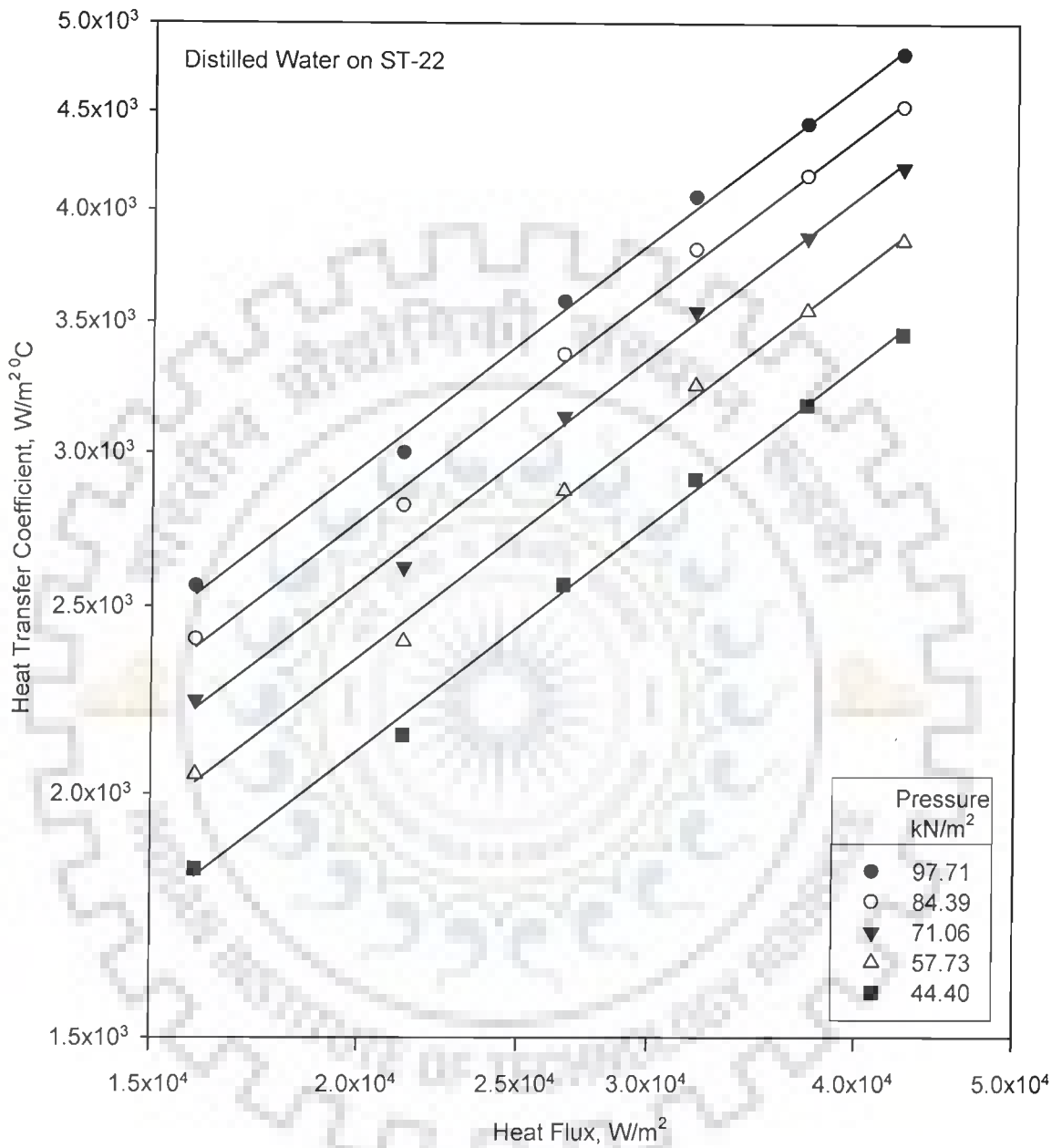


Fig. 5.26 Variation of heat transfer coefficient with heat flux for boiling of distilled water on a 22 μm thick copper coated heating tube surface with pressure as a parameter

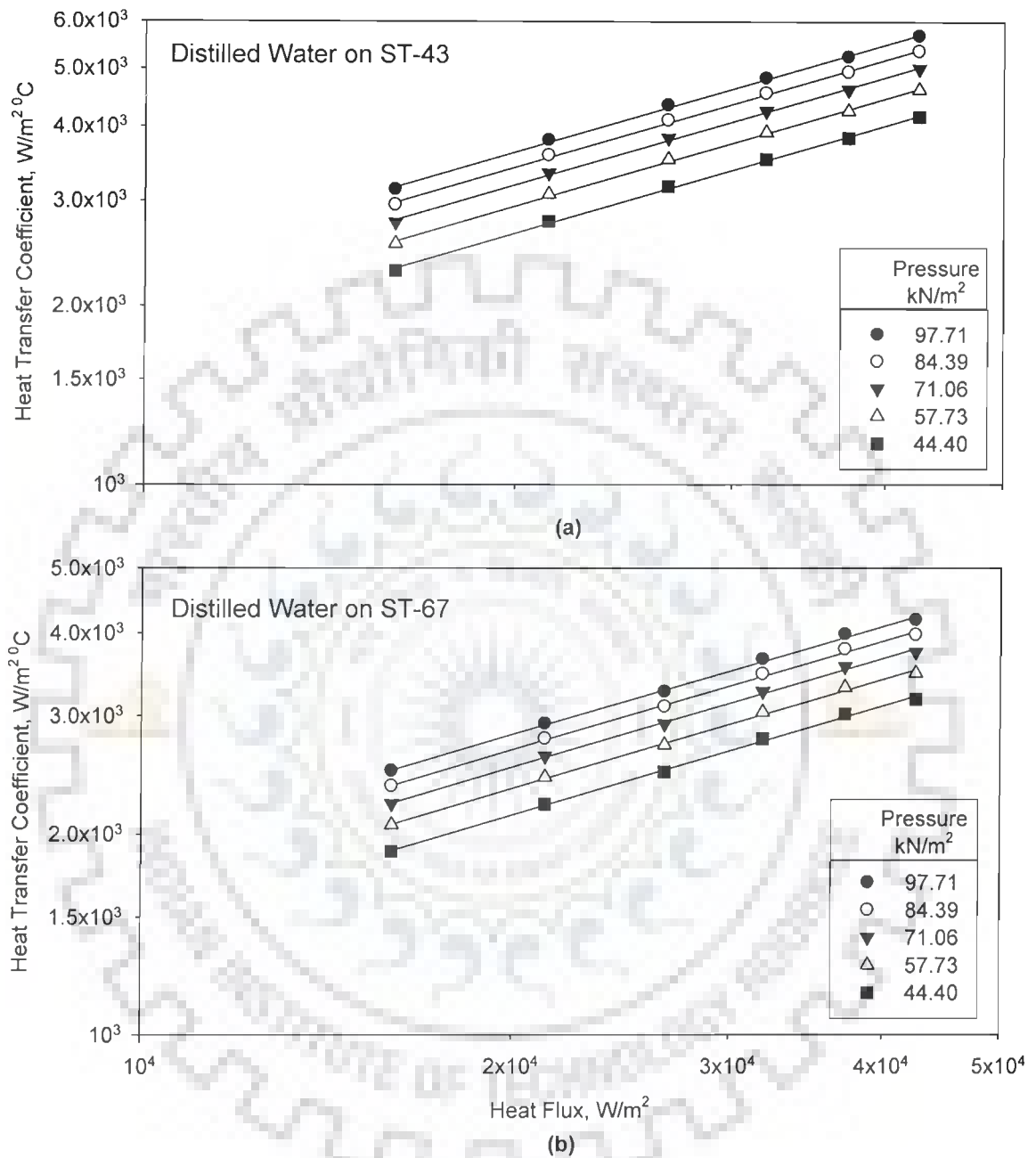


Fig. 5.27 Variation of heat transfer coefficient with heat flux for boiling of distilled water on 43 and 67 μm thick copper coated heating tubes with pressure as a parameter

heat flux in the same manner. Therefore, heat removal rate for boiling of distilled water on a heating surface covered with copper coating decreases with increase in thickness of coating as well as with heat flux. So, heat transfer coefficient – heat flux curve becomes steeper when thickness of coating is decreased. In other words, the slope of h versus q represented by exponent in relationship, $h \propto q^r$ decrease with increase in thickness of coating on a stainless steel heating tube. That is why, the value of exponent of q is found to be smaller on higher coating thickness coated tubes than that observed on smaller coating thickness coated tubes.

5.4.3 Heat transfer coefficient-heat flux relationship for distilled water on coated tubes

Above mentioned discussion indicates that heat transfer coefficient for the boiling of distilled water on a coated heating tube is a function of heat flux, pressure and liquid. Therefore, experimentally determined values of heat transfer coefficient for boiling of distilled water on a coated heating surface have been re-processed by regression analysis to obtain a correlation. It is as follows:

$$h = C_3 q^r p^s \quad (5.14)$$

where, constant, C_3 and exponents r and s depend upon the thickness coating on tube surface. The values of constants C_3 and exponents r and s for coated tubes of this investigation are listed in **Table 5.3**.

Table 5.3 Values of constant, C_3 and exponents, r and s for boiling of distilled water of Eq. (5.14)

S. No.	Tube	C_3	r	s
1	ST-22	0.61	0.66	0.42
2	ST-43	1.54	0.60	0.39
3	ST-67	2.69	0.54	0.35

Figure 5.28 shows a plot between experimentally-determined values of heat transfer coefficient and those predicted from **Eq. (5.14)** for the boiling of

distilled water on coated heating tube surfaces at atmospheric and sub-atmospheric pressures. The plot clearly indicates that the predicted values have matched excellently with the experimental values within a maximum error of $\pm 2.30\%$. Thus **Eq. (5.14)** has succeeded to correlate experimental data of boiling heat transfer for distilled water on coated heating tubes surfaces.

5.4.4 Comparison between boiling characteristics for distilled water on a coated heating tube and those on an uncoated heating tube

This section has been devoted to make a comparative study of boiling heat transfer characteristics of distilled water on tubes coated with copper of various thicknesses with that on an uncoated tube surface at atmospheric and subatmospheric pressures with an aim to obtain the effect of thickness of coating on boiling heat transfer coefficient.

Figure 5.29 represents a plot between heat transfer coefficient and heat flux for saturated boiling of distilled water on stainless steel tubes coated with copper of various thicknesses at atmospheric pressure. This plot also contains a curve for an uncoated tube surface to show comparison between the two. An inspection of this plot reveals following salient features:

- i. For a given heat flux, an increase in thickness of coating increases heat transfer coefficient up to a certain value and thereafter decreases
- ii. Heat transfer coefficient on coated tubes of various thicknesses is higher than that on an uncoated tube for a given value of heat flux.

Possible explanation for above behavior is as follows:

As explained in sub-section 5.4.1, coating of copper on an uncoated tube surface increases nucleation site density and reduces contact angle. Therefore, number of small sized vapor-bubbles emitting from a coated heating surface increases. This increases the population of vapor-bubbles which causes coalescence leading to form vapor agglomerates. As a result, heat removal rate decreases. In addition, coating also increases the magnitude of capillary action which, in turn, instigates liquid from pool to rush to inner portion of matrix structure with greater intensity to fill void caused by the departure of

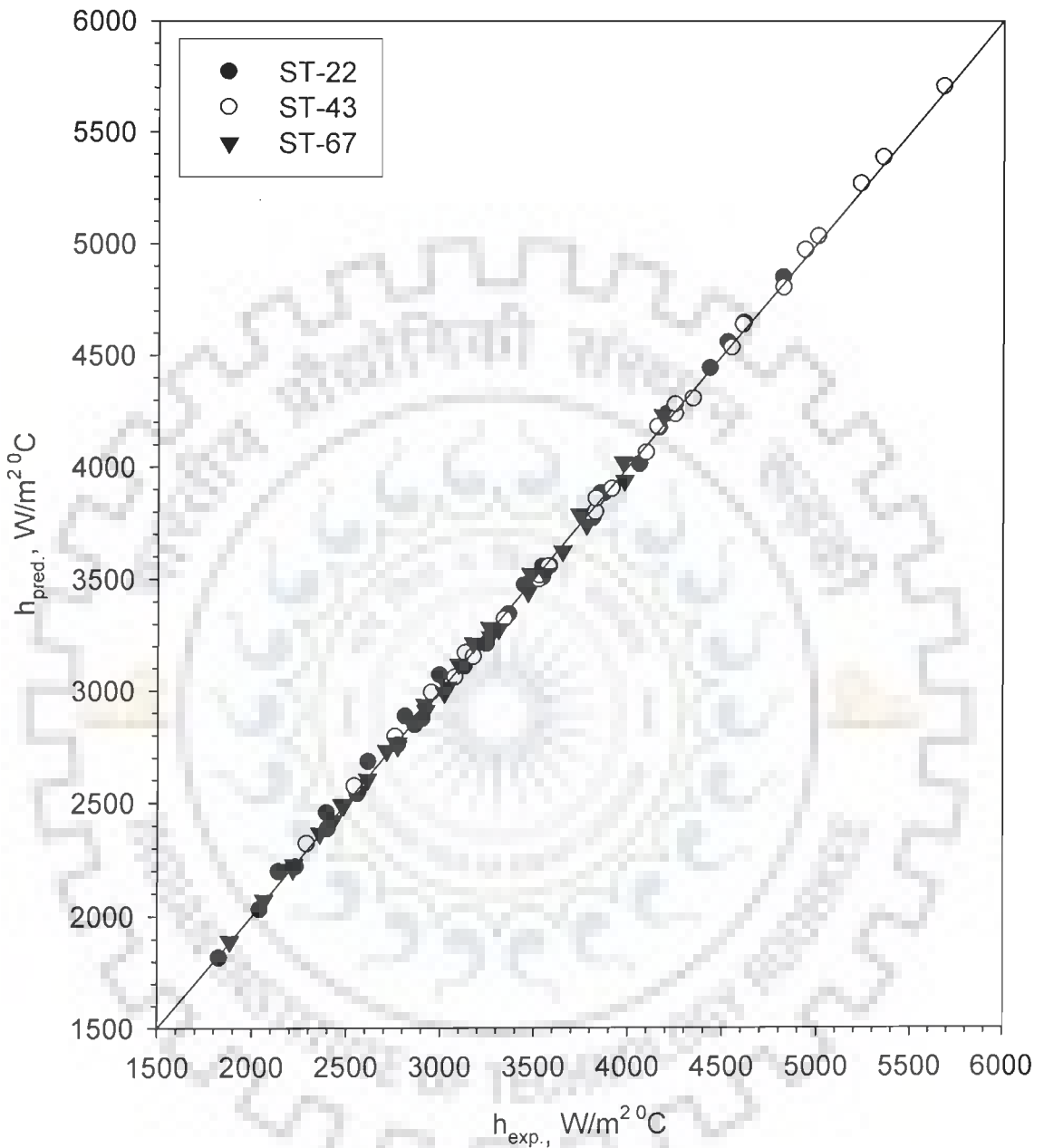


Fig. 5.28 Comparison of experimental heat transfer coefficients with those predicted from Eq. (5.14) for boiling of distilled water on coated heating tube surfaces at atmospheric and subatmospheric pressures

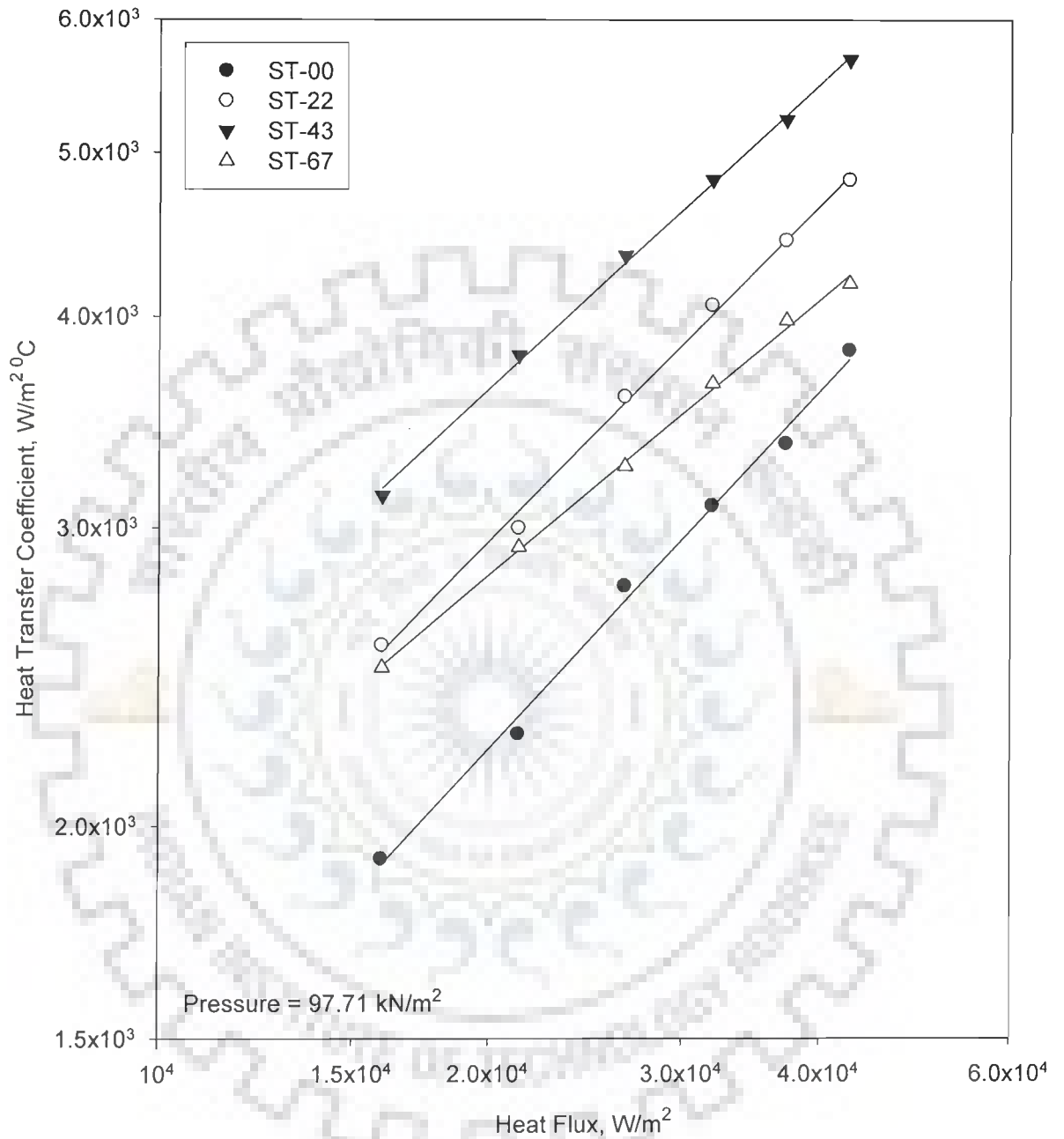


Fig. 5.29 Variation of heat transfer coefficient with heat flux for boiling of distilled water on copper coated tubes and on an uncoated tube at atmospheric pressure

vapor-bubbles from surface. In fact, it increases continuously with increase in coating thickness. This increases recirculation of liquid which leads to increase the intensity of turbulence near the heating surface and enhances heat removal rate. Thus, increase in thickness of coating produces two opposing phenomena reduction of heat removal rate due to the formation of vapor bubble-agglomerates and increase of heat removal rate owing to enhancement of capillary action. The resultant effect of coating thickness depends upon the magnitude of these phenomena. As a matter of fact, the effect of later seems to be more pronounced than that of former during initial stages of coating on a heating tube surface. That is why, heat transfer coefficient on a 22 μm thick coated surface is found to be more than that on an uncoated tube surface.

Above behavior also holds true when thickness of coating is increased from 22 to 43 μm . An increase in thickness of coating beyond 43 μm further enhances the population of vapor-bubbles and thereby vapors agglomerates which are responsible to decrease heat removal rate. However, it is also accomplished with the decrease of heat flow rate by conduction from substrate surface to various layers of coating owing to continuous replacement of liquid by vapor in matrix structure. As a result, heat removal rate decreases. Thus, both the above mentioned phenomena supplement each other to reduce heat removal rate from surface to liquid pool. No doubt, the intensity of recirculation rate due to capillary structure increases with thickness of coating, but its effect on heat removal rate does not seem to be as pronounced as that of vapor agglomerates. In other words, vapor agglomerates play a dominating role to affect heat transfer rate from coated surface. Since number of agglomerates increases with coating thickness, a reduction in heat removal rate and thereby heat transfer coefficient is bound to occur beyond a certain thickness of coating. In present investigation, heat transfer coefficient, at a given heat flux, is observed to decrease beyond a thickness of coating of 43 μm i.e. for coating thickness of 67 μm .

An increase in heat flux on a coated surface affects above phenomena considerably. When boiling of distilled water occurs on a coated surface, increase in vapor-bubble population occurs on account of increase in number of nucleation sites formed by various layers of coating as well as heat flux. As a consequence, many of them combine together to form vapor agglomerate which affects heat transfer coefficient adversely. Therefore, heat transfer rate in the region of high heat flux does not increase with the same rate as it does in the region of low heat flux. Thus, as can be seen from **Fig. 5.29**, slope of heat transfer coefficient-heat flux curve decreases with increase in coating thickness.

Figures 5.30 and 5.31 are typical plots showing the effect of coating thickness on heat transfer coefficient for boiling of distilled water at various subatmospheric pressures. These plots have essentially the same features as that of plot in **Fig. 5.29** for boiling of distilled water at atmospheric pressure.

On the basis of above, it can be said that coating of copper on an uncoated tube surface enhances heat transfer coefficient of boiling liquids significantly. For a given value of heat flux, heat transfer coefficient increases with increase in coating thickness up to a certain value and thereafter decreases. However, increase in heat transfer coefficient is not proportional to increase in coating thickness. Further, the rate of variation of heat transfer coefficient with heat flux depends upon coating thickness. In fact, it decreases with increase in thickness of coating. This continues and therefore, a thick coated heating tube surface may provide heat transfer coefficient lower than that of an uncoated heating tube surface depending up on the value of heat flux and pressure. The increase in magnitude of heat transfer coefficient has differed due to difference in physico-thermal properties of methanol and distilled water.

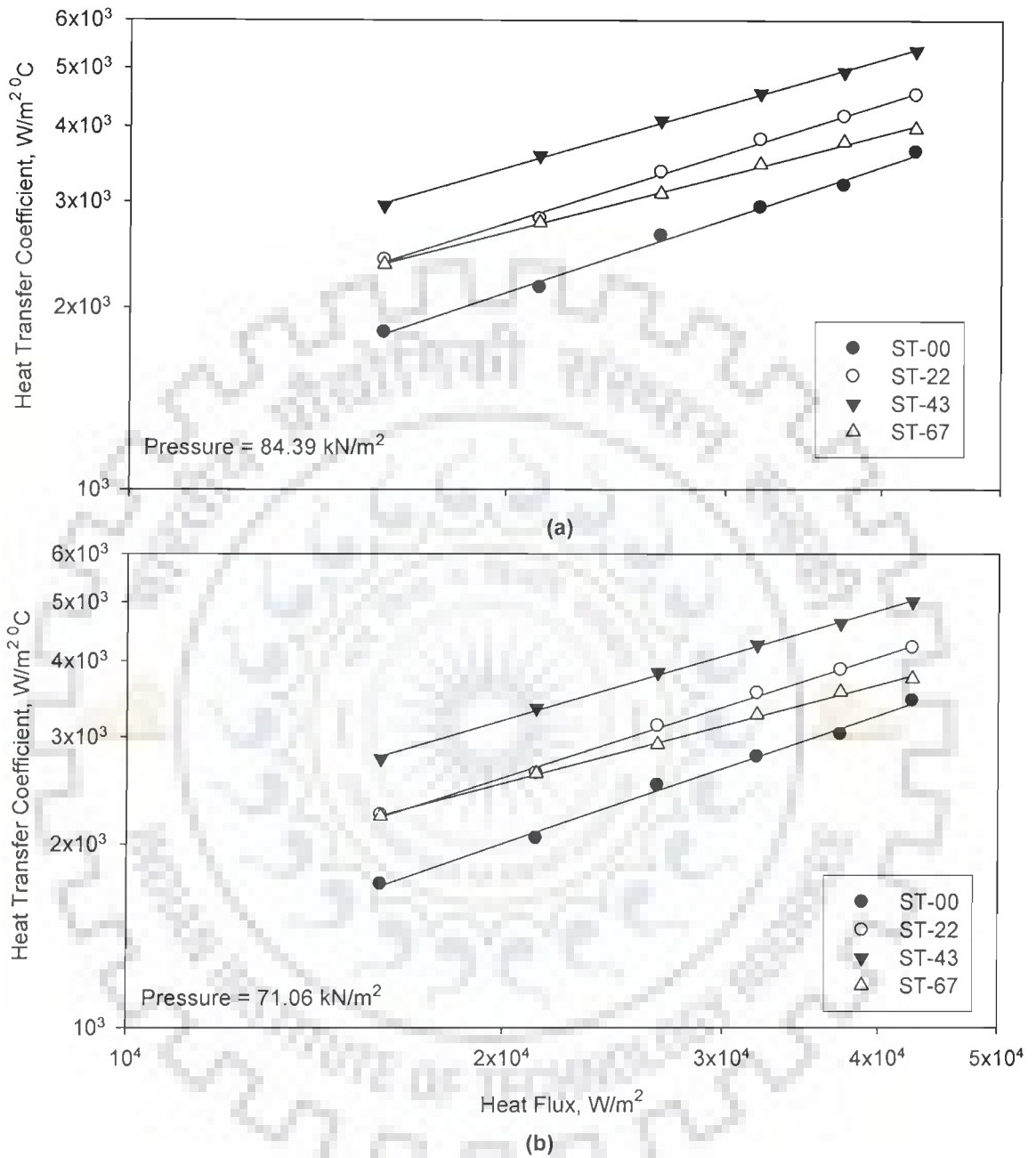


Fig. 5.30 Variation of heat transfer coefficient with heat flux for boiling of distilled water on copper coated tubes and uncoated tube at 84.39 kN/m² and 71.06 kN/m² subatmospheric pressures

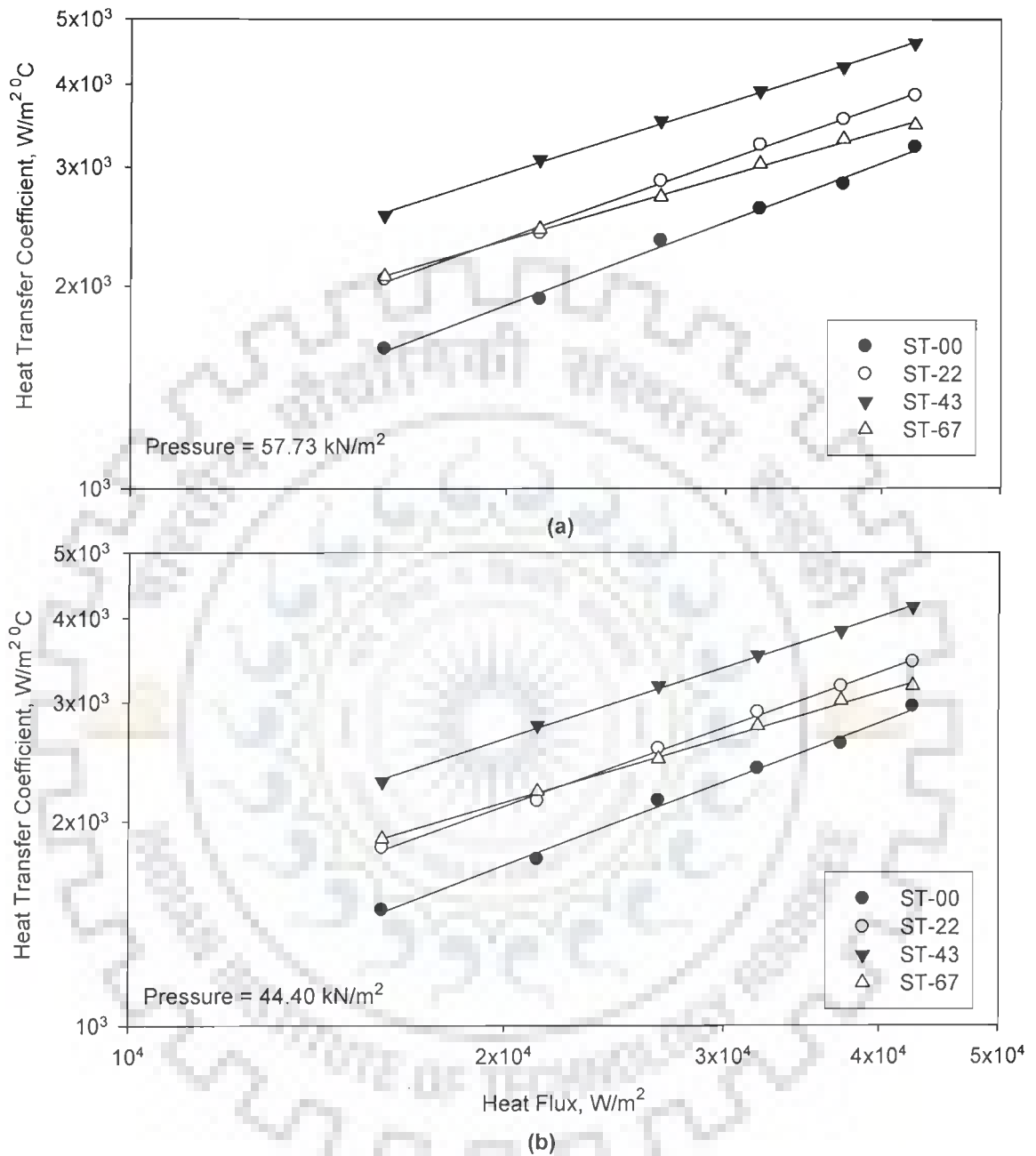


Fig. 5.31 Variation of heat transfer coefficient with heat flux for boiling of distilled water on copper coated tubes and uncoated tube at 57.73 kN/m^2 and 44.40 kN/m^2 subatmospheric pressures

5.5 NUCLEATE BOILING OF METHANOL ON A COATED HEATING TUBE

As mentioned in the preceding section, coating of a copper on a horizontal stainless steel tube enhances heat transfer coefficient for the boiling of distilled water at atmospheric and subatmospheric pressures. However, there exists a thickness of coating at which enhancement of heat transfer coefficient is maximum. In the present investigation 43 μm copper coated stainless steel heating tube has been found to provide the more heat transfer coefficient than 22 and 67 μm coated tubes. Thus, use of a 43 μm thick coated tube is advantageous. Keeping this in mind, it was considered adequate to investigate the pool boiling of saturated methanol on a 43 μm thick coated heating tube only. This was carried out due to constrain of time. Hence, following discussion pertains to the boiling of methanol on a 43 μm thick copper coated stainless steel tube at atmospheric and subatmospheric pressures.

Experimental data for boiling of saturated methanol on horizontal stainless steel tube coated with copper of 43 μm thickness at atmospheric and subatmospheric pressures are given in Tables B.6 of Annexure-B. Following subsections discuss the effect of heat flux and pressure on heat transfer coefficient for nucleate pool boiling of saturated methanol on a coated heating surface.

5.5.1 Boiling heat transfer characteristics for methanol on a coated tube

Figure 5.32 shows a plot between heat transfer coefficient and heat flux for the boiling of methanol on a 43 μm thick coated heating tube surface. Pressure is a parameter in this plot. This plot has the following salient features:

- i. At a given pressure, heat transfer coefficient increases with increase in heat flux and the variation between the two can be described by the relationship, $h \propto q^{0.60}$.
- ii. At a given value of heat flux, heat transfer coefficient increases with rise in pressure.

Above features are same as discussed earlier. Hence, same explanation holds true in this case also.

5.5.2 Heat transfer coefficient-heat flux relationship for methanol on a coated tube

Aforesaid discussion indicates that heat transfer coefficient of methanol, boiling on a 43 μm thick coated heating tube, is a function of heat flux and pressure. Therefore, experimentally determined values of heat transfer coefficient for boiling of methanol on a 43 μm thick coated heating surface have been re-processed by regression analysis to obtain a correlation. It is as follows:

$$h = 1.27q^{0.60}p^{0.39} \quad (5.15)$$

Figure 5.33 shows a plot between experimentally-determined values of heat transfer coefficient and those predicted from **Eq. (5.15)** for the boiling of methanol on a 43 μm thick coated heating tube at atmospheric and subatmospheric pressures. The plot clearly indicates that the predicted values have matched excellently with the experimental values within a maximum error of $\pm 3\%$. Thus **Eq. (5.15)** has succeeded to correlate experimental data of boiling heat transfer of saturated methanol on a 43 μm thick coated heating tube surface.

5.5.3 Comparison of boiling heat transfer characteristics on a coated and uncoated tube surfaces for methanol

This section has been devoted to make a comparative study of boiling heat transfer characteristics of methanol on a 43 μm thick coated tube with that on an uncoated tube surface at atmospheric and subatmospheric pressures with an objective to obtain the effect of coating on boiling heat transfer coefficient.

Figure 5.34 depicts a plot between heat transfer coefficient and heat flux for saturated boiling of methanol on a tube coated with 43 μm thickness of copper at atmospheric pressure. This plot also contains a curve for an uncoated tube surface for the sake of comparison. A close examination of this plot reveals that heat transfer coefficient for boiling of methanol on a 43 μm thick coated tube is higher than that on an uncoated tube for a given value of heat flux.

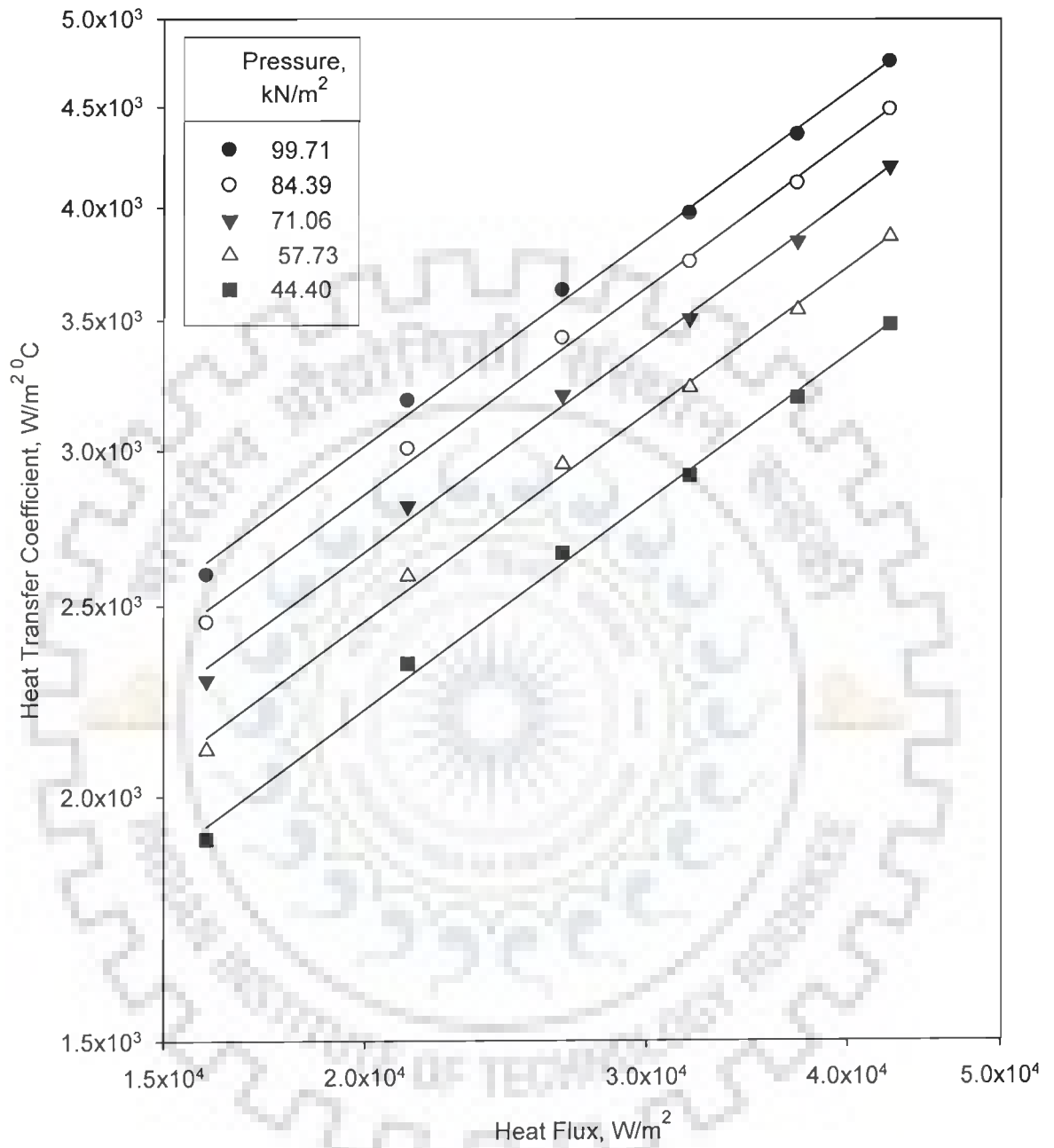


Fig. 5.32 Variation of heat transfer coefficient with heat flux for boiling of methanol on a 43 µm thick copper coated heating tube surface with pressure as a parameter

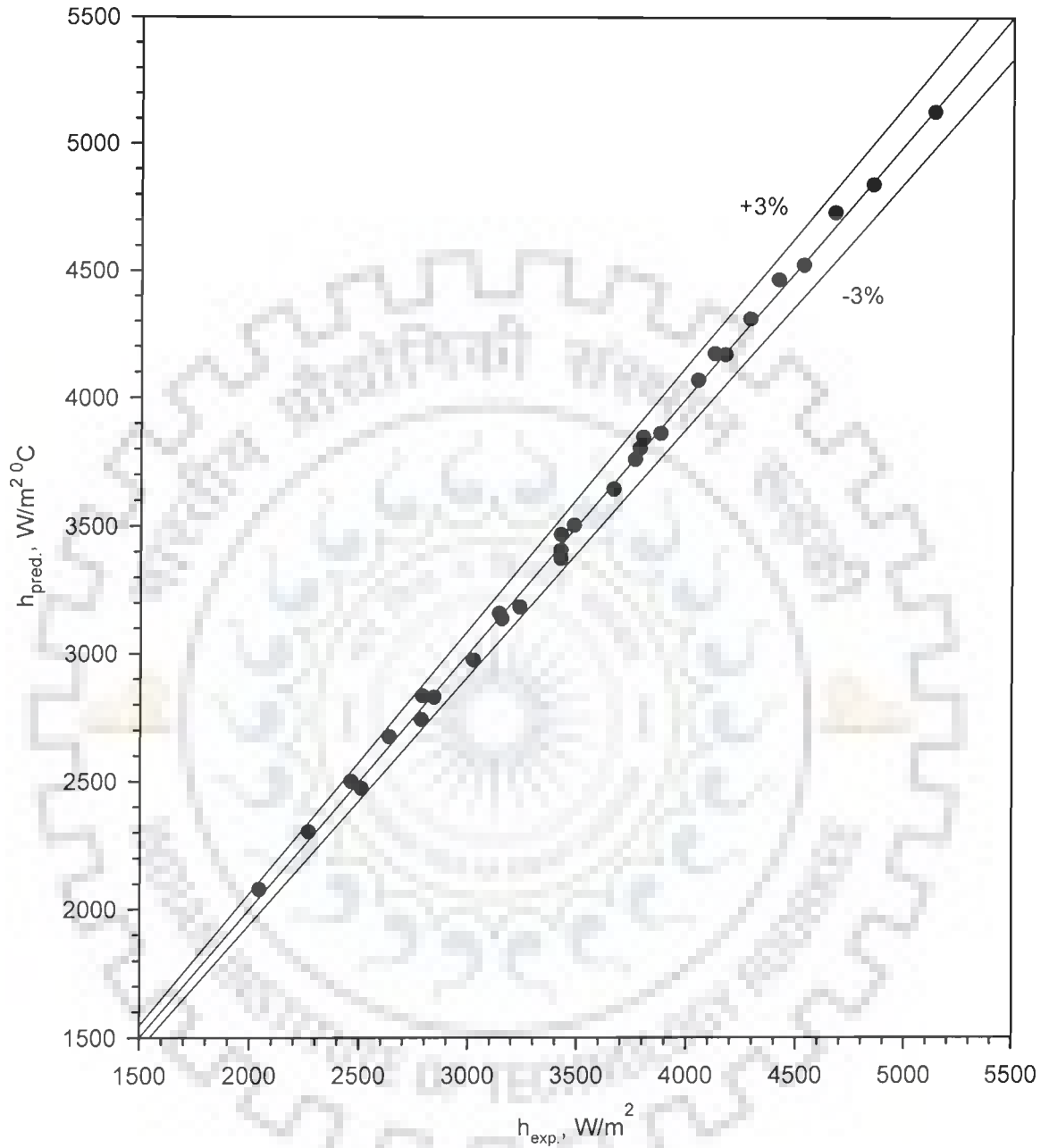


Fig. 5.33 Comparison of experimental heat transfer coefficients with those predicted from Eq. (5.15) for boiling of methanol on a 43 μm coated heating tube surfaces at atmospheric and subatmospheric pressures

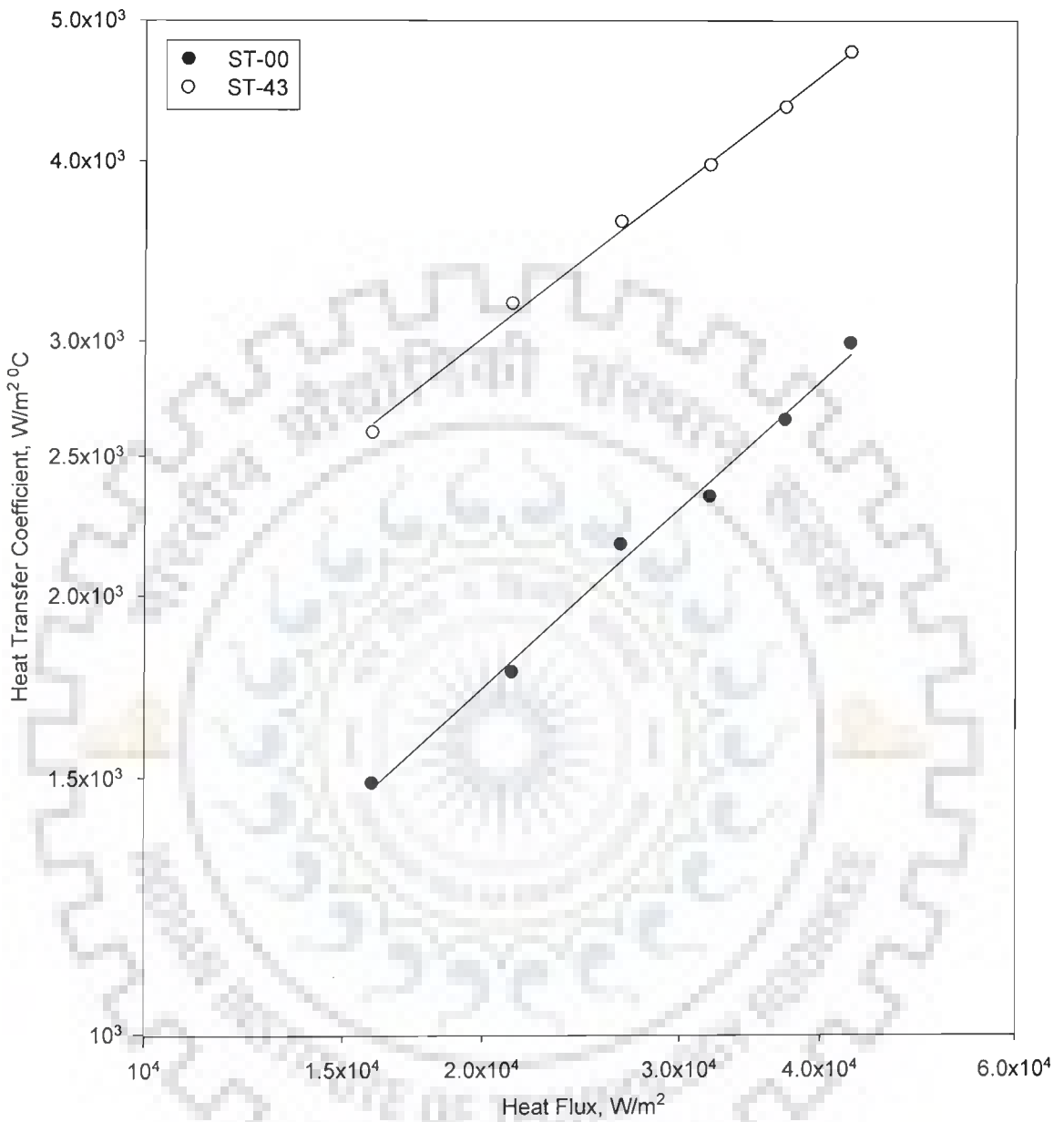


Fig. 5.34 Variation of heat transfer coefficient with heat flux for boiling of methanol on a 43 μm thick copper coated tube and on an uncoated tube at atmospheric pressure

Above feature is similar to that obtained for boiling of distilled water on a coated tube as discussed earlier. Hence, same explanation holds true in this case too.

Figures 5.35 and 5.36 are typical plots to represent the effect of coating on heat transfer coefficient for boiling of methanol at 84.39, 71.06, 57.73 and 44.40 kN/m² pressures, respectively. The features of these plots are similar to that drawn from **Fig. 5.34** at atmospheric pressure.

SUMMARY

On the basis of above it may be concluded that coating of copper on a stainless steel tube enhances heat transfer coefficient for the boiling of saturated liquids – distilled water and methanol at atmospheric and subatmospheric pressures. However, enhancement on a 43 μm thick coated tube has been found to be more than 22 and 67 μm thick coated tubes for the boiling of distilled water.

5.6 NUCLEATE BOILING OF A BINARY MIXTURE ON A COATED HEATING TUBE

As pointed out earlier, 43 μm thick coated heating tube was also selected to investigate heat transfer characteristic for the boiling of various compositions of methanol-distilled water binary mixture at atmospheric and subatmospheric pressures. Experimental data for the boiling of 5, 10, 30, 50, 80, 90 and 95 mole percent methanol-distilled water mixtures on a 43 μm thick copper coated stainless steel heating tube are listed in Tables B.14 to B.20 of Annexure-B. Following subsections describe the effect of heat flux, pressure and composition on heat transfer coefficient for the boiling of mixture on a coated heating tube.

5.6.1 *Boiling heat transfer characteristics for a binary mixture on a coated heating tube*

Figure 37 represents a typical plot between heat transfer coefficient and heat flux for the saturated boiling of 5 mol percent methanol-distilled water mixture on 43 μm thick copper coated heating tube surface. Pressure is a

parameter in this plot. Following important features emerged out from this plot:

- a. At a given pressure, heat transfer coefficient increases with heat flux and the variation between the two can be described by the functional relationship, $h \propto q^{0.60}$.
- b. An increase in pressure increases heat transfer coefficient at a given value of heat flux.

Boiling of other composition of methanol-distilled water mixture on a $43 \mu\text{m}$ coated tube surface also resulted similar plots as shown in **Figs. 5.38 to 5.40**. All of them have similar features as mentioned above.

The above mentioned behavior is same as has been observed for the boiling of mixtures on an uncoated tube surface. Further, the concentration (30 mol percent) at which turnaround phenomena has been observed is same as found in case of uncoated tube. Thus, coating of tube surface does not seem to change the behavior and also the turnaround concentration.

Thus, it may be said that boiling heat transfer characteristics of methanol-distilled water binary mixture on a $43 \mu\text{m}$ thick copper coated heating tube surface are alike with those of methanol, and distilled water. This is quite synonymous with the behavior on uncoated tube surface.

5.6.2 Heat transfer coefficient-heat flux relationship for a binary mixture on a coated heating tube

Using experimental data for the boiling of various compositions of methanol-distilled water mixture at a $43 \mu\text{m}$ thick copper coated heating tube surface at atmospheric and subatmospheric pressures, following dimensional correlation amongst heat transfer coefficient, heat flux and pressure has been obtained by regression analysis:

$$h = C_4 q^{0.60} p^{0.39} \quad (5.16)$$

where, C_4 is a constant whose value depends upon the percentage composition of the mixture, and surface characteristic. The values of constant, C_4 as determined for various compositions of methanol-distilled water mixtures are given in **Table 5.4**.

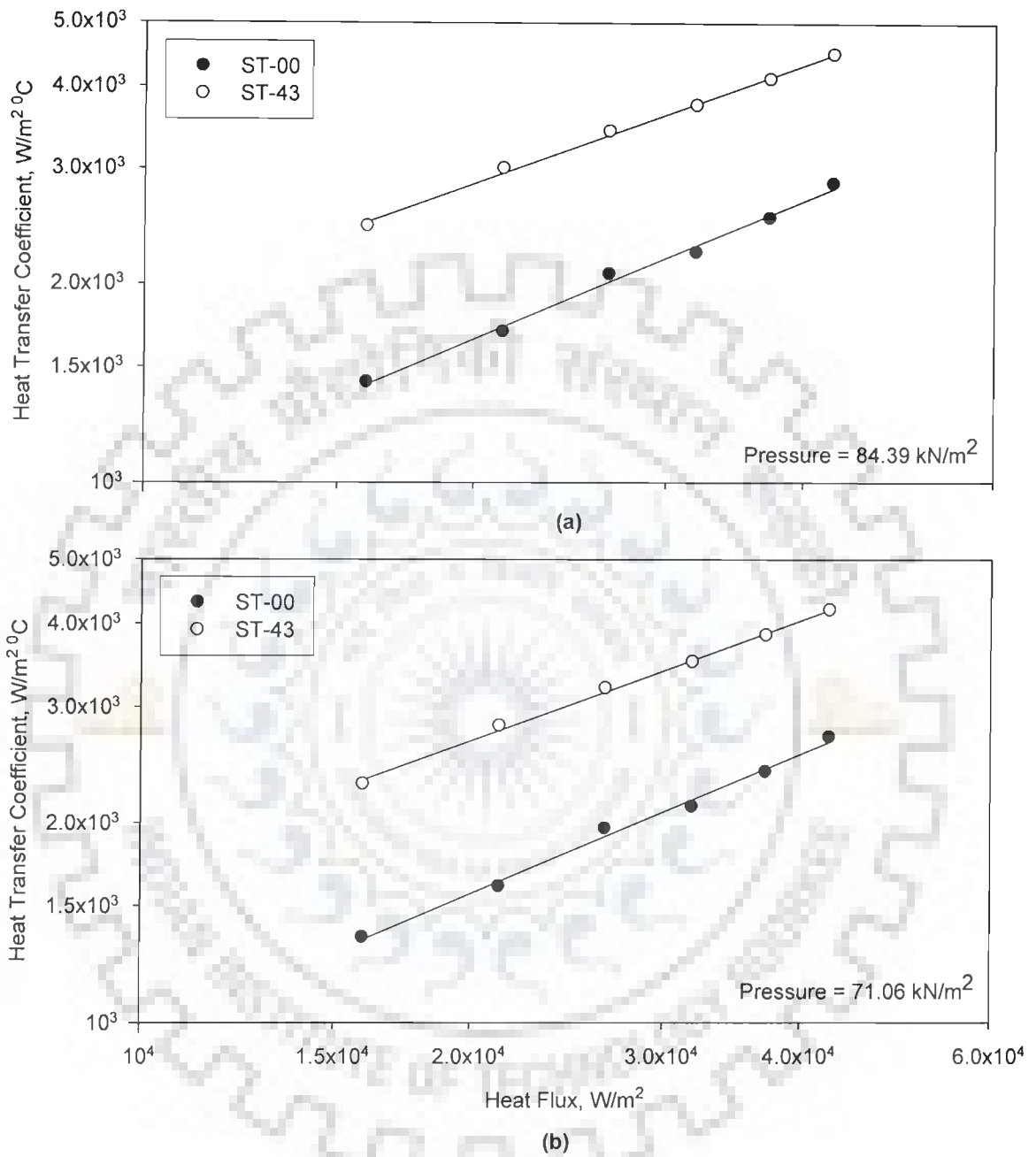


Fig. 5.35 Variation of heat transfer coefficient with heat flux for boiling of methanol on a 43 μm thick copper coated tube and on an uncoated tube at 84.39 and 71.06 kN/m^2 pressures

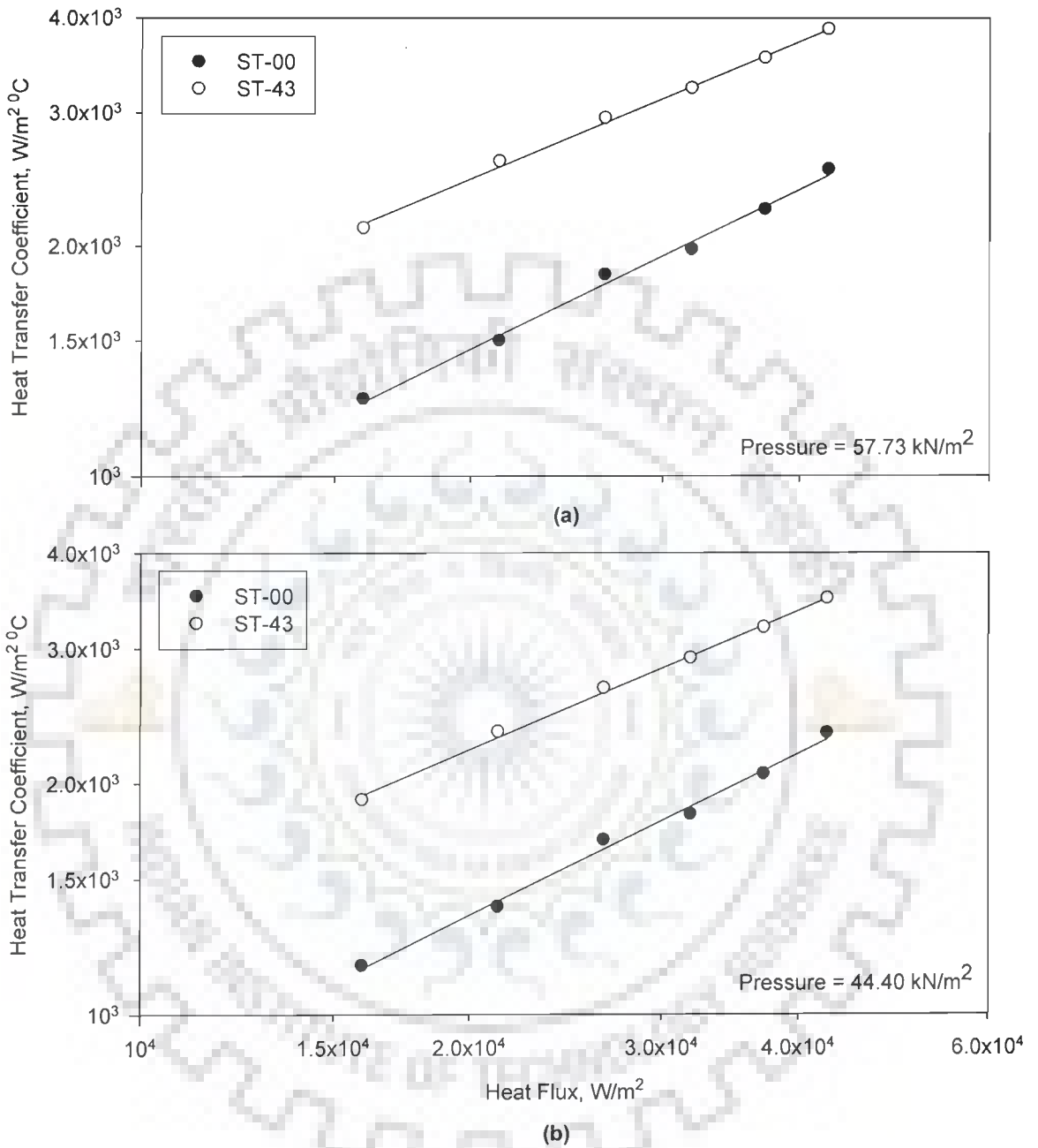


Fig. 5.36 Variation of heat transfer coefficient with heat flux for boiling of methanol on a 43 μm thick copper coated tube and on an uncoated tube at 57.73 and 44.40 kN/m² pressures

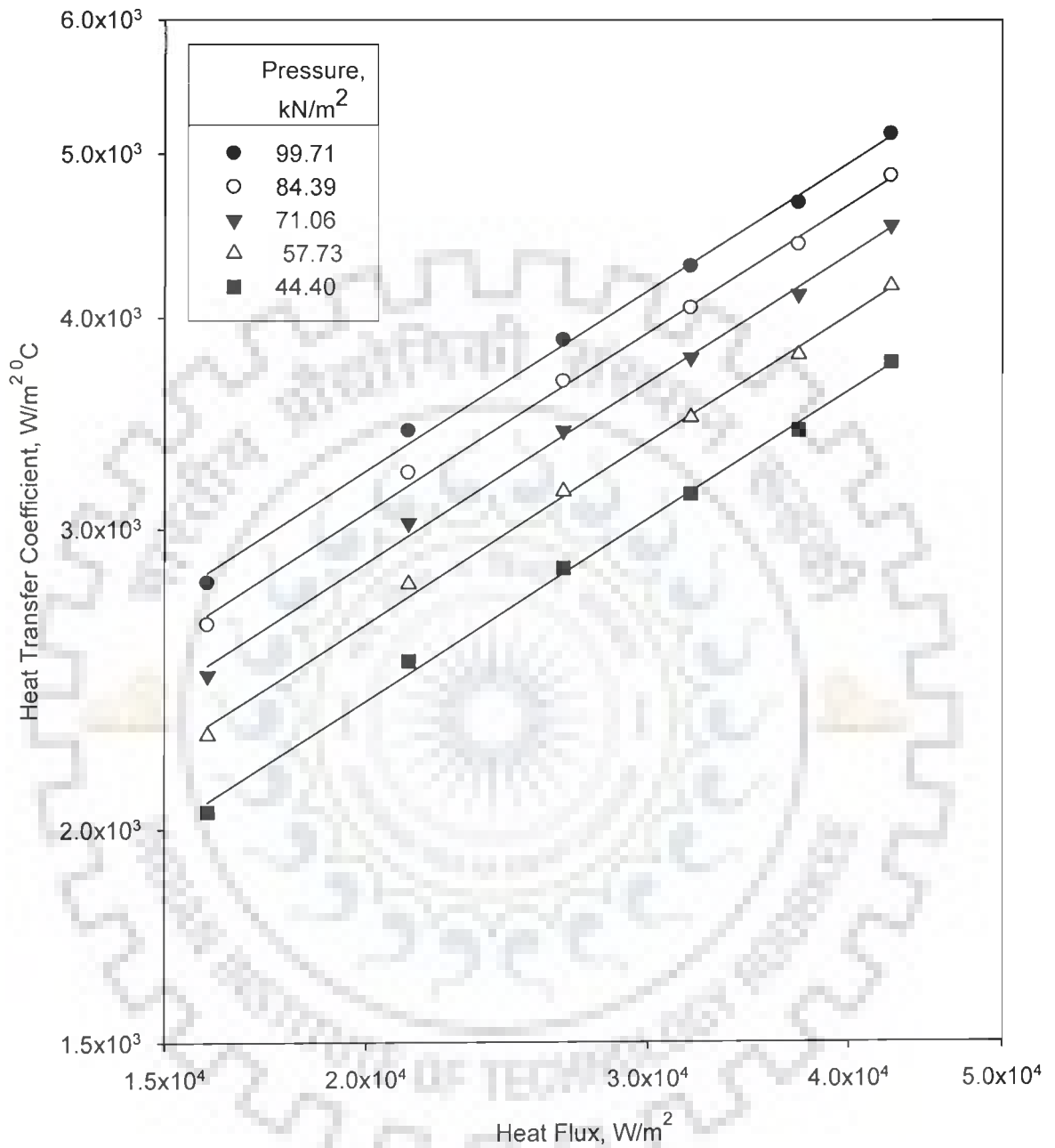


Fig. 5.37 Variation of heat transfer coefficient with heat flux for boiling of 5 mol% methanol-distilled water mixture on a 43 μm thick copper coated heating tube surface with pressure as a parameter

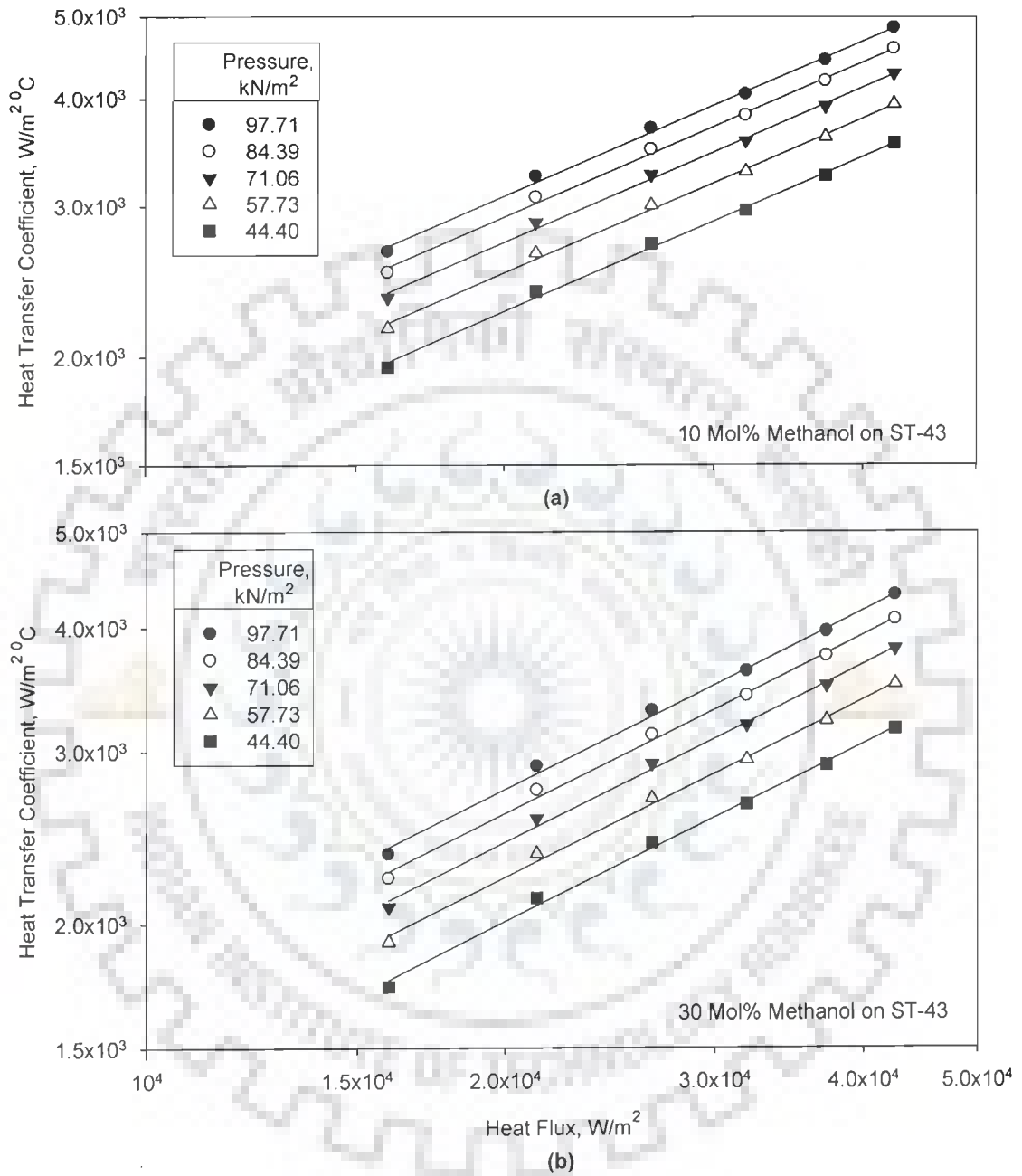


Fig. 5.38 Variation of heat transfer coefficient with heat flux for boiling of 10 and 30 mol% methanol-distilled water mixtures on a 43 μm thick copper coated heating tube surface with pressure as a parameter

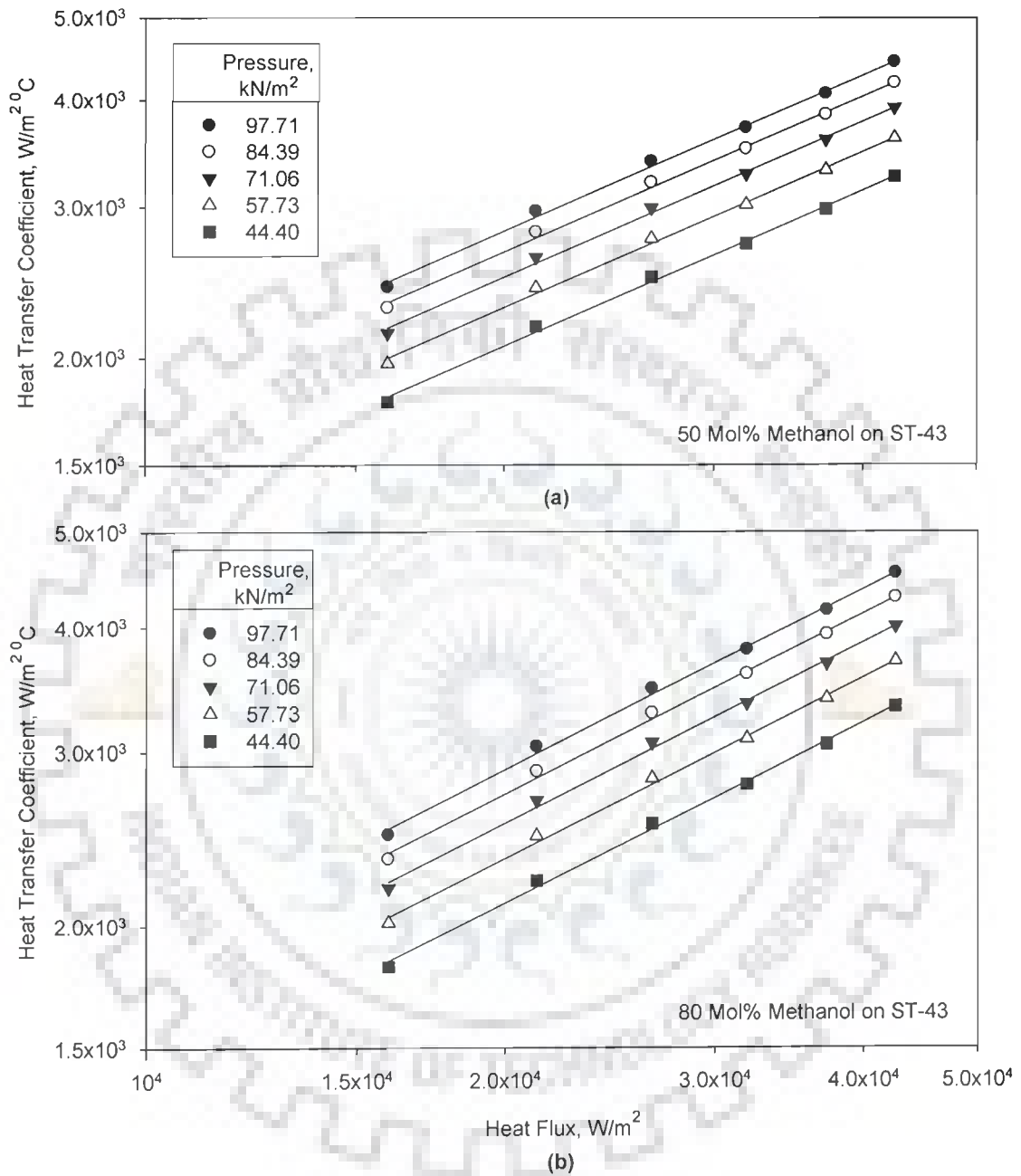


Fig. 5.39 Variation of heat transfer coefficient with heat flux for boiling of 50 and 80 mol% methanol-distilled water mixtures on a 43 μm thick copper coated heating tube surface with pressure as a parameter

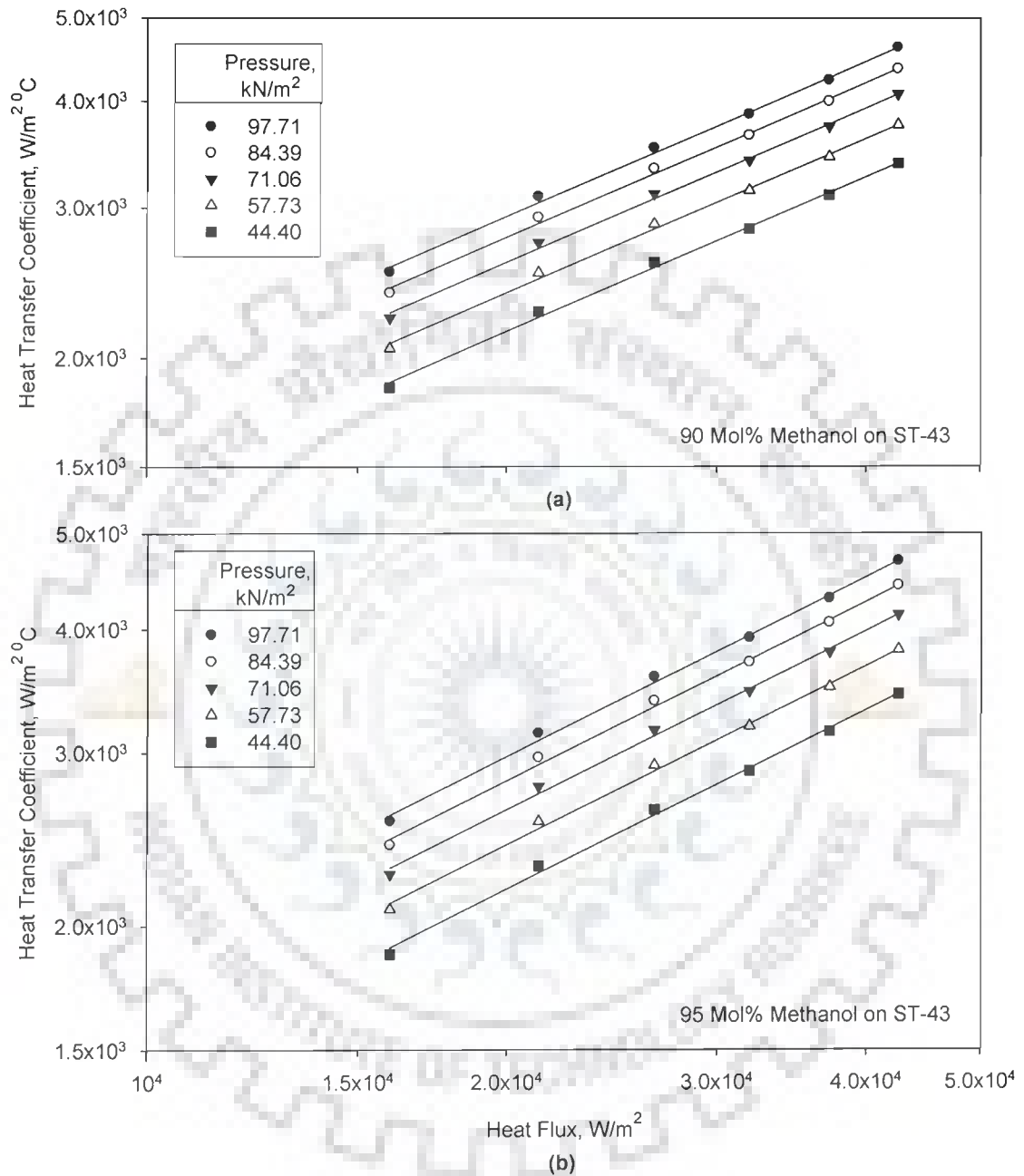


Fig. 5.40 Variation of heat transfer coefficient with heat flux for boiling of 90 and 95 mol% methanol-distilled water mixtures on a 43 μm thick copper coated heating tube surface with pressure as a parameter

Table 5.4 Value of constants C_4 of Eq. (5.16) for various compositions of methanol-distilled water mixtures

S. No.	Mixture Concentration (Mol% Methanol)	C_4
1.	5	1.337
2.	10	1.334
3.	30	1.170
4.	50	1.178
5.	80	1.202
6.	90	1.229
7.	95	1.244

Equation (5.16) is a simple and convenient equation for the calculation of heat transfer coefficient for the boiling of methanol-distilled water mixture on a 43 μm thick copper coated heating tube surface from the knowledge of heat flux and pressure provided the value of constant, C_4 is known.

Figure 5.41 shows a plot between experimentally determined values of heat transfer coefficient and those calculated by Eq. (5.16) for the boiling of various concentrations on a 43 μm thick copper coated heating tube surface at atmospheric and subatmospheric pressures. As can be seen from the plot, the predictions match the experimental values excellently within an error of $\pm 5\%$ only. Thus, it is concluded that Eq. (5.16) can be used to determine heat transfer coefficient for the boiling of methanol-distilled water mixtures on a 43 μm copper coated stainless steel heating tube from the knowledge of heat flux and pressure provided the values of constant C_4 are known.

5.6.3 Comparison of boiling heat transfer characteristics on a coated and uncoated tube surfaces for a binary mixture

Figure 5.42 has been drawn to show a comparison of heat transfer coefficient for the boiling of various composition of methanol-distilled water mixture on a 43 μm copper coated stainless steel heating tube surface with that on an uncoated tube at atmospheric pressure. Basically, it is a plot between h

and q for a coated as well as an uncoated tube surface. The plot clearly indicates that at a given value of heat flux, heat transfer coefficient on a coated tube is higher than that on an uncoated one. Same features have also been obtained for the boiling of mixtures at subatmospheric pressures, as can be seen from the plots contains in **Figs. 5.43 to 5.45**. The reason for this behavior is same as discussed earlier in case of liquids.

Keeping above in view, it may be said that coating of copper on a stainless steel heating tube enhances heat transfer coefficient for the boiling of methanol-distilled water binary mixtures at atmospheric and subatmospheric pressures. Further, the functional relationship between h and q described by the power law, of form, $h \propto q^n$ also changes. In fact, the value of exponent n decreases when boiling of liquid mixture occurs on a coated heating tube surface. It is also bring out the fact that coating of a tube does not affect the salient features. But it merely alters the rate of variation. This is in line with the behavior observed for the boiling of liquids on coated surfaces. Hence boiling behavior of methanol-distilled water mixture is as that for single component liquids – distilled water and methanol.

5.6.4 Variation of heat transfer coefficient of mixtures with composition for boiling on a coated tube

Figure 5.46b represents a typical plot between heat transfer coefficients for the boiling of various compositions of methanol-distilled water mixture on a $43 \mu\text{m}$ thick coated tube and concentration at atmospheric pressure to show the effect of concentration on heat transfer coefficient. Heat flux is parameter in this plot. Following important points emerges out from this plot:

- i. For a given heat flux, heat transfer coefficient decreases with increase in methanol concentration. This trend continues till the concentration reaches to 30 mol percent. Thereafter, any further increase in concentration increases the value of heat transfer coefficient.
- ii. At a given concentration heat transfer coefficient increases with increase in heat flux.

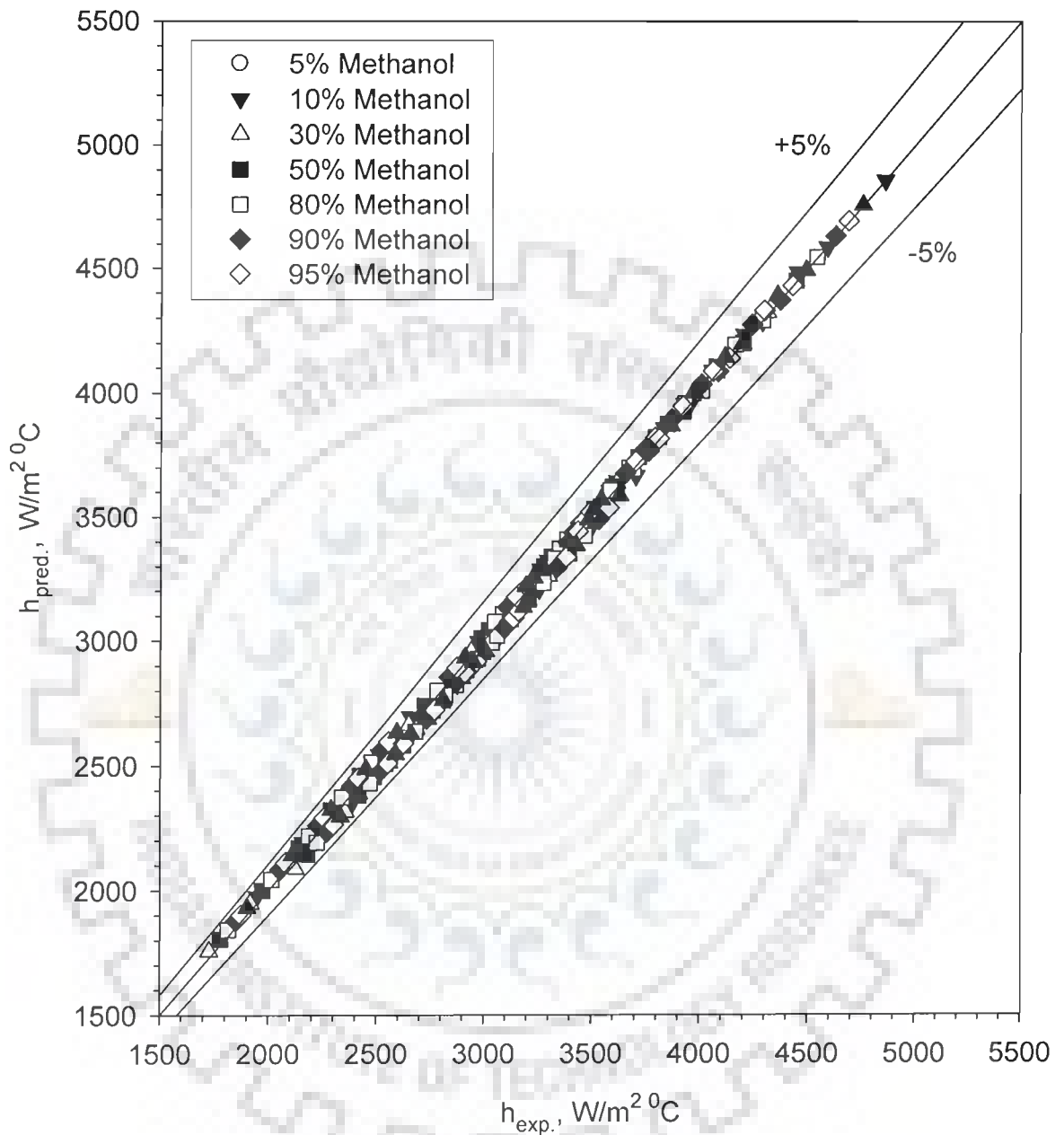


Fig. 5.41 Comparison of experimental heat transfer coefficients with those predicted from Eq. (5.16) for boiling of methanol-distilled water mixtures on a 43 μm coated heating tube surfaces at atmospheric and subatmospheric pressures

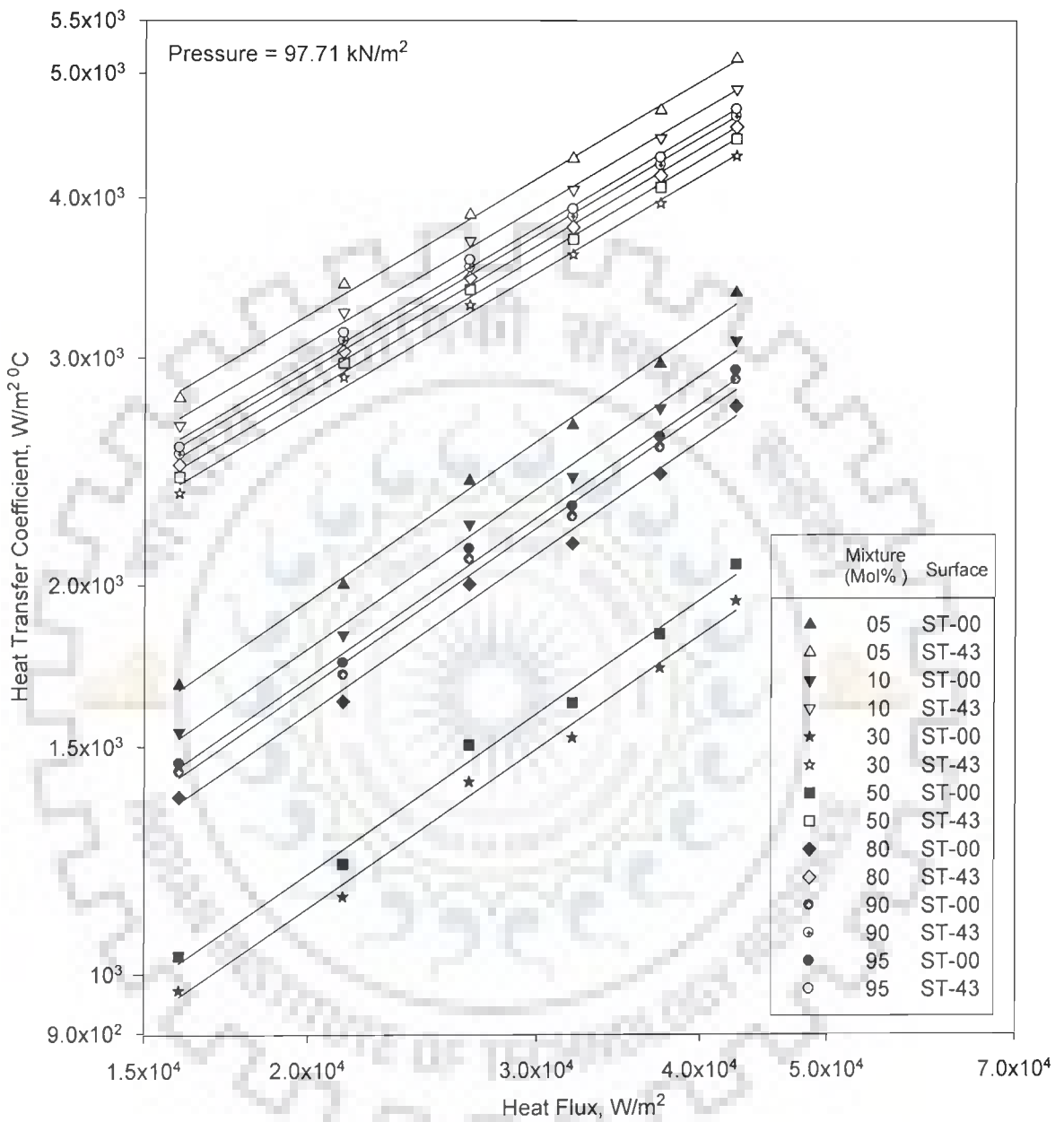


Fig. 5.42 Variation of heat transfer coefficient with heat flux for boiling of various methanol-distilled water mixtures on a 43 μ m thick copper coated tube and on an uncoated tube at atmospheric pressure

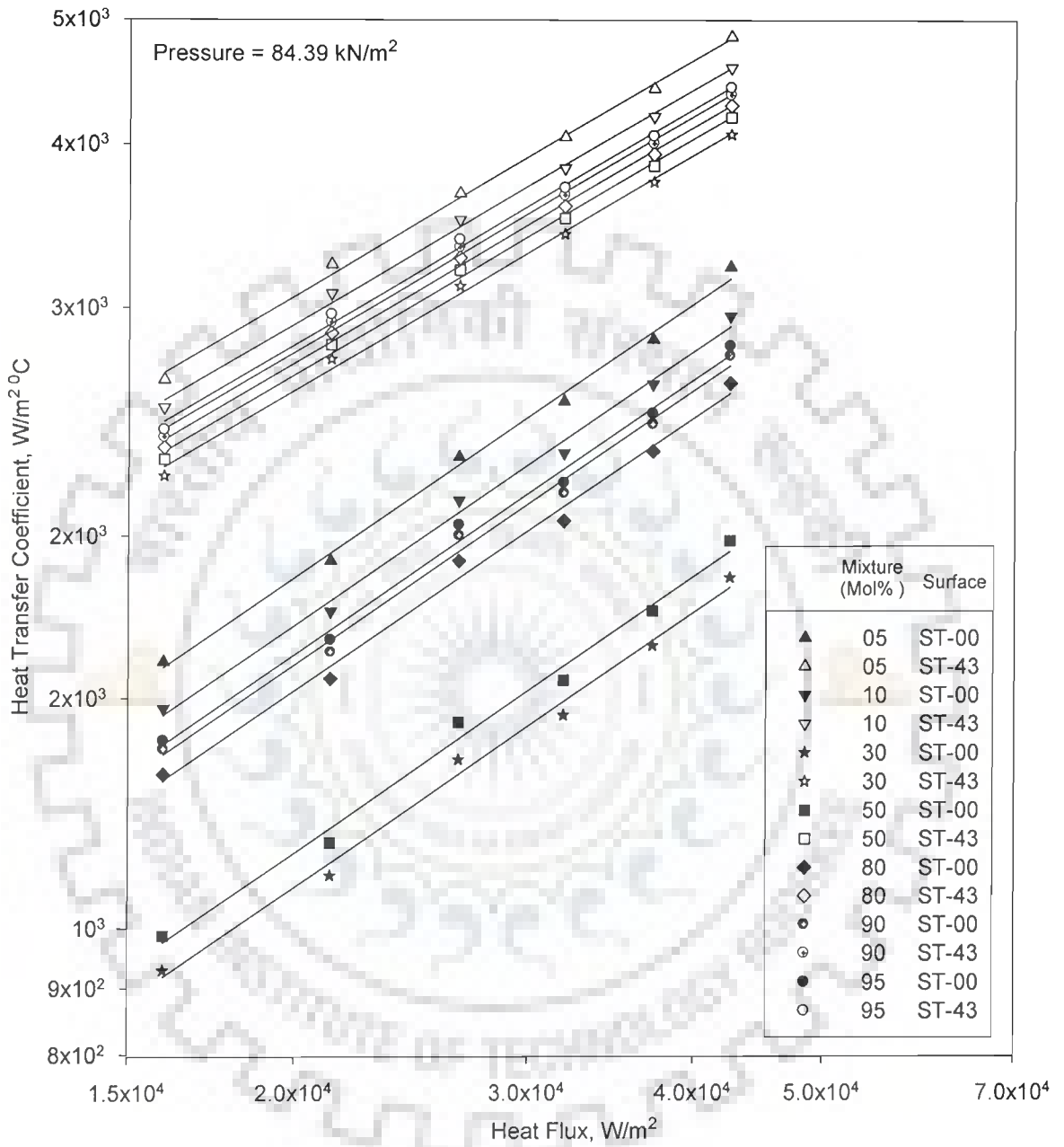


Fig. 5.43 Variation of heat transfer coefficient with heat flux for boiling of various methanol-distilled water mixtures on a 43 μm thick copper coated tube and on an uncoated tube at 84.39 kN/m² pressure

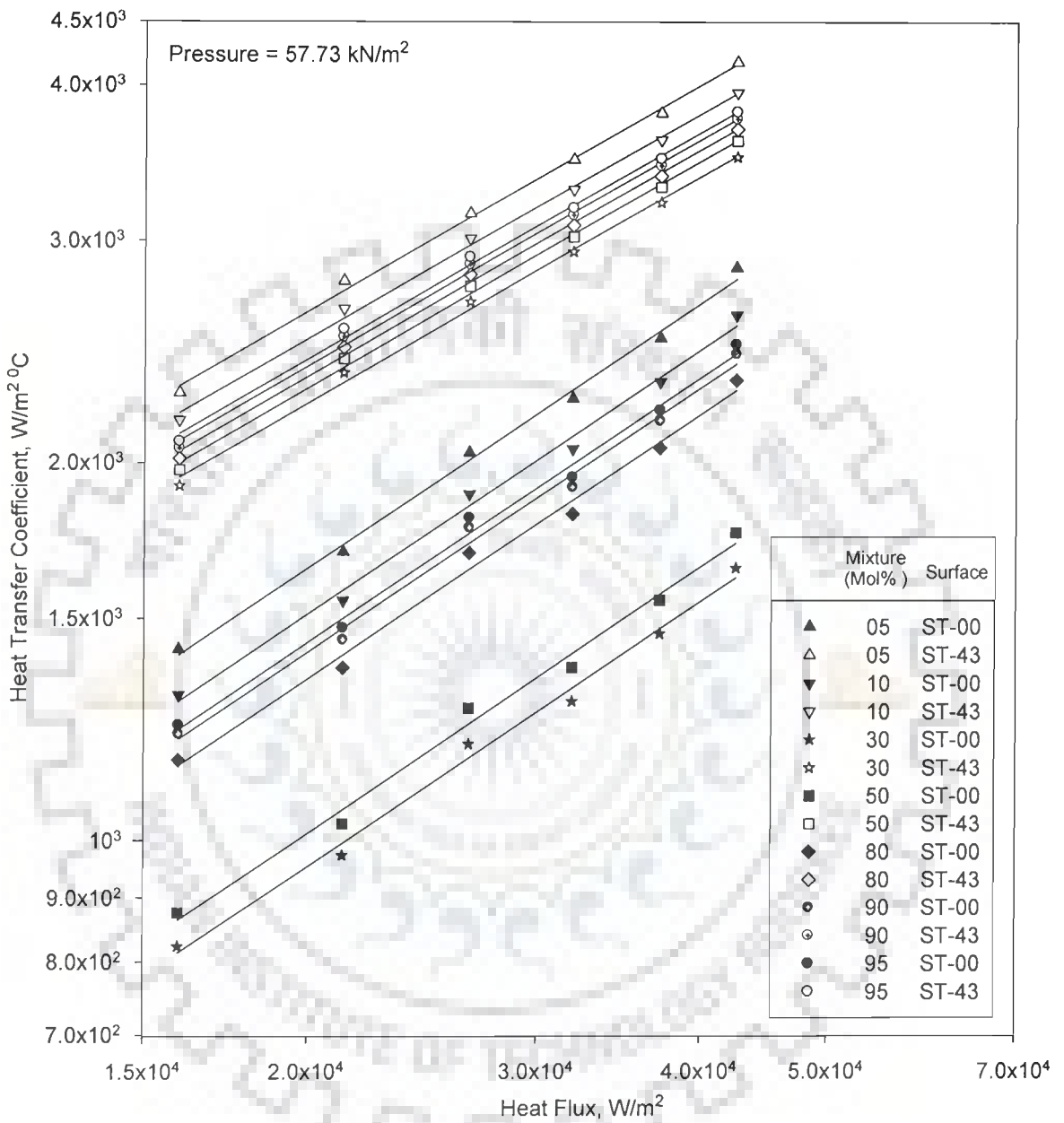


Fig. 5.44 Variation of heat transfer coefficient with heat flux for boiling of various methanol-distilled water mixtures on a 43 μm thick copper coated tube and on an uncoated tube at 57.73 kN/m² pressure

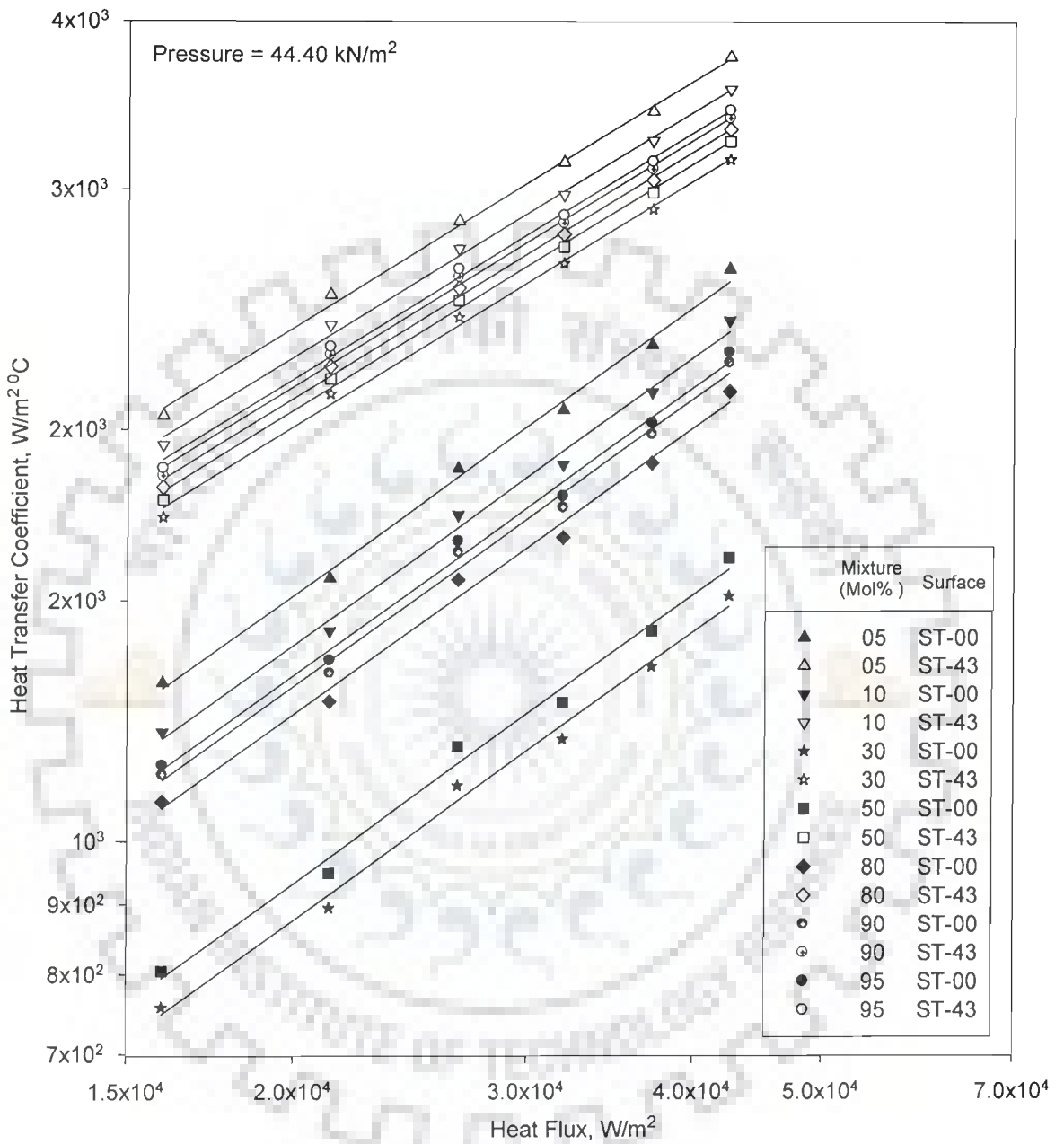


Fig. 5.45 Variation of heat transfer coefficient with heat flux for boiling of various methanol-distilled water mixtures on a 43 μ m thick copper coated tube and on an uncoated tube at 44.40 kN/m² pressure

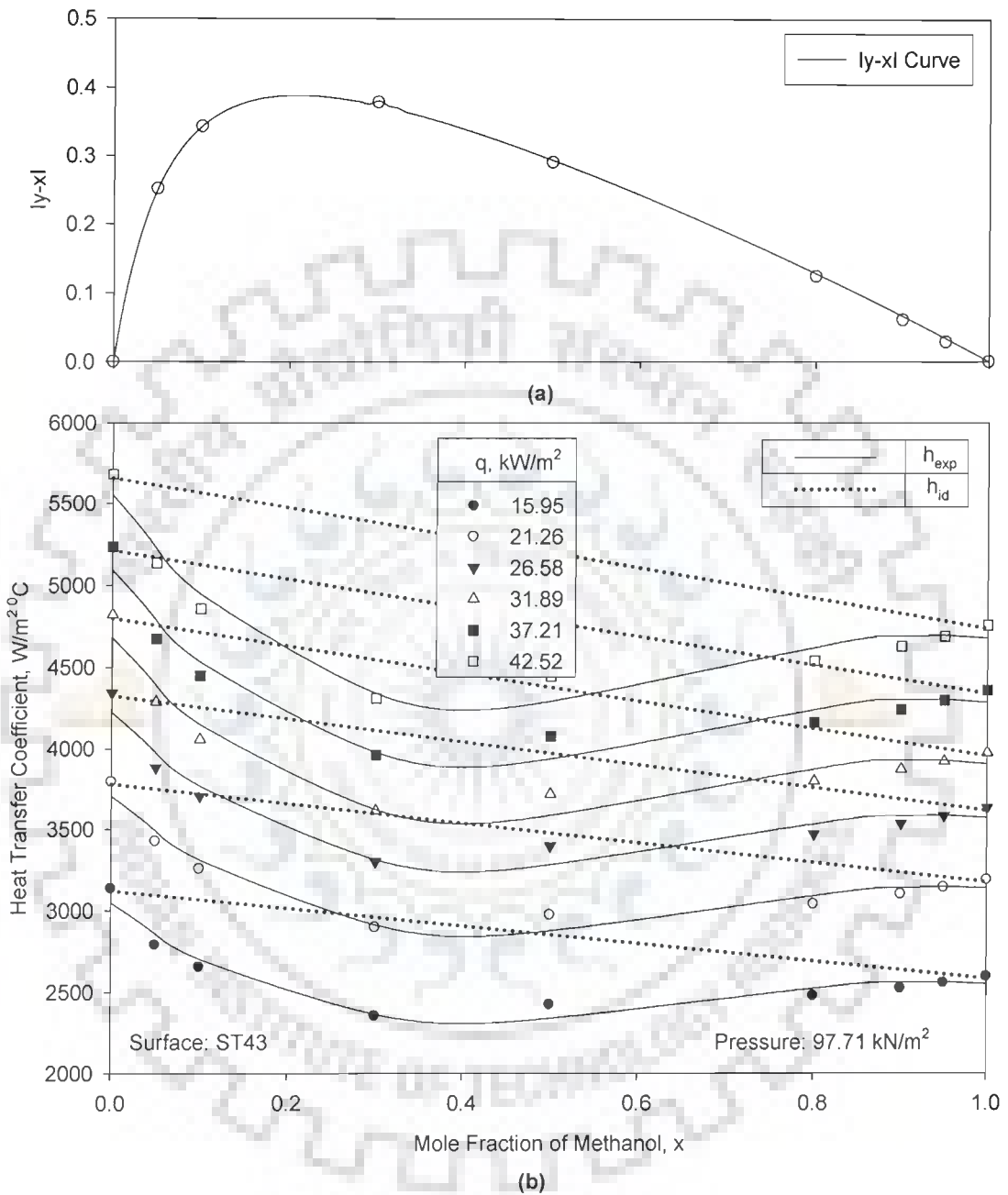


Fig. 5.46 Variation of heat transfer coefficient, and $|y - x|$ with mole fraction of methanol for methanol-water mixtures on 43 μm thickness copper coated tube at atmospheric pressure

Figures 5.47b to 5.49b represent variation of heat transfer coefficient on a 43 μm thick coated tube as a function of concentration at 84.39, 57.73 and 44.40 kN/m^2 , respectively. These plots also have essentially the same feature as discussed above.

To explain the behavior of above plots, phase equilibrium diagram of methanol-distilled water binary mixture as shown in **Fig. 5.46a** is examined. It may be pin pointed here that the experimental values of y and x as obtained from the analysis of liquid and vapor samples taken during the boiling of various compositions of binary mixture on coated surfaces have been found to be almost same as those obtained in the case of boiling on an uncoated tube. This is quite natural, thus it validates the correctness of experimental data taken on coated surfaces. Further, it also brings out the applicability of the phase equilibrium curves, as shown in **Fig. 5.22** for uncoated surface to boiling on coated tube surfaces also, hence the variation of heat transfer coefficients with mol percent of methanol and also for the existence of turnaround point given in Section 5.3.3 for the boiling of binary mixture on an uncoated tube surface holds true in this case too. The concentration at which turnaround in heat transfer coefficient occur is also found to be same i.e. 30 mole percent. Similar results have also been obtained for the boiling of various compositions of methanol-distilled water binary mixtures on coated tube surfaces at subatmospheric pressure. Based on above, it can said that boiling of various composition of methanol-distilled water binary mixture on a 43 μm copper coated heating tube surfaces is quite analogous to that on an uncoated surfaces at atmospheric and subatmospheric pressures. Hence it is governed by the same phenomena as in case an uncoated tube surface. This includes vaporization of unequal amounts of high- and low- volatile components of the mixture, and so the occurrence of simultaneous heat and mass transfer involved in this process. This is also responsible to vary potential and thereby heat transfer coefficient with concentration. Consequently, heat transfer coefficient for boiling of a given composition of methanol-distilled water mixture on a coated heating tube surface at atmospheric and subatmospheric

pressures can not be predicted by interpolation of heat transfer coefficients of the respective values of individual single component liquids. This is quite similar to the finding observed in case of boiling on an uncoated heating tube surface.

Above discussion has clearly shown that heat transfer coefficient of a binary mixture on a coated heating tube surface can not be determined by an interpolation of heat transfer coefficient of methanol and distilled water. This observation is quite similar to that obtained in case of an uncoated tube surface. Further, heat transfer coefficient on a coated tube has also been found to follow same pattern as that on an uncoated tube. In other words, coating of tube does not change the trend of h versus x curve. Therefore, it was thought to examine **Eq. (5.13)** for its validity on coated tube surface also. For convenience **Eq. (5.13)** is reproduced below:

$$\frac{h}{h_{id}} = \frac{\Delta T_{id}}{\Delta T} = \left[1 + |y - x| \left(\frac{\alpha}{D} \right)^{0.5} \right]^{-(0.8x+0.20)} \quad (5.13)$$

Figure 5.50 represents a plot between heat transfer coefficients calculated by the use of **Eq. (5.13)** and experimentally determined values for various compositions of methanol-distilled water mixture on a 43 μm copper coated heating tube surface at atmospheric pressure. The computed values of heat transfer coefficient have been obtained by determining h_{id} from **Eq. (5.13)** by using the respective values of heat transfer coefficients determined experimentally for the boiling of methanol and distilled water on a 43 μm copper coated heating tube surface and then by applying **Eq. (5.13)**.

The plot clearly indicates an excellent match between computed and experimental values within a maximum error of $\pm 20\%$. Thus, **Eq. (5.13)** has succeeded to predict heat transfer coefficient of methanol-distilled water mixture boiling on a 43 μm copper coated heating tube surface. Similar plots have also been prepared for the boiling of methanol-distilled water mixtures at various subatmospheric pressures as shown in **Fig. 5.51**. Predicted values have match excellently with experimental values within a maximum error of $\pm 20\%$. So, above correlation holds true for subatmospheric pressure range also.

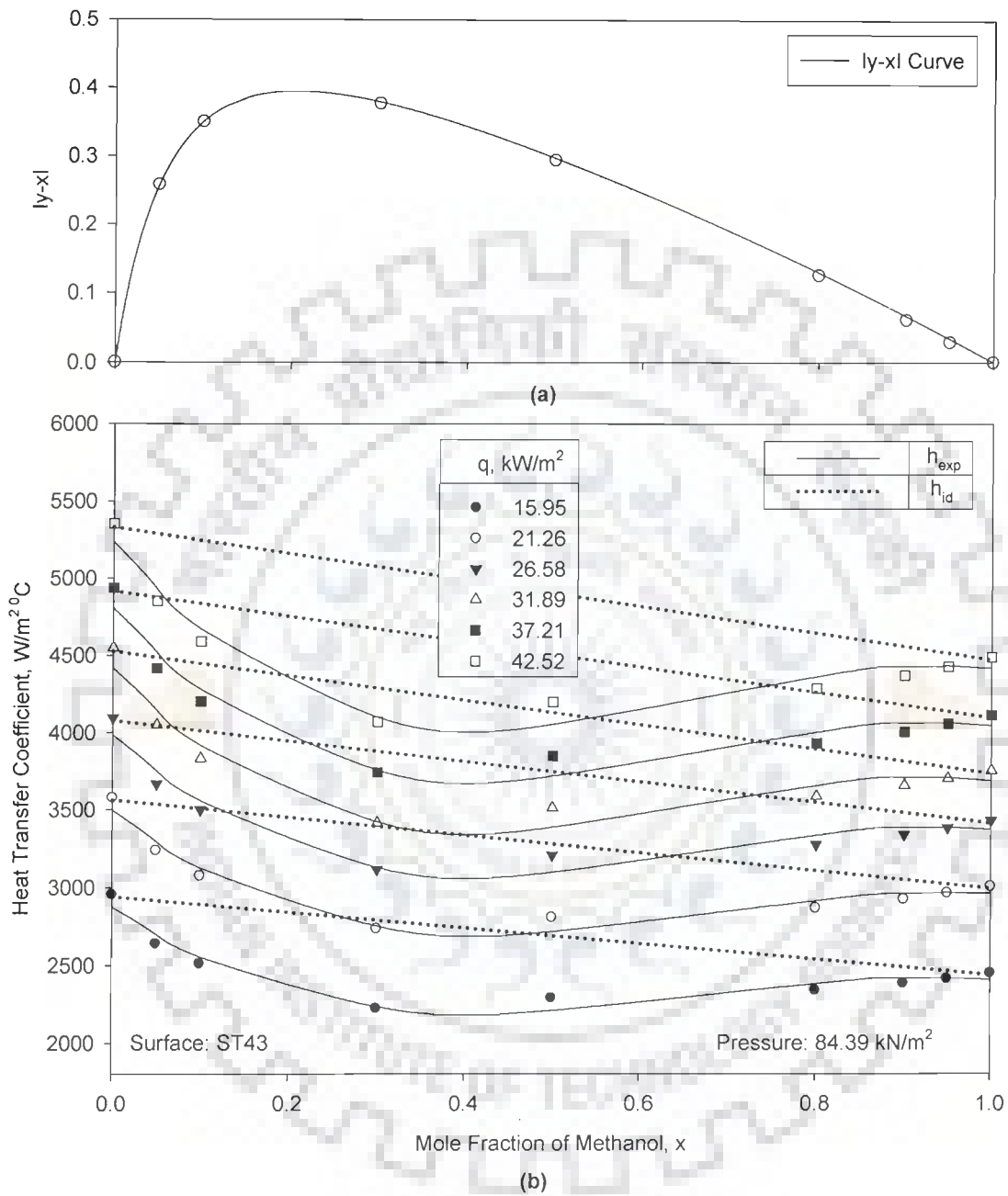


Fig. 5.47 Variation of heat transfer coefficient and $|y - x|$ with mole fraction of methanol for methanol-water mixtures on 43 μm thickness copper coated tube at 84.39 kN/m² pressure

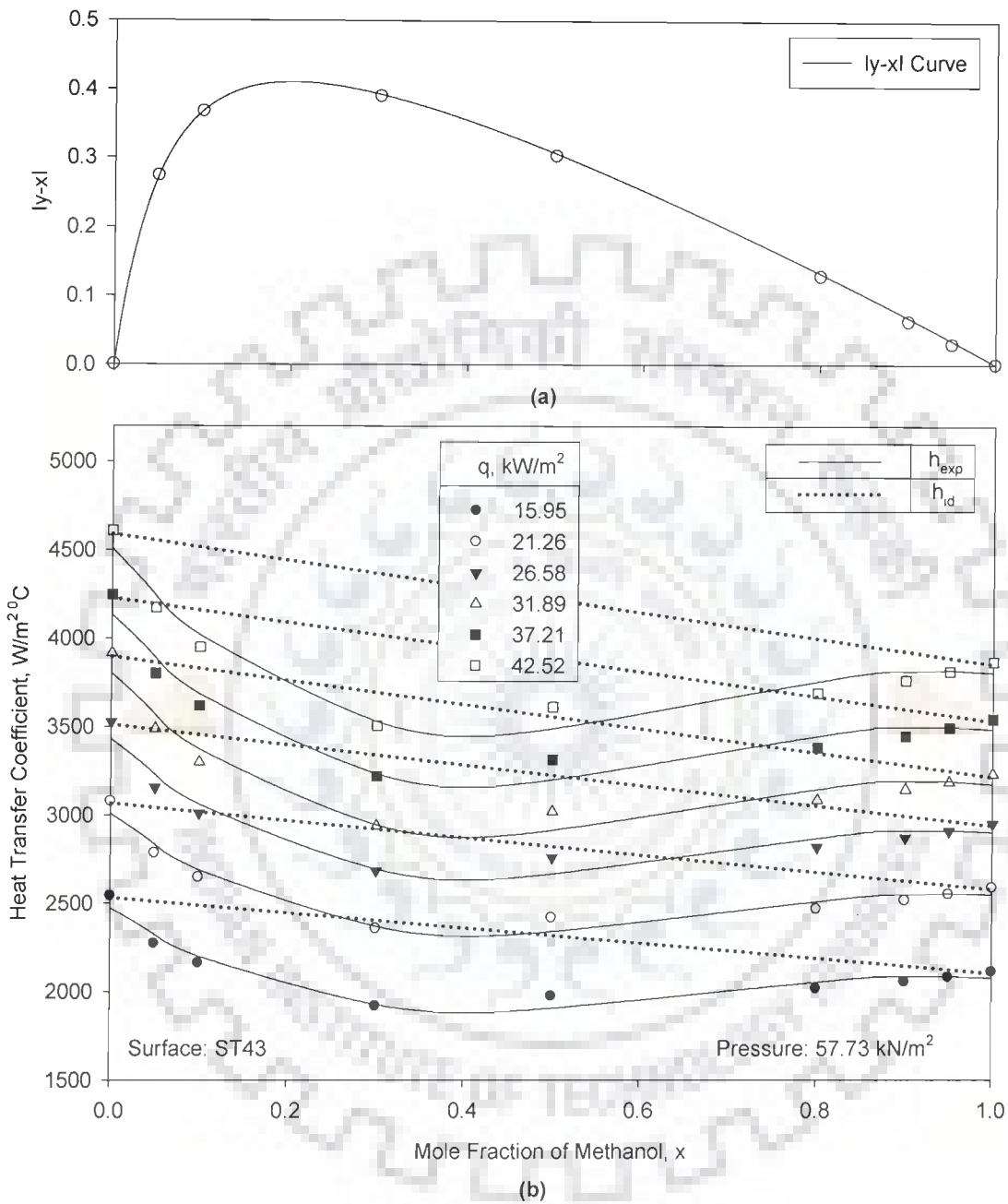


Fig. 5.48 Variation of heat transfer coefficient and $|y - x|$ with mole fraction of methanol for methanol-water mixtures on 43 μm thickness copper coated tube at 57.73 kN/m^2 pressure

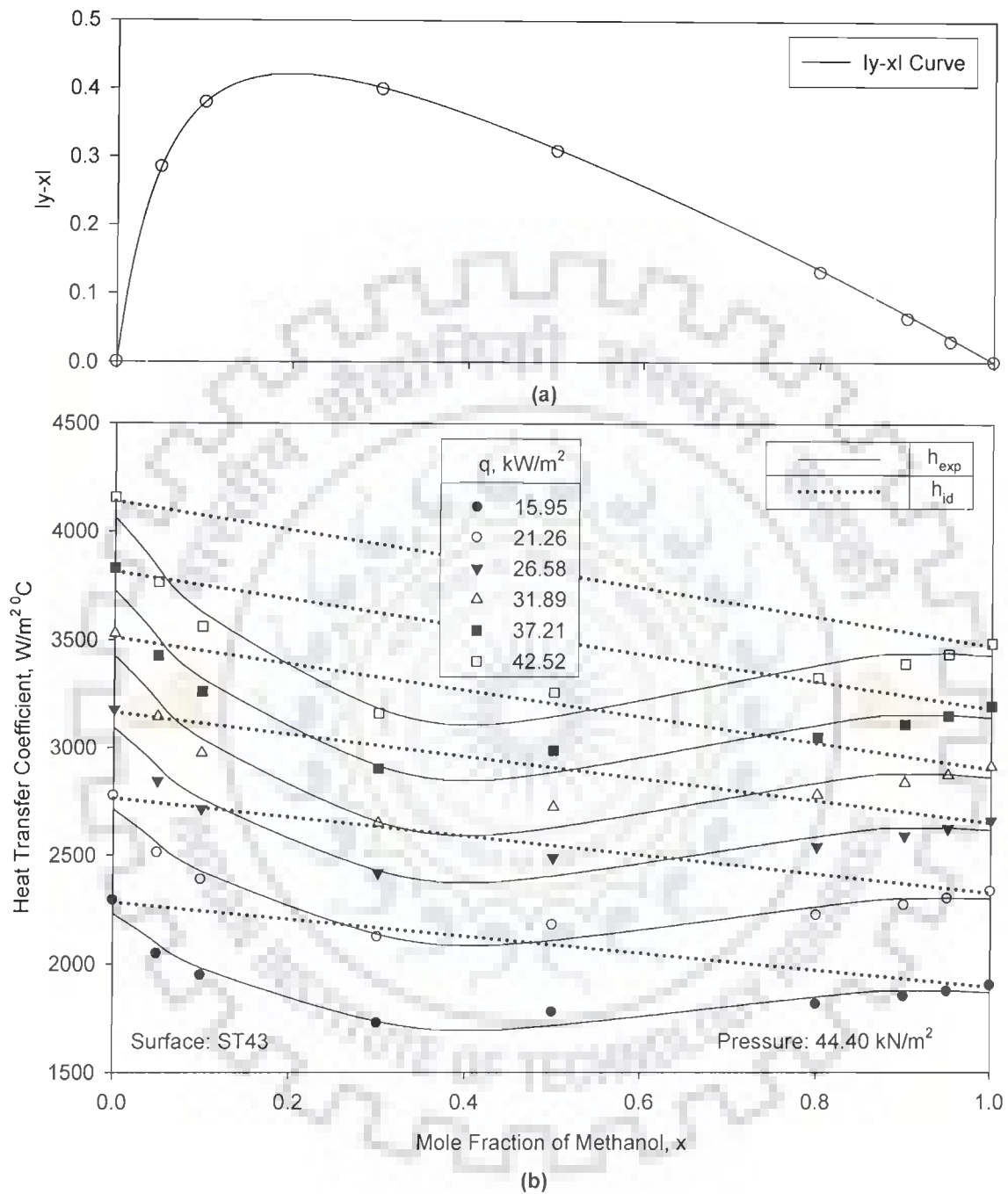


Fig. 5.49 Variation of heat transfer coefficient and $|y - x|$ with mole fraction of methanol for methanol-water mixtures on 43 μm thickness copper coated tube at 44.40 kN/m² pressure

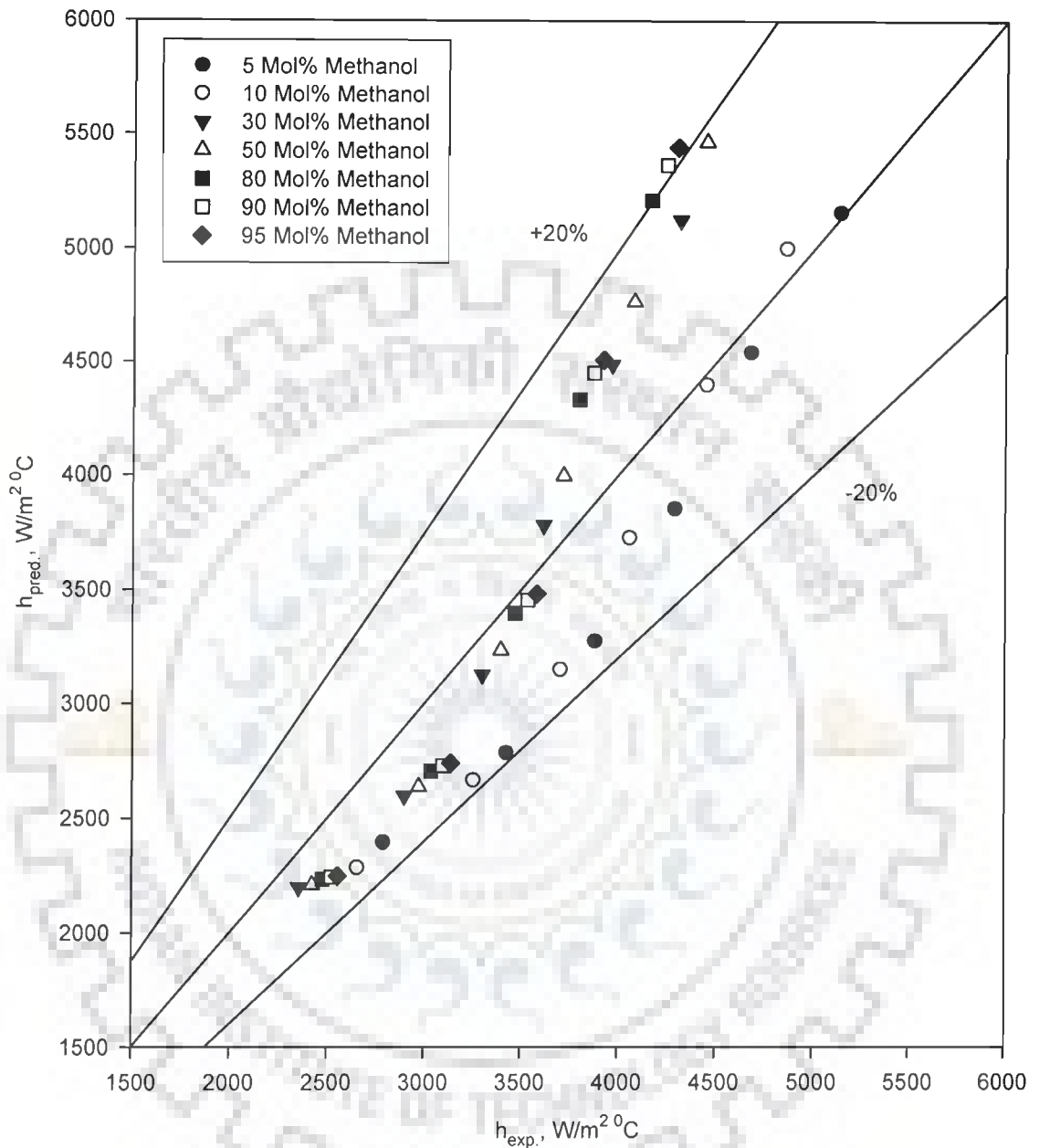


Fig. 5.50 Comparison of experimental heat transfer coefficients with those predicted from Eq. (5.13) for boiling of methanol-distilled water mixtures on a 43 μm copper coated heating tube surface at atmospheric pressure

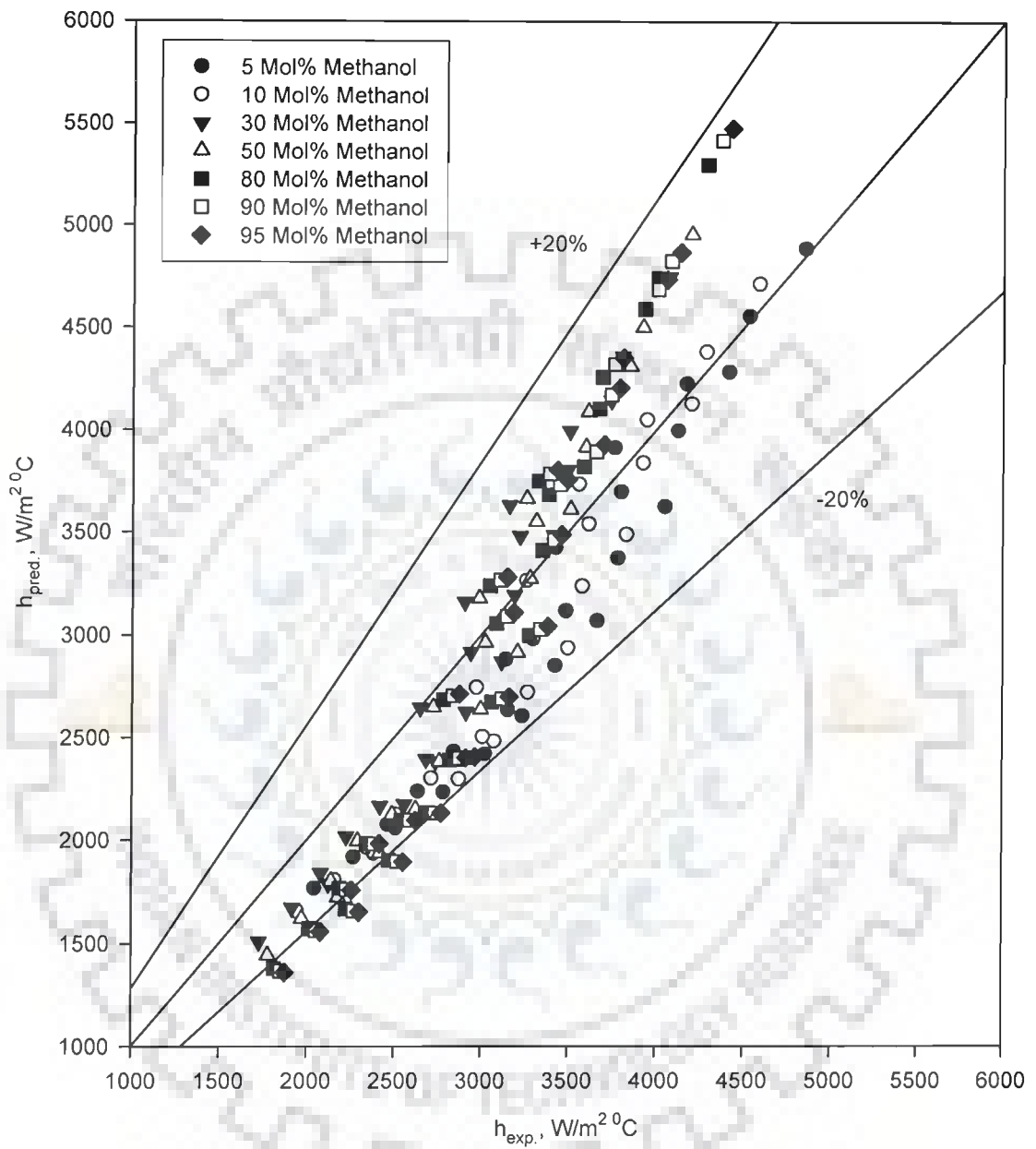


Fig. 5.51 Comparison of experimental heat transfer coefficients with those predicted from **Eq. (5.13)** for boiling of methanol-distilled water mixture on a 43 μm copper coated heating tube surface at subatmospheric pressures

Thus, it may be concluded that heat transfer coefficient of a boiling methanol-distilled water mixture can be determined by the use of **Eq. (5.13)** for both the cases – uncoated and coated tube surfaces. This makes **Eq. (5.13)** to be of general applicability. Above observation is quite obvious as may be obtained by a re-look of **Eqs. (5.9 & 5.13)**. Both of them considers mole fraction of methanol, physico-thermal properties and phase equilibrium diagram for the mixture only. In fact, they do not include any factor which depends upon heating surface characteristics. Hence, **Eqs. (5.9 & 5.13)** are applicable for the boiling of a liquid mixture irrespective of surface involved in boiling.

At this juncture, it may be recalled that in Section 5.4.3 and 5.5.2, **Eqs. (5.14 & 5.15)** have been developed for the prediction of heat transfer coefficient for the boiling of distilled water and methanol on a 43 μm copper coated heating tube surface. Therefore, above equations may also be used in **Eq. (5.9)** to obtain h_{ig} . However, it may be cautioned that **Eqs. (5.14 & 5.15)** can be used only when the value of constants appearing in them is known experimentally. In other words, above correlation, **Eq. (5.13)** requires experimentation for single component liquids – methanol and distilled water on a coated surface to determine boiling heat transfer coefficient of a binary mixture on the same surface.

Further, boiling heat transfer data for subatmospheric pressures can also be determined from the knowledge of heat transfer coefficient at atmospheric pressure by the application of **Eq. (5.6)**. Thus, **Eqs. (5.6, 5.9 & 5.13)** describes a complete procedure to obtain heat transfer coefficient of a given composition of a methanol-distilled water mixture from the known values of heat transfer coefficients of single component liquids at atmospheric pressure only. In other words, one needs not to conduct experiment for the boiling of methanol-distilled water mixtures at all. It necessitates experimentation of boiling heat transfer coefficient for single component liquids at atmospheric pressure only.

REMARKS

Above discussion is based on the data for the boiling of methanol-distilled water binary mixtures at atmospheric and subatmospheric pressures on a 43 μm copper coated heating tube surface. Although no study has been carried out on other similar binary mixtures and on other coated surfaces, yet the arguments advanced above clearly support that it should be valid for any binary mixture having same characteristics (non-azeotropic and non-ideal) and also for a surface irrespective of thickness of coating on it. Hence, no attempts should be made to extend the validity of above beyond its range of applicability i.e. non-azeotropic and non-ideal liquid mixtures similar to methanol-distilled water mixtures; atmospheric and subatmospheric pressures and copper coating on stainless steel heating tube surface.

SUMMARY

Boiling of methanol-distilled water binary mixtures on a copper coated heating tube surface at atmospheric and subatmospheric pressures has resulted similar behavior as that on an uncoated tube surface as regards the variation of heat transfer coefficient with respect to heat flux, pressure and concentration. Therefore, heat transfer coefficient can not be predicted from interpolation of respective values of heat transfer coefficients of single component liquids. However, it can be determined from the correlation, **Eq. (5.13)** developed above. These findings are quite similar to those obtained for uncoated heating tube surface. Hence, finally it can be said that boiling characteristics of a binary mixture remains unaltered irrespective of heating surface being coated or not.

5.7 THERMAL EFFECTIVENESS OF A COATED HEATING TUBE

It has been clearly pointed out in the preceding sections that heat transfer coefficient of liquids and mixtures boiling on a coated tube surface strongly depend upon heat flux, pressure and thickness of coating. In fact, boiling heat transfer coefficient on a coated surface is more than that on an uncoated heating tube surface for identical conditions. Apparently, coated tube

may be used as heating surface if it provides enhancement in heat transfer coefficient. Therefore, it is relevant to evaluate thermal effectiveness of such surfaces for the application of copper coating over heating tube surface for enhanced boiling of liquids and mixtures. Following section describes it in detail:

Thermal effectiveness of a coated heating tube surface for saturated boiling of a liquid may be defined as the ratio of heat transfer coefficient on a coated surface to that on an uncoated tube surface at the same values of heat flux and pressure. Mathematically, it is expressed as:

$$\zeta_{\delta} = \left(\frac{h_{\text{COATED_TUBE}}}{h_{\text{UNCOATED_TUBE}}} \right)_{q,p} \quad (5.17)$$

Thermal effectiveness for boiling of distilled water on 22 μm thick coated tube surface can be obtained from Eqs. (5.4 & 5.14) and is expressed by the following equation:

$$\zeta_{22} = C_5 q^{\alpha_1} p^{\beta_1} \quad (5.18)$$

where, the values of constant, C_5 and exponents, α_1 and β_1 for distilled water are given in Table 5.5.

The expression for thermal effectiveness for boiling of distilled water, methanol and their binary mixtures on a 43 μm thick coated tube surface is also obtained using Eqs. (5.4, 5.7, 5.14, 5.15 & 5.16) which is as follows:

$$\zeta_{43} = C_6 q^{\alpha_2} p^{\beta_2} \quad (5.19)$$

where, the values of constant, C_6 and exponents, α_2 and β_2 for distilled water, methanol and their various binary mixtures are given in Table 5.5.

Similarly, thermal effectiveness for the boiling of distilled water on a 67 μm thick coated tube surface is obtained by using Eqs. (5.4 & 5.14) as given below:

$$\zeta_{67} = C_7 q^{\alpha_3} p^{\beta_3} \quad (5.20)$$

where, the values of constant, C_7 and exponents, α_3 and β_3 for distilled water are also provided in Table 5.5.

Thus, thermal effectiveness of a coated heating tube surface for boiling of distilled water, methanol and their binary mixtures can be calculated using **Eqs. (5.18, 5.19 & 5.20)**, at a given value of heat flux and pressure, provided the constant appearing in these equations are known.

Table 5.5 Values of constants, C_5 , C_6 , C_7 and exponents, α_1 , α_2 , α_3 , β_1 , β_2 and β_3 of **Eqs. (5.18, 5.19 & 5.20)**

Coating Thickness $\delta = 22 \mu\text{m}$			
Liquid	C_5	α_1	β_1
Distilled Water	1.233	-0.04	0.10
Coating Thickness $\delta = 43 \mu\text{m}$			
Liquid	C_6	α_2	β_2
Distilled Water	3.128	-0.10	0.07
Methanol	3.273	-0.10	0.07
5% Methanol	3.099	-0.10	0.07
10% Methanol	3.358	-0.10	0.07
30% Methanol	4.551	-0.10	0.07
50% Methanol	4.461	-0.10	0.07
80% Methanol	4.369	-0.10	0.07
90% Methanol	3.311	-0.10	0.07
95% Methanol	3.318	-0.10	0.07
Coating Thickness $\delta = 67 \mu\text{m}$			
Liquid	C_7	α_3	β_3
Distilled Water	5.454	-0.16	0.03

Typical 3D plots drawn in **Figs. 5.52 to 5.54** demonstrate the effect of heat flux and pressure on thermal effectiveness for boiling of distilled water on stainless steel tubes coated with 22, 43 and 67 μm thicknesses of copper, respectively. These plots facilitate one to readily get the value of thermal effectiveness from the known values of heat flux and pressure on a coated tube. These plots clearly indicate that heat flux and pressure substantially affect

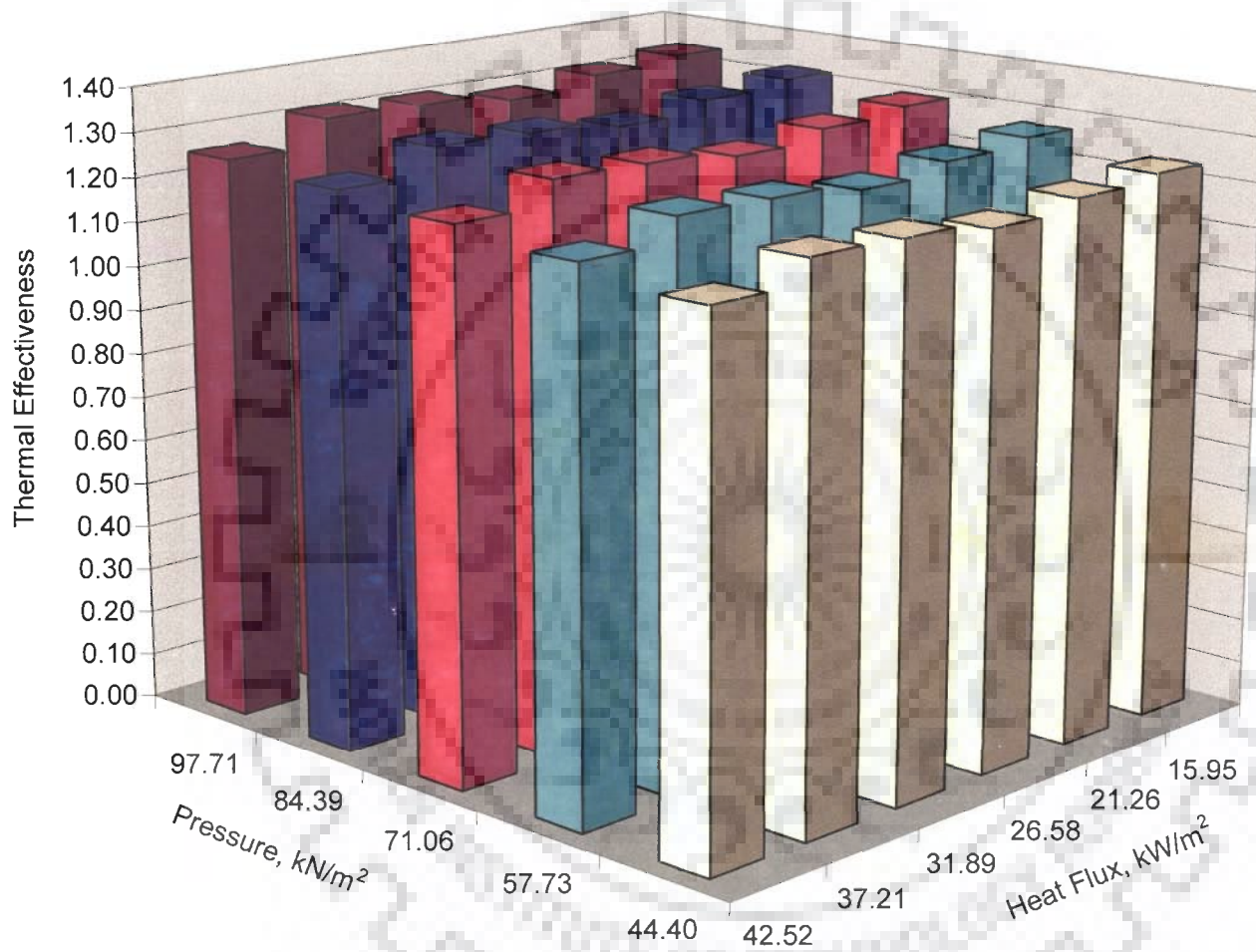


Fig. 5.52 Variation of thermal effectiveness with heat flux and pressure for the boiling of distilled water over a 22 μm thick copper coated heating tube surface

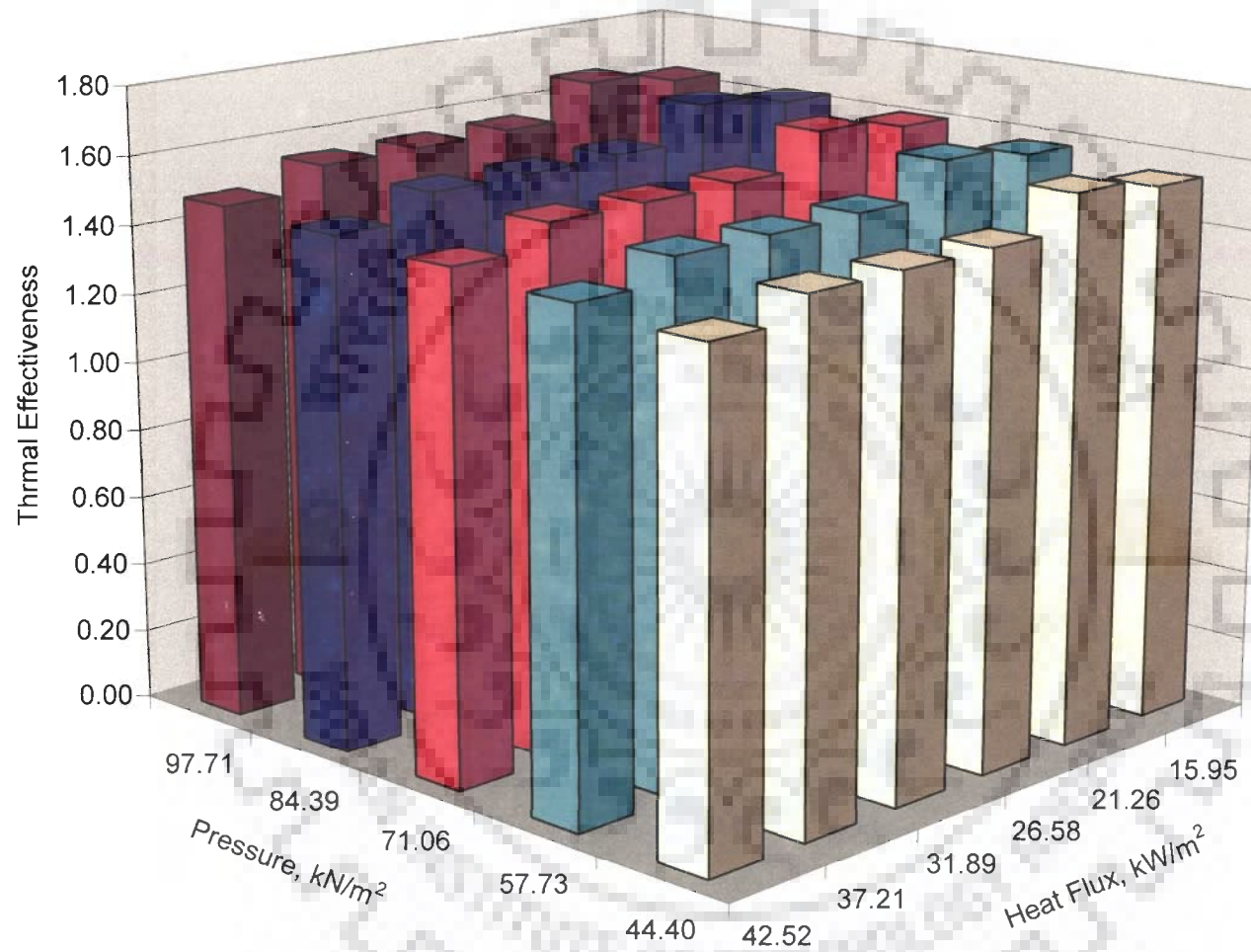


Fig. 5.53 Variation of thermal effectiveness with heat flux and pressure for the boiling of distilled water over a $43 \mu\text{m}$ thick copper coated heating tube surface

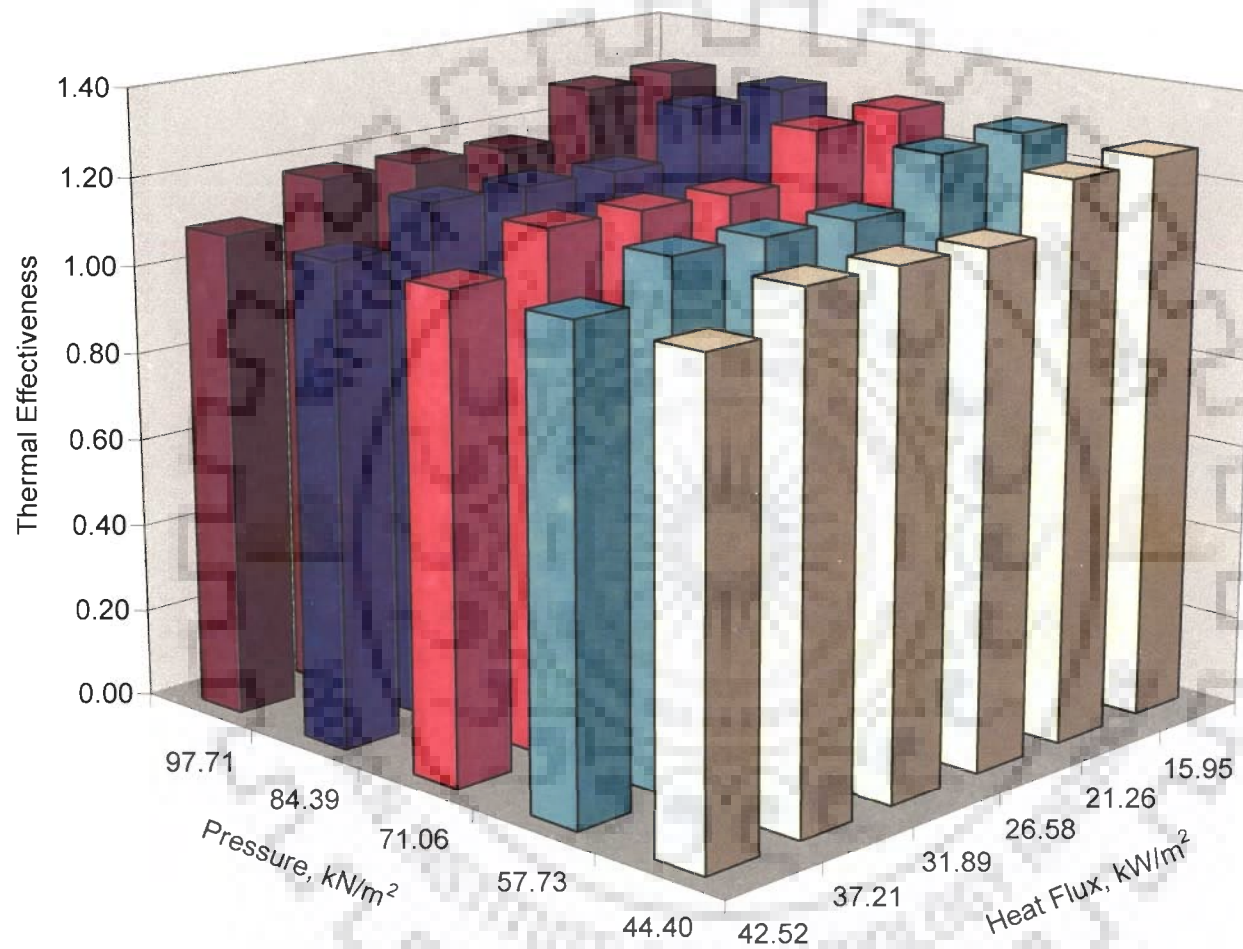


Fig. 5.54 Variation of thermal effectiveness with heat flux and pressure for the boiling of distilled water over a $67 \mu\text{m}$ thick copper coated heating tube surface

the value of thermal effectiveness for the boiling of distilled water on a tube coated with a given thickness of copper. Fortunately, the values of thermal effectiveness in all cases of this investigation are found to be greater than unity and hence such tubes may be used profitably for enhanced boiling of liquids. However, as pointed out earlier, thermal effectiveness, ζ depends upon the value of heat flux and pressure; so situation may arise when the value of thermal effectiveness becomes lower than unity. Naturally, the use of coated surfaces in above circumstances will not result any enhancement of heat transfer coefficient and hence their use for enhanced boiling of liquids may not be justified. Above conditions of heat flux, pressure and thickness of coating do exist during boiling of liquids on coated tubes. Therefore, it is necessary to investigate operating conditions which may provide value of thermal effectiveness to be greater than unity, as their application is required for enhanced boiling of liquids. Based upon it, the range of heat flux, pressure and thickness of coating for enhanced boiling of liquids on a coated heating tube surface is evaluated in the following paragraphs:

As discussed above, expression for enhanced boiling of distilled water on tube surface coated with copper of a given thickness are obtained by applying the condition, $\zeta > 1$ to **Eqs. (5.18 to 5.20)**. They are as follows:

(a) for 22 μm thick coated tube surface

$$q^{0.04} p^{-0.10} < 1.233 \quad (5.21a)$$

(b) for 43 μm thick coated tube surface

$$q^{0.10} p^{-0.07} < 3.128 \quad (5.21b)$$

(c) for 67 μm thick coated tube surface

$$q^{0.16} p^{-0.03} < 5.454 \quad (5.21c)$$

Figures 5.55 to 5.58 show 3D plots of thermal effectiveness as a function of heat flux and pressure for the boiling of methanol and methanol-distilled water binary mixtures on a 43 μm thick copper coated surface. These plots also indicate that the value of thermal effectiveness is always greater than unity for all the values of heat flux and pressure of this investigation. However,

separate criteria have been obtained for enhanced boiling of methanol and various methanol-distilled water binary mixtures by using the constraint, $\zeta > 1$ in Eqs. (5.19). These are as follows:

A. For the boiling of methanol on 43 μm thick coated tube surface

$$q^{0.01} p^{-0.07} < 3.273 \quad (5.22a)$$

B. For the boiling of 5 mol% methanol on 43 μm thick coated tube surface

$$q^{0.01} p^{-0.07} < 3.099 \quad (5.22b)$$

C. For the boiling of 10 mol% methanol on 43 μm thick coated tube surface

$$q^{0.01} p^{-0.07} < 3.358 \quad (5.22c)$$

D. For the boiling of 30 mol% methanol on 43 μm thick coated tube surface

$$q^{0.01} p^{-0.07} < 4.551 \quad (5.22d)$$

E. For the boiling of 50 mol% methanol on 43 μm thick coated tube surface

$$q^{0.01} p^{-0.07} < 4.461 \quad (5.22e)$$

F. For the boiling of 80 mol% methanol on 43 μm thick coated tube surface

$$q^{0.01} p^{-0.07} < 3.306 \quad (5.22f)$$

G. For the boiling of 90 mol% methanol on 43 μm thick coated tube surface

$$q^{0.01} p^{-0.07} < 3.311 \quad (5.22g)$$

H. For the boiling of 95 mol% methanol on 43 μm thick coated tube surface

$$q^{0.01} p^{-0.07} < 3.318 \quad (5.22h)$$

REMARKS

It is important to mention here that above expressions of thermal effectiveness have been developed using experimental data obtained for saturated boiling of distilled water, methanol and their binary mixtures over a stainless steel heating tube surface coated with copper of various thicknesses. Further, they have been developed for heat flux ranging from 15,946.84 W/m^2 to 42,524.62 W/m^2 and pressure from 44.40 kN/m^2 to 97.71 kN/m^2 . Therefore, the criterion obtained in this investigation for enhanced boiling heat transfer is valid only for above range of operating parameters. So, no attempt should be made to use above criterion for the determination of thermal effectiveness of a stainless steel tube coated with copper beyond the above range of parameters.

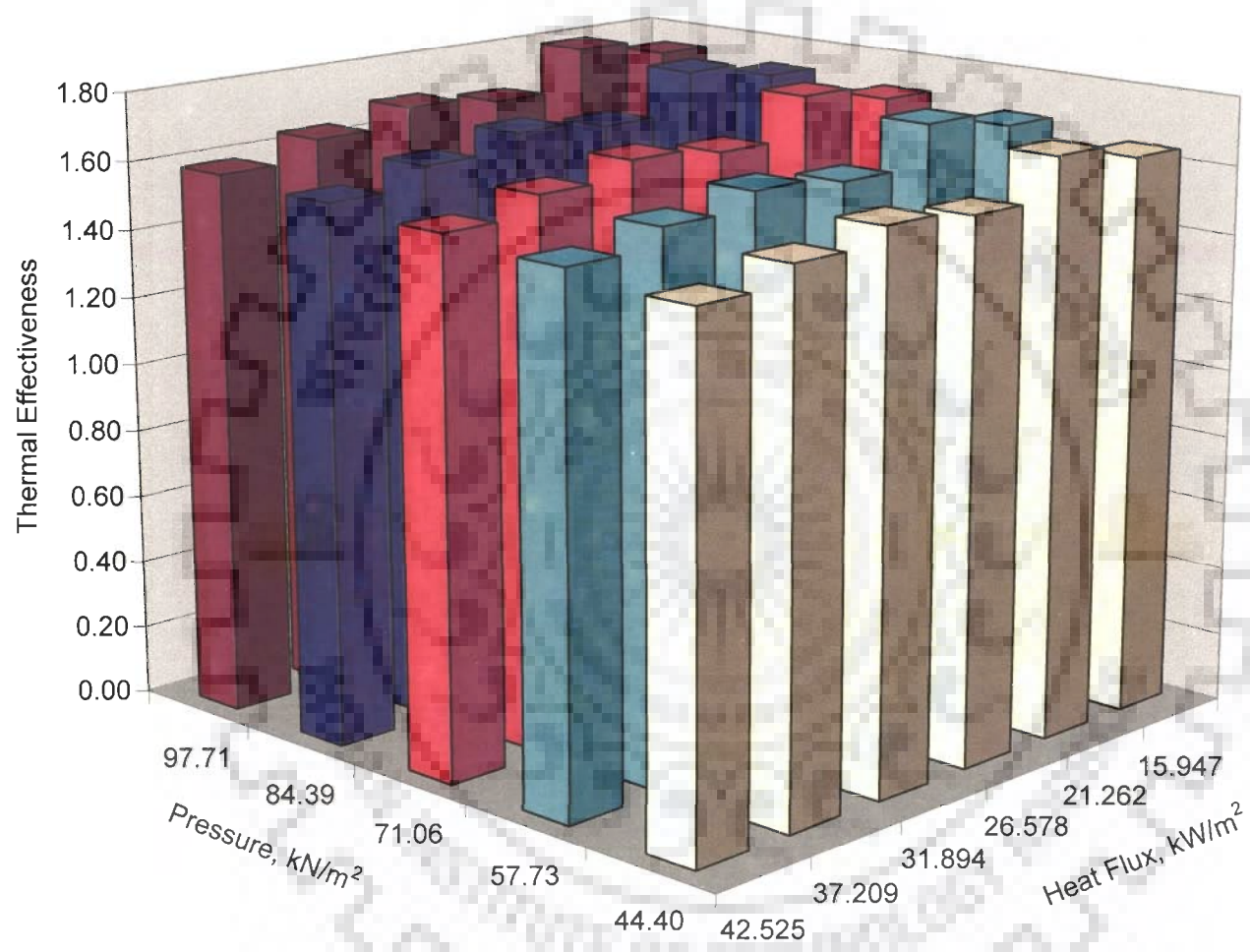


Fig. 5.55 Variation of thermal effectiveness with heat flux and pressure for the boiling of Methanol over a 43 μm thick copper coated heating tube surface

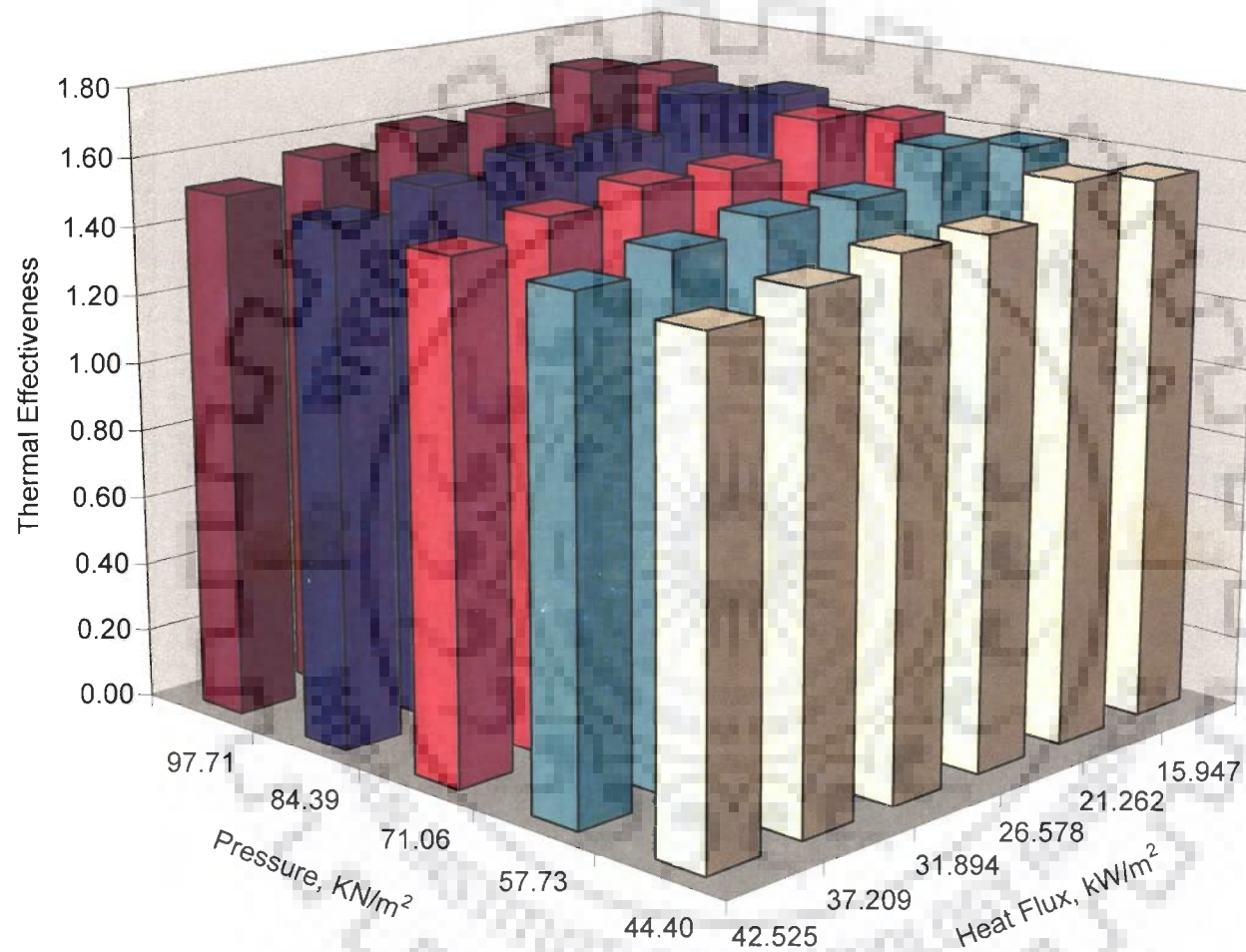


Fig. 5.56 Variation of thermal effectiveness with heat flux and pressure for the boiling of 5 mol% Methanol over a 43 μm thick copper coated heating tube surface

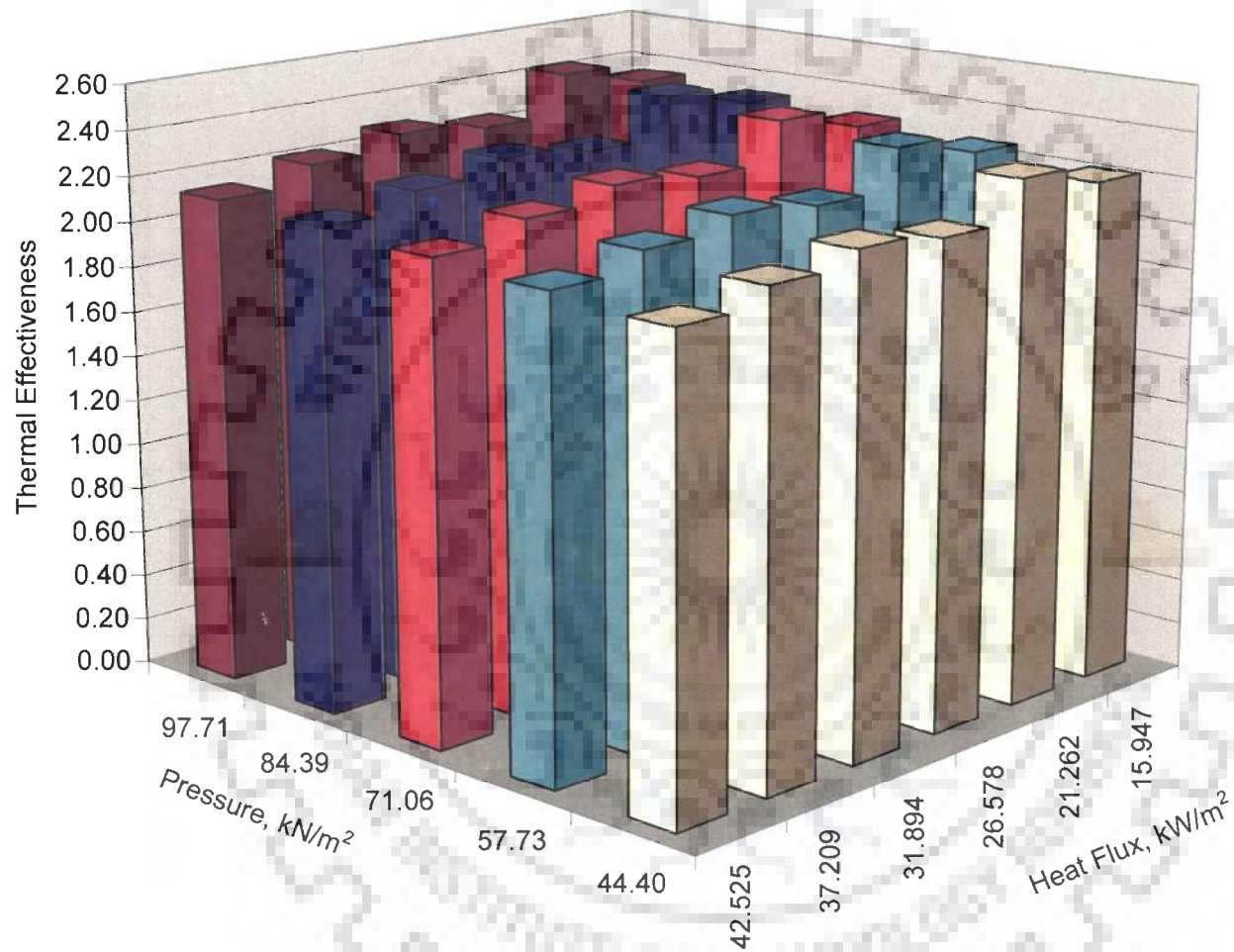


Fig. 5.57 Variation of thermal effectiveness with heat flux and pressure for the boiling of 50 mol% Methanol over a 43 μm thick copper coated heating tube surface

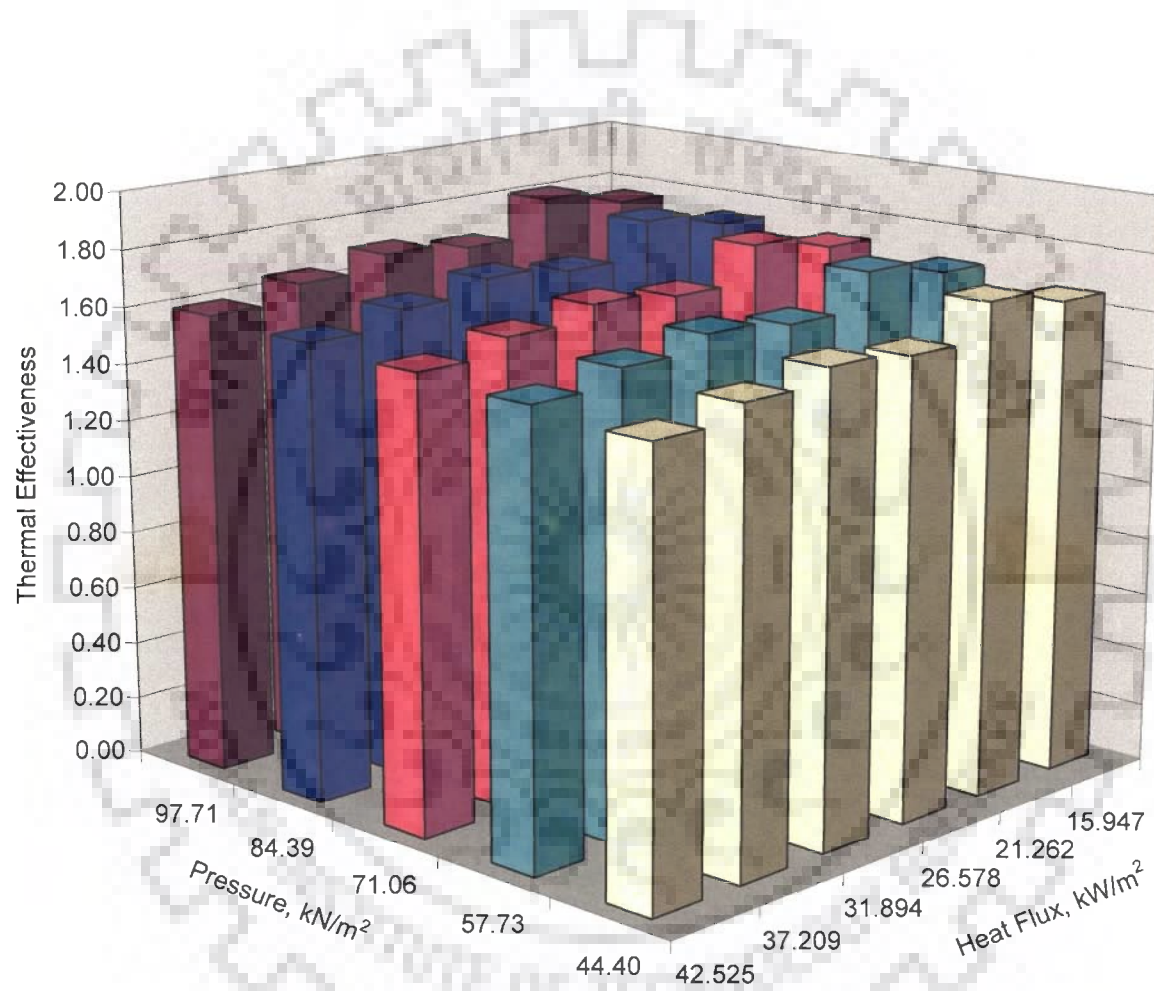


Fig. 5.58 Variation of thermal effectiveness with heat flux and pressure for the boiling of 90 mol% Methanol over a 43 μm thick copper coated heating tube surface

SUMMARY

Present investigation on nucleate pool boiling of distilled water, methanol and their binary mixtures from stainless steel tube coated with copper of various thicknesses has indicated the feasibility of using copper coating as a potential passive technique for augmentation of heat transfer coefficient at atmospheric and subatmospheric pressures. In fact, thickness of coating has been found to affect boiling heat transfer coefficient. In fact, enhancement in heat transfer coefficient depends upon the value of heat flux, pressure, boiling liquid and thickness of coating. The present investigation has resulted an enhancement of heat transfer coefficient for saturated boiling of methanol, distilled water and their binary mixtures with in the domain of heat flux and pressure studied herein.

Thermal effectiveness of coated tube surface has been evaluated for saturated boiling of methanol, distilled water and their mixtures at atmospheric and sub-atmospheric pressures and has been found to be a function of operating parameters mentioned above. A criterion has been developed for enhanced boiling of these liquids and mixtures on stainless steel tube coated with copper of various thicknesses. It enables to determine the range of heat flux for enhanced boiling of liquids and mixtures on a stainless steel heating tube surface coated with copper of a given thickness at a given pressure or alternatively the span of operating pressure to get enhanced boiling of liquids and mixtures on a coated tube surface subjected to a given value of heat flux.

Chapter-6

Conclusions and Recommendations

This chapter deals with the conclusions and recommendations of the study

CONCLUSIONS AND RECOMMENDATIONS

6.1 CONCLUSIONS

As a result of present investigation, following important conclusions have emerged out:

1. Experimental data for nucleate pool boiling of distilled water, and methanol on an uncoated heating tube surface have been generated for a wide range of heat flux at atmospheric and subatmospheric pressures. Analysis of the data has shown that surface temperature, for a given value of heat flux, increases from bottom to side to top position and thus value of local heat transfer coefficient increases continuously from top to side to bottom position. The value of local heat transfer coefficient, at a given circumferential position, has been found to vary with heat flux according to power law relationship, $h_v \propto q^{0.7}$ for all the values of pressures of this investigation. In addition, an equation relating local heat transfer coefficient with heat flux and pressure has also been developed by regression analysis within an error of $\pm 7\%$.
2. Average heat transfer coefficient of a liquid boiling on a plain tube at atmospheric and subatmospheric pressures has been found to vary with heat flux by power law relationship, $h \propto q^{0.7}$. Raising pressure has improved the value of heat transfer coefficient. Thus, heat transfer coefficient has been expressed as function of heat flux and pressure by relationship, $h = C_1 q^{0.7} p^{0.32}$, where C_1 is a constant representing surface liquid combination factor. Further, this equation has been reduced into a non-dimensional form: $(h^*/h_1^*) = (p/p_1)^{0.32}$ where h^* represents $(h/q^{0.7})$ and subscript 1 denotes atmospheric pressure condition. Above equation is tested against experimental data for the boiling of distilled water and methanol on an uncoated heating surface of this investigation; of water, methanol, carbon-tetrachloride and n-butanol on a brass tube

surface by Cryder & Finalborgo [39]; of n-heptane on a copper plate surface by Cichelli & Bonilla [33]; of distilled water, methanol, ethanol and isopropanol on a brass tube surface by Vittala et al. [148,149]; of distilled water on a stainless steel tube surface by Bansal [8]; of distilled water, benzene and toluene on a stainless steel surface by Bhaumik [16]; of distilled water on a mild steel heating tube surface by Alam et al. [4]; of methanol on a mild steel heating tube surface by Prasad et al. [105]; and of isopropanol on a mild steel heating tube surface by Prasad [106] and found to correlate them excellently within an error of ranging from -12 to +9%.

Further, this non-dimensional equation can be used to generate heat transfer coefficient for the boiling of liquids at subatmospheric pressures without resorting to experimentation from the knowledge of experimentally determined value of heat transfer coefficient at atmospheric pressure only. Another important point is that it can also be used to examine the consistency of heat transfer data taken for the boiling of various liquids on heating surfaces of differing surface characteristics of atmospheric and subatmospheric pressures.

3. The experimental data for the pool boiling of methanol-distilled water binary mixtures at atmospheric and subatmospheric pressures has shown analogous boiling characteristic as that of individual liquids. Hence, the variation of average heat transfer coefficient of a binary liquid mixture with respect to heat flux and pressure remains the same as that of an individual liquid. It can be represented by the relationship, $h = C_2 q^{0.7} p^{0.32}$, which has been obtained by regression analysis within an error of $\pm 7.5\%$, where, C_2 is a constant whose value depends upon the composition of the mixture, and surface characteristic. Further, above equation has been reduced into a non-dimensional form: $(h^*/h_1^*) = (p/p_1)^{0.32}$. It has been tested against experimental data for the boiling of various composition of methanol-distilled water mixtures on a uncoated stainless steel surface at atmospheric and subatmospheric pressures of this investigation; and of methanol-water mixtures, ethanol-

- water mixtures, and isopropanol-water mixtures due to Pandey [102] on a plain stainless steel surface at atmospheric and subatmospheric pressures and found to correlate them with the maximum deviation ranging from of -12 to +20%.
4. Heat transfer coefficient of methanol-distilled water mixture has been found to decrease with increase in concentration of methanol and attains a distinct minimum i.e. turnaround concentration at 30 mole percent of methanol concentration. Beyond this concentration, heat transfer coefficient increases with increase in concentration of methanol. Further, increase in pressure has led to increase the value of heat transfer coefficient of the mixture but does not alter the turnaround concentration. Based upon it, a correlation, $h/h_{id} = [1 + |y - x|(\alpha/D)^{0.5}]^{-(0.8x+0.2)}$ has been developed to determine heat transfer coefficient of a binary mixture from the knowledge of heat transfer coefficients of individual components, phase equilibrium data, and physico-thermal properties of the mixtures. This equation has correlated all the experimental data of this investigation within an error of $\pm 15\%$ as well as those predicted by correlations of [22, 50, 60, 76, 114, 121, 132, 134] within an average error of $\pm 25\%$.
 5. Experimental data for nucleate pool boiling of distilled water on stainless steel tubes coated with various thicknesses (22, 43 and 67 μm) of copper have been generated for different values of heat flux and pressure. Analysis has shown that heat transfer coefficient is related to heat flux by the relationship, $h \propto q^r$ where the value of exponent, r depends upon the thickness of copper coating. In fact, the value of exponent r is always less than 0.7 which generally holds true for boiling of liquids on an uncoated surface. Further, it has also been found to decrease with increase in thickness of coating. Thus, heat transfer coefficient of distilled water has been found to increase. This phenomenon continues up to a particular value of coating thickness and thereafter decreases with further increase in thickness of coating. Enhancement on a 43 μm thick coated tube has been found to be more

than that on 22 and 67 μm thick coated tubes for the boiling of distilled water. A dimensional relationship $h = C_3 q' p^s$ has been obtained to relate heat transfer coefficient for boiling of distilled water on coated surfaces with heat flux and pressure. The value of constant, C_3 and exponents, r and s in this relationship depend upon thickness of coating and heating surface characteristics.

Similar observations have also been made for the boiling of methanol on a 43 μm thick coated tube surface. A dimensional relationship, $h = 1.27 q'^{0.60} p^{0.39}$ has been developed to obtain heat transfer coefficient for the boiling of methanol on a 43 μm thick coated tube surface.

6. The experimental data for pool boiling of methanol-distilled water binary mixtures at atmospheric and subatmospheric pressure on a 43 μm copper coated tube have shown the same trend as obtained for the boiling of liquids on a plain tube. A functional relationship amongst heat transfer coefficient, heat flux and pressure on a 43 μm copper coated stainless steel tube has been obtained by least squares method in the following form: $h = C_4 q'^{0.60} p^{0.39}$, where the value of constant, C_4 depends upon individual components concentration in the binary mixture and heating surface characteristics.
7. It has been observed that application of copper coating on stainless steel heating tube surface does not alter the methanol turnaround concentration. In addition, the correlation, $h/h_{id} = [1 + |y - x|(\alpha/D)^{0.5}]^{-(0.8x+0.2)}$ has been developed for boiling of mixtures on a plain tube is also valid for the boiling of liquid mixtures on a 43 μm thick copper coated tube as well. This correlation has been compared with the experimental data for the boiling of methanol-distilled water mixtures on a 43 μm thick copper coated tube and found to match very well within an error of $\pm 20\%$.
8. Thermal effectiveness of a stainless steel heating tube surface coated with copper of various thicknesses has been evaluated as a ratio of heat transfer coefficient of a boiling liquid over a coated tube to that on an

uncoated tube surface subjected to same heat flux and pressure. This has been carried out to determine the applicability of copper coating on an uncoated tube for the boiling of liquids and their mixtures. Analysis has shown that thermal effectiveness is related to heat flux and pressure by the following functional correlation, $\zeta = k q^\alpha p^\beta$. Considering the condition, $\zeta > 1$, a criterion $q^{-\alpha} p^{-\beta} < k$ has been established for applicability of coated heating tube in enhanced boiling of liquids. This criterion can be used for the determination of range of pressure required for enhanced boiling of liquids at a given value of heat flux. Alternatively it can also be used to predict range of heat flux at which enhanced boiling of a liquid occurs at a given value of pressure.

Above criterion is also applicable to enhanced boiling of methanol-distilled water mixtures on a stainless steel heating tube surface coated with copper of a given thickness.

6.2 RECOMMENDATIONS

Following is recommended for future research work:

1. The present experimentation has been confined to saturated pool boiling of water, methanol and their binary liquid mixtures on an uncoated stainless steel heating tube surface for various values of heat flux at atmospheric and sub-atmospheric pressures. Therefore, correlations developed in this investigation are valid only for operating conditions of this investigation. It is desirable that experimental data at pressures higher than one atmosphere be generated and thereby correlations be developed. Further, investigation should also include other industrially important liquids like refrigerants, hydrocarbons, cryogenics, solvents, etc. to obtain generalized inferences.
2. In present investigation, effect of thickness of copper coating on a stainless steel tube for the boiling liquids and their mixtures has been determined. However, it will be worthwhile to investigate the effect of other metallic coating materials such as silver, molybdenum, cadmium,

zinc, aluminum, etc. on boiling heat transfer coefficient. Further, substrate material such as copper, bronze, zinc, brass, etc. should also be investigated to obtain their effect on enhanced boiling of liquids.

3. Measurement of contact angle made by liquid droplet over uncoated as well as coated tube surfaces could not be made in this investigation due to lack of sophisticated instrumental facilities. However, it is desirable to include such a study as it likely to provide strength to arguments advanced for phenomena occurring therein.
4. Electroplating technique is employed in this investigation for coating of copper on stainless steel tube. It is recommended that other techniques such as thermal-spraying, sintering, vapor deposition, sputtering etc. should also be investigated to obtain their role in enhancement of boiling heat transfer coefficient on coated tubes.
5. This investigation has been confined for the boiling of distilled water-methanol binary mixtures only. It is recommended that experiments on other industrially important liquid binary mixtures such as water-acetic acid, water-acetone, etc., and ternary mixtures should also be conducted to obtain the generalized conclusions. Besides, it will also be order to investigate azeotropic liquid mixtures to obtain a complete rational phenomenon of the boiling occurring therein.

Annexure -A

Coating Procedure of Heating Tubes

This describes the procedure for coating of copper over uncoated tube and measurement of coating thickness

PREPARATION OF COATED HEATING TUBES

This annexure describes the procedure adopted in the present study for the copper coating over the uncoated stainless steel tube. It also describes various precautions taken during coating procedure, and includes the procedure adopted for the measurement of coating thickness. All heating tubes except uncoated tube (ST-00) used in this investigation were processed to obtain desired copper coating thicknesses.

The coatings of three stainless steel heating tubes (ST-22, ST-43, & ST-67) were made by electroplating technique at M/s Plating Sheen Chem. India Pvt. Ltd., New Delhi, India.

A.1 Electroplating Process

Electroplating is the process of applying a metallic coating to an article by passing an electric current through an electrolyte in contact with the article, thereby forming a surface having properties or dimensions different from those of the article. The essential components of an electroplating process are an electrode to be plated i.e. the cathode or substrate, a second electrode to complete the circuit i.e. the anode, an electrolyte containing the metal ions to be deposited, and a direct current power source. The electrodes are immersed in the electrolyte with the anode connected to the positive leg of the power supply and the cathode to the negative leg. The schematic diagram of an electroplating process is given in **Fig. A.1**.

Electroplating equipment available with M/s Plating Sheen Chem. India Pvt. Ltd., New Delhi, India was used for application of coating on heating tubes. It consist a mild steel tank made of 5 mm thick double welded M.S. sheet. Inner side of the tank was lined with rubber and outer side was provided with thermal insulation of 40 mm thick glass wool covered with 16 gauge aluminum sheets. Heating tubes to be plated were used as cathode and electrolytic grade copper sheet was used as an anode. DC power supply to the equipment was provided by a solid-state silicon rectifier.

Following sub-sections illustrate briefly the electroplating process and its operating parameters.

A.1.1 Preliminary Treatment

This coating process essentially requires a conductive surface free from oil, grease, dirt and other volatile material. Therefore, preliminary treatment process employed prior to electroplating process to clean the substrate surface. The process consists of pretreatment, alkaline cleaning, acid dipping, followed by strike plating of copper.

The processes employed for cleaning of all heating tube surfaces are as follows:

- The pretreatment steps include removal of oil, grease, polishing and buffing compounds. It was done prior to normal cleaning by dipping all the three heating tube in organic solvents, trichloroethylene (20 ml/l) for 5 min at a temperature of 90 °C.
- Heating tubes were further cleaned by an alkaline cleaner sodium carbonate or sodium hydroxide (50 g/l) for 5 min at a temperature of 70 °C to dislodge surface soil.
- Acid dipping was used to remove oxide films on heating tubes formed in the alkaline cleaning step and to neutralize the alkaline film. 0.2M HCl solution was used as an acid dip.
- The copper strike plating step was employed to applying a thin layer of copper in a copper cyanide solution to enhance the conductive properties of the heating tubes.

A.1.2 Operating Procedure of Coating

Rochelle cyanide copper plating process was used for coating of copper on stainless steel heating tubes. Operating parameters used in this process are summarized in **Table A.1**.

Table A.1 Operating parameters for cyanide copper plating process

Operating Parameters	Value
Rochelle Copper cyanide (g/l)	150
Temperature ($^{\circ}\text{C}$)	55
Cathode current density (amp/dm^2)	3.0
Anode current density (amp/dm^2)	3.0
Bath Voltage (V)	6
Copper metal (g/l)	20
Free sodium cyanide (g/l)	8
Rochelle salt (g/l)	48

Steps involved in coating of heating tube surface are as follows:

- Properly cleaned tank was filled with two-third full of de-ionized water. Required quantity of the Rochelle copper cyanide salt was added slowly into the tank with vigorous stirring, which was continued till the salt get dissolved completely. Further, water was added up to the required final volume, and again solution was stirred thoroughly.
- The solution was then filtered with PCI Elefil process filters to remove dust and other fine particles. It was necessary to make solution free from these type of impurities, which otherwise interfere in the performance of the bath solution.
- The tank solution was heated up to the operating temperature and thereafter, the process equipments were arranged as shown in **Fig. A.1**.
- A dummy specimen was prepared which was used at the initiation of the process to qualify the surface preparation, the surface cleanliness, thickness, and adhesion, which must be in accordance with the present requirements.
- For this purpose a dummy specimen was first tested by hanging it with the cathode support rod, which is connected to the negative terminal of

the DC power source. Positive terminal of power source is connected with the anode support rod, from which the copper anode is hanging.

- DC power supply was turned on and the process was allowed to continue for a predetermined time.
- After completion of electroplating process, the power supply was turned off and both copper anode and dummy specimen (cathode) were carefully removed from the bath.
- Weight loss was determined by weighing the anode before the start and after the completion of the coating process. The loss in weight of the anode equals the gain in weight of the cathode.
- Approximate calculation for operating parameters and process time were made to obtain the desired coating thickness. The coating thickness of the dummy specimen was then measured to verify the desired coating thickness.
- After that, heating tube was attached to the cathode support rod in place of dummy specimen and process was repeated with determined operating parameters for a predetermined time. This is carried out to obtain desired coating thickness over the heating tube. The coating thickness of the prepared specimen was then measured to verify the desired coating thickness.
- Similar procedure was repeated for rest of the two stainless steel tubes to obtain desired coating thickness over them. However, every time approximate calculation of operating parameters was made to obtain the various desired coating thicknesses.

A.1.3 Precautions during Coating of Heating Tube Surface

The following precautions are taken during coating of heating tube to produce the most uniform coating thickness of the best possible quality.

- The substrate surface was cleaned properly by pretreatment process to increase conductivity and adhesion capabilities.
- It is very important for an electrolyte to be free from dust and other fine invisible particles. These particles interfere in the performance of the

bath solution. Therefore, electrolyte solution was filtered by appropriate filters to maintain clean solution in the bath all the time.

- Replenishment addition of sodium cyanide and Rochelle copper salt was made by adopting analytical measures. The purpose of this addition was to obtain a uniform coating over heating tubes by maintaining the content bath same throughout the process.
- Uniform DC Power supply was maintained all through the coating process.
- Rochelle copper plating bath solution is alkaline in nature and contains sodium cyanide and copper metal, which are toxic in nature. Therefore, great care was taken during the entire process in its handling. The spent solution was collected in a suitable tank, and remaining copper was removed from it by electroplating process with dummy cathodes. Then detoxification of cyanide was done by usual method of adding stable bleaching powder or sodium hypochlorite solution or by passing chlorine gas. Thereafter, all waste materials were discarded in accordance with local authority regulations.

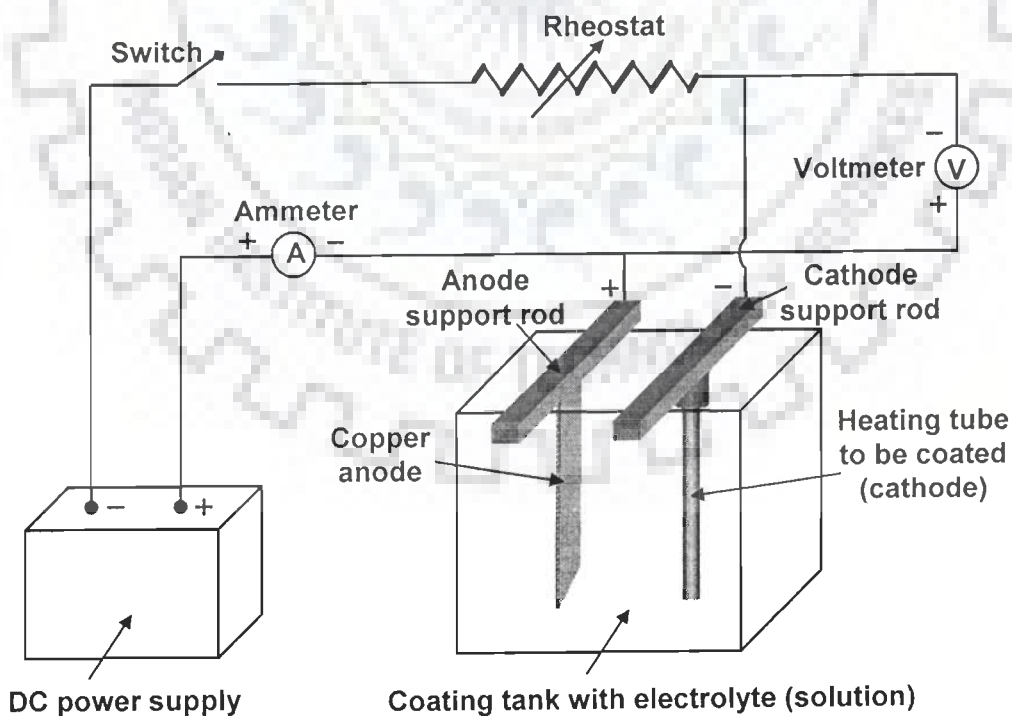


Fig. A.1 Schematic diagram for electroplating circuits

A.2 Measurement of Coating Thickness of Heating Tube

The coating thicknesses employed over the three heating tubes were verified with a magnetic coating thickness gauge. This instrument has an accuracy of $\pm 1\mu\text{m}$. Following steps were taken for the measurement of copper coating over the heating tubes:

- The instrument was switched on by connecting its power cord to the power plug.
- The surface of the heating tube and bottom surface of the probe of the instrument were cleaned thoroughly to avoid imprecision in calibrating the instrument which otherwise give erroneous thickness measurement data.
- Probe of the instrument was placed on an uncoated base material by holding the outer holder so that spring loading may ensure constant pressure on the surface. Zero control was adjusted to read 0.
- A known thickness of calibrated foil was kept between the probe and bare material and subsequently, instrument indicated the value of thickness. If the measured value of thickness was equal to the known thickness of the foil, then the instrument was ready for the measurement of unknown coating thickness. Otherwise, it was adjusted to zero setting again and calibration was done until it provided the known thickness of the foil.
- After calibration, probe of the instrument was placed randomly at different locations on the surface of the heating tube and the displayed values of coating thickness were noted. The arithmetic mean of these values represented true value of thickness of copper coating. It may be mentioned here that no significant variations in the values of coating thickness at different locations was observed which ensures that the coating was uniform over the entire surface of the heating tubes.

The above mentioned procedure was adopted for measuring the coating thickness of copper on all the coated tubes (ST-22, ST-43 and ST-67) and their values are given in **Table 3.1**.

Annexure –B

Tabulation of Experimental Data

This presents tabulation of experimental data

Table B.1 Boiling heat transfer data of distilled water over a horizontal uncoated tube

Run No.	Heat Input, Q W	Heat Flux, q W/m ²	Wall Temperature, T _w , °C				Liquid Pool Temperature, T _{lm} , °C				Wall Super Heat, ΔT _w °C	Heat Transfer Coefficient, h W/m ² °C
			Top	Side	Bottom	Side	Top	Side	Bottom	Side		
Pressure : 97.71 kN/m ²												
1	240	15946.8	112.35	111.25	110.33	111.31	99.15	99.17	99.18	99.18	8.33	1913.4
2	320	21262.5	114.64	113.85	112.18	113.79	99.15	99.17	99.18	99.18	9.37	2268.7
3	400	26578.1	116.14	115.13	113.91	115.24	99.15	99.17	99.18	99.18	9.60	2769.8
4	480	31893.7	117.91	117.27	115.92	117.31	99.15	99.17	99.18	99.18	10.32	3089.6
5	560	37209.3	120.57	119.11	117.58	119.20	99.15	99.17	99.18	99.18	11.07	3362.1
6	640	42524.9	121.86	120.47	119.02	120.47	99.15	99.17	99.18	99.18	11.14	3817.1
Pressure : 84.39 kN/m ²												
7	240	15946.8	108.47	107.40	106.34	107.45	94.80	94.91	94.83	94.91	8.75	1822.4
8	320	21262.5	110.81	110.07	108.22	109.99	94.80	94.91	94.83	94.91	9.84	2161.5
9	400	26578.1	112.32	111.34	109.97	111.45	94.80	94.91	94.83	94.91	10.07	2639.7
10	480	31893.7	114.10	113.52	112.01	113.56	94.80	94.91	94.83	94.91	10.83	2944.7
11	560	37209.3	116.83	115.39	113.69	115.48	94.80	94.91	94.83	94.91	11.61	3204.7
12	640	42524.9	118.13	116.76	115.14	116.74	94.80	94.91	94.83	94.91	11.69	3638.9
Pressure : 71.06 kN/m ²												
13	240	15946.8	104.42	103.32	102.30	103.33	90.19	90.34	90.35	90.30	9.24	1725.1
14	320	21262.5	106.82	106.07	104.22	105.94	90.19	90.34	90.35	90.30	10.39	2046.1
15	400	26578.1	108.34	107.34	106.00	107.41	90.19	90.34	90.35	90.30	10.64	2499.0
16	480	31893.7	110.16	109.58	108.08	109.58	90.19	90.34	90.35	90.30	11.44	2786.9
17	560	37209.3	112.97	111.47	109.78	111.53	90.19	90.34	90.35	90.30	12.27	3033.6
18	640	42524.9	114.27	112.85	111.24	112.79	90.19	90.34	90.35	90.30	12.35	3444.2

Table B.1 Contd.

Run No.	Heat Input, Q W	Heat Flux, q W/m ²	Wall Temperature, T _{wo} , °C				Liquid Pool Temperature, T _{lm} , °C				Wall Super Heat, ΔT _w °C	Heat Transfer Coefficient, h W/m ² °C
			Top	Side	Bottom	Side	Top	Side	Bottom	Side		
Pressure : 57.73 kN/m ²												
19	240	15946.8	100.13	98.82	97.74	98.87	85.18	85.21	85.23	85.19	9.88	1614.1
20	320	21262.5	102.60	101.68	99.70	101.57	85.18	85.21	85.23	85.19	11.11	1914.2
21	400	26578.1	104.15	102.95	101.52	103.05	85.18	85.21	85.23	85.19	11.37	2337.1
22	480	31893.7	106.01	105.24	103.66	105.27	85.18	85.21	85.23	85.19	12.23	2607.8
23	560	37209.3	108.92	107.19	105.39	107.27	85.18	85.21	85.23	85.19	13.11	2838.4
24	640	42524.9	110.22	108.57	106.86	108.53	85.18	85.21	85.23	85.19	13.20	3222.8
Pressure : 44.40 kN/m ²												
25	240	15946.8	94.48	93.07	91.90	93.14	78.55	78.59	78.62	78.59	10.75	1483.2
26	320	21262.5	97.06	96.06	93.91	95.96	78.55	78.59	78.62	78.59	12.08	1759.5
27	400	26578.1	98.63	97.32	95.78	97.46	78.55	78.59	78.62	78.59	12.37	2148.8
28	480	31893.7	100.53	99.71	98.00	99.76	78.55	78.59	78.62	78.59	13.30	2397.7
29	560	37209.3	103.60	101.72	99.77	101.83	78.55	78.59	78.62	78.59	14.26	2609.1
30	640	42524.9	104.90	103.10	101.26	103.09	78.55	78.59	78.62	78.59	14.36	2962.1

Table B.2 Boiling heat transfer data of distilled water over a 22 μm thick horizontal coated tube

Run No.	Heat Input, Q W	Heat Flux, q W/m ²	Wall Temperature, T_{wo} , °C				Liquid Pool Temperature, T_{lm} , °C				Wall Super Heat, ΔT_w °C	Heat Transfer Coefficient, h W/m ² °C
			Top	Side	Bottom	Side	Top	Side	Bottom	Side		
Pressure : 97.77 kN/m ²												
31	240	15950.4	110.01	109.10	108.52	109.09	99.13	99.15	99.15	99.16	6.23	2559.3
32	320	21267.2	111.97	111.39	110.52	111.37	99.13	99.15	99.15	99.16	7.09	2997.7
33	400	26584.0	113.69	112.98	112.00	112.95	99.13	99.15	99.15	99.16	7.42	3584.0
34	480	31900.8	115.50	114.71	113.66	114.57	99.13	99.15	99.15	99.16	7.86	4060.3
35	560	37217.6	117.44	116.30	115.62	116.30	99.13	99.15	99.15	99.16	8.39	4434.2
36	640	42534.4	119.18	118.08	117.11	118.10	99.13	99.15	99.15	99.16	8.82	4819.7
Pressure : 84.43 kN/m ²												
37	240	15950.4	106.35	105.30	104.83	105.29	94.92	95.00	95.05	95.04	6.64	2403.1
38	320	21267.2	108.59	107.63	106.74	107.55	94.92	95.00	95.05	95.04	7.55	2815.2
39	400	26584.0	110.58	109.02	108.34	109.02	94.92	95.00	95.05	95.04	7.90	3366.3
40	480	31900.8	112.48	110.72	110.06	110.64	94.92	95.00	95.05	95.04	8.36	3814.0
41	560	37217.6	113.91	112.79	111.81	112.76	94.92	95.00	95.05	95.04	8.93	4165.4
42	640	42534.4	115.81	114.37	113.67	114.33	94.92	95.00	95.05	95.04	9.39	4527.6
Pressure : 71.17 kN/m ²												
43	240	15950.4	102.22	101.30	100.20	101.27	90.24	90.35	90.32	90.31	7.14	2234.2
44	320	21267.2	104.51	103.55	102.47	103.48	90.24	90.35	90.32	90.31	8.12	2617.4
45	400	26584.0	106.19	105.13	104.10	105.13	90.24	90.35	90.32	90.31	8.49	3129.8
46	480	31900.8	108.58	106.57	105.91	106.58	90.24	90.35	90.32	90.31	9.00	3545.2
47	560	37217.6	109.85	108.96	107.40	108.95	90.24	90.35	90.32	90.31	9.61	3872.8
48	640	42534.4	111.83	110.67	109.11	110.61	90.24	90.35	90.32	90.31	10.10	4208.8

Table B.2 Contd.

Run No.	Heat Input, Q W	Heat Flux, q W/m ²	Wall Temperature, T _w , °C				Liquid Pool Temperature, T _{lm} , °C				Wall Super Heat, ΔT _w °C	Heat Transfer Coefficient, h W/m ² °C
			Top	Side	Bottom	Side	Top	Side	Bottom	Side		
Pressure : 57.81 kN/m ²												
49	240	15950.4	97.54	96.81	95.98	96.79	85.14	85.18	85.22	85.18	7.79	2046.0
50	320	21267.2	100.17	99.05	98.27	99.01	85.14	85.18	85.22	85.18	8.87	2397.0
51	400	26584.0	101.81	100.80	99.84	100.74	85.14	85.18	85.22	85.18	9.27	2866.1
52	480	31900.8	103.82	102.64	101.41	102.58	85.14	85.18	85.22	85.18	9.82	3247.4
53	560	37217.6	105.68	104.57	103.46	104.50	85.14	85.18	85.22	85.18	10.49	3546.8
54	640	42534.4	107.44	106.33	105.33	106.32	85.14	85.18	85.22	85.18	11.03	3855.3
Pressure : 44.52 kN/m ²												
55	240	15950.4	92.07	90.84	90.37	90.84	78.47	78.51	78.55	78.53	8.71	1830.6
56	320	21267.2	94.61	93.50	92.41	93.48	78.47	78.51	78.55	78.53	9.91	2144.6
57	400	26584.0	96.14	95.23	94.34	95.16	78.47	78.51	78.55	78.53	10.36	2564.7
58	480	31900.8	98.61	96.85	96.10	96.84	78.47	78.51	78.55	78.53	10.98	2905.9
59	560	37217.6	100.53	98.92	98.10	98.91	78.47	78.51	78.55	78.53	11.72	3173.6
60	640	42534.4	102.30	100.88	99.92	100.84	78.47	78.51	78.55	78.53	12.33	3449.8

Table B.3 Boiling heat transfer data of distilled water over a 43 μm thick horizontal coated tube

Run No.	Heat Input, Q W	Heat Flux, q W/m ²	Wall Temperature, T_{wo} , °C				Liquid Pool Temperature, T_{lm} , °C				Wall Super Heat, ΔT_w °C	Heat Transfer Coefficient, h W/m ² °C
			Top	Side	Bottom	Side	Top	Side	Bottom	Side		
Pressure : 97.71 kN/m ²												
61	240	15946.8	108.76	108.12	107.24	108.10	99.12	99.17	99.20	99.15	5.09	3134.1
62	320	21262.5	110.51	109.84	109.19	109.81	99.12	99.17	99.20	99.15	5.60	3793.8
63	400	26578.1	112.72	111.40	110.96	111.41	99.12	99.17	99.20	99.15	6.12	4343.6
64	480	31893.7	114.22	113.40	112.42	113.48	99.12	99.17	99.20	99.15	6.61	4822.4
65	560	37209.3	116.18	115.19	114.11	115.12	99.12	99.17	99.20	99.15	7.11	5233.7
66	640	42524.9	117.79	116.85	115.69	116.83	99.12	99.17	99.20	99.15	7.49	5680.7
Pressure : 84.37 kN/m ²												
67	240	15946.8	105.17	103.96	103.42	103.97	94.99	94.93	94.87	94.93	5.40	2955.0
68	320	21262.5	107.30	105.83	104.83	105.82	94.99	94.93	94.87	94.93	5.94	3577.8
69	400	26578.1	109.15	107.51	106.85	107.52	94.99	94.93	94.87	94.93	6.49	4096.6
70	480	31893.7	110.61	109.45	108.72	109.43	94.99	94.93	94.87	94.93	7.01	4548.6
71	560	37209.3	112.88	111.13	110.21	111.14	94.99	94.93	94.87	94.93	7.54	4937.3
72	640	42524.9	114.74	112.77	111.80	112.76	94.99	94.93	94.87	94.93	7.94	5353.9
Pressure : 71.11 kN/m ²												
73	240	15946.8	100.87	99.81	98.90	99.81	90.20	90.27	90.32	90.28	5.77	2761.5
74	320	21262.5	102.68	101.70	100.74	101.69	90.20	90.27	90.32	90.28	6.36	3342.8
75	400	26578.1	105.31	103.21	102.48	103.20	90.20	90.27	90.32	90.28	6.94	3827.6
76	480	31893.7	106.73	105.25	104.31	105.24	90.20	90.27	90.32	90.28	7.50	4249.8
77	560	37209.3	108.60	107.12	106.02	107.11	90.20	90.27	90.32	90.28	8.07	4612.5
78	640	42524.9	110.43	108.90	107.41	108.89	90.20	90.27	90.32	90.28	8.49	5006.6

Table B.3 Contd.

Run No.	Heat Input, Q W	Heat Flux, q W/m ²	Wall Temperature, T _{w0} , °C				Liquid Pool Temperature, T _{lm} , °C				Wall Super Heat, ΔT _w °C	Heat Transfer Coefficient, h W/m ² °C
			Top	Side	Bottom	Side	Top	Side	Bottom	Side		
Pressure : 57.68 kN/m ²												
79	240	15946.8	97.08	95.22	94.11	95.22	85.28	85.34	85.36	85.36	6.27	2543.4
80	320	21262.5	98.82	97.24	95.96	97.23	85.28	85.34	85.36	85.36	6.91	3079.2
81	400	26578.1	100.99	99.02	97.82	99.02	85.28	85.34	85.36	85.36	7.54	3525.9
82	480	31893.7	103.05	101.09	99.12	101.09	85.28	85.34	85.36	85.36	8.15	3914.8
83	560	37209.3	105.30	102.74	101.09	102.73	85.28	85.34	85.36	85.36	8.76	4248.8
84	640	42524.9	107.00	104.42	103.01	104.40	85.28	85.34	85.36	85.36	9.23	4608.5
Pressure : 44.44 kN/m ²												
85	240	15946.8	90.60	89.26	88.37	89.26	78.57	78.60	78.63	78.64	6.96	2292.6
86	320	21262.5	93.07	91.09	90.14	91.07	78.57	78.60	78.63	78.64	7.66	2775.9
87	400	26578.1	95.18	93.03	92.02	93.02	78.57	78.60	78.63	78.64	8.36	3178.2
88	480	31893.7	97.17	94.90	94.07	94.89	78.57	78.60	78.63	78.64	9.04	3528.9
89	560	37209.3	99.04	96.96	95.83	96.98	78.57	78.60	78.63	78.64	9.71	3830.1
90	640	42524.9	100.99	98.88	97.37	98.70	78.57	78.60	78.63	78.64	10.23	4157.3

Table B.4 Boiling heat transfer data of distilled water over a 67 μm thick horizontal coated tube

Run No.	Heat Input, Q W	Heat Flux, q W/m ²	Wall Temperature, T_{wo} , °C				Liquid Pool Temperature, T_{lm} , °C				Wall Super Heat, ΔT_w °C	Heat Transfer Coefficient, h W/m ² °C
			Top	Side	Bottom	Side	Top	Side	Bottom	Side		
Pressure : 97.76 kN/m ²												
91	240	15955.4	110.12	109.44	108.42	109.43	99.09	99.12	99.15	99.13	6.42	2483.5
92	320	21273.8	112.04	111.64	110.73	111.50	99.09	99.12	99.15	99.13	7.28	2920.1
93	400	26592.3	114.39	113.87	112.42	113.79	99.09	99.12	99.15	99.13	8.15	3260.6
94	480	31910.8	116.78	115.47	114.22	115.41	99.09	99.12	99.15	99.13	8.74	3649.7
95	560	37229.2	118.25	117.55	116.13	117.51	99.09	99.12	99.15	99.13	9.35	3977.5
96	640	42547.7	120.46	119.66	118.11	119.54	99.09	99.12	99.15	99.13	10.17	4180.5
Pressure : 84.37 kN/m ²												
97	240	15955.4	106.10	105.63	104.65	105.62	94.88	94.94	94.96	94.95	6.76	2357.5
98	320	21273.8	108.58	107.59	106.94	107.58	94.88	94.94	94.96	94.95	7.67	2772.5
99	400	26592.3	110.72	109.91	108.88	109.91	94.88	94.94	94.96	94.95	8.58	3096.0
100	480	31910.8	112.78	111.83	110.56	111.80	94.88	94.94	94.96	94.95	9.20	3465.9
101	560	37229.2	114.88	113.59	112.59	113.58	94.88	94.94	94.96	94.95	9.85	3776.9
102	640	42547.7	116.67	116.00	114.51	115.97	94.88	94.94	94.96	94.95	10.71	3969.7
Pressure : 71.67 kN/m ²												
103	240	15955.4	102.10	101.27	100.61	101.26	90.29	90.33	90.35	90.32	7.18	2220.4
104	320	21273.8	104.40	103.51	102.75	103.50	90.29	90.33	90.35	90.32	8.14	2611.3
105	400	26592.3	106.66	105.91	104.66	105.89	90.29	90.33	90.35	90.32	9.11	2916.1
106	480	31910.8	108.94	107.49	106.92	107.47	90.29	90.33	90.35	90.32	9.77	3264.4
107	560	37229.2	110.94	109.62	108.50	109.57	90.29	90.33	90.35	90.32	10.46	3557.8
108	640	42547.7	112.93	111.85	110.73	111.86	90.29	90.33	90.35	90.32	11.37	3739.2

Table B.4 Contd.

Run No.	Heat Input, Q W	Heat Flux, q W/m ²	Wall Temperature, T _w , °C				Liquid Pool Temperature, T _{lm} , °C				Wall Super Heat, ΔT _w °C	Heat Transfer Coefficient, h W/m ² °C
			Top	Side	Bottom	Side	Top	Side	Bottom	Side		
Pressure : 58.01 kN/m ²												
109	240	15955.4	97.42	96.75	95.83	96.65	85.11	85.14	85.16	85.14	7.72	2065.3
110	320	21273.8	99.84	98.91	98.20	98.90	85.11	85.14	85.16	85.14	8.75	2429.0
111	400	26592.3	102.06	101.31	100.45	101.29	85.11	85.14	85.16	85.14	9.80	2712.5
112	480	31910.8	104.26	103.21	102.36	103.16	85.11	85.14	85.16	85.14	10.50	3036.4
113	560	37229.2	106.36	105.28	104.21	105.19	85.11	85.14	85.16	85.14	11.24	3309.5
114	640	42547.7	108.75	107.64	106.14	107.50	85.11	85.14	85.16	85.14	12.23	3478.3
Pressure : 44.72 kN/m ²												
115	240	15955.4	90.83	90.07	90.72	90.72	78.49	78.52	78.54	78.53	8.46	1884.6
116	320	21273.8	93.03	92.40	93.01	93.01	78.49	78.52	78.54	78.53	9.59	2216.5
117	400	26592.3	95.34	94.62	95.33	95.33	78.49	78.52	78.54	78.53	10.74	2475.1
118	480	31910.8	97.30	96.69	97.20	97.20	78.49	78.52	78.54	78.53	11.51	2771.0
119	560	37229.2	99.77	98.56	99.51	99.51	78.49	78.52	78.54	78.53	12.32	3020.2
120	640	42547.7	102.07	100.99	102.06	102.06	78.49	78.52	78.54	78.53	13.40	3174.6

Table B.5 Boiling heat transfer data of methanol over a horizontal uncoated tube

Run No.	Heat Input, Q W	Heat Flux, q W/m ²	Wall Temperature, T _w , °C				Liquid Pool Temperature, T _{lm} , °C				Wall Super Heat, ΔT _w °C	Heat Transfer Coefficient, h W/m ² °C
			Top	Side	Bottom	Side	Top	Side	Bottom	Side		
Pressure : 97.71 kN/m ²												
121	240	15946.8	78.58	77.84	76.99	77.67	63.26	63.26	63.25	63.18	10.73	1486.8
122	320	21262.5	81.13	80.28	79.26	80.55	63.26	63.26	63.25	63.18	11.99	1772.7
123	400	26578.1	82.52	81.91	80.95	81.97	63.26	63.26	63.25	63.18	12.25	2168.8
124	480	31893.7	85.69	84.33	83.31	84.55	63.26	63.26	63.25	63.18	13.62	2340.9
125	560	37209.3	86.92	86.43	85.25	86.15	63.26	63.26	63.25	63.18	14.07	2644.4
126	640	42524.9	88.79	87.60	86.47	87.62	63.26	63.26	63.25	63.18	14.24	2986.9
Pressure : 84.69 kN/m ²												
127	240	15946.8	76.03	75.11	74.35	75.18	61.17	61.13	61.13	61.18	11.21	1422.4
128	320	21262.5	78.34	77.88	76.96	77.89	61.17	61.13	61.13	61.18	12.54	1695.4
129	400	26578.1	80.54	79.19	78.12	79.40	61.17	61.13	61.13	61.18	12.82	2073.0
130	480	31893.7	83.02	82.08	80.95	82.02	61.17	61.13	61.13	61.18	14.26	2237.0
131	560	37209.3	84.71	83.66	82.79	83.87	61.17	61.13	61.13	61.18	14.73	2526.8
132	640	42524.9	86.06	85.30	84.12	85.31	61.17	61.13	61.13	61.18	14.90	2853.6
Pressure : 71.26 kN/m ²												
133	240	15946.8	72.44	71.73	70.69	71.94	56.04	56.05	56.00	56.07	11.86	1345.1
134	320	21262.5	75.29	74.45	73.32	74.43	56.04	56.05	56.00	56.07	13.26	1603.6
135	400	26578.1	76.95	75.79	75.16	75.85	56.04	56.05	56.00	56.07	13.55	1961.2
136	480	31893.7	79.66	78.73	77.61	78.87	56.04	56.05	56.00	56.07	15.07	2116.8
137	560	37209.3	81.63	80.66	78.69	80.95	56.04	56.05	56.00	56.07	15.56	2390.8
138	640	42524.9	82.90	81.91	80.94	82.00	56.04	56.05	56.00	56.07	15.75	2699.9

Table B.5 Contd.

Run No.	Heat Input, Q W	Heat Flux, q W/m ²	Wall Temperature, T _w , °C				Liquid Pool Temperature, T _{lm} , °C				Wall Super Heat, ΔT _w °C	Heat Transfer Coefficient, h W/m ² °C
			Top	Side	Bottom	Side	Top	Side	Bottom	Side		
Pressure : 57.73 kN/m ²												
139	240	15946.8	68.64	67.65	66.86	67.88	51.30	51.32	51.28	51.25	12.67	1259.1
140	320	21262.5	71.44	70.49	69.61	70.57	51.30	51.32	51.28	51.25	14.17	1500.6
141	400	26578.1	72.69	72.22	71.20	72.32	51.30	51.32	51.28	51.25	14.48	1835.3
142	480	31893.7	76.12	74.97	73.79	75.10	51.30	51.32	51.28	51.25	16.10	1980.9
143	560	37209.3	78.14	76.86	75.51	76.67	51.30	51.32	51.28	51.25	16.63	2237.1
144	640	42524.9	79.30	78.06	77.21	78.47	51.30	51.32	51.28	51.25	16.83	2526.5
Pressure : 45.05 kN/m ²												
145	240	15946.8	63.74	63.35	62.60	63.30	45.66	45.71	45.71	45.61	13.77	1158.0
146	320	21262.5	67.13	66.12	65.12	66.25	45.66	45.71	45.71	45.61	15.41	1379.6
147	400	26578.1	69.21	67.47	66.81	67.56	45.66	45.71	45.71	45.61	15.75	1687.4
148	480	31893.7	71.68	70.83	69.76	70.91	45.66	45.71	45.71	45.61	17.51	1821.0
149	560	37209.3	73.74	72.65	71.46	72.71	45.66	45.71	45.71	45.61	18.09	2056.6
150	640	42524.9	74.72	74.26	73.17	74.35	45.66	45.71	45.71	45.61	18.30	2323.1

Table B.6 Boiling heat transfer data of methanol over a 43 μm thick horizontal coated tube

Run No.	Heat Input, Q W	Heat Flux, q W/m ²	Wall Temperature, T_{wo} , °C				Liquid Pool Temperature, T_{lm} , °C				Wall Super Heat, ΔT_w °C	Heat Transfer Coefficient, h W/m ² °C
			Top	Side	Bottom	Side	Top	Side	Bottom	Side		
Pressure : 97.76 kN/m ²												
151	240	15946.8	74.49	73.91	73.50	73.98	63.91	64.08	64.09	63.99	6.15	2593.9
152	320	21262.5	76.93	75.67	74.74	75.75	63.91	64.08	64.09	63.99	6.68	3182.5
153	400	26578.1	78.63	77.66	76.69	77.76	63.91	64.08	64.09	63.99	7.32	3628.5
154	480	31893.7	80.76	79.58	78.51	79.78	63.91	64.08	64.09	63.99	8.03	3973.5
155	560	37209.3	82.57	81.17	80.75	81.26	63.91	64.08	64.09	63.99	8.54	4356.9
156	640	42524.9	84.02	83.09	82.12	83.22	63.91	64.08	64.09	63.99	8.95	4753.4
Pressure : 85.13 kN/m ²												
157	240	15946.8	70.97	70.52	69.79	70.57	60.17	60.13	60.13	60.18	6.51	2451.1
158	320	21262.5	73.45	72.11	71.36	72.26	60.17	60.13	60.13	60.18	7.07	3006.4
159	400	26578.1	75.43	74.01	73.44	74.11	60.17	60.13	60.13	60.18	7.75	3427.5
160	480	31893.7	77.28	76.19	75.29	76.28	60.17	60.13	60.13	60.18	8.50	3752.9
161	560	37209.3	79.05	78.02	77.16	78.06	60.17	60.13	60.13	60.18	9.04	4114.8
162	640	42524.9	80.73	79.79	78.66	79.91	60.17	60.13	60.13	60.18	9.47	4489.0
Pressure : 70.97 kN/m ²												
163	240	15946.8	67.37	66.99	66.41	67.21	55.92	56.99	55.99	56.01	6.96	2290.4
164	320	21262.5	69.84	68.97	67.81	68.86	55.92	56.99	55.99	56.01	7.57	2809.9
165	400	26578.1	71.84	70.81	69.86	70.98	55.92	56.99	55.99	56.01	8.30	3202.7
166	480	31893.7	74.00	72.83	71.94	72.96	55.92	56.99	55.99	56.01	9.09	3507.2
167	560	37209.3	75.83	74.72	73.67	74.92	55.92	56.99	55.99	56.01	9.68	3845.2
168	640	42524.9	77.22	76.12	75.76	76.96	55.92	56.99	55.99	56.01	10.14	4194.5

Table B.6 Contd.

Run No.	Heat Input, Q W	Heat Flux, q W/m ²	Wall Temperature, T _w , °C				Liquid Pool Temperature, T _{lm} , °C				Wall Super Heat, ΔT _w °C	Heat Transfer Coefficient, h W/m ² °C
			Top	Side	Bottom	Side	Top	Side	Bottom	Side		
Pressure : 58.15 kN/m ²												
169	240	15946.8	62.87	62.41	61.68	62.46	50.99	51.00	51.01	51.00	7.55	2111.0
170	320	21262.5	65.42	64.18	63.26	64.28	50.99	51.00	51.01	51.00	8.21	2588.7
171	400	26578.1	67.37	66.33	65.26	66.42	50.99	51.00	51.01	51.00	9.01	2950.9
172	480	31893.7	69.69	68.46	67.21	68.53	50.99	51.00	51.01	51.00	9.87	3231.2
173	560	37209.3	71.17	70.50	69.30	70.54	50.99	51.00	51.01	51.00	10.50	3543.0
174	640	42524.9	73.13	72.11	71.13	72.21	50.99	51.00	51.01	51.00	11.00	3865.1
Pressure : 44.82 kN/m ²												
175	240	15946.8	57.86	57.24	56.57	57.28	45.03	45.05	45.08	45.05	8.38	1902.7
176	320	21262.5	60.51	59.12	58.10	59.22	45.03	45.05	45.08	45.05	9.11	2333.9
177	400	26578.1	62.45	61.32	60.26	61.50	45.03	45.05	45.08	45.05	9.99	2660.1
178	480	31893.7	64.66	63.49	62.73	63.58	45.03	45.05	45.08	45.05	10.95	2912.8
179	560	37209.3	66.76	65.47	64.51	65.57	45.03	45.05	45.08	45.05	11.65	3193.8
180	640	42524.9	68.51	67.42	66.15	67.53	45.03	45.05	45.08	45.05	12.21	3484.0

Table B.7 Boiling heat transfer data of 5% methanol over a horizontal uncoated tube

Run No.	Heat Input, Q W	Heat Flux, q W/m ²	Wall Temperature, T _w , °C				Liquid Pool Temperature, T _{lm} , °C				Wall Super Heat, ΔT _w °C	Heat Transfer Coefficient, h W/m ² °C
			Top	Side	Bottom	Side	Top	Side	Bottom	Side		
Pressure : 97.70 kN/m ²												
181	240	15946.8	106.14	105.39	104.10	105.32	91.99	92.09	92.06	92.07	9.38	1699.6
182	320	21262.5	108.42	107.94	106.12	107.86	91.99	92.09	92.06	92.07	10.46	2032.1
183	400	26578.1	110.04	109.63	108.28	109.59	91.99	92.09	92.06	92.07	11.00	2417.0
184	480	31893.7	112.23	111.46	110.00	111.60	91.99	92.09	92.06	92.07	11.66	2734.2
185	560	37209.3	114.34	113.87	111.51	113.41	91.99	92.09	92.06	92.07	12.36	3011.5
186	640	42524.9	115.92	114.79	113.24	114.97	91.99	92.09	92.06	92.07	12.54	3392.3
Pressure : 85.05 kN/m ²												
187	240	15946.8	102.71	101.69	101.08	101.71	88.02	88.03	88.04	88.03	9.96	1600.9
188	320	21262.5	105.15	104.22	103.33	104.18	88.02	88.03	88.04	88.03	11.12	1912.9
189	400	26578.1	106.94	105.99	104.85	105.93	88.02	88.03	88.04	88.03	11.56	2299.8
190	480	31893.7	109.19	108.24	107.13	108.27	88.02	88.03	88.04	88.03	12.57	2538.1
191	560	37209.3	111.00	110.07	108.99	110.09	88.02	88.03	88.04	88.03	13.13	2833.7
192	640	42524.9	112.72	111.11	110.50	111.17	88.02	88.03	88.04	88.03	13.20	3222.0
Pressure : 71.28 kN/m ²												
193	240	15946.8	98.56	97.76	96.85	97.65	83.36	83.38	83.39	83.37	10.52	1515.4
194	320	21262.5	101.05	100.29	99.14	100.29	83.36	83.38	83.39	83.37	11.74	1810.5
195	400	26578.1	102.98	101.92	100.95	101.86	83.36	83.38	83.39	83.37	12.21	2176.9
196	480	31893.7	105.27	104.27	103.14	104.37	83.36	83.38	83.39	83.37	13.28	2402.1
197	560	37209.3	107.18	106.12	105.10	106.11	83.36	83.38	83.39	83.37	13.87	2682.1
198	640	42524.9	108.67	107.59	106.23	107.37	83.36	83.38	83.39	83.37	13.94	3049.7

208

Table B.7 Contd.

Run No.	Heat Input, Q W	Heat Flux, q W/m ²	Wall Temperature, T _w , °C				Liquid Pool Temperature, T _{lm} , °C				Wall Super Heat, ΔT _w °C	Heat Transfer Coefficient, h W/m ² °C
			Top	Side	Bottom	Side	Top	Side	Bottom	Side		
Pressure : 57.32 kN/m ²												
199	240	15946.8	94.06	93.06	92.12	92.86	77.95	77.97	78.00	77.98	11.24	1418.3
200	320	21262.5	96.26	95.39	94.93	95.81	77.95	77.97	78.00	77.98	12.55	1694.4
201	400	26578.1	98.46	97.37	96.13	97.49	77.95	77.97	78.00	77.98	13.05	2037.1
202	480	31893.7	100.88	99.67	98.92	99.61	77.95	77.97	78.00	77.98	14.19	2248.0
203	560	37209.3	102.53	101.65	100.86	101.67	77.95	77.97	78.00	77.98	14.83	2509.9
204	640	42524.9	104.46	103.02	101.60	103.01	77.95	77.97	78.00	77.98	14.90	2853.8
Pressure : 45.41 kN/m ²												
205	240	15946.8	89.33	88.37	87.67	88.45	72.39	72.43	72.44	72.43	12.23	1304.2
206	320	21262.5	92.12	91.21	90.02	91.21	72.39	72.43	72.44	72.43	13.65	1558.1
207	400	26578.1	93.89	92.99	91.94	92.99	72.39	72.43	72.44	72.43	14.19	1873.3
208	480	31893.7	96.60	95.24	94.70	95.31	72.39	72.43	72.44	72.43	15.43	2067.1
209	560	37209.3	98.79	97.30	96.33	97.28	72.39	72.43	72.44	72.43	16.12	2307.8
210	640	42524.9	99.83	98.85	97.44	98.97	72.39	72.43	72.44	72.43	16.21	2624.2

Table B.8 Boiling heat transfer data of 10% methanol over a horizontal uncoated tube

Run No.	Heat Input, Q W	Heat Flux, q W/m ²	Wall Temperature, T _w , °C				Liquid Pool Temperature, T _{lm} , °C				Wall Super Heat, ΔT _w °C	Heat Transfer Coefficient, h W/m ² °C
			Top	Side	Bottom	Side	Top	Side	Bottom	Side		
Pressure : 97.71 kN/m ²												
211	240	15946.8	102.92	101.89	101.73	102.00	87.96	87.98	88.00	87.98	10.35	1540.2
212	320	21262.5	105.72	104.73	103.48	104.78	87.96	87.98	88.00	87.98	11.63	1829.0
213	400	26578.1	107.36	106.12	105.39	106.13	87.96	87.98	88.00	87.98	11.93	2227.3
214	480	31893.7	109.99	108.27	107.90	108.84	87.96	87.98	88.00	87.98	13.16	2422.9
215	560	37209.3	111.58	110.10	109.82	110.28	87.96	87.98	88.00	87.98	13.59	2738.0
216	640	42524.9	112.99	111.80	110.99	111.71	87.96	87.98	88.00	87.98	13.75	3093.2
Pressure : 84.49 kN/m ²												
217	240	15946.8	99.28	98.69	97.66	98.65	83.93	83.94	83.95	83.95	10.82	1473.5
218	320	21262.5	101.97	100.95	100.12	101.65	83.93	83.94	83.95	83.95	12.16	1749.0
219	400	26578.1	103.79	102.71	101.84	102.73	83.93	83.94	83.95	83.95	12.48	2129.1
220	480	31893.7	106.21	105.13	104.49	105.46	83.93	83.94	83.95	83.95	13.77	2315.9
221	560	37209.3	108.04	107.03	106.04	107.06	83.93	83.94	83.95	83.95	14.22	2616.4
222	640	42524.9	109.47	108.62	107.01	108.81	83.93	83.94	83.95	83.95	14.39	2955.3
Pressure : 71.11 kN/m ²												
223	240	15946.8	95.68	94.67	93.50	94.67	79.36	79.37	79.41	79.40	11.44	1394.3
224	320	21262.5	98.05	97.13	96.72	97.30	79.36	79.37	79.39	79.40	12.85	1655.0
225	400	26578.1	99.94	98.83	97.94	98.94	79.36	79.37	79.39	79.40	13.19	2015.0
226	480	31893.7	102.62	101.34	100.66	101.55	79.36	79.37	79.39	79.40	14.55	2191.7
227	560	37209.3	104.48	103.22	102.20	103.24	79.36	79.37	79.39	79.40	15.03	2476.1
228	640	42524.9	106.00	104.76	103.32	104.84	79.36	79.37	79.39	79.40	15.20	2796.8

Table B.8 Contd.

Run No.	Heat Input, Q W	Heat Flux, q W/m ²	Wall Temperature, T _{w0} , °C				Liquid Pool Temperature, T _{lm} , °C				Wall Super Heat, ΔT _w °C	Heat Transfer Coefficient, h W/m ² °C
			Top	Side	Bottom	Side	Top	Side	Bottom	Side		
Pressure : 57.73 kN/m ²												
229	240	15946.8	91.13	90.06	89.11	89.77	73.97	73.98	74.03	74.00	12.22	1305.1
230	320	21262.5	93.49	92.87	91.86	92.96	73.97	73.98	74.03	74.00	13.73	1549.0
231	400	26578.1	95.21	94.42	93.34	94.74	73.97	73.98	74.03	74.00	14.09	1885.9
232	480	31893.7	98.16	97.06	96.16	97.24	73.97	73.98	74.03	74.00	15.55	2050.8
233	560	37209.3	99.85	98.98	97.89	98.99	73.97	73.98	74.03	74.00	16.06	2317.1
234	640	42524.9	101.88	100.36	99.10	100.21	73.97	73.98	74.03	74.00	16.25	2617.3
Pressure : 44.40 kN/m ²												
235	240	15946.8	85.46	84.57	83.61	84.57	67.45	67.46	67.47	67.45	13.29	1200.1
236	320	21262.5	88.70	87.35	86.33	87.46	67.45	67.46	67.47	67.45	14.93	1424.3
237	400	26578.1	90.99	88.71	87.92	88.89	67.45	67.46	67.47	67.45	15.33	1733.9
238	480	31893.7	93.44	91.86	90.70	91.91	67.45	67.46	67.47	67.45	16.91	1885.9
239	560	37209.3	94.68	93.84	92.75	93.93	67.45	67.46	67.47	67.45	17.46	2130.8
240	640	42524.9	96.86	95.09	94.03	95.11	67.45	67.46	67.47	67.45	17.67	2406.5

Table B.9 Boiling heat transfer data of 30% methanol over a horizontal uncoated tube

Run No.	Heat Input, Q W	Heat Flux, q W/m ²	Wall Temperature, T _w , °C				Liquid Pool Temperature, T _{lm} , °C				Wall Super Heat, ΔT _w °C	Heat Transfer Coefficient, h W/m ² °C
			Top	Side	Bottom	Side	Top	Side	Bottom	Side		
Pressure : 97.82 kN/m ²												
241	240	15946.8	99.96	99.21	98.34	99.22	78.91	78.99	78.93	78.98	16.42	971.0
242	320	21262.5	103.61	102.50	101.53	102.54	78.91	78.99	78.93	78.98	18.52	1148.3
243	400	26578.1	105.25	104.18	102.92	104.32	78.91	78.99	78.93	78.98	18.87	1408.3
244	480	31893.7	108.52	107.43	106.60	107.47	78.91	78.99	78.93	78.98	20.94	1523.0
245	560	37209.3	110.49	109.36	108.39	109.49	78.91	78.99	78.93	78.98	21.60	1722.6
246	640	42524.9	112.19	111.08	109.67	111.04	78.91	78.99	78.93	78.98	21.89	1942.4
Pressure : 84.37 kN/m ²												
247	240	15946.8	96.56	95.87	95.04	95.95	74.85	74.89	74.90	74.90	17.17	929.0
248	320	21262.5	100.45	99.18	98.29	99.35	74.85	74.89	74.90	74.90	19.36	1098.1
249	400	26578.1	102.17	100.76	100.08	100.84	74.85	74.89	74.90	74.90	19.74	1346.6
250	480	31893.7	105.45	104.33	103.42	104.41	74.85	74.89	74.90	74.90	21.91	1455.7
251	560	37209.3	107.41	106.31	105.23	106.49	74.85	74.89	74.90	74.90	22.60	1646.4
252	640	42524.9	109.02	107.92	106.82	108.01	74.85	74.89	74.90	74.90	22.91	1855.9
Pressure : 71.00 kN/m ²												
253	240	15946.8	92.84	92.25	91.76	92.28	70.29	70.35	70.36	70.36	18.14	879.1
254	320	21262.5	97.17	96.23	93.69	96.35	70.29	70.35	70.36	70.36	20.45	1039.8
255	400	26578.1	98.43	97.12	96.32	98.28	70.29	70.35	70.36	70.36	20.86	1274.3
256	480	31893.7	102.35	101.25	99.45	101.32	70.29	70.35	70.36	70.36	23.14	1378.1
257	560	37209.3	104.09	103.25	101.68	103.36	70.29	70.35	70.36	70.36	23.88	1558.3
258	640	42524.9	105.62	104.70	103.56	104.86	70.29	70.35	70.36	70.36	24.20	1757.0

Table B.9 Contd.

Run No.	Heat Input, Q W	Heat Flux, q W/m ²	Wall Temperature, T _w , °C				Liquid Pool Temperature, T _{lm} , °C				Wall Super Heat, ΔT _w °C	Heat Transfer Coefficient, h W/m ² °C
			Top	Side	Bottom	Side	Top	Side	Bottom	Side		
Pressure : 57.68 kN/m ²												
259	240	15946.8	89.58	88.51	88.20	88.76	65.57	65.58	65.61	65.57	19.38	823.0
260	320	21262.5	93.43	92.72	91.20	92.69	65.57	65.58	65.61	65.57	21.86	972.8
261	400	26578.1	95.31	94.02	93.34	94.17	65.57	65.58	65.61	65.57	22.29	1192.5
262	480	31893.7	98.78	97.49	97.46	97.96	65.57	65.58	65.61	65.57	24.73	1289.6
263	560	37209.3	101.04	99.92	98.95	100.00	65.57	65.58	65.61	65.57	25.52	1458.2
264	640	42524.9	102.80	101.48	100.41	101.69	65.57	65.58	65.61	65.57	25.87	1644.1
Pressure : 44.84 kN/m ²												
265	240	15946.8	84.37	83.97	83.59	84.08	59.11	59.13	59.12	59.13	21.07	756.7
266	320	21262.5	89.09	87.88	86.92	87.94	59.11	59.13	59.12	59.13	23.76	894.9
267	400	26578.1	90.43	89.57	89.12	89.68	59.11	59.13	59.12	59.13	24.24	1096.6
268	480	31893.7	94.41	93.71	92.44	93.95	59.11	59.13	59.12	59.13	26.89	1185.9
269	560	37209.3	96.10	95.92	95.00	95.99	59.11	59.13	59.12	59.13	27.75	1340.8
270	640	42524.9	98.41	97.14	96.80	97.25	59.11	59.13	59.12	59.13	28.13	1511.8

Table B.10 Boiling heat transfer data of 50% methanol over a horizontal uncoated tube

Run No.	Heat Input, Q W	Heat Flux, q W/m ²	Wall Temperature, T _{w0} , °C				Liquid Pool Temperature, T _{lm} , °C				Wall Super Heat, ΔT _w °C	Heat Transfer Coefficient, h W/m ² °C
			Top	Side	Bottom	Side	Top	Side	Bottom	Side		
Pressure : 97.74 kN/m ²												
271	240	15946.8	93.05	92.43	91.72	92.33	73.11	73.13	73.14	73.13	15.45	1032.3
272	320	21262.5	96.90	95.43	94.46	95.87	73.11	73.13	73.14	73.13	17.47	1217.3
273	400	26578.1	98.12	97.10	96.11	97.23	73.11	73.13	73.14	73.13	17.67	1504.1
274	480	31893.7	101.82	100.19	99.45	100.24	73.11	73.13	73.14	73.13	19.69	1619.9
275	560	37209.3	103.34	102.37	101.17	102.42	73.11	73.13	73.14	73.13	20.32	1831.0
276	640	42524.9	104.75	103.76	102.76	103.84	73.11	73.13	73.14	73.13	20.50	2073.9
Pressure : 84.56 kN/m ²												
277	240	15946.8	89.92	89.07	88.69	89.06	69.21	69.23	69.24	69.24	16.15	987.2
278	320	21262.5	93.59	92.66	91.39	92.62	69.21	69.23	69.24	69.24	18.26	1164.2
279	400	26578.1	95.88	93.98	92.57	93.78	69.21	69.23	69.24	69.24	18.49	1437.8
280	480	31893.7	98.61	97.21	96.60	97.32	69.21	69.23	69.24	69.24	20.60	1548.2
281	560	37209.3	100.23	99.43	98.65	99.17	69.21	69.23	69.24	69.24	21.27	1749.7
282	640	42524.9	102.00	100.75	99.72	100.87	69.21	69.23	69.24	69.24	21.46	1981.3
Pressure : 71.00 kN/m ²												
283	240	15946.8	86.78	85.36	85.10	85.52	64.82	64.84	64.84	64.83	17.05	935.0
284	320	21262.5	90.22	89.12	88.19	89.27	64.82	64.84	64.84	64.83	19.29	1102.0
285	400	26578.1	91.14	90.29	89.39	91.98	64.82	64.84	64.84	64.83	19.53	1360.9
286	480	31893.7	95.21	94.14	93.21	94.26	64.82	64.84	64.84	64.83	21.77	1465.2
287	560	37209.3	97.32	96.03	95.18	96.17	64.82	64.84	64.84	64.83	22.47	1656.1
288	640	42524.9	99.18	97.16	96.72	97.55	64.82	64.84	64.84	64.83	22.67	1875.5

Table B.10 Contd.

Run No.	Heat Input, Q W	Heat Flux, q W/m ²	Wall Temperature, T _w , °C				Liquid Pool Temperature, T _{lm} , °C				Wall Super Heat, ΔT _w °C	Heat Transfer Coefficient, h W/m ² °C
			Top	Side	Bottom	Side	Top	Side	Bottom	Side		
Pressure : 58.05 kN/m ²												
289	240	15946.8	82.47	81.66	80.88	81.77	59.64	59.65	59.68	59.68	18.23	874.9
290	320	21262.5	86.34	85.15	84.71	85.22	59.64	59.65	59.68	59.68	20.62	1031.2
291	400	26578.1	87.90	86.90	85.77	86.94	59.64	59.65	59.68	59.68	20.87	1273.5
292	480	31893.7	91.54	90.50	89.42	90.65	59.64	59.65	59.68	59.68	23.26	1371.4
293	560	37209.3	93.67	92.39	91.66	92.48	59.64	59.65	59.68	59.68	24.01	1549.8
294	640	42524.9	95.06	93.99	93.02	94.08	59.64	59.65	59.68	59.68	24.23	1755.1
Pressure : 44.61 kN/m ²												
295	240	15946.8	78.65	77.81	77.50	77.98	54.34	54.36	54.38	54.37	19.82	804.7
296	320	21262.5	82.76	81.70	80.99	81.98	54.34	54.36	54.38	54.37	22.42	948.3
297	400	26578.1	84.64	83.26	82.35	83.33	54.34	54.36	54.38	54.37	22.69	1171.2
298	480	31893.7	88.30	87.14	86.36	87.25	54.34	54.36	54.38	54.37	25.29	1261.0
299	560	37209.3	90.28	89.33	88.37	89.42	54.34	54.36	54.38	54.37	26.11	1425.0
300	640	42524.9	91.82	90.44	90.27	90.91	54.34	54.36	54.38	54.37	26.35	1613.6

Table B.11 Boiling heat transfer data of 80% methanol over a horizontal uncoated tube

Run No.	Heat Input, Q W	Heat Flux, q W/m ²	Wall Temperature, T _w , °C				Liquid Pool Temperature, T _{lm} , °C				Wall Super Heat, ΔT _w °C	Heat Transfer Coefficient, h W/m ² °C
			Top	Side	Bottom	Side	Top	Side	Bottom	Side		
Pressure : 97.66 kN/m ²												
301	240	15946.8	83.22	82.55	81.70	82.50	67.00	67.05	67.07	67.08	11.64	1370.5
302	320	21262.5	86.24	85.13	84.15	85.31	67.00	67.05	67.07	67.08	13.09	1624.7
303	400	26578.1	87.56	86.58	85.83	86.71	67.00	67.05	67.07	67.08	13.28	2001.5
304	480	31893.7	90.30	89.49	88.64	89.50	67.00	67.05	67.07	67.08	14.82	2151.5
305	560	37209.3	92.31	91.22	90.00	91.29	67.00	67.05	67.07	67.08	15.28	2435.6
306	640	42524.9	93.76	92.69	91.53	92.68	67.00	67.05	67.07	67.08	15.47	2748.5
Pressure : 84.07 kN/m ²												
307	240	15946.8	79.85	79.32	78.49	79.41	63.30	63.31	63.33	63.33	12.15	1312.7
308	320	21262.5	83.19	81.97	81.12	82.05	63.30	63.31	63.33	63.33	13.69	1552.9
309	400	26578.1	84.62	83.51	82.48	83.64	63.30	63.31	63.33	63.33	13.90	1911.7
310	480	31893.7	87.57	86.40	85.32	86.56	63.30	63.31	63.33	63.33	15.54	2052.5
311	560	37209.3	89.06	88.27	87.12	88.42	63.30	63.31	63.33	63.33	16.02	2322.1
312	640	42524.9	90.74	89.67	88.64	89.71	63.30	63.31	63.33	63.33	16.23	2620.2
Pressure : 70.95 kN/m ²												
313	240	15946.8	76.47	75.68	74.96	75.64	59.01	59.04	59.06	59.05	12.84	1241.6
314	320	21262.5	79.44	78.53	77.93	78.56	59.01	59.04	59.06	59.05	14.50	1466.4
315	400	26578.1	81.16	80.03	79.10	80.13	59.01	59.04	59.06	59.05	14.72	1805.3
316	480	31893.7	84.21	83.02	82.11	83.17	59.01	59.04	59.06	59.05	16.48	1935.5
317	560	37209.3	85.91	84.79	84.12	84.85	59.01	59.04	59.06	59.05	17.00	2189.0
318	640	42524.9	87.40	86.40	85.41	86.37	59.01	59.04	59.06	59.05	17.21	2470.4

Table B.11 Contd.

Run No.	Heat Input, Q W	Heat Flux, q W/m ²	Wall Temperature, T _{w0} , °C				Liquid Pool Temperature, T _{lm} , °C				Wall Super Heat, ΔT _w °C	Heat Transfer Coefficient, h W/m ² °C
			Top	Side	Bottom	Side	Top	Side	Bottom	Side		
Pressure : 57.71 kN/m ²												
319	240	15946.8	72.98	71.91	71.51	72.05	54.52	54.54	54.56	54.57	13.76	1158.8
320	320	21262.5	75.87	75.26	74.15	75.22	54.52	54.54	54.56	54.57	15.50	1371.4
321	400	26578.1	77.42	76.63	75.57	76.80	54.52	54.54	54.56	54.57	15.72	1690.9
322	480	31893.7	80.75	79.69	78.72	79.67	54.52	54.54	54.56	54.57	17.55	1817.2
323	560	37209.3	82.34	81.32	81.01	81.48	54.52	54.54	54.56	54.57	18.12	2054.0
324	640	42524.9	84.13	83.00	81.79	83.05	54.52	54.54	54.56	54.57	18.30	2323.8
Pressure : 44.32 kN/m ²												
325	240	15946.8	68.39	67.68	66.98	67.78	48.94	48.97	48.98	48.96	14.94	1067.4
326	320	21262.5	71.68	70.78	70.06	70.94	48.94	48.97	48.98	48.96	16.83	1263.5
327	400	26578.1	73.36	72.37	71.44	72.43	48.94	48.97	48.98	48.96	17.10	1554.5
328	480	31893.7	76.59	75.71	74.63	75.76	48.94	48.97	48.98	48.96	19.10	1669.6
329	560	37209.3	78.56	77.43	76.61	77.48	48.94	48.97	48.98	48.96	19.68	1890.7
330	640	42524.9	79.86	79.06	78.04	79.20	48.94	48.97	48.98	48.96	19.93	2133.5

Table B.12 Boiling heat transfer data of 90% methanol over a horizontal uncoated tube

Run No.	Heat Input, Q W	Heat Flux, q W/m ²	Wall Temperature, T _w , °C				Liquid Pool Temperature, T _{lm} , °C				Wall Super Heat, ΔT _w °C	Heat Transfer Coefficient, h W/m ² °C
			Top	Side	Bottom	Side	Top	Side	Bottom	Side		
Pressure : 97.68 kN/m ²												
331	240	15946.8	81.00	79.96	79.30	79.96	65.12	65.14	65.14	65.13	11.12	1434.3
332	320	21262.5	83.70	82.63	81.70	82.73	65.12	65.14	65.14	65.13	12.48	1703.1
333	400	26578.1	84.76	83.89	83.48	84.57	65.12	65.14	65.14	65.13	12.70	2092.9
334	480	31893.7	87.77	86.89	85.91	86.93	65.12	65.14	65.14	65.13	14.13	2256.4
335	560	37209.3	89.62	88.56	87.60	88.61	65.12	65.14	65.14	65.13	14.59	2551.0
336	640	42524.9	91.43	89.85	88.93	89.93	65.12	65.14	65.14	65.13	14.76	2881.0
Pressure : 84.55 kN/m ²												
337	240	15946.8	77.94	76.82	76.57	76.98	61.65	61.63	61.67	61.66	11.62	1372.4
338	320	21262.5	80.56	80.10	78.66	79.81	61.65	61.63	61.67	61.66	13.06	1628.4
339	400	26578.1	82.02	81.35	80.33	81.41	61.65	61.63	61.67	61.66	13.29	2000.5
340	480	31893.7	85.01	84.32	82.77	84.10	61.65	61.63	61.67	61.66	14.79	2156.7
341	560	37209.3	86.69	85.66	85.08	85.76	61.65	61.63	61.67	61.66	15.27	2437.6
342	640	42524.9	88.46	87.02	86.37	87.15	61.65	61.63	61.67	61.66	15.45	2752.3
Pressure : 70.77 kN/m ²												
343	240	15946.8	74.30	73.56	72.84	73.59	57.46	57.52	57.50	57.49	12.28	1299.1
344	320	21262.5	77.46	76.23	75.38	76.35	57.46	57.52	57.50	57.49	13.79	1541.9
345	400	26578.1	79.12	77.81	76.70	77.83	57.46	57.52	57.50	57.49	14.03	1893.8
346	480	31893.7	81.63	80.74	79.78	80.75	57.46	57.52	57.50	57.49	15.62	2041.3
347	560	37209.3	83.45	82.49	81.52	82.51	57.46	57.52	57.50	57.49	16.13	2307.6
348	640	42524.9	85.26	83.83	82.79	83.94	57.46	57.52	57.50	57.49	16.32	2605.7

Table B.12 Contd.

Run No.	Heat Input, Q W	Heat Flux, q W/m ²	Wall Temperature, T _{w0} , °C				Liquid Pool Temperature, T _{lm} , °C				Wall Super Heat, ΔT _w °C	Heat Transfer Coefficient, h W/m ² °C
			Top	Side	Bottom	Side	Top	Side	Bottom	Side		
Pressure : 57.02 kN/m ²												
349	240	15946.8	70.35	69.28	68.91	69.51	52.54	52.55	52.69	52.58	13.12	1215.6
350	320	21262.5	73.51	72.37	71.32	72.40	52.54	52.55	52.69	52.58	14.74	1442.7
351	400	26578.1	74.77	74.19	73.08	73.66	52.54	52.55	52.69	52.58	15.00	1772.2
352	480	31893.7	78.06	76.75	75.93	76.84	52.54	52.55	52.69	52.58	16.70	1910.2
353	560	37209.3	79.69	78.61	77.72	78.78	52.54	52.55	52.69	52.58	17.23	2159.1
354	640	42524.9	81.50	79.89	79.27	80.04	52.54	52.55	52.69	52.58	17.44	2438.0
Pressure : 43.60 kN/m ²												
355	240	15946.8	65.81	65.02	64.29	65.11	46.96	46.99	46.99	46.97	14.28	1117.1
356	320	21262.5	69.12	67.92	67.13	68.18	46.96	46.99	46.99	46.97	16.04	1325.7
357	400	26578.1	70.16	69.68	68.86	69.84	46.96	46.99	46.99	46.97	16.32	1628.6
358	480	31893.7	73.86	72.78	71.48	72.89	46.96	46.99	46.99	46.97	18.17	1755.6
359	560	37209.3	75.55	74.55	73.65	74.68	46.96	46.99	46.99	46.97	18.75	1984.5
360	640	42524.9	77.10	76.06	75.12	76.14	46.96	46.99	46.99	46.97	18.98	2240.5

Table B.13 Boiling heat transfer data of 95% methanol over a horizontal uncoated tube

Run No.	Heat Input, Q W	Heat Flux, q W/m ²	Wall Temperature, T _w , °C				Liquid Pool Temperature, T _{lm} , °C				Wall Super Heat, ΔT _w °C	Heat Transfer Coefficient, h W/m ² °C
			Top	Side	Bottom	Side	Top	Side	Bottom	Side		
Pressure : 97.70 kN/m ²												
361	240	15946.8	79.73	78.59	78.17	78.79	64.04	64.04	64.10	64.08	10.95	1456.2
362	320	21262.5	82.56	81.27	80.23	81.37	64.04	64.04	64.10	64.08	12.22	1739.7
363	400	26578.1	84.18	82.78	81.62	82.91	64.04	64.04	64.10	64.08	12.47	2132.1
364	480	31893.7	86.52	85.51	84.44	85.72	64.04	64.04	64.10	64.08	13.87	2298.8
365	560	37209.3	88.21	87.31	86.21	87.31	64.04	64.04	64.10	64.08	14.32	2599.1
366	640	42524.9	90.34	88.32	87.65	88.56	64.04	64.04	64.10	64.08	14.51	2931.5
Pressure : 84.07 kN/m ²												
367	240	15946.8	76.75	75.75	75.16	75.87	60.62	60.63	60.64	60.64	11.45	1393.0
368	320	21262.5	79.36	78.62	77.45	78.51	60.62	60.63	60.64	60.64	12.78	1663.8
369	400	26578.1	80.82	80.16	78.79	80.29	60.62	60.63	60.64	60.64	13.04	2038.2
370	480	31893.7	83.80	82.82	81.58	82.83	60.62	60.63	60.64	60.64	14.52	2197.2
371	560	37209.3	85.62	84.45	83.40	84.48	60.62	60.63	60.64	60.64	14.98	2484.0
372	640	42524.9	87.07	85.84	85.03	85.91	60.62	60.63	60.64	60.64	15.18	2801.1
Pressure : 70.99 kN/m ²												
373	240	15946.8	73.50	72.76	71.97	72.81	56.85	56.80	56.89	56.89	12.10	1318.0
374	320	21262.5	76.27	75.23	74.68	75.58	56.85	56.80	56.89	56.89	13.51	1573.6
375	400	26578.1	78.66	77.02	75.21	77.02	56.85	56.80	56.89	56.89	13.78	1928.4
376	480	31893.7	81.05	80.02	78.05	80.11	56.85	56.80	56.89	56.89	15.34	2078.6
377	560	37209.3	82.54	81.41	80.88	81.42	56.85	56.80	56.89	56.89	15.83	2350.1
378	640	42524.9	84.03	83.02	82.06	83.07	56.85	56.80	56.89	56.89	16.05	2650.3

Table B.13 Contd.

Run No.	Heat Input, Q W	Heat Flux, q W/m ²	Wall Temperature, T _{w0} , °C				Liquid Pool Temperature, T _{lm} , °C				Wall Super Heat, ΔT _w °C	Heat Transfer Coefficient, h W/m ² °C
			Top	Side	Bottom	Side	Top	Side	Bottom	Side		
Pressure : 57.61 kN/m ²												
379	240	15946.8	69.42	68.58	67.99	68.67	51.94	51.95	51.96	51.95	12.91	1235.0
380	320	21262.5	72.60	71.55	70.08	71.58	51.94	51.95	51.96	51.95	14.43	1473.6
381	400	26578.1	73.98	72.75	72.34	72.98	51.94	51.95	51.96	51.95	14.73	1805.0
382	480	31893.7	76.95	75.86	74.99	75.97	51.94	51.95	51.96	51.95	16.39	1946.2
383	560	37209.3	78.76	77.67	76.82	77.71	51.94	51.95	51.96	51.95	16.91	2199.9
384	640	42524.9	80.52	79.15	78.03	79.25	51.94	51.95	51.96	51.95	17.14	2480.7
Pressure : 44.34 kN/m ²												
385	240	15946.8	64.67	63.90	62.99	63.87	45.98	46.03	46.01	45.99	14.05	1135.0
386	320	21262.5	67.65	66.79	65.75	66.88	45.98	46.03	46.01	45.99	15.69	1355.1
387	400	26578.1	69.55	68.29	67.25	68.34	45.98	46.03	46.01	45.99	16.01	1659.7
388	480	31893.7	72.67	71.30	70.26	71.50	45.98	46.03	46.01	45.99	17.82	1789.3
389	560	37209.3	74.26	73.38	72.00	73.46	45.98	46.03	46.01	45.99	18.40	2022.8
390	640	42524.9	75.94	74.82	73.65	74.76	45.98	46.03	46.01	45.99	18.64	2280.9

Table B.14 Boiling heat transfer data of 5% methanol over a 43 μm thick horizontal coated tube

Run No.	Heat Input, Q W	Heat Flux, q W/m ²	Wall Temperature, T_{w0} , °C				Liquid Pool Temperature, T_{lm} , °C				Wall Super Heat, ΔT_w °C	Heat Transfer Coefficient, h W/m ² °C
			Top	Side	Bottom	Side	Top	Side	Bottom	Side		
Pressure : 97.71 kN/m ²												
391	240	15946.8	102.68	101.89	101.72	101.98	92.47	92.57	92.59	92.57	5.71	2791.7
392	320	21262.5	105.01	103.83	102.75	103.72	92.47	92.57	92.59	92.57	6.21	3426.0
393	400	26578.1	106.88	105.50	104.95	105.65	92.47	92.57	92.59	92.57	6.85	3880.8
394	480	31893.7	108.61	107.54	106.63	107.61	92.47	92.57	92.59	92.57	7.44	4289.0
395	560	37209.3	110.41	109.24	108.50	109.39	92.47	92.57	92.59	92.57	7.96	4676.4
396	640	42524.9	112.20	110.73	110.29	110.68	92.47	92.57	92.59	92.57	8.28	5136.3
Pressure : 84.43 kN/m ²												
397	240	15946.8	98.94	98.17	97.34	98.24	87.56	88.58	88.59	88.56	6.04	2639.3
398	320	21262.5	100.94	100.01	98.76	100.15	87.56	88.58	88.59	88.56	6.57	3237.5
399	400	26578.1	103.35	101.65	100.94	101.71	87.56	88.58	88.59	88.56	7.25	3666.9
400	480	31893.7	104.89	103.69	102.78	103.87	87.56	88.58	88.59	88.56	7.87	4051.9
401	560	37209.3	107.11	105.41	104.42	105.56	87.56	88.58	88.59	88.56	8.42	4417.6
402	640	42524.9	108.73	107.25	105.60	107.35	87.56	88.58	88.59	88.56	8.77	4851.6
Pressure : 71.09 kN/m ²												
403	240	15946.8	94.73	94.23	93.59	94.38	83.93	83.95	83.98	83.97	6.47	2465.1
404	320	21262.5	97.31	95.77	95.34	95.83	83.93	83.95	83.98	83.97	7.03	3024.4
405	400	26578.1	99.04	98.02	97.03	98.15	83.93	83.95	83.98	83.97	7.76	3425.3
406	480	31893.7	100.73	99.87	99.46	99.93	83.93	83.95	83.98	83.97	8.43	3785.5
407	560	37209.3	103.00	101.74	100.80	101.87	83.93	83.95	83.98	83.97	9.02	4127.1
408	640	42524.9	104.49	103.37	102.48	103.61	83.93	83.95	83.98	83.97	9.38	4532.4

Table B.14 Contd.

Run No.	Heat Input, Q W	Heat Flux, q W/m ²	Wall Temperature, T _{w0} , °C				Liquid Pool Temperature, T _{lm} , °C				Wall Super Heat, ΔT _w °C	Heat Transfer Coefficient, h W/m ² °C
			Top	Side	Bottom	Side	Top	Side	Bottom	Side		
Pressure : 57.96 kN/m ²												
409	240	15946.8	89.98	89.39	88.60	89.45	78.53	78.53	78.54	78.53	7.02	2271.6
410	320	21262.5	92.29	91.13	90.18	91.35	78.53	78.53	78.54	78.53	7.63	2786.3
411	400	26578.1	94.21	93.28	92.35	93.34	78.53	78.53	78.54	78.53	8.42	3155.9
412	480	31893.7	96.37	95.14	94.24	95.39	78.53	78.53	78.54	78.53	9.15	3487.3
413	560	37209.3	98.34	97.15	95.98	97.30	78.53	78.53	78.54	78.53	9.79	3802.0
414	640	42524.9	99.80	98.92	97.69	99.03	78.53	78.53	78.54	78.53	10.18	4175.6
Pressure : 44.71 kN/m ²												
415	240	15946.8	83.96	83.64	82.91	83.65	71.93	71.95	71.98	71.94	7.79	2047.7
416	320	21262.5	86.97	85.12	84.51	85.32	71.93	71.93	71.98	71.94	8.46	2512.2
417	400	26578.1	88.56	87.55	86.69	87.69	71.93	71.93	71.98	71.94	9.34	2845.0
418	480	31893.7	90.64	89.69	88.68	89.78	71.93	71.93	71.98	71.94	10.14	3144.0
419	560	37209.3	92.67	91.64	90.64	91.75	71.93	71.93	71.98	71.94	10.86	3427.5
420	640	42524.9	94.47	93.27	92.39	93.40	71.93	71.93	71.98	71.94	11.30	3764.3

Table B.15 Boiling heat transfer data of 10% methanol over a 43 μm thick horizontal coated tube

Run No.	Heat Input, Q W	Heat Flux, q W/m ²	Wall Temperature, T_{wo} , °C				Liquid Pool Temperature, T_{lm} , °C				Wall Super Heat, ΔT_w °C	Heat Transfer Coefficient, h W/m ² °C
			Top	Side	Bottom	Side	Top	Side	Bottom	Side		
Pressure : 97.77 kN/m ²												
421	240	15946.8	98.20	97.64	97.09	97.66	87.71	87.84	87.95	87.86	6.00	2657.4
422	320	21262.5	100.39	99.45	98.36	99.58	87.71	87.84	87.95	87.86	6.53	3255.8
423	400	26578.1	102.27	101.22	100.55	101.40	87.71	87.84	87.95	87.86	7.18	3703.3
424	480	31893.7	104.45	103.19	102.35	103.24	87.71	87.84	87.95	87.86	7.86	4057.4
425	560	37209.3	106.11	105.02	104.08	105.10	87.71	87.84	87.95	87.86	8.36	4450.2
426	640	42524.9	107.62	106.79	105.66	106.88	87.71	87.84	87.95	87.86	8.75	4858.0
Pressure : 84.43 kN/m ²												
427	240	15946.8	94.90	93.91	93.39	94.04	83.86	83.96	83.94	83.87	6.35	2511.8
428	320	21262.5	96.83	95.85	94.93	95.95	83.86	83.96	83.94	83.87	6.91	3076.8
429	400	26578.1	99.11	97.75	96.52	98.00	83.86	83.96	83.94	83.87	7.60	3499.1
430	480	31893.7	100.94	99.73	98.71	99.96	83.86	83.96	83.94	83.87	8.32	3833.3
431	560	37209.3	102.70	101.49	100.43	101.91	83.86	83.96	83.94	83.87	8.85	4203.9
432	640	42524.9	104.71	103.08	102.35	103.14	83.86	83.96	83.94	83.87	9.27	4589.0
Pressure : 71.47 kN/m ²												
433	240	15946.8	90.52	90.04	89.36	90.07	79.38	79.39	79.43	79.39	6.80	2346.3
434	320	21262.5	92.77	91.81	90.91	91.98	79.38	79.39	79.43	79.39	7.40	2874.2
435	400	26578.1	95.70	93.71	92.25	93.80	79.38	79.39	79.43	79.39	8.13	3268.8
436	480	31893.7	97.06	96.13	94.22	96.24	79.38	79.39	79.43	79.39	8.91	3580.9
437	560	37209.3	98.59	97.69	96.97	97.75	79.38	79.39	79.43	79.39	9.47	3927.2
438	640	42524.9	100.39	99.46	98.43	99.56	79.38	79.39	79.43	79.39	9.92	4287.1

Table B.15 Contd.

Run No.	Heat Input, Q W	Heat Flux, q W/m ²	Wall Temperature, T _w , °C				Liquid Pool Temperature, T _{lm} , °C				Wall Super Heat, ΔT _w °C	Heat Transfer Coefficient, h W/m ² °C
			Top	Side	Bottom	Side	Top	Side	Bottom	Side		
Pressure : 57.81 kN/m ²												
439	240	15946.8	85.74	85.04	84.66	85.17	73.93	73.94	74.02	73.98	7.38	2161.4
440	320	21262.5	88.06	87.11	86.01	87.12	73.93	73.94	74.02	73.98	8.03	2647.7
441	400	26578.1	90.13	89.10	88.12	89.20	73.93	73.94	74.02	73.98	8.83	3011.3
442	480	31893.7	92.23	91.18	90.34	91.24	73.93	73.94	74.02	73.98	9.67	3298.7
443	560	37209.3	94.16	93.05	92.14	93.18	73.93	73.94	74.02	73.98	10.28	3617.9
444	640	42524.9	95.85	94.80	93.94	94.94	73.93	73.94	74.02	73.98	10.77	3948.9
Pressure : 44.32 kN/m ²												
445	240	15946.8	80.02	79.59	78.74	79.66	67.49	67.51	67.57	67.48	8.18	1948.6
446	320	21262.5	82.91	81.33	80.26	81.48	67.49	67.51	67.57	67.48	8.91	2387.0
447	400	26578.1	84.83	83.47	82.67	83.60	67.49	67.51	67.57	67.48	9.79	2715.2
448	480	31893.7	86.98	85.77	84.77	85.86	67.49	67.51	67.57	67.48	10.72	2974.3
449	560	37209.3	88.73	87.84	86.73	87.90	67.49	67.51	67.57	67.48	11.41	3262.1
450	640	42524.9	90.81	89.66	88.13	89.82	67.49	67.51	67.57	67.48	11.94	3560.7

Table B.16 Boiling heat transfer data of 30% methanol over a 43 μm thick horizontal coated tube

Run No.	Heat Input, Q W	Heat Flux, q W/m ²	Wall Temperature, T_{wo} , °C				Liquid Pool Temperature, T_{lm} , °C				Wall Super Heat, ΔT_w °C	Heat Transfer Coefficient, h W/m ² °C
			Top	Side	Bottom	Side	Top	Side	Bottom	Side		
Pressure : 97.76 kN/m ²												
451	240	15946.8	90.23	89.27	88.67	89.33	78.75	78.83	78.79	78.82	6.77	2355.0
452	320	21262.5	91.78	91.33	90.33	91.42	78.75	78.83	78.79	78.82	7.34	2896.5
453	400	26578.1	94.01	93.37	91.95	93.46	78.75	78.83	78.79	78.82	8.06	3297.9
454	480	31893.7	95.91	95.40	94.16	95.46	78.75	78.83	78.79	78.82	8.83	3613.5
455	560	37209.3	98.25	97.02	95.91	97.10	78.75	78.83	78.79	78.82	9.40	3960.3
456	640	42524.9	99.94	98.70	97.81	98.79	78.75	78.83	78.79	78.82	9.87	4310.4
Pressure : 84.83 kN/m ²												
457	240	15946.8	86.45	85.76	85.24	85.84	74.82	74.84	74.88	74.86	7.16	2225.8
458	320	21262.5	88.64	87.71	86.61	87.80	74.82	74.84	74.88	74.86	7.77	2737.4
459	400	26578.1	90.89	89.64	88.56	89.78	74.82	74.84	74.88	74.86	8.53	3116.4
460	480	31893.7	92.93	91.72	90.67	91.88	74.82	74.84	74.88	74.86	9.34	3414.0
461	560	37209.3	94.60	93.65	92.69	93.75	74.82	74.84	74.88	74.86	9.95	3741.3
462	640	42524.9	96.50	95.38	94.42	95.48	74.82	74.84	74.88	74.86	10.45	4071.0
Pressure : 71.32 kN/m ²												
463	240	15946.8	82.46	82.35	81.38	82.06	70.36	71.34	70.32	70.36	7.67	2080.4
464	320	21262.5	85.09	83.93	82.87	84.03	70.36	71.34	70.32	70.36	8.31	2558.1
465	400	26578.1	87.10	86.00	84.98	86.18	70.36	71.34	70.32	70.36	9.13	2911.5
466	480	31893.7	89.17	88.14	87.23	88.26	70.36	71.34	70.32	70.36	10.00	3189.5
467	560	37209.3	91.17	90.01	89.08	90.20	70.36	71.34	70.32	70.36	10.64	3495.7
468	640	42524.9	92.78	91.94	90.88	92.08	70.36	71.34	70.32	70.36	11.18	3804.4

Table B.16 Contd.

Run No.	Heat Input, Q W	Heat Flux, q W/m ²	Wall Temperature, T _w , °C				Liquid Pool Temperature, T _{lm} , °C				Wall Super Heat, ΔT _w °C	Heat Transfer Coefficient, h W/m ² °C
			Top	Side	Bottom	Side	Top	Side	Bottom	Side		
Pressure : 58.08 kN/m ²												
469	240	15946.8	77.81	77.18	76.61	77.17	65.06	65.04	65.07	65.10	8.32	1916.7
470	320	21262.5	80.27	79.02	78.09	79.28	65.06	65.04	65.07	65.10	9.02	2356.3
471	400	26578.1	82.23	81.38	80.22	81.44	65.06	65.04	65.07	65.10	9.91	2682.5
472	480	31893.7	84.51	83.52	82.54	83.55	65.06	65.04	65.07	65.10	10.85	2938.9
473	560	37209.3	86.60	85.41	84.50	85.49	65.06	65.04	65.07	65.10	11.55	3220.7
474	640	42524.9	88.34	87.32	86.32	87.42	65.06	65.04	65.07	65.10	12.14	3504.3
Pressure : 45.02 kN/m ²												
475	240	15946.8	72.71	72.12	71.52	72.26	59.11	59.12	59.13	59.12	9.23	1728.2
476	320	21262.5	75.32	74.21	73.13	74.14	59.11	59.12	59.13	59.12	10.01	2124.3
477	400	26578.1	77.39	76.45	75.38	76.57	59.11	59.12	59.13	59.12	10.99	2418.4
478	480	31893.7	79.70	78.75	77.65	78.97	59.11	59.12	59.13	59.12	12.04	2649.1
479	560	37209.3	81.96	80.68	79.79	80.82	59.11	59.12	59.13	59.12	12.82	2903.3
480	640	42524.9	83.64	82.77	81.65	82.83	59.11	59.12	59.13	59.12	13.46	3159.8

Table B.17 Boiling heat transfer data of 50% methanol over a 43 μm thick horizontal coated tube

Run No.	Heat Input, Q W	Heat Flux, q W/m ²	Wall Temperature, T_{wo} , °C				Liquid Pool Temperature, T_{lm} , °C				Wall Super Heat, ΔT_w °C	Heat Transfer Coefficient, h W/m ² °C
			Top	Side	Bottom	Side	Top	Side	Bottom	Side		
Pressure : 97.59 kN/m ²												
481	240	15946.8	84.61	84.03	83.40	84.02	73.61	73.63	73.64	73.63	6.58	2423.5
482	320	21262.5	86.90	85.73	84.93	85.87	73.61	73.63	73.64	73.63	7.16	2970.9
483	400	26578.1	88.62	87.84	86.73	88.03	73.61	73.63	73.64	73.63	7.83	3393.0
484	480	31893.7	90.92	89.67	88.97	89.74	73.61	73.63	73.64	73.63	8.59	3714.7
485	560	37209.3	92.69	91.57	90.67	91.62	73.61	73.63	73.64	73.63	9.13	4074.6
486	640	42524.9	94.28	93.37	92.29	93.44	73.61	73.63	73.64	73.63	9.57	4443.5
Pressure : 84.74 kN/m ²												
487	240	15946.8	81.28	80.39	79.96	80.43	69.73	69.74	69.77	69.75	6.96	2291.1
488	320	21262.5	83.37	82.26	81.49	82.46	69.73	69.74	69.77	69.75	7.57	2807.8
489	400	26578.1	85.38	84.29	83.37	84.48	69.73	69.74	69.77	69.75	8.29	3206.3
490	480	31893.7	87.50	86.38	85.43	86.47	69.73	69.74	69.77	69.75	9.09	3509.6
491	560	37209.3	89.33	88.23	87.24	88.37	69.73	69.74	69.77	69.75	9.67	3849.4
492	640	42524.9	91.26	89.75	89.22	89.87	69.73	69.74	69.77	69.75	10.13	4197.8
Pressure : 70.87 kN/m ²												
493	240	15946.8	77.15	76.58	75.96	76.65	65.32	65.33	65.33	65.34	7.45	2140.5
494	320	21262.5	79.52	78.52	77.47	78.54	65.32	65.33	65.33	65.34	8.11	2622.9
495	400	26578.1	81.51	80.53	79.54	80.60	65.32	65.33	65.33	65.34	8.87	2995.6
496	480	31893.7	83.71	82.64	81.65	82.66	65.32	65.33	65.33	65.34	9.73	3279.1
497	560	37209.3	85.52	84.53	83.58	84.58	65.32	65.33	65.33	65.34	10.35	3596.4
498	640	42524.9	87.26	86.36	85.22	86.45	65.32	65.33	65.33	65.34	10.84	3921.3

Table B.17 Contd.

Run No.	Heat Input, Q W	Heat Flux, q W/m ²	Wall Temperature, T _{w0} , °C				Liquid Pool Temperature, T _{lm} , °C				Wall Super Heat, ΔT _w °C	Heat Transfer Coefficient, h W/m ² °C
			Top	Side	Bottom	Side	Top	Side	Bottom	Side		
Pressure : 57.56 kN/m ²												
499	240	15946.8	72.61	72.07	71.51	72.13	60.18	60.20	60.20	60.19	8.08	1972.8
500	320	21262.5	74.90	74.21	72.82	74.32	60.18	60.20	60.20	60.19	8.80	2416.9
501	400	26578.1	77.41	76.19	74.85	76.22	60.18	60.20	60.20	60.19	9.63	2759.4
502	480	31893.7	79.37	78.34	77.28	78.45	60.18	60.20	60.20	60.19	10.56	3021.2
503	560	37209.3	81.14	80.32	79.31	80.43	60.18	60.20	60.20	60.19	11.23	3313.6
504	640	42524.9	83.04	82.18	80.97	82.27	60.18	60.20	60.20	60.19	11.77	3611.7
Pressure : 44.57 kN/m ²												
505	240	15946.8	67.69	67.00	66.51	67.21	54.33	54.32	54.37	54.32	8.97	1778.7
506	320	21262.5	70.24	69.15	68.01	69.25	54.33	54.32	54.37	54.32	9.76	2179.2
507	400	26578.1	72.35	71.34	70.31	71.43	54.33	54.32	54.37	54.32	10.68	2487.8
508	480	31893.7	74.49	73.38	72.24	74.49	54.33	54.32	54.37	54.32	11.71	2723.5
509	560	37209.3	76.59	75.78	74.47	75.82	54.33	54.32	54.37	54.32	12.46	2986.8
510	640	42524.9	78.65	77.34	76.72	77.42	54.33	54.32	54.37	54.32	13.05	3257.9

Table B.18 Boiling heat transfer data of 80% methanol over a 43 μm thick horizontal coated tube

Run No.	Heat Input, Q W	Heat Flux, q W/m ²	Wall Temperature, T_{wo} , °C				Liquid Pool Temperature, T_{lm} , °C				Wall Super Heat, ΔT_w °C	Heat Transfer Coefficient, h W/m ² °C
			Top	Side	Bottom	Side	Top	Side	Bottom	Side		
Pressure : 98.02 kN/m ²												
511	240	15946.8	78.43	77.81	77.09	77.90	67.54	67.57	67.57	67.57	6.44	2476.0
512	320	21262.5	80.66	79.61	78.62	79.68	67.54	67.57	67.57	67.57	7.01	3034.8
513	400	26578.1	82.60	81.53	80.53	81.63	67.54	67.57	67.57	67.57	7.67	3465.9
514	480	31893.7	84.58	83.54	82.60	83.58	67.54	67.57	67.57	67.57	8.40	3795.0
515	560	37209.3	86.45	85.26	84.35	85.47	67.54	67.57	67.57	67.57	8.94	4161.1
516	640	42524.9	88.08	87.16	85.85	87.22	67.54	67.57	67.57	67.57	9.37	4538.9
Pressure : 84.45 kN/m ²												
517	240	15946.8	75.17	74.51	73.68	74.55	63.78	63.83	63.90	63.92	6.81	2340.3
518	320	21262.5	77.31	76.31	75.26	76.49	63.78	63.83	63.90	63.92	7.41	2868.0
519	400	26578.1	79.37	78.37	77.11	78.41	63.78	63.83	63.90	63.92	8.12	3274.8
520	480	31893.7	81.47	80.22	79.40	80.36	63.78	63.83	63.90	63.92	8.90	3584.8
521	560	37209.3	83.06	82.27	81.08	82.39	63.78	63.83	63.90	63.92	9.47	3930.3
522	640	42524.9	85.17	83.98	82.52	84.01	63.78	63.83	63.90	63.92	9.92	4287.2
Pressure : 71.23 kN/m ²												
523	240	15946.8	71.31	70.72	70.12	70.75	59.51	59.65	59.70	59.66	7.29	2187.1
524	320	21262.5	73.61	72.61	71.61	72.72	59.51	59.65	59.70	59.66	7.94	2679.5
525	400	26578.1	75.77	74.56	73.66	74.63	59.51	59.65	59.70	59.66	8.69	3060.0
526	480	31893.7	77.74	76.75	75.65	76.90	59.51	59.65	59.70	59.66	9.52	3350.2
527	560	37209.3	79.66	78.52	77.73	78.63	59.51	59.65	59.70	59.66	10.13	3672.8
528	640	42524.9	81.45	80.39	79.28	80.43	59.51	59.65	59.70	59.66	10.62	4006.1

Table B.18 Contd.

Run No.	Heat Input, Q W	Heat Flux, q W/m ²	Wall Temperature, T _{w0} , °C				Liquid Pool Temperature, T _{lm} , °C				Wall Super Heat, ΔT _w °C	Heat Transfer Coefficient, h W/m ² °C
			Top	Side	Bottom	Side	Top	Side	Bottom	Side		
Pressure : 57.83 kN/m ²												
529	240	15946.8	66.95	66.39	65.51	66.36	54.56	54.59	54.59	54.60	7.91	2015.2
530	320	21262.5	69.29	68.17	67.35	68.28	54.56	54.59	54.59	54.60	8.61	2469.0
531	400	26578.1	71.26	70.34	69.37	70.45	54.56	54.59	54.59	54.60	9.43	2818.5
532	480	31893.7	73.52	72.51	71.52	72.57	54.56	54.59	54.59	54.60	10.34	3085.9
533	560	37209.3	75.46	74.43	73.45	74.50	54.56	54.59	54.59	54.60	11.00	3383.8
534	640	42524.9	77.37	76.35	74.97	76.33	54.56	54.59	54.59	54.60	11.52	3690.4
Pressure : 44.64 kN/m ²												
535	240	15946.8	61.60	61.07	60.46	60.96	48.34	48.46	48.54	48.39	8.78	1815.6
536	320	21262.5	64.03	63.08	61.92	63.23	48.34	48.46	48.54	48.39	9.56	2224.6
537	400	26578.1	66.05	65.24	64.36	65.30	48.34	48.46	48.54	48.39	10.46	2540.3
538	480	31893.7	68.53	67.45	66.55	67.51	48.34	48.46	48.54	48.39	11.47	2781.4
539	560	37209.3	70.54	69.53	68.43	69.56	48.34	48.46	48.54	48.39	12.20	3049.5
540	640	42524.9	72.32	71.49	70.27	71.39	48.34	48.46	48.54	48.39	12.79	3326.1

Table B.19 Boiling heat transfer data of 90% methanol over a 43 μm thick horizontal coated tube

Run No.	Heat Input, Q W	Heat Flux, q W/m ²	Wall Temperature, T_{wo} , °C				Liquid Pool Temperature, T_{lm} , °C				Wall Super Heat, ΔT_w °C	Heat Transfer Coefficient, h W/m ² °C
			Top	Side	Bottom	Side	Top	Side	Bottom	Side		
Pressure : 97.71 kN/m ²												
541	240	15946.8	75.84	75.29	74.72	75.48	65.13	65.13	65.29	65.28	6.32	2523.1
542	320	21262.5	78.29	77.09	76.07	77.16	65.13	65.13	65.29	65.28	6.87	3094.5
543	400	26578.1	80.15	79.03	78.00	79.13	65.13	65.13	65.29	65.28	7.53	3531.8
544	480	31893.7	82.20	80.99	79.97	81.09	65.13	65.13	65.29	65.28	8.24	3868.6
545	560	37209.3	83.77	82.92	81.57	83.18	65.13	65.13	65.29	65.28	8.77	4240.6
546	640	42524.9	85.58	84.44	83.63	84.55	65.13	65.13	65.29	65.28	9.19	4625.7
Pressure : 84.69 kN/m ²												
547	240	15946.8	72.67	72.24	71.32	72.29	61.62	61.63	61.63	61.68	6.69	2384.9
548	320	21262.5	75.09	73.68	73.36	73.80	61.62	61.63	61.63	61.68	7.27	2924.2
549	400	26578.1	76.85	76.02	74.75	76.15	61.62	61.63	61.63	61.68	7.96	3337.0
550	480	31893.7	78.78	78.06	76.86	78.19	61.62	61.63	61.63	61.68	8.73	3654.8
551	560	37209.3	80.88	79.73	78.79	79.81	61.62	61.63	61.63	61.68	9.29	4005.8
552	640	42524.9	82.51	81.51	80.47	81.57	61.62	61.63	61.63	61.68	9.73	4369.3
Pressure : 71.26 kN/m ²												
553	240	15946.8	69.24	69.01	68.32	69.06	57.92	57.93	58.02	57.93	7.16	2228.6
554	320	21262.5	71.62	70.91	69.72	70.97	57.92	57.93	58.02	57.93	7.78	2732.3
555	400	26578.1	73.91	72.79	71.67	72.89	57.92	57.93	58.02	57.93	8.52	3118.1
556	480	31893.7	75.86	74.85	73.95	74.93	57.92	57.93	58.02	57.93	9.34	3415.0
557	560	37209.3	77.77	76.79	75.70	76.81	57.92	57.93	58.02	57.93	9.94	3742.9
558	640	42524.9	78.88	78.82	77.42	78.92	57.92	57.93	58.02	57.93	10.42	4082.6

Table B.19 Contd.

Run No.	Heat Input, Q W	Heat Flux, q W/m ²	Wall Temperature, T _{w0} , °C				Liquid Pool Temperature, T _{lm} , °C				Wall Super Heat, ΔT _w °C	Heat Transfer Coefficient, h W/m ² °C
			Top	Side	Bottom	Side	Top	Side	Bottom	Side		
Pressure : 57.73 kN/m ²												
559	240	15946.8	65.39	64.54	63.99	64.61	53.01	53.08	53.07	53.09	7.77	2053.4
560	320	21262.5	67.49	66.70	65.29	66.84	53.01	53.08	53.07	53.09	8.45	2517.5
561	400	26578.1	69.48	68.74	67.51	68.90	53.01	53.08	53.07	53.09	9.25	2872.0
562	480	31893.7	71.98	70.72	69.66	70.86	53.01	53.08	53.07	53.09	10.14	3146.2
563	560	37209.3	73.80	72.66	71.56	72.89	53.01	53.08	53.07	53.09	10.79	3448.4
564	640	42524.9	75.66	74.50	73.32	74.57	53.01	53.08	53.07	53.09	11.31	3761.4
Pressure : 45.05 kN/m ²												
565	240	15946.8	60.01	59.48	58.76	59.58	47.00	47.07	47.06	47.03	8.61	1851.2
566	320	21262.5	62.78	61.37	60.29	61.48	47.00	47.07	47.06	47.03	9.37	2269.5
567	400	26578.1	64.63	63.60	62.66	63.68	47.00	47.07	47.06	47.03	10.26	2589.9
568	480	31893.7	66.98	65.84	64.81	65.95	47.00	47.07	47.06	47.03	11.24	2836.3
569	560	37209.3	68.94	67.81	66.88	67.92	47.00	47.07	47.06	47.03	11.97	3108.7
570	640	42524.9	70.81	69.75	68.42	69.92	47.00	47.07	47.06	47.03	12.54	3390.7

Table B.20 Boiling heat transfer data of 95% methanol over a 43 μm thick horizontal coated tube

Run No.	Heat Input, Q W	Heat Flux, q W/m ²	Wall Temperature, T_{wo} , °C				Liquid Pool Temperature, T_{lm} , °C				Wall Super Heat, ΔT_w °C	Heat Transfer Coefficient, h W/m ² °C
			Top	Side	Bottom	Side	Top	Side	Bottom	Side		
Pressure : 97.86 kN/m ²												
571	240	15946.8	75.07	74.42	73.83	74.47	64.35	64.41	64.39	64.46	6.24	2555.3
572	320	21262.5	77.31	76.19	75.18	76.34	64.35	64.41	64.39	64.46	6.78	3136.7
573	400	26578.1	79.20	77.92	77.48	78.08	64.35	64.41	64.39	64.46	7.43	3578.4
574	480	31893.7	81.25	80.07	79.14	80.13	64.35	64.41	64.39	64.46	8.14	3918.9
575	560	37209.3	83.03	81.84	80.91	81.97	64.35	64.41	64.39	64.46	8.66	4296.5
576	640	42524.9	84.65	83.59	82.58	83.66	64.35	64.41	64.39	64.46	9.07	4686.3
Pressure : 84.46 kN/m ²												
577	240	15946.8	71.74	71.04	70.40	71.10	60.65	60.66	60.67	60.67	6.60	2415.7
578	320	21262.5	74.03	72.74	71.94	72.92	60.65	60.66	60.67	60.67	7.17	2964.6
579	400	26578.1	75.83	74.74	74.07	74.81	60.65	60.66	60.67	60.67	7.86	3381.1
580	480	31893.7	77.92	76.67	76.22	76.73	60.65	60.66	60.67	60.67	8.61	3702.2
581	560	37209.3	79.92	78.64	77.52	78.74	60.65	60.66	60.67	60.67	9.17	4058.8
582	640	42524.9	81.47	80.35	79.35	80.49	60.65	60.66	60.67	60.67	9.61	4426.7
Pressure : 71.29 kN/m ²												
583	240	15946.8	68.31	67.47	66.77	67.53	56.61	56.65	56.72	56.63	7.07	2256.9
584	320	21262.5	70.29	69.35	68.51	69.43	56.61	56.65	56.72	56.63	7.68	2769.7
585	400	26578.1	72.51	71.20	70.55	71.35	56.61	56.65	56.72	56.63	8.41	3159.2
586	480	31893.7	74.60	73.42	72.37	73.52	56.61	56.65	56.72	56.63	9.22	3459.4
587	560	37209.3	76.58	75.35	74.00	75.42	56.61	56.65	56.72	56.63	9.81	3792.2
588	640	42524.9	78.19	76.93	76.13	77.04	56.61	56.65	56.72	56.63	10.28	4136.1

Table B.20 Contd.

Run No.	Heat Input, Q W	Heat Flux, q W/m ²	Wall Temperature, T _w , °C				Liquid Pool Temperature, T _{lm} , °C				Wall Super Heat, ΔT _w °C	Heat Transfer Coefficient, h W/m ² °C
			Top	Side	Bottom	Side	Top	Side	Bottom	Side		
Pressure : 57.90 kN/m ²												
589	240	15946.8	64.05	63.33	62.74	63.42	51.72	51.95	51.98	52.00	7.67	2079.5
590	320	21262.5	66.22	65.34	64.26	65.44	51.72	51.95	51.98	52.00	8.33	2551.7
591	400	26578.1	68.45	67.23	66.54	67.32	51.72	51.95	51.98	52.00	9.13	2910.5
592	480	31893.7	70.65	69.36	68.67	69.43	51.72	51.95	51.98	52.00	10.01	3186.7
593	560	37209.3	72.53	71.42	70.31	71.50	51.72	51.95	51.98	52.00	10.65	3493.6
594	640	42524.9	74.31	73.17	72.10	73.29	51.72	51.95	51.98	52.00	11.16	3810.3
Pressure : 44.50 kN/m ²												
595	240	15946.8	59.12	58.30	58.00	58.39	46.12	46.15	46.13	46.15	8.51	1874.6
596	320	21262.5	61.59	60.35	59.32	60.55	46.12	46.15	46.13	46.15	9.24	2300.7
597	400	26578.1	63.99	62.56	61.23	62.66	46.12	46.15	46.13	46.15	10.13	2623.9
598	480	31893.7	65.73	64.85	63.76	65.05	46.12	46.15	46.13	46.15	11.10	2873.2
599	560	37209.3	67.97	66.73	65.74	66.89	46.12	46.15	46.13	46.15	11.82	3149.2
600	640	42524.9	69.90	68.37	67.89	68.50	46.12	46.15	46.13	46.15	12.38	3434.9

Annexure –C

Sample Calculation

This describes procedure involve in calculation of heat transfer coefficient and thermal effectiveness

SAMPLE CALCULATION

The experimental data as recorded by various thermocouples and other measuring instruments for nucleate pool boiling of liquids over uncoated as well as coated heating tube surface are listed in tabular form in Annexure-B. Following section explains step by step procedure adopted to calculate surface area of heating tube, heat flux, wall superheat, local heat transfer coefficient and average heat transfer coefficient for a set of data for uncoated as well as for a coated tube.

C.1 HEATING TUBE DETAILS

In the present investigation four heating tubes; one uncoated and three coated tubes are taken to obtain boiling heat transfer data of pure liquids and their binary mixtures. An AISI 304 stainless steel tube has been used as substrate material and copper as a coating material. The thermal conductivity of the heating tube and coating material are 16.4 and 389.34 W/m⁰C [103], respectively. The details of heating tube dimensions are given in the following **Table C.1**.

Table C.1 Detail Dimensions of Heating Tube

Heating Tube Nomenclature	O.D. of Tube before Coating d , (m)	O.D. of Tube after Coating d_o , (m)	I.D. of Tube d_i , (m)	Pitch Circle Diameter d_h , (m)	Effective Length L , (m)	Coating thickness δ , (μm)
ST-00	0.031940	0.031940	0.01804	0.0250	0.1500	0
ST-22	0.031930	0.031974	0.01799	0.0250	0.1500	22
ST-43	0.031940	0.032026	0.01801	0.0250	0.1500	43
ST-67	0.031920	0.032054	0.01800	0.0250	0.1510	67

C.2 HEAT TRANSFER COEFFICIENT ON UNCOATED HEATING TUBE: FOR PURE LIQUIDS

The steps involved in the calculation of local as well as average heat transfer coefficient for boiling of pure liquids on uncoated tube are shown below by taking the data of Run no. 1 from Table B.1 of Annexure-B. This experimental run corresponds to the data of boiling of distilled water over uncoated heating tube. For convenience, the data corresponding to this run are reproduced below:

Power Input, $Q = 240 \text{ W}$				Pressure, $P = 97.71 \text{ kN/m}^2$			
Wall Temperature, $T_{wm}, ^\circ\text{C}$				Liquid Temperature, $T_{lm}, ^\circ\text{C}$			
Top	Side	Bottom	Side	Top	Side	Bottom	Side
112.35	111.25	110.33	111.31	99.15	99.17	99.18	99.18

C.2.1 Heat Transfer Surface Area of Heating Tube, A

$$\begin{aligned}
 A &= \pi d_o L && \text{(C.1)} \\
 &= \pi \times 0.03194 \times 0.150 \\
 &= 0.01505 \text{ m}^2
 \end{aligned}$$

C.2.2 Heat Flux, q

$$\begin{aligned}
 q &= \frac{Q}{A} && \text{(C.2)} \\
 &= \frac{240}{0.01505} \\
 &= 15946.84 \text{ W/m}^2
 \end{aligned}$$

C.2.3 Outer Surface Temperature of Heating Tube, T_{wo}

The outer surface temperature of heating tube is calculated by subtracting the temperature drop in the tube wall, δT_w from the measured wall temperature, T_{wm} as follows,

$$T_{wo} = T_{wm} - \delta T_w \quad \text{(C.3)}$$

where, temperature drop δT_w is calculated by using Fourier's heat conduction equation for thin cylinders. It is as follows,

$$\begin{aligned}\delta T_w &= \frac{qd_o}{2k_w} \ln\left(\frac{d_o}{d_h}\right) \quad (C.4) \\ &= \left(\frac{15946.84 \times 0.03194}{2 \times 16.4}\right) \ln\left(\frac{0.03194}{0.02500}\right) \\ &= 3.8^\circ\text{C}\end{aligned}$$

Now, the surface temperatures of heating tube at top, side and bottom positions are calculated by using the Eq. (C.3). The calculated values are given below in tabular form:

Position, ψ	Temperature, $^\circ\text{C}$		
	T_{wm}	δT_w	T_{wo}
Top	112.35	3.8	108.55
Side	111.25	3.8	107.45
Bottom	110.33	3.8	106.52
Side	111.31	3.8	107.51

C.2.4 Local Wall Superheat, $\Delta T_{w\psi}$

Values of local wall superheat at top, bottom and two side positions, around the circumference of heating tube are calculated by subtracting the liquid temperature from the corresponding outer surface temperature, i.e.

$$\Delta T_{w\psi} = T_{wo} - T_{lm} \quad (C.5)$$

The calculated values of local wall super heat using the above equation are given below in tabular form,

Position, ψ	Temperature, $^\circ\text{C}$		
	T_{wo}	T_{lm}	$\Delta T_{w\psi}$
Top	108.55	99.15	9.40
Side	107.45	99.17	8.28
Bottom	106.52	99.18	7.34
Side	107.51	99.18	8.33

C.2.5 Local Heat Transfer Coefficient, h_{ψ}

Local heat transfer coefficient at top, bottom and two side positions, around the circumference of the heating tube is calculated using the following equation:

$$h_{\psi} = \frac{q}{\Delta T_{w\psi}} \quad (\text{C.6})$$

The values of Local heat transfer coefficient obtained using the above equation are given below in tabular form,

Position, ψ	q , W/m ²	$\Delta T_{w\psi}$, °C	h_{ψ} , W/m ² /°C
Top	15946.84	9.40	1696.73
Side	15946.84	8.28	1927.64
Bottom	15946.84	7.34	2171.49
Side	15946.84	8.33	1916.06

C.2.6 Average Outer Surface Temperature of Heating Tube, \bar{T}_{wo}

The average outer surface temperature is calculated by taking arithmetic mean of outer surface temperature measured respectively at top, side, bottom and side of the heating tube. It is expressed by the following equation:

$$\bar{T}_{wo} = \frac{1}{4} (T_{(wo)t} + T_{(wo)s} + T_{(wo)b} + T_{(wo)s}) \quad (\text{C.7})$$

Where, subscripts t, s and b represent top, side and bottom positions on heating tube surface, respectively.

Hence,

$$\begin{aligned} \bar{T}_{wo} &= \frac{1}{4} (108.55 + 107.45 + 106.52 + 107.51) \\ &= 107.50^{\circ} \text{C} \end{aligned}$$

C.2.7 Average Liquid Temperature, \bar{T}_{lm}

The average liquid temperature is calculated by taking arithmetic mean of liquid pool temperature measured at top, two sides and bottom positions of the heating tube. It is expressed by the following equation;

$$\bar{T}_{lm} = \frac{1}{4} (T_{(lm)t} + T_{(lm)s} + T_{(lm)b} + T_{(lm)s}) \quad (C.8)$$

hence,

$$\begin{aligned} \bar{T}_{lm} &= \frac{1}{4} (99.15 + 99.17 + 99.18 + 99.18) \\ &= 99.17^{\circ}\text{C} \end{aligned}$$

C.2.8 Wall Superheat, ΔT_w

The wall superheat of the heating tube is calculated by subtracting the average liquid temperature from the average outer surface temperature. It is expressed as:

$$\Delta T_w = \bar{T}_{wo} - \bar{T}_{lm} \quad (C.9)$$

hence,

$$\begin{aligned} \Delta T_w &= 107.50 - 99.17 \\ &= 8.33^{\circ}\text{C} \end{aligned}$$

C.2.9 Average Heat Transfer Coefficient, h

The average boiling heat transfer coefficient is calculated using following equation;

$$\begin{aligned} h &= \frac{q}{\Delta T_w} \quad (C.10) \\ &= \frac{15946.84}{8.26} = 1913.37 \text{ W/m}^2/^{\circ}\text{C} \end{aligned}$$

C.3 HEAT TRANSFER COEFFICIENT ON UNCOATED HEATING TUBE: FOR BINARY MIXTURE

The procedure involved in the calculation of boiling heat transfer coefficient for binary mixture on an uncoated tube is similar to that mentioned above for pure liquids on the same heating tube. Run no. 271 from Table B.10 of Annexure-B is taken to show the procedure for the calculation of heat transfer coefficient in the pool boiling of 50 mole percent methanol-distilled water mixture on an uncoated tube. The data are reproduced below:

Power Input, $Q = 240 \text{ W}$				Pressure, $P = 97.71 \text{ kN/m}^2$			
Wall Temperature, T_{wm}				Liquid Temperature, T_{lm}			
Top	Side	Bottom	Side	Top	Side	Bottom	Side
93.05	92.43	91.72	92.33	73.11	73.13	73.14	73.13

The parameters required for calculation of heat transfer coefficients for binary mixtures on an uncoated tube such as outer diameter, pitch circle diameter, heat transfer surface area and heat flux are same as used in previous case. Further, calculation for outer surface temperature, temperature drop, local wall superheat, and local heat transfer coefficients at top, bottom and the two side positions were carried out by using the procedure described above for pure liquids on an uncoated tube. The calculated values are listed below:

Position	$q, \text{ W/m}^2$	Temperature, $^{\circ}\text{C}$					h_{ψ} $\text{W/m}^2/^{\circ}\text{C}$
		T_{wm}	δT_w	T_{wo}	T_{lm}	$\Delta T_{w\psi}$	
Top	15946.84	93.05	3.80	89.24	73.11	16.13	988.60
Side	15946.84	92.43	3.80	88.62	73.13	15.49	1029.31
Bottom	15946.84	91.72	3.80	87.91	73.14	14.77	1079.11
Side	15946.84	92.33	3.80	88.52	73.13	15.39	1036.07

The other parameters average value of outer surface temperature, liquid temperature, wall superheat and heat transfer coefficient are calculated in the same manner as mentioned above for pure liquids on an uncoated heating tube. The calculated values are as follows:

$$\begin{aligned} \text{The average outer surface temperature} &= 88.58 \\ \text{The average liquid temperature} &= 73.13 \text{ }^{\circ}\text{C} \\ \text{The wall superheat} &= 15.45 \text{ }^{\circ}\text{C} \\ \text{The average boiling heat transfer coefficient} &= 1032.28 \text{ W/m}^2/^{\circ}\text{C} \end{aligned}$$

C.4 HEAT TRANSFER COEFFICIENT ON COATED HEATING TUBE:

The procedure involved in the calculation of boiling heat transfer coefficient both for pure liquids and their binary mixtures on coated heating tube is similar to that mentioned above for uncoated heating tube. Thus, to

demonstrate the calculation procedure for coated tube, Run no. 61 from Table B. 3 of Annexure-B is taken. It corresponds to the data of boiling of distilled water over a 43 μm thick copper coated tube. The data is reproduced below:

Power Input, $Q = 240 \text{ W}$				Pressure, $P = 97.71 \text{ kN/m}^2$			
Wall Temperature, T_{wm}				Liquid Temperature, T_{lm}			
Top	Side	Bottom	Side	Top	Side	Bottom	Side
108.76	108.12	107.24	108.10	99.12	99.17	99.20	99.15

For coated tubes, the outer diameter and the pitch circle diameter of the tubes are given in Table C.1. The other parameters such as the heat transfer surface area and heat flux are calculated using various equations given for uncoated heating tube. These values are as follows:

$$\text{Heat transfer surface area} = 0.01505 \text{ m}^2$$

$$\text{Heat flux} = 15946.84 \text{ W/m}^2$$

It is important to mention here that the outer wall surface temperature of coated surface was calculated by neglecting the temperature drop across copper coating thickness. Thus, the calculations of heat transfer coefficient are based on substrate temperature only. Based upon this, calculation for outer surface temperature, temperature drop and local heat transfer coefficient were carried out by using the procedure described above for uncoated tube. Following table lists the values of measured surface temperature, outer surface temperature, local wall superheat and local heat transfer coefficient at top, bottom and the two side positions of coated heating tube:

Position	$q, \text{ W/m}^2$	Temperature, $^{\circ}\text{C}$					h_{ψ} $\text{W/m}^2\text{ }^{\circ}\text{C}$
		T_{wm}	δT_w	T_{wo}	T_{lm}	$\Delta T_{w\psi}$	
Top	15946.84	108.76	3.80	104.96	99.12	5.84	2735.13
Side	15946.84	108.12	3.80	103.32	99.17	5.15	3100.76
Bottom	15946.84	107.24	3.80	103.44	99.20	4.24	3771.82
Side	15946.84	108.10	3.80	103.30	99.15	5.15	3095.64

The average value of outer surface temperature, liquid temperature, wall superheat and heat transfer coefficient for the coated heating tube are calculated in the same manner as mentioned above for uncoated heating tube.

The calculated values are as follows:

The average outer surface temperature	= 104.26 °C
The average liquid temperature	= 99.16 °C
The wall superheat	= 5.10 °C
The average boiling heat transfer coefficient	= 3134.12 W/m ² /°C

C.5 THERMAL EFFECTIVENESS OF COATED HEATING TUBE

Thermal effectiveness of a coated heating tube surface is given by

$$\zeta_{\delta} = \left(\frac{h_{\text{COPPERCOATED}}}{h_{\text{PLAIN TUBE}}} \right)_{q, p} \quad (\text{C.10})$$

For 43 µm thick coated tube, the value of heat flux, pressure and heat transfer coefficient given in Run no. 66 from Table B.3 of Annexure – B, is as follows:

Heat flux	= 42524.92 W/m ²
Pressure	= 97.71 kN/m ²
Heat transfer coefficient	= 5680.65 W/m ² /°C

Similarly, for uncoated tube, the value of heat flux, pressure and heat transfer coefficient given in Run no. 6 from Table B.1 of Annexure – B, is as follows:

Heat flux	= 42524.92 W/m ²
Pressure	= 97.71 kN/m ²
Heat transfer coefficient	= 3817.07 W/m ² /°C

$$\zeta_{40} = \frac{5680.65}{3817.07} = 1.49$$

Hence, thermal effectiveness of a 43 µm thick copper coated stainless steel tube for a heat flux of 42,524.92 W/m² and a pressure of 97.71 kN/m² is 1.49.

Uncertainty Analysis

This presents analysis of uncertainty involved in various data of this investigation

UNCERTAINTY ANALYSIS

The present investigation involves the measurement of basic parameters like power input, temperature of heating tube surface along its circumference at top, bottom, and two sides, the corresponding temperature of test liquid around the heating tube surface and surface area of the heating tube. These data are taken during the experiment and are processed further to calculate heat transfer coefficient. The measurement of these data is carried out by different type of instruments, e.g. a digital wattmeter is used to measure the power input to the heater, a digital multi-meter to measure the temperatures of heating tube surface and test liquid, a vernier caliper to measure the physical dimensions of heating tube and a coating thickness gauge to measure the thickness of coating over the tube surface. However, all instruments have some inherent limitation due to manufacturing constrains and therefore the measured values are limited by their own least count. Besides, the method employed in the calculation is also not free from uncertainties. As a result the recorded data have some degree of uncertainty. In other words, the calculation of heat transfer coefficient, which includes recorded data of all instruments, has an uncertainty. Therefore, it is necessary to calculate the uncertainty of each data recorded by various instruments so that the degree of uncertainty associated with the calculated heat transfer coefficient may be realized. Following is the details of uncertainty analysis performed to determine the degree of uncertainty associated with heat transfer coefficient

Schultz & Cole [115] have given the following method which can be used to determine the maximum and minimum possible uncertainty in the calculation of heat transfer coefficient. According to them, the dependent variable x is to be expressed as a function of independent measured quantities ($y_1, y_2, y_3, \dots, y_n$) in the following form:

$$x = f(y_1, y_2, y_3, \dots, y_n)$$

The uncertainty, U_x associated with the variable x , is defined as the absolute value of the maximum expected deviation from the reported experimental values and is given mathematically in the following form:

$$U_x = \left[\sum_{i=1}^n \left\{ \left(\frac{\partial x}{\partial y_i} \right) U_{y_i} \right\}^2 \right]^{\frac{1}{2}} \quad (\text{D.1})$$

Where, U_{y_i} is the uncertainty associated in a quantity y_i .

In order to visualize the uncertainty associated with the calculated average heat transfer coefficient a demo calculation is shown below by taking data for the Run no. 6 of Table B.1 of Annexure-B for the boiling of distilled water over uncoated heating tube. The set of data taken is given again below for ready reference.

Power input = 640W				Pressure = 97.71 kN/m ²			
Liquid Temperature, T_{lm}				Wall Temperature, T_{wm}			
Top	Side	Bottom	Side	Top	Side	Bottom	Side
99.15	99.17	99.18	99.18	121.86	120.47	119.02	120.47

D.1 Uncertainty in Power Input, U_Q

A digital wattmeter having a least count 1 Watt was used in the present investigation to measure the power supplied to the heater. Therefore, the maximum possible uncertainty associated in the measurement of power supply was of 1 Watt.

Hence,
$$U_Q = \left[(1)^2 \right]^{\frac{1}{2}} = 1 \text{ W}$$

D.2 Uncertainty in the Surface Area of the Heating Tube, U_A

The surface area of the plain heating tube is given by,

$$\begin{aligned} A &= \pi d_o l \\ &= \pi \times 0.031940 \times 0.150 \\ &= 0.01505 \text{ m}^2 \end{aligned}$$

Therefore, uncertainty associated with heating tube surface area is given by the following expression:

$$U_A = \left[(\pi d_0 U_l)^2 + (\pi l U_{d_0})^2 \right]^{\frac{1}{2}} \quad (D.2)$$

Where, U_l and U_{d_0} are the uncertainties associated in the measurement of length and outside diameter of heating tube, respectively. The measurement of effective length and outside diameter of the heating tube was done with the help of a vernier caliper having a least count of 0.01 mm.

So, $U_l = U_{d_0} = 1 \times 10^{-5} \text{ m}$

Putting the values of U_l and U_{d_0} in the above equation, we get:

$$U_A = \left[(\pi \times 0.031940 \times 1 \times 10^{-5})^2 + (\pi \times 0.150 \times 1 \times 10^{-5})^2 \right]^{\frac{1}{2}}$$

$$U_A = 0.00000482 \text{ m}^2$$

Thus the uncertainty in the measurement of surface area of the heating tube varies from 0.0150452 to 0.01505482 m^2 .

D.3 Uncertainty in Heat Flux, U_q

The heat flux is given by,

$$q = Q/A = 640/0.01505 = 42524.92 \text{ W/m}^2$$

Therefore, the uncertainty associated with heat flux is given by the following expression,

$$U_q = \left[\left(\frac{U_Q}{A} \right)^2 + \left(-\frac{QU_A}{A^2} \right)^2 \right]^{\frac{1}{2}} \quad (D.3)$$

Where, U_Q is the uncertainty associated with the measurement of power and is equal to 1 W.

$$U_q = \left[\left(\frac{1}{0.01505} \right)^2 + \left(-\frac{640 \times 0.00000482}{(0.01505)^2} \right)^2 \right]^{\frac{1}{2}} = 67.83 \text{ W/m}^2$$

Thus, the uncertainty in the measurement of heat flux varies from 42458.09 to 42592.75 W/m^2 .

D.4 Uncertainty in Heating Tube Surface Temperature, $U_{T_{wm}}$

Copper constantan thermocouples were used to measure the heating tube wall and liquid temperature. The e.m.f. values of thermocouples were measured with the help of a digital multimeter having a least count of 0.001 mV. From e.m.f.-temperature chart, it is found that the value of 0.001 mV corresponds to 0.021°C .

Thus, uncertainty in the measurement of tube wall and liquid temperature is of 0.021°C .

Hence, $U_{T_{wm}} = U_{T_{lm}} = 0.021^{\circ}\text{C}$

Outer surface temperature = Measured wall temperature – Temperature drop

i.e. $T_{wo} = T_{wm} - \delta T_w$

where, temperature drop, δT_w , is given by:

$$\delta T_w = \frac{qd_0}{2k_w} \ln\left(\frac{d_0}{d_h}\right)$$

$$\begin{aligned} \delta T_w &= \left(\frac{42524.92 \times 0.031940}{2 \times 16.4}\right) \ln\left(\frac{0.031940}{0.02500}\right) \\ &= 10.14^{\circ}\text{C} \end{aligned}$$

Therefore, the uncertainty associated with the temperature drop is given by the following expression,

$$\begin{aligned} U_{\delta T_w} &= \left[\left\{ \frac{d_0}{2k_w} \ln\left(\frac{d_0}{d_h}\right) U_q \right\}^2 + \left\{ \left(\frac{q}{2k_w} \ln\left(\frac{d_0}{d_h}\right) + \frac{q}{2k_w} \right) U_{d_0} \right\}^2 \right. \\ &\quad \left. + \left\{ \frac{-qd_0}{2k_w^2} \ln\left(\frac{d_0}{d_h}\right) U_{k_w} \right\}^2 + \left\{ \frac{qd_0}{2k_w} \left(\frac{-1}{d_h}\right) U_{d_h} \right\}^2 \right]^{1/2} \end{aligned} \quad (\text{D.4})$$

where, U_{k_w} is the uncertainty in the value of thermal conductivity of the heating tube material. Here U_{k_w} is assumed to be equal to zero since the value of thermal conductivity of stainless steel is taken from Perry & Green [103].

Therefore,

$$\begin{aligned}
 U_{\delta T_w} &= \left[\left\{ \frac{0.031940}{2 \times 16.4} \ln \left(\frac{0.031940}{0.02500} \right) \times 67.83 \right\}^2 + \left\{ \left(\frac{42524.92}{2 \times 16.4} \ln \left(\frac{0.031940}{0.02500} \right) + \frac{42524.92}{2 \times 16.4} \right) \times 1 \times 10^{-5} \right\}^2 \right. \\
 &\quad \left. + \left\{ \frac{-42524.92 \times 0.031940}{2 \times (16.4)^2} \ln \left(\frac{0.031940}{0.02500} \right) \times 0.0 \right\}^2 + \left\{ \left(\frac{42524.92 \times 0.031940}{2 \times 16.4} \left(\frac{-1}{0.02500} \right) \right) \times 1 \times 10^{-5} \right\}^2 \right]^{\frac{1}{2}} \\
 &= 0.02822662 \text{ } ^\circ\text{C}
 \end{aligned}$$

Now, values surface temperature of the heating tube around its circumference at top, bottom and two side positions are obtained by subtracting δT_w from measured wall temperature. The details are given in a tabular form in the following table.

Position, ψ	Temperature, $^\circ\text{C}$		
	T_{wm}	δT_w	T_{wo}
Top	121.86	10.14	111.72
Side	120.47	10.14	110.33
Bottom	119.02	10.14	108.88
Side	120.47	10.14	110.33

Hence, the uncertainty in outer surface temperature $U_{T_{wo}}$ is given by,

$$\begin{aligned}
 U_{T_{wo}} &= \left[\left(U_{T_{wm}} \right)^2 + \left(-U_{\delta T_w} \right)^2 \right]^{\frac{1}{2}} \quad (D.5) \\
 &= \left[(0.021)^2 + (0.02822662)^2 \right]^{\frac{1}{2}} \\
 &= 0.035182 \text{ } ^\circ\text{C}
 \end{aligned}$$

Thus, uncertainty associated in the measurement of temperature of outer surface at top, sides and bottom of the heating tube is $0.035182 \text{ } ^\circ\text{C}$.

However, in the calculation of average heat transfer coefficient, we need to calculate average outer surface temperature and uncertainty associated in it.

The average outer surface temperature is calculated by taking arithmetic mean of surface temperature of the heating tube at top, sides and bottom positions.

Mathematically,

$$\bar{T}_{wo} = \frac{1}{4}(T_{wo,t} + T_{wo,s} + T_{wo,b} + T_{wo,s})$$

where, subscripts t, s and b refer to top, side and bottom position on heating tube respectively.

So,

$$\begin{aligned}\bar{T}_{wo} &= \frac{1}{4}(111.72 + 110.33 + 108.88 + 110.33) \\ &= 110.32^{\circ}\text{C}\end{aligned}$$

Now, the uncertainty associated with average outer surface temperature is given by the following expression,

$$U_{\bar{T}_{wo}} = \left[\frac{1}{4} \left\{ (U_{T_{wo,t}})^2 + (U_{T_{wo,s}})^2 + (U_{T_{wo,b}})^2 + (U_{T_{wo,s}})^2 \right\} \right]^{\frac{1}{2}} \quad (\text{D.6})$$

$$\begin{aligned}U_{\bar{T}_{wo}} &= \left[\frac{1}{4} \left\{ (0.02822662)^2 + (0.02822662)^2 \right\} + (0.02822662)^2 + (0.02822662)^2 \right]^{\frac{1}{2}} \\ U_{\bar{T}_{wo}} &= 0.02822662^{\circ}\text{C}\end{aligned}$$

D.5 Uncertainty in Liquid Temperature, $U_{T_{lm}}$

As mentioned in section D.4 the uncertainty in the measurement of liquid temperature is 0.021°C .

Hence,

$$U_{T_{lm}} = 0.021^{\circ}\text{C}$$

Like average surface temperature, we need to calculate average liquid temperature and to find out the uncertainty associated with it. The average liquid temperature \bar{T}_l is given by,

$$\bar{T}_l = \frac{1}{4}(T_{lm,t} + T_{lm,s} + T_{lm,b} + T_{lm,s})$$

$$\bar{T}_l = \frac{1}{4}(99.15 + 99.17 + 99.18 + 99.18)$$

$$\bar{T}_l = 99.17^{\circ}\text{C}$$

Now, the uncertainty associated with average liquid temperature is given by the following expression:

$$U_{T_{lm}} = \left[\frac{1}{4} \left\{ (U_{T_{lm,t}})^2 + (U_{T_{lm,s}})^2 + (U_{T_{lm,b}})^2 + (U_{T_{lm,s}})^2 \right\} \right]^{\frac{1}{2}} \quad (\text{D.7})$$

$$U_{T_{im}} = \left[\frac{1}{4} \left\{ (0.021)^2 + (0.021)^2 + (0.021)^2 + (0.021)^2 \right\} \right]^{\frac{1}{2}}$$

$$\begin{aligned} U_{\bar{T}_{im}} &= \left[\frac{1}{3} \left\{ (0.021)^2 + (0.021)^2 + (0.021)^2 \right\} \right]^{\frac{1}{2}} \\ &= 0.021^{\circ}\text{C} \end{aligned}$$

D.6 Uncertainty in Wall Superheat, $U_{\Delta T_w}$

The wall superheat calculated as follows;

$$\begin{aligned} \Delta T_w &= \bar{T}_{wo} - \bar{T}_i \\ &= 110.32 - 99.17 \\ &= 11.14^{\circ}\text{C} \end{aligned}$$

So, the uncertainty associated with the wall superheat is given by the following expression:

$$U_{\Delta T_w} = \left[\left(U_{\bar{T}_{wo}} \right)^2 + \left(-U_{\bar{T}_i} \right)^2 \right]^{\frac{1}{2}} \quad (\text{D.8})$$

$$\begin{aligned} U_{\Delta T_w} &= \left[(0.02822662)^2 + (-0.021)^2 \right]^{\frac{1}{2}} \\ &= 0.035182^{\circ}\text{C} \end{aligned}$$

D.7 Uncertainty in Heat Transfer Coefficient, $U_{\bar{h}}$

The average value of heat transfer coefficient can be calculated from the following expression,

$$\begin{aligned} \bar{h} &= \frac{q}{\Delta T_w} \\ &= \frac{42524.92}{11.14} \\ &= 3817.07 \text{ W/m}^2\text{ }^{\circ}\text{C} \end{aligned}$$

So, the uncertainty associated with average heat transfer coefficient is given by,

$$U_{\bar{h}} = \left[\left(\frac{U_q}{\Delta T_w} \right)^2 + \left(-\frac{q U_{\Delta T_w}}{\Delta T_w^2} \right)^2 \right]^{\frac{1}{2}} \quad (\text{D.9})$$

$$= \left[\left(\frac{66.45}{11.14} \right)^2 + \left(- \frac{42524.92 \times 0.035182}{(11.14)^2} \right)^2 \right]^{\frac{1}{2}}$$
$$= 13.43 \text{ W/m}^2 \text{ } ^\circ\text{C}$$

Thus, the uncertainty in the measurement of average heat transfer coefficient may vary from 3803.64 to 3830.50 W/m² °C i.e. ±0.35% of the experimental value. Similar procedure has been used to calculate uncertainty associated with the measurement of average heat transfer coefficient of all experimental runs of this investigation. The maximum value of uncertainty is found to be ±1.13% which is well within the acceptable limit. Therefore, the experimental data obtained in the present investigation may be considered to be reliable and consistent within the acceptable limits.



Annexure –E

PHYSICO-THERMAL PROPERTIES EVALUATION

This presents the thermo-physical properties used in this study and their method of calculation

PHYSICO-THERMAL PROPERTIES EVALUATION

Physico-thermal properties of pure liquids used in the present investigation, namely distilled water and methanol, are readily available in the literature in different system of units. However, property data tables available in open literature are generally do not provide properties at every pressure and temperature. Therefore, the physico-thermal properties of distilled water and methanol have been calculated using various correlations and methods at various temperature and pressures used in the present investigation.

In addition, physico-thermal properties of methanol-distilled water binary mixtures are available for limited range of temperature and concentration only. Thus, various methods have been used to predict the properties of methanol-distilled water binary mixtures. These methods are discussed in following sections:

E.1 Liquid and Vapor Densities

The liquid density was calculated at the respective saturation temperature of a given mixture with the assumption that for these mixtures the partial molar volume of each component in the mixture is equal to its pure component volume at the same temperature and pressure. The liquid densities for distilled water, methanol and their binary mixtures are plotted in **Fig. E.1**.

The vapor density was calculated by employing Redlich-Kwong equation of state [103]. The vapor density variation as a function of saturation temperature for distilled water, methanol and their binary mixtures are shown in **Fig. E.2**.

E.2 Thermal Conductivity

Thermal conductivity of binary liquid mixtures has been predicted employing Filippov & Novoselova [110] equation, which is given below:

$$k_{\text{mix.}} = k_1x_1 + k_2x_2 - 0.72(k_2 - k_1)(x_1x_2) \quad (\text{E.1})$$

where, x_2 is the mole fraction of component having the larger value of k . The calculated values are plotted in **Fig. E.3**.

E.3 Surface Tension

Surface tension of the methanol-distilled water binary mixtures has been calculated using the method of Chunxi et al. [32], which is given below:

$$\sigma_{\text{mix.}} = (x_1\sigma_1 + x_2\sigma_2) - \frac{x_1x_2RT}{x_2 + x_1\Lambda_{21}} \left(\frac{\partial\Lambda_{21}}{\partial A} \right) \times \left[1 - \frac{1}{\Lambda_{21}} \right] \quad (\text{E.2})$$

$$\text{Where, } \Lambda_{21} = \frac{v_1}{v_2} \exp\left(\frac{U_{12} - U_{11}}{RT}\right)$$

For methanol-water system:

$$\left(\frac{U_{12} - U_{11}}{R} \right) = 625.5; \quad \frac{\partial(U_{12} - U_{11})}{(10^{-5}R)\partial A} = 561.22$$

$$v_1 = 4.072 \times 10^{-2} \text{ m}^3/\text{kg-mol}; \quad v_2 = 1.808 \times 10^{-2} \text{ m}^3/\text{kg-mol}$$

In these equations v is the molar volume, σ is the surface tension, and suffix 1 and 2 refers to methanol and water, respectively.

The values of surface tension for methanol-water mixtures have been calculated using above procedure, and are plotted in **Fig. E.4**.

E.4 Viscosity

Viscosity of the methanol-distilled water binary mixtures has been calculated using the correlation given by Tamura & Kurata [110]. The correlation is provided below:

$$\mu_{\text{mix.}} = x_1\phi_1\mu_1 + x_2\phi_2\mu_2 + 2(x_1x_2\phi_1\phi_2)^{1/2}\mu_{12} \quad (\text{E.3})$$

where, x is the mole fraction, μ is the viscosity, ϕ is the volume fraction, and suffix 1 and 2 refers to methanol and water, respectively.

The values of viscosities for distilled water-methanol binary liquid mixtures have been calculated using above procedure, and the values are plotted in **Fig. E.5**.

E.5 Diffusivity Estimation

Diffusivity of the methanol-distilled water binary mixtures has been calculated using the method given by Lesffer and Cullinan [103], which is given below:

$$D_{AB}\mu_{mix} = (D_{AB}^0\mu_B)^{x_B} (D_{BA}^0\mu_A)^{x_A} \left[1 + \frac{\partial \ln \gamma_A}{\partial \ln x_A} \right] \quad (E.4)$$

where, D_{AB}^0 is the diffusivity of A at infinite dilution in B and D_{BA}^0 is the diffusivity of B at infinite dilution in A. D_{AB}^0 and D_{BA}^0 were calculated by the empirical correlation of Wilke & Chang [103]. The activity coefficient γ_A can be typically obtained by the vapor-liquid equilibrium data.

Wilke & Chang [103] correlation:

$$D_{AB}^0 = 117.3 \times 10^{-18} \frac{(\psi_B M_B)^{0.5} T}{\mu_A v_A^{0.6}} \quad (E.5)$$

where, M_B is the molecular weight of solvent, kg/kmol; T is the temperature, K; μ is the solution viscosity, kg/ms; v_A is the solute molar volume at normal boiling point, $m^3/kmol$; ψ is the association factor for the solvent. ψ is equal to 2.26 for water as a solvent, and is 1.19 for methanol as solvent.

The values of diffusivity for the methanol-distilled water binary mixtures have been calculated using above procedure, and the resulted values are plotted in Fig. E.6.

E.5 Specific Heat and Latent Heat of Vaporization

The specific heat and latent heat of vaporization for the methanol-distilled water binary mixtures has been calculated by weighted average method. Following correlations have been used for calculation these properties:
Specific heat:

$$C_{p,mix} = xC_{p,1} + (1-x)C_{p,2} \quad (E.6)$$

Latent heat of vaporization:

$$\lambda_{mix} = x\lambda_1 + (1-x)\lambda_2 \quad (E.7)$$

where, x is the mole fraction of methanol in water, C_p is the specific heat, and λ is the latent heat of vaporization.

The values of specific heat and latent heat of vaporization for aqueous binary liquid mixtures as calculated by above procedure are plotted in Figs. E.7 and E.8.

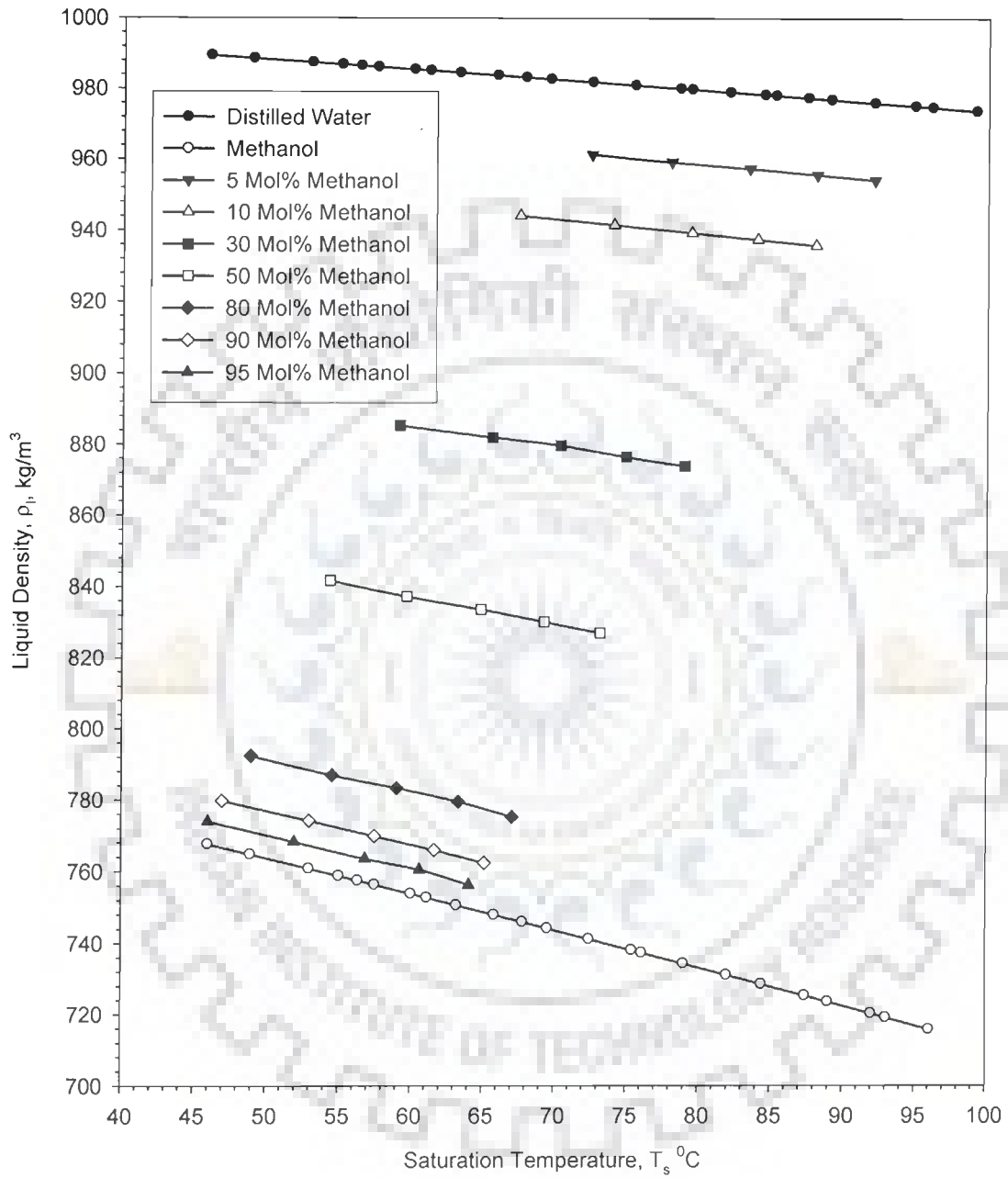


Fig. E.1 Variation of liquid density of distilled water, methanol and their binary mixtures with saturation temperature

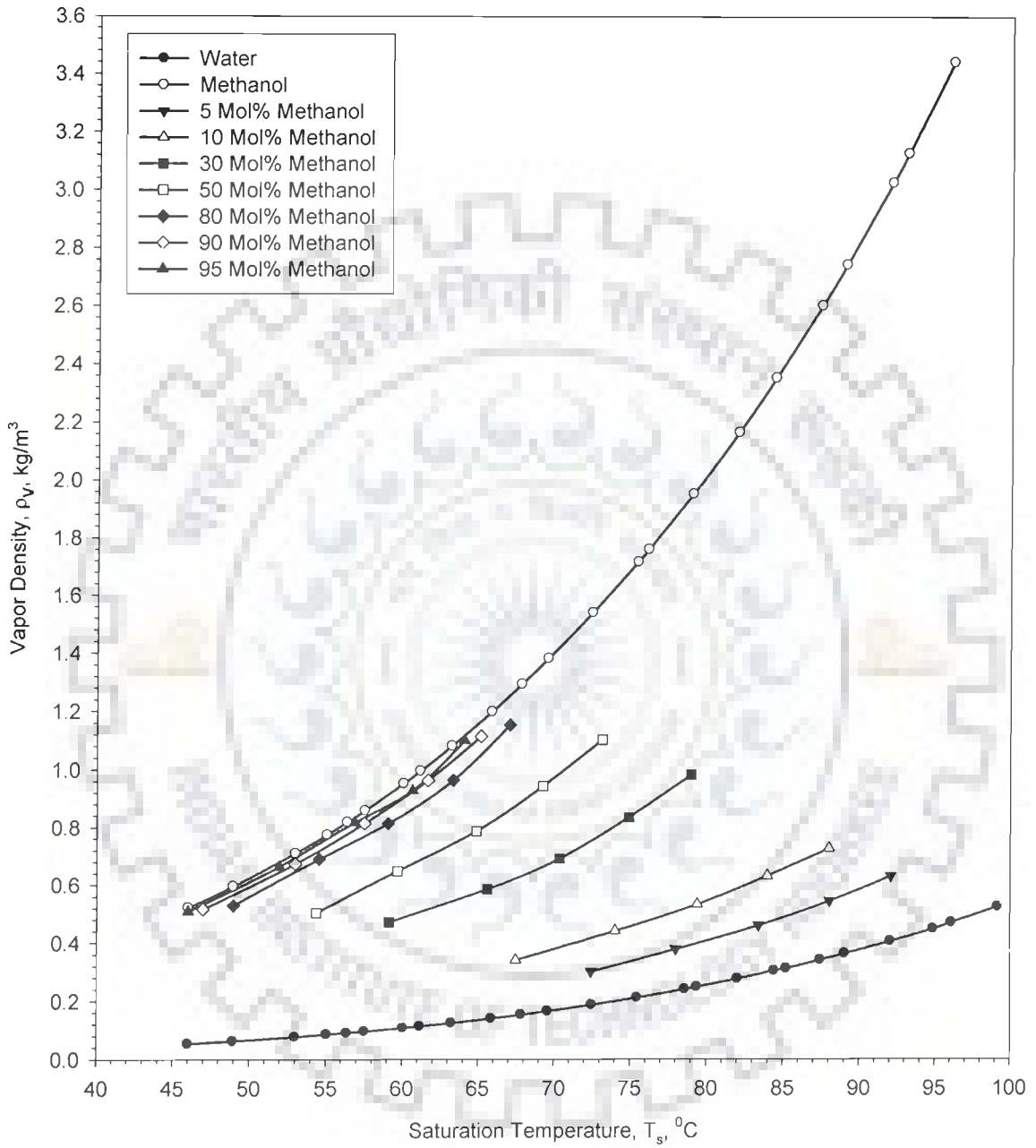


Fig. E.2 Variation of vapor density of distilled water, methanol and their binary mixtures with saturation temperature

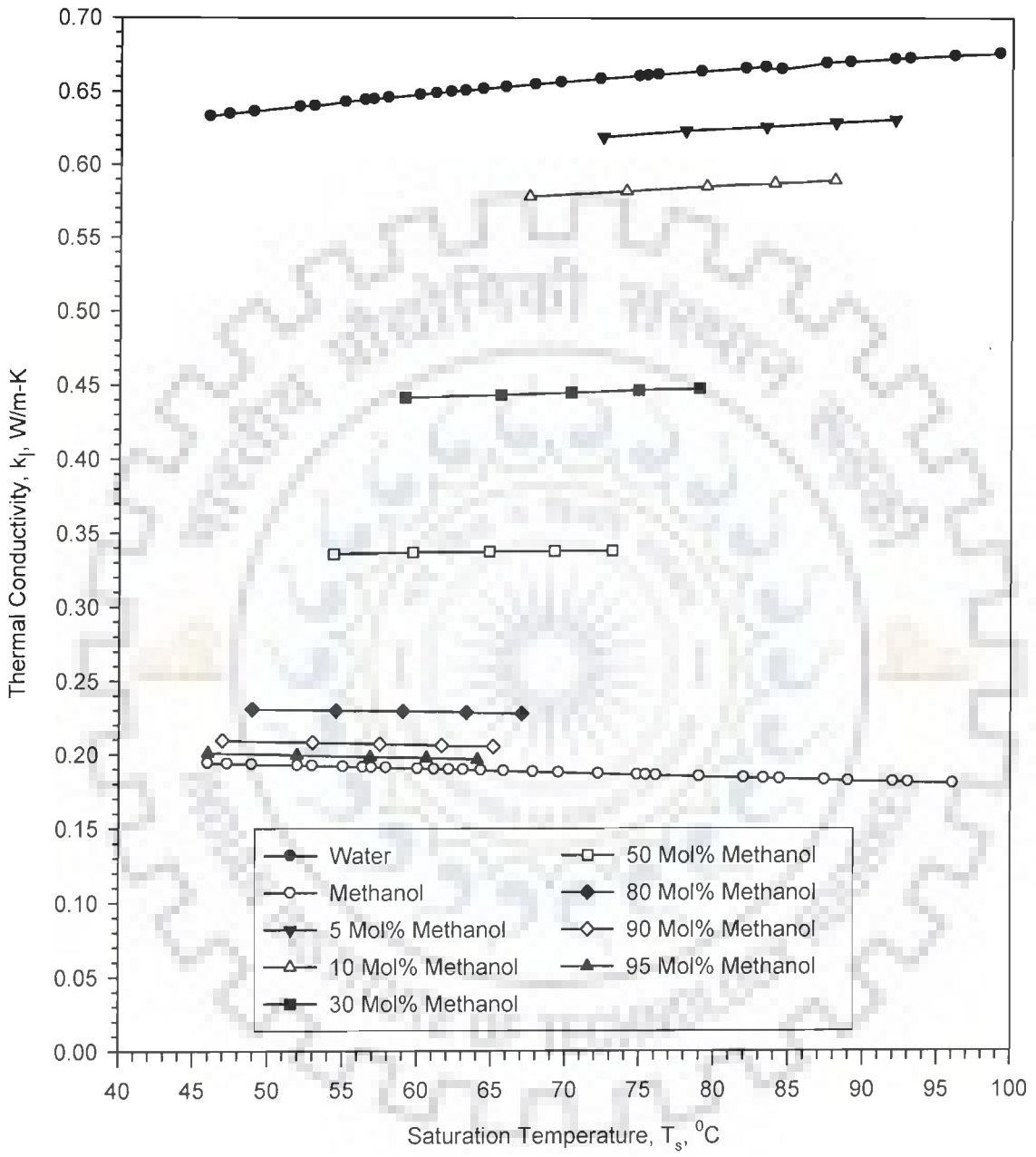


Fig. E.3 Variation of thermal conductivity of distilled water, methanol and their binary mixtures with saturation temperature (Mole% Basis)

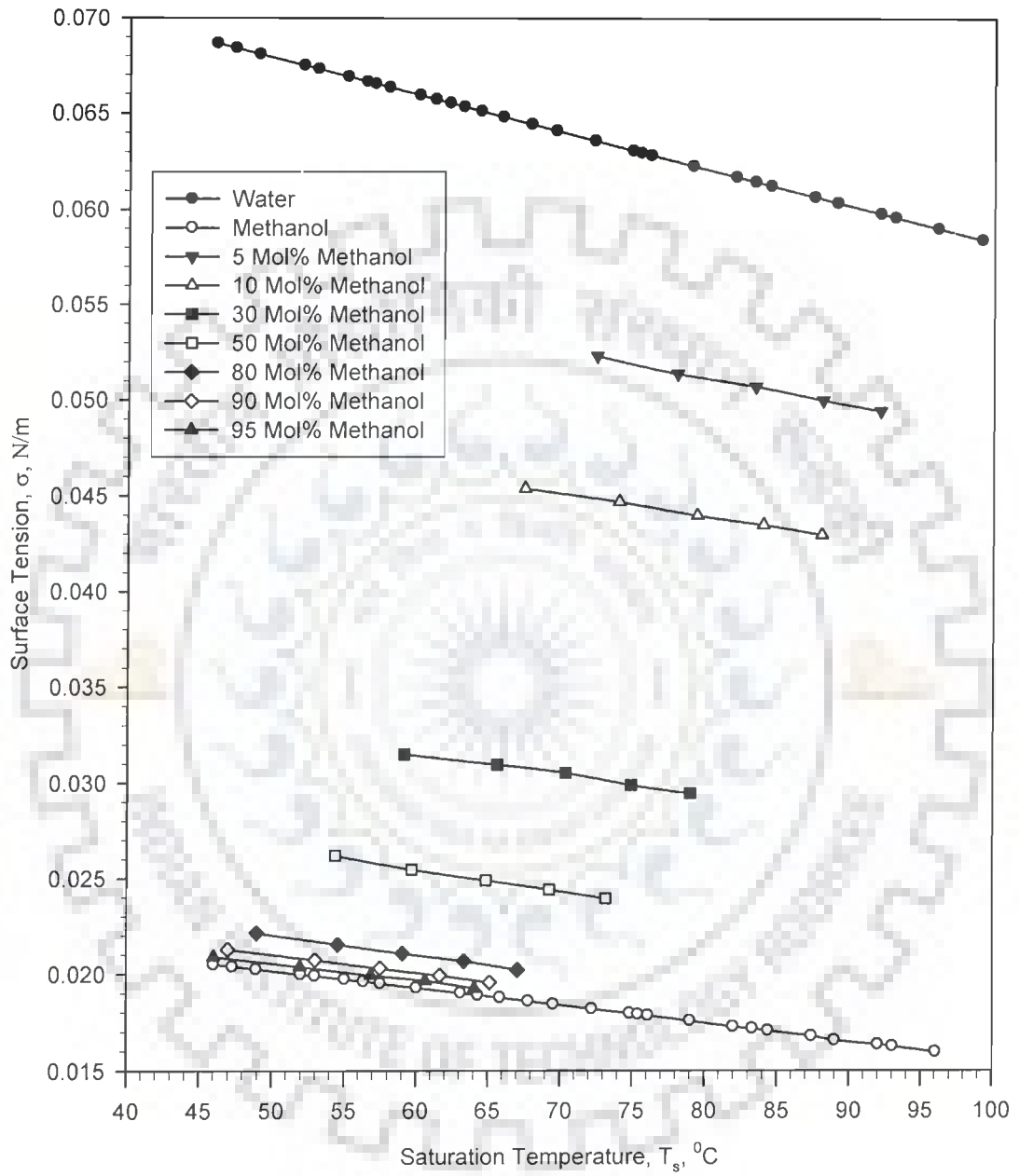


Fig. E.4 Variation of surface tension of distilled water, methanol and their binary mixtures with saturation temperature

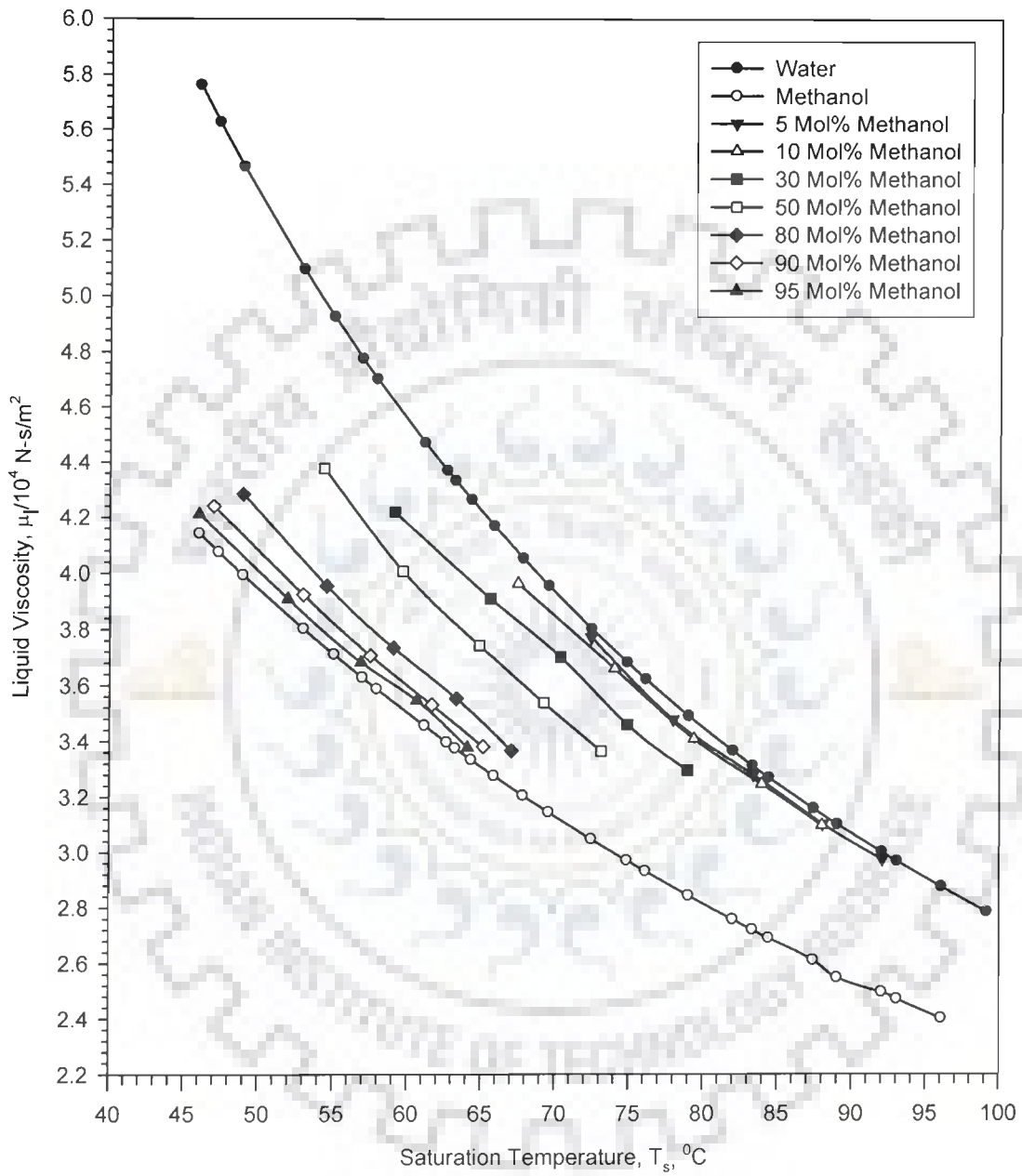


Fig. E.5 Variation of liquid viscosity of distilled water, methanol and their binary mixtures with saturation temperature

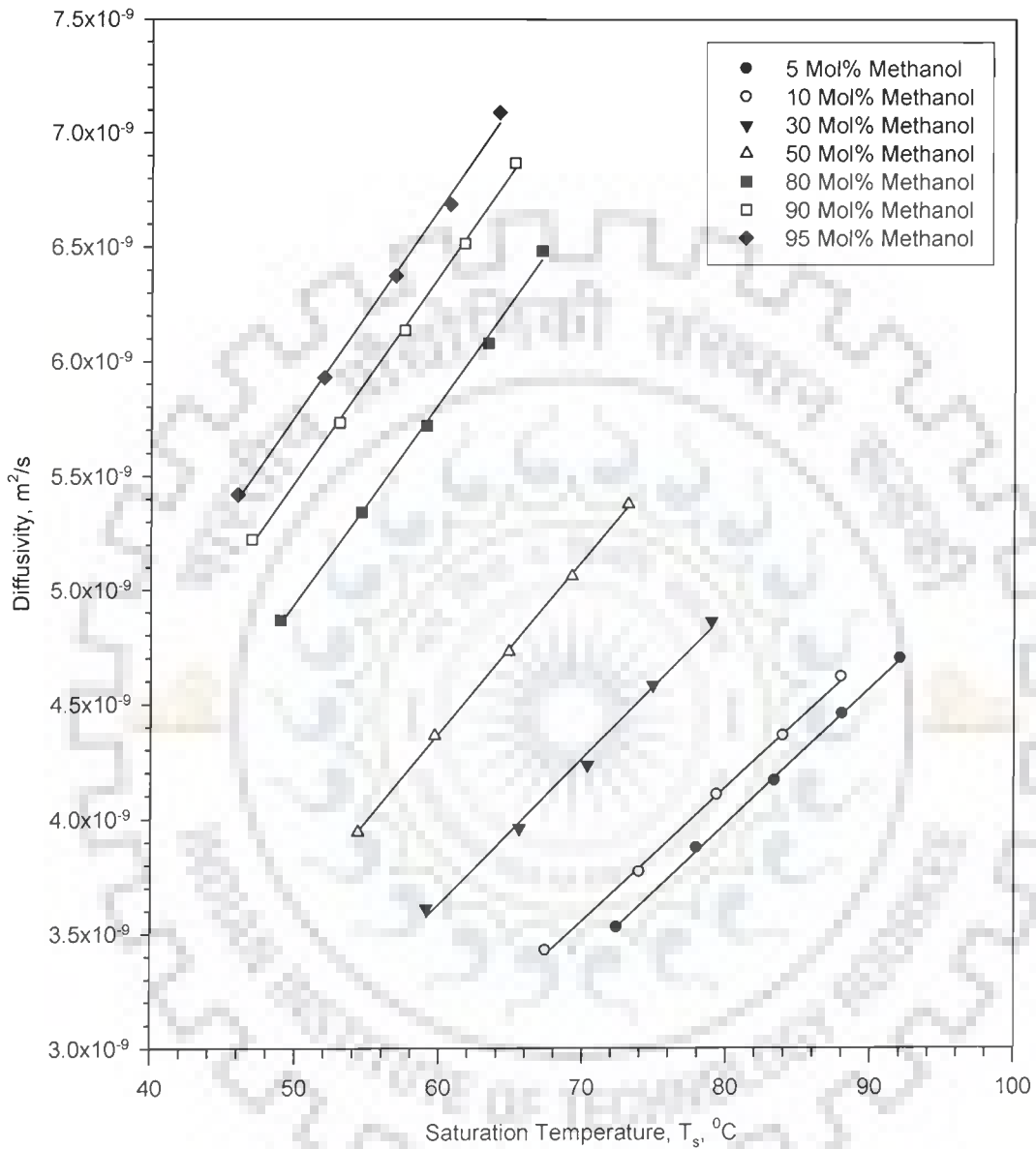


Fig. E.6 Variation of Diffusivity of methanol-distilled water mixtures with saturation temperature

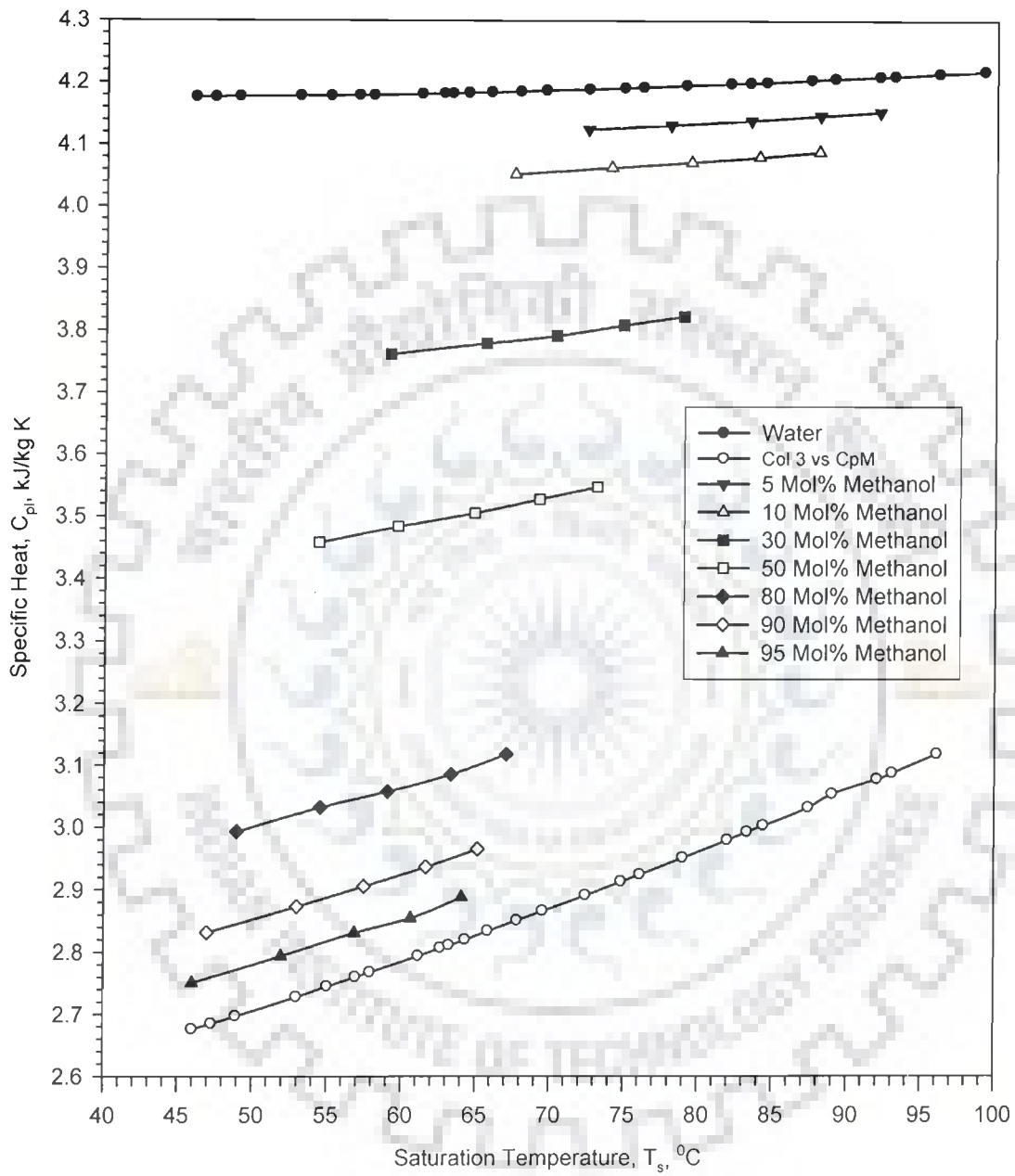


Fig. E.7 Variation of specific heat of distilled water, methanol and their binary mixtures with saturation temperature

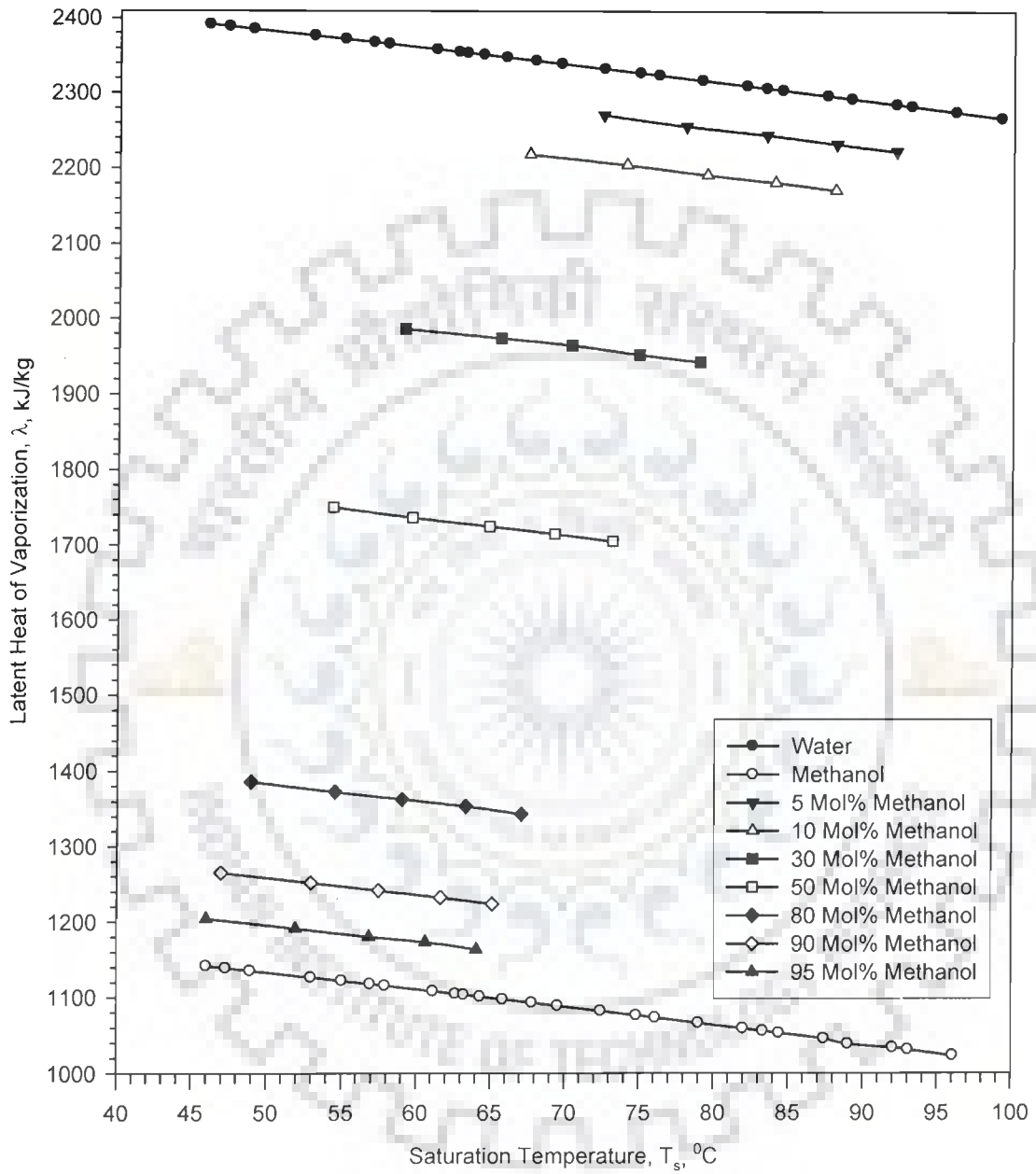


Fig. E.8 Variation of latent heat of vaporization of distilled water, methanol and their binary mixtures with saturation temperature

The slide features a yellow paper-like corner in the top-left, secured by a green pushpin. A large, faint watermark of a gear with text inside is centered in the background. The word "References" is written in a large, bold, orange font with a black outline.

References

*This provides various publications
referred during this study*

REFERENCES

1. Afgan, N.H., Jovic, L.A., Kovalev, S.A. and Lenykov, V.A., Boiling heat transfer from surfaces with porous layers, *Int. J. Heat Mass Transfer*, Vol. 28, No. 2, pp 415-422, 1985.
2. Afgan, N.H., Boiling heat transfer and burnout heat flux of ethyl alcohol-benzene mixtures, 3rd *Int. Heat Transfer Conf.*, Chicago, 98, Vol. III, August, pp 175-185, 1966.
3. Ahmed, S., and Carey, V.P., Effects of gravity on the boiling of binary fluid mixtures, *Int. J. Heat Mass Transfer*, Vol. 41, No. 16, pp 2469-2483, 1998.
4. Alam, M.S., Prasad, L., Gupta, S.C., and Agarwal, V.K., Enhanced boiling of saturated water on copper coated surfaces, *Chem. Eng. Process*, Vol. 47, No. 1, pp 159-167, 2008.
5. Alam, S.S., and Varshney, B.S., Pool boiling of liquid mixtures, Presented at 2nd *National Heat and Mass Transfer Conference*, IIT Kanpur, Paper No. B-6, pp 13-15 Dec., 1973.
6. Alpay, H.E., and Balkan, F., Nucleate pool boiling performance of acetone-ethanol and methylene chloride-ethanol binary mixture, *Int. J. Heat Mass Transfer*, Vol. 32, No. 12, pp 2403-2408, 1989.
7. Bajorek, S.M., and Lloyd, J.R., Recent advances in the evaluation of nucleate boiling in multicomponent liquids, *Int. Symp. on the Physics of Heat Transfer in Boiling and Condensation*, Moscow, pp. 1-8, 1997.
8. Bansal, G.D., Studies of Nucleate pool boiling of liquids on in-line horizontal cylinders of different materials, Ph.D. Thesis, Mechanical Engineering Department, University of Roorkee, 1985.
9. Benjamin, R.J., and Balakrishnan, A.R., Nucleation pool boiling heat transfer of pure liquids at low to moderate heat fluxes, *Int. J. Heat Mass Transfer*, Vol. 39, No. 12, pp 2495-2504, 1996.

10. Benjamin, R.J., and Balakrishnan, A.R., Nucleate boiling heat transfer of binary mixtures at low to moderate heat fluxes, *Trans. ASME J. Heat Transfer*, Vol. 121, pp 365-375, 1999.
11. Berenson, P.J., Experiments on pool-boiling heat transfer, *Int. J. Heat Mass Transfer*, Vol. 5, pp 985-999, 1962.
12. Bergles, A.E., Techniques to enhance heat transfer, Chapter 11 in *Handbook of Heat Transfer*, W. M. Rohsenow, J. P. Hartnett, and Y. I. Cho, (eds.), 3rd ed., pp 11.1- 11.76, McGraw Hill, 1998.
13. Bergles, A.E., Bakhru, N. and Shires, J.W. Jr., Cooling of high power-density computer components, M.I.T. Engineering Projects Laboratory, Report No. DSR 70712-60, Nov., 1968.
14. Bergles, A.E., Enhancement of pool boiling, *Int. J. Refrig.*, Vol. 20, No. 8, pp 545-551, 1997.
15. Bhaumik, S., Agrawal, V.K., and Gupta, S.C., A generalized correlation of nucleate pool boiling of liquids, *Indian Journal of Chemical Technology*, Vol. 11, pp 719-725, Sept., 2004.
16. Bhaumik, S., Nucleate pool boiling of saturated liquids on PTFE coated horizontal heating tube, Ph.D. Thesis, Chemical Engineering Department, IIT Roorkee, 2003.
17. Bliss, F.E. Jr., Hsu, S.T., and Crawford, M., An investigation into the effects of various platings on the film coefficient during nucleate boiling from horizontal tubes, *Int. J. Heat Mass Transfer*, Vol. 12, pp 1061-1072, 1969.
18. Bonilla C.F., and Perry, C.W., Heat transmission to boiling binary liquid mixtures, *Trans. AIChE*, Vol. 37, pp 686-705, 1941.
19. Borishanskii, V.M., Bobrovich, G.I., and Minchenko, F.P., Heat transfer from a tube to water and to ethanol in nucleate pool boiling, in 'Problems of Heat Transfer and Hydraulics of Two-phase Media', Symposium, S.S. Kutateladze (ed.), Pergamon Press, pp 85-106, 1969.

20. Borishanskii, V.M., Use of thermodynamic similarity in generalizing experimental data on heat transfer, Processing of the International Heat Transfer Conference, pp 975, 1962.
21. Calus, W.F., and Leonidopoulos, D.J., Pool boiling - binary liquid mixtures, *Int. J. Heat Mass Transfer*, Vol. 17, pp 249-256, 1974.
22. Calus, W.F., and Rice, P., Pool boiling - binary liquid mixtures, *Chem. Eng. Sci.*, Vol. 27, pp 1687-1697, 1972.
23. Chang, J.Y., and You, S.M., Boiling heat transfer phenomena from micro-porous and porous surfaces in saturated FC-72, *Int. J. Heat Mass Transfer*, Vol. 40, No. 18, pp 4437-4447, 1997.
24. Chang, J.Y., and You, S.M., Enhanced boiling heat transfer from micro-porous cylindrical surfaces in saturated FC-87 and R-123, *Trans. ASME, J. Heat Transfer*, Vol. 119, No. 18, pp 319-325, May, 1997.
25. Chang, J.Y., and You, S.M., Heater orientation effects on pool boiling of micro-porous-enhanced surfaces in saturated FC-72, *J. Heat Transfer*, Vol. 118, No. 118, pp 937-943, Nov., 1996.
26. Chaudri, I.H., and McDougall, I.R., Aging studies in nucleate pool boiling of isopropyl acetate and perchloroethylene, *Int. J. Heat Mass Transfer*, Vol. 12, pp 681-688, 1969.
27. Chen, Y., Groll, M., Mertz, R., and Kulenovic, R., Pool boiling heat transfer of propane, isobutane and their mixtures on enhanced tubes with reentrant channels, *Int. J. of Heat and Mass Transfer*, Vol. 48, pp 2310-2322, 2005.
28. Chernobylskii, I.I., and Lukach, Y.E., Calculation of the heat transfer coefficient during boiling of binary mixtures, *Khim. Prom.*, pp 362-263, 1957.
29. Chien, L.H., and Webb, R.L., Measurement of bubble dynamics on an enhanced boiling surface, *Exp. Thermal Fluid Sc.*, Vol. 16, pp 177-186, 1998.

30. Chowdhury, S.K.R., and Winterton, R.H.S., Surface effects in pool boiling, *Int. J. Heat Mass Transfer*, Vol. 28, No. 10, pp 1881-1889, 1985.
31. Chun, M.H., and Kang, M.G., Effects of heat exchanger and tube parameters on nucleate pool boiling heat transfer, *Trans. ASME, J. Heat Transfer*, Vol. 120, pp 468-476, May, 1998.
32. Chunxi, L., Wenchuan, W., and Zihao, W., A surface tension model for liquid mixtures based on the Wilson equation, *Fluid Phase Equilibria*, Vol. 175, pp 185-196, 2000.
33. Cichelli, T.M., and Bonilla, C.F., Heat transfer to liquids boiling under pressure, *AIChE J.*, Vol. 41, pp 755-787, 1945.
34. Cieslinski, J.T., Nucleate pool boiling on porous metallic coatings, *Exp. Thermal Fluid Sc.*, Vol. 25, pp 557-564, 2002.
35. Clements, L.D., and Colver, C.P., Nucleate boiling of light hydrocarbons and their mixtures, *Proceedings of the Heat Transfer and Fluid Mechanics Institute* (edited by Landis, R.B. and Hardeman, G.J.), Stanford University Press, pp 417-430, 1972.
36. Cooper, M.G., Heat flow rates in saturated nucleate pool boiling-A wide ranging examination using reduced properties, in *Advances Heat Transfer*, Vol. 16, pp 157-239, Academic Press Inc., 1984.
37. Cornwell, K. and Houston, S.D., Nucleate pool boiling on horizontal tubes: a convection-based correlation, *Int. J. Heat Mass Transfer*, Vol. 37, pp 303-309, 1994.
38. Corty, C., and Foust, A.S., Surface variables in nucleate boiling, *Chem. Eng. Prog. Symp. Ser.*, Vol. 51, No. 17, pp 1-12, 1955.
39. Cryder, D.S., and Finalborgo, A.C., Heat transmission from metal surfaces to boiling liquids: Effect of temperature of the liquid on the liquid film coefficient, *AIChE J.*, pp 346-361, 1937.
40. Cryder, D.S., and Gilliland, E.R., *Ind. Eng. Chem.*, Vol. 24, pp 1382-1387, 1932.

41. Danilova, G.N., and Tikhonov, A.V., Enhancement of heat transfers in the boiling of R-113, refrigerant on various kinds of surface, Heat Transfer.Soviet Research, Vol. 16, No. 1, pp 59-66, 1984.
42. Das, M.K., A study of nucleate boiling of saturated liquids on copper coated heating tube surface, Ph.D. Thesis, Chemical Engineering Department, IIT Roorkee, 2005.
43. Dhir, V.K., and Liaw, S.P., Framework for a unified model for nucleate and transition pool boiling heat transfer, ASME J. Heat Transfer, Vol. 111, pp 739-746, 1989.
44. Drew, T.B., and Mueller, C., Boiling, Trans. AIChE, Vol. 33, pp 449-473, 1937.
45. Filatkin, V.N., Boiling heat transfer to water ammonia mixtures, problem of heat transfer and hydraulics of two-phase media, a Symposium edited in Russian by S.S. Kutateladze and translated by O.M. Blunn, Pergamon Press, London, pp 131-136, 1969.
46. Foster, H. K., and Zuber, N., Dynamics of vapor bubble and boiling heat transfer, AIChE J., Heat Transfer, Vol. 27, No. 3, pp 216-228, 1955.
47. Foster, K.E., and Greif, R., Heat transfer to boiling liquid – mechanism and correlations, Trans. ASME, J. Heat Transfer, Vol. 81, pp 43-53, Feb., 1959.
48. Fritz, W., Maximum volume of vapour bubble, Physik, Zeitschr, Vol. 36, pp 379-393, 1935.
49. Fujita, Y., and Tsutsui, M., Experimental investigation in pool boiling heat transfer of ternary mixture and heat transfer correlation, Exp. Therm. Fluid Sci., Vol. 26, pp 237–244, 2002.
50. Fujita, Y., and Tsutsui, M., Heat transfer in nucleate pool boiling of binary mixtures, Int. J. Hear Mass Transfer, Vol. 37, Suppl. 1. pp 291-302, 1994.

51. Fujita, Y., and Tsutsui, M., Nucleate boiling of two and three-component mixtures, *Int. J. of Heat and Mass Transfer* Vol. 47, pp 4637-4648, 2004.
52. Gaertner, R.F., Effect of surface Chemistry on the level of burnout heat flux in pool boiling, General Electric Research Laboratory, Report No. 63-RL-3449C, Sep., 1963.
53. Gilmour, C.H., Nucleate boiling-A correlation, *Chem. Eng. Prog.*, Vol. 54, No. 10, pp 77-79, 1958.
54. Griffith, P., and Wallis, J.D., The role of surface conditions in nucleate boiling, *Chem. Engg. Prog. Symp. Ser.*, Vol. 56, No. 30, pp 49-63, 1960.
55. Gupta, A., Saini, J.S., and Varma, H.K., Boiling heat transfer in small horizontal tube bundles at low cross-flow velocities, *Int. J. Heat Mass Transfer*, Vol. 38, No. 4, pp 599-605, 1995.
56. Gupta, S.C., and Varshney, B.S., A method for generalizing nucleate pool boiling heat transfer data for subatmospheric pressures, *Indian J. Chem. Technology*, Vol. 17, pp 331-334, Sept., 1979.
57. Gupta, S.C., and Varshney, B.S., Boiling heat transfer from a horizontal cylinder to a liquid pool, *Inst. of Engineers (CH)*, Vol. 61, Oct., 1980.
58. Haider, S.I., and Webb, R.L., A transient micro-convection model of nucleate pool boiling, *Int. J. Heat Mass Transfer*, Vol. 40, No. 15, pp 3675-3688, 1997.
59. Han, C.Y., and Griffith, P., The mechanism of heat transfer in nucleate pool boiling- part I: Bubble initiation, growth and departure, *Int. J. Heat Mass Transfer*, Vol. 8, pp. 887-904, 1965.
60. Happel, O., and Stephan, K., Heat transfer from nucleate to film boiling in binary mixtures, 5th *Int. Heat Transfer Conf. Tokyo*, Paper B 7.8, AICHE, N.Y., 1974.
61. Hinrichs, T., Hennecke, E. and Yasuda, H., The effect of plasma-deposited polymers on the nucleate boiling behavior of copper heat transfer surfaces, *Int. J. Heat Mass Transfer*, Vol. 24, No. 8, pp 1359-1368, 1981.

62. Hongji, Z., and Li, C., Investigation on boiling heat transfer from powder-porous surfaces, Proc. Int. Symp. on Phase Change Heat Transfer, Chengjing, Sichuan, China, X. Mingdao (ed.), pp 442-447, May 20-23, 1988.
63. Hsieh, S.S., and Hsu, P.T., Nucleate boiling characteristics of R-114, distilled water and R-134a on plain and rib-roughened tube geometries, Int. J. Heat Mass Transfer, Vol. 37, No. 10, pp 1423-1432, 1994.
64. Hsieh, S.S., and Weng, C.J., Nucleate pool boiling from coated surfaces in saturated R-134a and R-407c, Int. J. Heat Mass Transfer, Vol. 40, No. 3, pp 519-532, 1997.
65. Hughmark, G.A., Statistical analysis of nucleate pool boiling data, AIChE National Meeting. Cleveland, Abstract 41, 1961.
66. Hui, T.O., and Thome, J. R., A study of binary mixture boiling: boiling site density and subcooled heat transfer, Int. J. Heat Mass Transfer, Vol. 28, No. 5, pp 919-928, 1985.
67. Inoue, T., and Monde, M., Nucleate pool boiling heat transfer in binary mixtures, Wärme and Stoffübertragung, Vol. 29, pp 171-180, 1994.
68. Inoue, T., Kawae, N., and Monde, M., Characteristics of heat transfer coefficient during nucleate pool boiling of binary mixtures, Heat and Mass Transfer Vol. 33, pp 337-344, 1998.
69. Inoue, T., Monde, M., and Teruya, Y., Pool boiling heat transfer in binary mixtures of ammonia/water, Int. J. of Heat and Mass Transfer, Vol. 45, pp 4409-4415, 2002.
70. Insinger, T.H., and Bliss, H., Transmission of heat to boiling liquids, Trans. AIChE, Vol. 36, pp 491-516, 1940.
71. Ivanov, O.P., Heat transfer studies in boiling of F-12 and F-22 mixtures, Kholod. Tekhnika, Vol. 43, No 4, pp 27-29, 1966.
72. Jakob, M., and Linke, W., Physik Z., Vol. 36, pp 267-280, 1935.
73. Jakob, M., Heat transfer in evaporation and condensation, Mechanical Engineering, Vol. 58, No. 10, pp 643-660, Oct., 1936.

74. Jung, D., Song, K., Ahn, K., and Kim, J., Nucleate boiling heat transfer coefficients of mixtures containing HFC32, HFC125, and HFC134a, *Int. J. of Refrigeration*, Vol. 26, pp 764-771, 2003.
75. Jung, D.S., and Venart, J.E.S., Effects of enhanced surfaces and surface orientation on nucleate and film boiling heat transfer in R-11, *Int. J. Heat Mass Transfer*, Vol. 30, No. 12, pp 2623-2639, 1987.
76. Jungnickel, H., Wassilew, P., and Kraus, W.E., Investigations on the heat transfer of boiling binary refrigerant mixtures, *Int. J. Refrigeration*, Vol. 3, pp 129-133, 1980.
77. Kajikawa, T., Takazawa, H., and Mizuki, M., Heat transfer performance of metal fiber sintered surfaces, *Heat Transfer Engineering*, Vol. 4, No.1, pp 57-66, Jan.-Mar., 1983.
78. Kang M.G., Effect of surface roughness on pool boiling heat transfer, *Int. J. Heat Mass Transfer*, Vol. 43, pp 4073-4085, 2000.
79. Kim, J.H., Rainey, K.N., You, S.M., and Pak, J.Y., Mechanism of nucleate boiling heat transfer enhancement from microporous surfaces in saturated FC-72, *Trans. ASME, J. Heat Transfer*, Vol. 124, pp 500-506, 2002.
80. Köster, Ralf, Herres, G., and Kaupmann, P., and Hübner, P., Influence of the heat flux in mixture boiling: experiments and correlations, *Int. J. Refrigeration*, Vol. 20, No. 8, pp 598-605, 1997.
81. Krupiczka, R., Rotkegel, A., and Ziobrowski, Z., The influence of mass transport on the heat transfer coefficients during the boiling of multicomponent mixtures, *Int. J. Therm. Sci.*, Vol. 39, pp 667-672, 2000.
82. Kruzhilin, G.N., and Averin, Y.K., Generalization of experimental data for boiling heat transfer of liquids under conditions of natural convection, *Izv. Akad. Nauk. SSR. Otdel. Tekh. Nauk*, No. 10, 1955.
83. Kurihara, H.M., and Myers, J.E., The effects of superheat and surface roughness on boiling coefficients, *AIChE J.*, Vol. 6, pp 83-91, 1960.

84. Kutateladze, S.S., *Fundamentals of Heat Transfer*, Edward Arnold (Publishers) Ltd., London, 1963.
85. Labuntsov, D.A., Heat transfer Correlations for nucleate boiling of liquids, *Teploenergetika*, No. 5, 1960.
86. Lee, H.C., Kim, J., Oh, B.D., and Kim, M.H., Single bubble growth in saturated pool boiling of binary mixtures, *Int. J. of Multiphase Flow*, Vol. 30, pp 697-710, 2004.
87. Lu, S.M., and Chang, R.H., Pool boiling from a surface with a porous layer, *AIChE J.*, Vol. 33, No. 11, pp 1813-1828, Nov., 1987.
88. Luke, A., Pool boiling heat transfer from horizontal tubes with different surface roughness, *Int. J. Refrig.*, Vol. 20, No. 8, pp 561-574, 1997.
89. Magrini, U., and Nannei, E., On the influence of the thickness and thermal properties of heating walls on the heat transfer coefficients in nucleate pool boiling, *Trans. ASME, J. Heat Transfer*, Vol. 97, pp 173-178, May, 1975.
90. Marto, P.J., Moulson, J.A., and Maynard, M.D., Nucleate pool boiling of nitrogen with different surface conditions, *Trans. ASME, J. Heat Transfer*, Vol. 90, pp 437-444, Nov., 1968.
91. McNelly, M.J., A correlation of rates of heat transfer to nucleate boiling of liquids, *J. Imperial Coll., Chem. Engg. Sci.*, Vol. 7, pp 18-34, 1953.
92. Minchenko, F.P., and Firsova, E.V., Heat transfer to water and water-lithium salt solutions in nucleate pool boiling, pp 137-151, in 'Problems of Heat Transfer and Hydraulics of Two-phase Media', Symposium edited by S.S. Kutateladze, Pergamon Press, 1969.
93. Mostinskii, I.L., Calculation of heat transfer and internal heat fluxes in boiling liquids, *Teploenergetika* (10/4), pp 66, 1963.
94. Nahra, Z., and Næss, E., Heat transfer in pool boiling of binary and ternary non-azeotropic mixtures, *Heat Mass Transfer*, DOI 10.1007/s00231-007-0294-z, 2008.

95. Nakayama, W., Daikoku, T., and Nakajima, T., Effects of pore diameter and system pressure on saturated pool nucleate boiling heat transfer from porous surfaces, *Trans. ASME*, Vol. 104, pp 286-291, May, 1982.
96. Nakayama, W., Daikoku, T., Kuwahara, H., and Nakajima, T., Dynamic model of enhanced boiling heat transfer on porous surfaces -Part II: Analytical modeling, *Trans. ASME*, Vol. 102, pp 451-456, 1980.
97. Nakayama, W., Daikoku, T., Kuwahara, H., and Nakajima, T., Dynamic model of enhanced boiling heat transfer on porous surfaces-Part I: Experimental investigation, *Trans. ASME*, Vol. 102, pp 445-450, 1980.
98. Nishikawa, K., and Ito, T., Augmentation of nucleate boiling heat transfer by prepared surfaces, in *Heat Transfer in Energy Problems*, Mizushima, T. and Wang, W.J. (eds.), pp 111-118, Hemisphere Publishing Corporation, New York, 1982.
99. Nishikawa, K., Ito, T., and Tanaka, K., Enhanced heat transfer by nucleate boiling on a sintered metal layer, *Heat Transfer-Japanese Research*, Vol. 8, pp 65-81, 1979.
100. Nukiyama, S., The maximum and minimum values of the heat Q transmitted from metal to boiling water under atmospheric pressure, *Int. J. Heat Mass Transfer*, Vol. 9, pp. 1419-1433, 1966 [Paper originally published in *J. Japan Soc. Mech. Engrs.*, Vol. 37, pp 367-374, 1934 in Japanese language.
101. Palen, J.W., and Small, W.M., A new way to design kettle and internal reboilers, *Hydrocarbon processing*, Vol. 43, No. 11, pp 199-208, 1964.
102. Pandey, S.K., Nucleate pool boiling of liquids and their mixtures at subatmospheric pressure, Ph.D. Thesis, Chemical Engineering Department, University of Roorkee, 1982.
103. Perry, R.H., and Green, D.W., *Perry's Chemical Engineers' Handbook*, VII edition, McGraw Hill Book Company Inc., New York, 1997.
104. Piore, I.L., Experimental evaluation of constants for the Rohsenow pool boiling correlation, *Int. J. Heat Mass Transfer*, Vol. 42, pp 2003-2013, 1999.

105. Prasad, L., Alam, M.S, Gupta, S.C., and Agarwal, V.K., Enhanced boiling of methanol on copper coated surfaces, *Chemical Engineering and Technology*, Vol. 30, No. 7, pp 901-906, 2007.
106. Prasad, L., Enhanced boiling of saturated liquids on copper coated heating tube surface, Ph.D. Thesis, Chemical Engineering Department, IIT Roorkee, 2005.
107. Rainey, K.N., and You, S.M., Effects of heater size and orientation on pool boiling heat transfer from microporous coated surfaces, *Int. J. Heat Mass Transfer*, Vol. 44, pp 2589-2599, 2001.
108. Rallis, C.J., and Jawurek, H.H., Latent heat transport in saturated nucleate boiling, *Int. J. Heat Mass Transfer*, Vol. 7, pp 1051-1068, 1964.
109. Rao, G.V., and Balakrishnan, A.R., Heat transfer in nucleate pool boiling of multicomponent mixtures, *Experimental Thermal and Fluid Science*, Vol. 29, pp 87-103, 2004.
110. Reid, R.C., Prausnitz, J.M., and Sherwood, T.K., *The properties of Gases and liquid*, 3rd Edition, McGraw Hill Book Co., N.Y., 1977.
111. Rice, P., and Calus, W.F., Pool boiling-single component liquids, *Chem. Engg. Sci.*, Vol. 27, pp 1677-1686, 1972.
112. Rohsenow, W.M., A method of correlating heat-transfer data for surface boiling of liquids, *Trans. ASME, J. Heat Transfer*, Vol. 74, pp 969 - 976, August, 1952.
113. Schade, S.S., and Park, E.L. Jr., Effect of a plasma deposited polymer coating on the nucleate boiling behaviour of Freon-113, in 'Multiphase Transport- Fundamentals, Reactor Safety, and Applications' edited by. T. Nejarat Veziroglu, Vol. 2, pp 711-726, Hemisphere Publishing Corporation, Washington D.C., 1980.
114. Schlünder, Heat transfer in nucleate boiling of mixtures, *Int. Chem. Eng.*, Vol. 23, No. 4, pp, 589-599, 1983.
115. Schultz, R.R., and Cole, R., Uncertainty analysis in boiling nucleation, *AIChE Symposium Series*, Vol. 75, pp 32-39, 1979.

116. Sciance, C.T., Colver, C.P., and Sliepcevich, C.M., Nucleate pool boiling and burnout of liquefied hydrocarbon gases, *Chem. Engg. Prog. Syst. Ser.*, Vol. 63, No. 77, pp 109-114, 1967.
117. Scurlock, R.G., Enhanced boiling heat transfer surfaces, *Cryogenics*, Vol. 35, pp 233-237, 1995.
118. Shen, J., Spindler, K., and Hahne, E., Pool boiling heat transfer of refrigerant mixtures R32/R125, *Int. Comm. Heat Mass Transfer*, Vol. 26, No. 8, pp 1091-1102, 1999.
119. Shi, M.H., and Liu, H.Y., The effects of thermal properties of the wall on nucleate pool boiling heat transfer, *Symposium on 'Multiphase flow and Heat Transfer'*, Vol. 1, Xue-Jun Chen, T.N. Veziroglu and C.L. Tien (eds.), pp 304-311, Hemisphere Publishing Corporation, Washington D.C., 1989.
120. Stephan, K., and Abdelsalam, M., Heat transfer correlations for natural convection boiling, *Int. J. Heat Mass Transfer*, Vol. 23, pp 73-87, 1980.
121. Stephan, K., and Körner, M., Calculation of heat transfer in evaporating binary liquid mixtures, *Chemie - Ingenieur - Technik*, Vol. 41, No. 7, pp 409-417, 1969.
122. Stephan, K., and Preuseer, P., Heat transfer in natural convection boiling of polynary mixtures, *6th Int. Heat Transfer Conf. Ontario*, Paper PB-13, pp 187-192, August 7th to 11th, 1978.
123. Stephan, K., and Preusser, P., Heat transfer and critical heat flux in pool boiling of binary and ternary mixtures, *Ger. Chem. Eng.*, Vol. 2, No. 3, pp 161-169, June, 1979.
124. Stephan, K., and Preusser, P., Heat transfer and maximum heat flux density in the vessel boiling of binary and ternary liquid mixtures, *Chem. Eng. Tech.*, Vol. 51, No. 1, pp 37, 1979.
125. Sternling, G.V., and Tichacek, L.J., Heat transfer coefficient for boiling mixtures – Experimental data for binary mixtures of large relative volatility, *Chemical Engineering Society*, Vol. 16, pp 297-337, 1961.

126. Sun, Z., Gong, M., Qi, Y., Li, Z., and Wu, J., Nucleate pool boiling heat transfer of pure refrigerants and binary mixtures, *J. of Thermal Science*, Vol. 13, No.3, pp 259-263, 2004.
127. Sun, Z., Gong, M., Li, Z., and Wu, J., Nucleate pool boiling heat transfer coefficients of pure HFC134a, HC290, HC600a and their binary and ternary mixtures, *Int. J. of Heat and Mass Transfer*, Vol. 50, pp 94-104, 2007.
128. Táboas, F., Vallès, M. I., and Bourouis, M., and Coronas, A., Pool boiling of ammonia/water and its pure components: Comparison of experimental data in the literature with the predictions of standard correlations, *Int. J. of Refrigeration*, Vol. 30, pp 778-788, 2007.
129. Takeda, E., Hayakawa, I., and Fujita, S., Boiling heat transfer coefficients of binary liquid mixtures, *Kagaku Kogaku*, Vol. 34, No. 7, pp 751-757, 1970.
130. Tehvir, J., Influence of porous coating on the boiling burnout heat flux, *Trans. Tallinn Technical University*, Tallinn, Estonia, Report no. 726, pp 80-90, 1991.
131. Tehvir, J., Sui, H., and Temkina, V., Heat transfer and hysteresis phenomena in boiling on porous plasma-sprayed surface, *Exp. Thermal Fluid Sc.*, Vol. 5, pp 714-727, 1992.
132. Thome, J.R., Prediction of binary mixture boiling heat transfer coefficients using only phase equilibrium data, *Int. J. Heat Mass Transfer*, Vol. 26, pp 965-974, 1983.
133. Thome, J.R. and Bold, W.B., Nucleate pool boiling in cryogenic binary mixtures, *Proc. Int. Cryog. Eng. Conf.*, Vol. 7, pp 523-530, 1978.
134. Thome, J.R., and Shakir, S., A new correlation for nucleate pool boiling of aqueous mixtures, *AIChE Symp. Ser.*, Vol. 83, No. 257, pp 46-51, 1987.
135. Thome, J.R., *Enhanced Boiling Heat Transfer*, Hemisphere Publishing Corporation, Washington D.C., 1990.

136. Tien, C.L., A hydrodynamic model for nucleate pool boiling, *Int. J. Heat Mass Transfer*, Vol. 5, pp 533-548, 1962.
137. Tolubinskii, V.I., Kriveshko, A.A., Ostrovskiy, Y.N., and Pisarev, V. Y., Effect of pressure on the boiling heat transfer rate in water-alcohol mixtures, *Heat Transfer-Soviet Research*, Vol. 5, No.3, pp 66-68, May-June, 1973.
138. Tolubinskii, V.I, and Ostrovskii, Y. N., Mechanism of vapor formation and rate of heat transfer during boiling of binary solutions, *Akad Nauk, Urk. SSSR Reshul Mezhevdom*, pp 7-16, 1966.
139. Tolubinskii, V.I. and Kostanchuk, D.M., Effect of pressure on heat transfer during subcooled water boiling, *Vop. Tekh. Teplofic*, No. 3, pp 58-61, 1971.
140. Tolubinskii, V.I., and Ostrovskii, Y.N., Mechanism of heat transfers in boiling of binary mixtures, *Heat Transfer - Soviet Research*, Vol. 1, No. 6, pp 6-11, 1969.
141. Tolubinskii, V.I., Ostrovskii, Y.N., and Kriveshko, A.A., Heat transfer to boiling water-glycerin mixtures, *Heat Transfer - Soviet Research*, Vol. 2, No.1, pp 22-24, Jan., 1970.
142. Ünal, H.C., Prediction of nucleate pool boiling heat transfer coefficients for binary mixtures, *Int. J. Heat Mars Transfer* Vol. 29, No. 4, pp 637-640, 1986.
143. Vachon, R.L., Nix, G.H., Tanger, G.E., and Cobb, R.O., Pool boiling heat transfer from teflon-coated stainless steel, *Trans. ASME, J. Heat Transfer*, Vol. 91, pp 364-370, Aug., 1969.
144. Vachon, R.L., Nix, G.H., Tanger, G.E., Evaluation of constants for the Rohsenow pool-boiling correlation, *Trans. ASME, J. Heat Transfer*, Vol. 90, pp 239-247, May, 1968.
145. Van Wijk W.R., Vos, A.S., and Van Stralen, S.J.D., Heat transfer to boiling binary liquid mixtures, *Chem. Engng. Sci.* Vol. 5, pp 68-80, 1956.

146. Vasiliev, L.L., Zhuravlev, A.S., Ovsyannik, A.V., Novikov, M.N., and Vasilievjr, L.L., Heat transfer in propane boiling on surfaces with a capillary-porous structure, *Heat Transfer Research*, Vol. 35, No. 6, pp 436-456, 2004.
147. Vemuri, S., and Kim, K., Pool boiling of saturated FC-72 on nano-porous surface, *Int. Comm. Heat Mass Transfer*, Vol. 32, No.1, pp 27-31, 2005.
148. Vittala, C.B.V., Gupta, S.C., and Agarwal, V.K., Boiling heat transfer from a PTFE coated heating tube to alcohols, *Exp. Thermal Fluid Sc.*, Vol. 25, pp 125-130, 2001.
149. Vittala, C.B.V., Gupta, S.C., and Agarwal, V.K., Pool boiling of distilled water on PTFE-coated heating tube, *Heat Transfer Engineering*, Vol. 21, No. 6, pp 26-33, 2000.
150. Wang, C.H., and Dhir, V.K., Effect of surface wettability on active nucleation site density during pool boiling of water on a vertical surface, *Trans. ASME, J. Heat Transfer*, Vol.115, pp 659-669, 1993.
151. Warner, D.F., Park, E.L. Jr., and Mayhan, K.G., Nucleate boiling heat transfer of liquid nitrogen from plasma deposited polymer coated surfaces, *Int. J. Heat Mass Transfer*, Vol. 21, pp 137-144, 1978.
152. Webb, R.L., *Principles of Enhanced Heat Transfer*, John Wiley & Sons, Inc. 1994.
153. Westwater, J.W., and Strangelo, J.G., Photographic study of boiling, *Ind. Engg. Chem.*, Vol. 47, pp 1605, 1955.
154. Wright, R.D., Clements, L.D., and Colver, C.P., Nucleate and film boiling of ethane-ethylene Mixtures, *AIChE J.*, Vol. 17, No. 3, pp 626, 1971.
155. Young, R.K., and Hummel, R.L., Improved nucleate boiling heat transfer, *Chem. Engg. Prog.*, Vol. 60, No. 7, pp 53-58, July, 1964.
156. Zhang, Y., and Zhang, H., Boiling heat transfer from a thin powder porous layer at low and moderate heat flux, pp 358-366, *II Int. Symp. on Multiphase Flow and Heat Transfer*, New York, X.J. Chen, T.N. Veziroglu, C.L. Tien (eds.), Hemisphere Publishing Corporation, Washington D.C., 1992.

157. Zhao, Y.H., Diao, Y.H. and Takaharu, T., Experimental investigation in nucleate pool boiling of binary refrigerant mixtures, *Applied Thermal Engineering*, Vol. 28, pp 110-115, 2008.
158. Zhou, X., and Bier, K., Pool boiling heat transfer from a horizontal tube coated with oxide ceramics, *Int. J. Refrig.*, Vol. 20, No. 8, pp 552-560, 1997.
159. Zuber, N., Nucleate boiling – the region of isolated bubbles and the similarity with natural convection, *Int. J. Heat Mass Transfer*, Vol. 6, pp 53-78, 1963.

